DEVELOPMENT OF REMOTE SENSING BASED GEOTHERMIC TECHNIQUES IN EARTHQUAKE STUDIES

A THESIS

Submitted in fulfilment of the requirements for the award of the degree of

DOCTOR OF PHILOSOPHY

in

EARTH SCIENCES

By

SWAPNAMITA CHOUDHURY

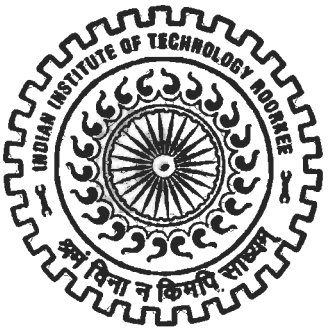

DEPARTMENT OF EARTH SCIENCES
INDIAN INSTITUTE OF TECHNOLOGY ROORKEE
ROORKEE-247 667 (INDIA)

JULY, 2005

INDIAN INSTITUTE OF TECHNOLOGY ROORKEE
ROORKEE

CANDIDATE'S DECLARATION

I hereby certify that the work which is being presented in this thesis, entitled "**DEVELOPMENT OF REMOTE SENSING BASED GEOTHERMIC TECHNIQUES IN EARTHQUAKE STUDIES**", in fulfilment of the requirement for the award of the degree of **DOCTOR OF PHILOSOPHY** and submitted in the **Department of Earth Sciences** of the Indian Institute of Technology Roorkee, is an authentic record of my own work carried out during a period from August 2001 to June 2005 under the supervision of **Dr. Arun K. Saraf**.

The matter embodied in this thesis has not been submitted by me for the award of any other degree of this or any other Institute/University.

Date: 4 July, 2005

Swapnamita Choudhury
(SWAPNAMITA CHOUDHURY)

This is to certify that the above statement made by the candidate is correct to the best of my knowledge.

Date: 04 July 2005

(DR. ARUN K. SARAF)

Department of Earth Sciences
Indian Institute of Technology Roorkee
ROORKEE-247 667

The Ph. D. viva-voce examination of **Swapnamita Choudhury**, Research Scholar was held on 09/09/05

Signature of Supervisor **Signature of H. O. D.** **Signature of External Examiner**

ABSTRACT

Earthquakes, the most unexpected and perhaps the most devastating natural calamity on earth, have imbibed interest in scientists from time immemorial. Studies on mechanism, cause, measurement of intensity and magnitude and not to mention prediction of earthquakes are still ambiguous. Generally, it is true that earthquakes cannot be predicted, but then devastating earthquakes keep coming and foster challenges to researchers world over. While analyzing past earthquakes and their characteristics perhaps a better understanding about this complex phenomenon can be made. That tectonics play a major role as the causative force behind an earthquake is now clear. Plate boundaries and fault zones are the most seismically active regions on the earth's crust and almost all past major earthquakes have been located along plate margins. Any pressure built-up due to tectonic activities, and also associated subsurface degassing due to closing of micro-pores with increasing stress, might create changes in the temperature regime near land surface. Charge carriers in rocks can be free electrons or deficient electrons (positive hole pairs or PHPs). PHPs dissociate under high pressure. When p-holes arrive at the earth's surface, they recombine by taking electrons from the surrounding and release heat. If by any technique, this change in thermal regime is detected, it can perhaps provide important clue to some impending earthquake activity. If earthquakes forewarn us before they strike, it is of utmost importance that we understand and pick up the clues. Satellite based radiometers, which can sense the thermal emission originating from the earth's surface and the intervening atmosphere, can be used to study any thermal anomaly developing near surface of the earth. Such satellite-derived detection of land surface temperature (LST) anomaly related to an earthquake is an important breakthrough for earthquake research. The concept that prior to earthquakes the LST increases has been validated by the study of 12 recent past earthquakes around the world. In the present study, LST maps derived from thermal NOAA-AVHRR data sets have been prepared and used to study the thermal scenario for the earthquakes in Bhuj (India) [26 January 2001 (M_w 7.7)], Boumerdes

(Algeria) [21 May 2003 (M_w 6.8)], Bam [26 December 2003 (M_w 6.6)] and Zarand in Iran [22 February 2005 (M_w 6.4)], Southeast Iran [13 March 2005 (M_w 6.0)] and in Banda-Aceh (Sumatra) [26 December 2004 (M_w 9.0)]. The earthquakes in Xinjiang [24 February 2003 (M_w 6.4)] and Zhangbei [10 January 1998 (M_w 6.2)] (China), Izmit / Kocaeli (Turkey) [17 August 1999 (M_w 7.6)], two earthquakes in Hindukush (Afghanistan) [3 March and 25 March 2002 (M_w 7.4 and 6.1)], and Kalat (Pakistan) [4 March 1990 (M_w 6.1)], have been studied using passive microwave SSM/I data sets. The Bhuj earthquake (India) has been analyzed using both AVHRR and SSM/I data sets. It has been observed that for all the above earthquakes studied, there were decipherable short-term temporal anomalies in the LST maps before the earthquakes. This thermal anomaly went away along with the earthquake events. The anomalies appeared a few days to a few hours preceding the earthquakes. The increase in temperature varied from 5-13° C than the usual temperature of the region around the epicentral area and also varied from earthquake to earthquake. Air temperature collected by meteorological stations situated near and around the epicentral area was obtained for the earthquake in Bhuj (India) and the several earthquakes in Iran. Temperature variation curves (TVC) were constructed using these data sets. The TVCs for these earthquakes also showed peaks of temperature increase before the earthquakes, which became normal again after the earthquakes. Air temperature normals were also constructed for the earthquakes in India and Iran, averaging data of several years. The amplitude of variation from normal was analyzed and was observed that the temperature was normal in all those years, unlike in the year in which the earthquake occurred. It has also been observed that the generation of thermal anomalies, their spatial extent, intensity and the days of their appearance prior to an earthquake depends on the magnitude, focal depth of the earthquake, terrain and meteorological conditions etc.

ACKNOWLEDGEMENT

I acknowledge my deepest gratitude for my supervisor, Dr. Arun K. Saraf, Department of Earth Sciences, Indian Institute of Technology Roorkee, for his connoisseur guidance, limitless support, endless optimism and motivation while carrying out this research work. Your association has created a different person in me. To adopt your strife for perfection will be my endeavor in all I do.

I express my heartfelt thanks to Prof. V. N. Singh, Head of the Department of Earth Sciences, Indian Institute of Technology Roorkee, and former HODs, Prof. A. K. Awasthi and Prof. B. Parkash, for providing the necessary facilities to accomplish the research work. I especially thank Prof. Singh, for all the support and endowing motivation to cultivate the research spirit. I also thank Prof. Sri Niwas, Chairman, DRC, Department of Earth Sciences, for constructive suggestions and appreciation.

I thank Department of Science and Technology (DST), New Delhi for the support towards the research project (PI: Dr. Saraf) and Council for Scientific and Industrial Research (CSIR), New Delhi for the financially supporting me as a Senior Research Fellow.

I duly thank National Institute of Oceanography (NIO), Goa, India Meteorological Department (IMD), Ahmedabad and University of Dundee, U.K., for providing valuable data sets for this study.

Heartfelt gratitude goes to my senior, Dr. Biswajit Sarma, for introducing me to team spirit in the lab. Fond remembrance and thanks is due to Parthapratim Ghosh, for many good days in the lab and otherwise. I also remember the days with Chandramani, Tanima, Bhavani and Sudipta Tapan Sinha.

The enormous collaboration and efforts put in by Ajanta, Santosh, Prabhu, Sudipta Dasgupta, Hemlata and Chetna cannot ever be forgotten. The association of especially Sudipta Dasgupta, towards the final stages of this work was wonderful. I cannot thank them all enough for their contribution and for creating the best working environment there can be.

I thank the Department technical and non-technical staff for all their help all these years, especially Shri A. R. J. G. Nair. The selfless, dedicated and round the clock service of the lab helper, Shri Rahil Hassan, is deeply appreciated.

I am deeply indebted in gratitude to my parents for their faith in me throughout, for their inspiration and for being with me through all troubles and tribulations. I dedicate my work to them. I also thank my brother for his support all along.

I also thank my dear friends Geetashree, Arunima, Anup, Rashmi and Shuchita for standing by me in all times. I thank Nabanita and Chetna for making the final days very memorable. I also appreciate the whole Earth Sciences Sarojini group for making my stay in Roorkee very interesting. I am beyond words while thanking Shalini, Suwagmani, Pratim and Prantajyoti for their regular cajoling and their faith in me.

Last but not the least I thank all those who have helped me directly or indirectly at various stages of this work.

CONTENTS

LIST OF FIGURES

LIST OF TABLES

1.1 INTRODUCTION

The evolving techniques of remote sensing have the potential to contribute and assist human research studies in evaluating natural processes and events occurring daily on the earth's surface on a global basis. Remote sensing now provides repetitive coverage, unbiased recordings of earth's surface and events, cost effective technology, which consumes less time and multi-spectral information. The use of visible remote sensing in association with Geographic Information Systems (GIS) in earthquake studies have been a great stride in the last few years in disaster mitigation by delineating earthquake hazard zones and inducing management, analyzing spatial variables, monitoring of earthquake prone areas, in assessment and in identifying gap areas. While GIS provides efficient analysis of natural hazards assessments, locating emergency areas, assisting in rehabilitations, remote sensing apart from identification of damaged areas, monitor the earth on a real time basis for future signs for an impending danger (Gupta, 2000). Now thermal remote sensing introduces more avenues for studying the earth. The earth's emissivity can unfold many unknown natural processes associated with earthquakes. Any thermal anomaly in tectonically active regions occurring on the land surface can be monitored regularly and any abnormality, when other meteorological conditions, are normal may be an indication for an impending earthquake.

Remote sensing for earthquake studies has probably traveled a long way and has become an integral part of earthquake disaster management. Till now, perhaps the lack of knowledge in this field, complexity of the phenomenon called 'earthquakes', availability of good resolution data for damage studies, cost of high resolution data, temporal resolution (revisit cycle of a satellite) etc. have been a major obstacle to such studies.

Earthquakes, perhaps the most devastating of all natural phenomena, have been an intriguing part of research interest for scientists since time immemorial. An earthquake is a sudden movement of the earth, caused by the abrupt release of strain that has accumulated over a long time. This short-time natural force has created havoc in mankind, destructing life, property, economy, thus paralyzing progress of the earthquake struck region for a long time. Whereas, most of the earthquakes originate at plate boundaries, where the plates of the earth's crust (called lithospheric plates) are converging, diverging or sliding past one another, few earthquakes also originate due to volcanism etc. or maybe man induced due to detonation of subsurface atomic explosives. Earthquakes associated with plate boundaries and plate subduction zones are the most powerful and account for more than half of the world's seismic events.

1.2 OBJECTIVES OF WORK

Time and again attempts at earthquake predictions have gripped scientists with enthusiasm, though complete success till now has never been ascertained. Geller et al. (1997) have even declared, "Earthquakes cannot be predicted", providing more, challenges to earth scientists for earthquake studies once again. Now with thermal remote sensing studies and satellite detection of land surface temperature (LST) anomaly related to an earthquake in this regard is an important breakthrough for earthquake studies.

Sensors like, Advanced Very High Resolution Radiometer (AVHRR) on board the American National Oceanic and Atmospheric Administration (NOAA) series of satellites, Moderate Resolution Imaging Spectroradiometer (MODIS) and Advanced Spaceborne Thermal Emission and Reflection Radiometer (ASTER) on Terra and Aqua satellites, Multi-channel Visible and Infra-red Scan Radiometer (MVISR), on board Chinese series of satellites Feng Yun (FY), all senses in the thermal infrared parts of the electromagnetic spectrum. The Spatial Sensor Microwave Imager (SSM/I) flown aboard the American Defense Meteorological Satellite Program (DMSP) is a passive microwave imager. These sensors can sense the thermal emission originating from the earth's surface and

provide unique opportunities to study any thermal anomaly developing on the land surface.

Chapter 2 discusses the background of earthquake studies, the understanding of the probable causes of earthquakes and attempts at earthquake predictions by seismologists around the world. The cause of earthquakes is now almost clear. Tectonic locations like plate boundary regions are the most seismically active zones. In India, there are five important seismic zones, according to the vulnerability of a region to any intensity of earthquake. The phenomenon of thermal abnormality can be understood to be due to several conditions and changes on rocks due to stresses generated prior to an earthquake. These explanations as given by different workers around the world have been discussed in Chapter 2.

Chapter 3 introduces different remote sensing data sets used to study the concept of 'thermal anomalies as associated with earthquakes'. For the study, 12 major recent past earthquakes were selected on the basis of availability of data. Pressure induces a rise in temperature. In tectonically active regions, stresses may build up. These stresses may augment the LST of the near ground surface. Further, these stresses may also bring about sub-surface degassing. These gases upon their escape to the atmosphere may create a localized greenhouse effect and increase the temperature of the region, thus creating a thermal anomaly in the surrounding region. This anomaly may be followed by an earthquake. The very recent explanation to the built-up of a thermal anomaly before an earthquake is given by Freund (2003). Charge carriers in the ground can be free electrons called positive hole pairs (PHPs). Upon induced pressure (as generated before an earthquake) PHP dissociate and try to attain stability. In the earth's surface they recombine and in the process release energy in the form of heat. This is manifested as LST anomaly prior to an earthquake event. Such thermal anomalies generated can provide important clues to impending earthquakes.

The present study is a post-event attempt to observe and analyze the appearance of short-term pre-earthquake thermal anomalies. This attempt is

towards developing knowledge about the appearance and correlation of pre-earthquake thermal anomalies and earthquakes and their detection by thermal remote sensing technique. This work is not intended towards forecasting or prediction of earthquakes. However, with regular monitoring and integrated approach based on other precursors, this might lead towards the same. In this study, thermal Infrared NOAA-AVHRR and passive microwave DMSP-SSM/I data sets were used to detect any built-up of pre-earthquake thermal anomalies for 12 past major earthquakes around the world. LST maps using NOAA-AVHRR data sets have been prepared and used to study the thermal scenario for the earthquakes in Bhuj (India), Boumerdes (Algeria), Bam and Zarand in Iran and Banda-Aceh (Sumatra) (table 1.1). The earthquakes in Xinjiang and Zhangbei (China), Izmit / Kocaeli (Turkey), two earthquakes in Hindukush (Afghanistan) and Kalat (Pakistan) have been studied with SSM/I data sets (table 1.2). The Bhuj earthquake (India) has been analyzed using both by AVHRR and SSM/I data sets. Air temperature conditions for the earthquakes in India and a few earthquakes in Iran, collected by meteorological stations around the epicenter, were also analyzed and the trend of temperature variations in the period when the earthquake occurred was observed. Past several years' data was also used to construct temperature normals to compare the thermal trend with regard to the year and time of the earthquakes. Terra-MODIS and NOAA-AVHRR data have been used to study the sea turbidity conditions induced by the tsunami after the megathrust earthquake and the underwater thrust, in Banda-Aceh in Sumatra.

Table 1.1: Details of the earthquakes studied using NOAA-AVHRR data sets

S. N.	Earthquake	Origin		Location (in DD)		Magnitude (M_w) (USGS)	Focal Depth (km)
		Date	Time (UTC)	Lat (N)	Long (E)		
1	Bhuj, India	26.01.01	03:16:41	23.41	70.23	7.9	16
2	Boumerdes, Algeria	21.05.03	18:44:19	36.90	03.71	6.8	10
3	Bam, Iran	26.12.03	01:56:52	29.00	58.34	6.6	10
4	Zarand, Iran	22.02.05	02:25:22	30.74	56.90	6.4	14
5	Southeast Iran	13.03.05	03:31:23	27.15	61.88	6.0	55
6	Banda-Aceh, Sumatra	26.12.04	00:58:53	3.31	95.95	9.0	30

Table 1.2: Details of the earthquakes studied using DMSP-SSM/I data sets

S. N.	Earthquake	Origin		Location (in DD)		Magnitude (M_w) (USGS)	Focal Depth (km)
		Date	Time (UTC)	Lat (N)	Long (E)		
1	Kalat, Pakistan	04.03.90	19:46:19	28.92	66.33	6.1	10
2	Zhangbei, China	10.01.98	03:50:41	41.08	114.50	6.2	30
3	Izmit, Turkey	17.08.99	00:01:39	40.74	29.86	7.6	17
4	Bhuj, India	26.01.01	03:16:41	23.41	70.23	7.7	16
5	Double Earthquakes of Hindukush, Afghanistan	03.03.02	12:08:06	36.44	70.45	6.2	195
		03.03.02	12.08.22	36.54	70.42	7.4	256
6	Hindukush, Afghanistan	25.03.02	14:56:37	35.97	69.18	6.1	33
7	Southern Xinjiang, China	24.02.03	02:03:41	39.61	77.24	6.4	11

Chapter 4 discusses the thermal remote sensing based analysis and observations in the earthquakes around the world. The analysis yield successful results in identifying definite built-up of thermal anomalies prior to all the earthquakes studied. The locations of the epicenters of all the earthquakes studied here are in the vicinity of plate boundary regions or active faulting and

thrusting. The observations led to some significant observations, which have also been discussed in this Chapter.

Chapter 5 summarizes the analysis, observations and the conclusions drawn from the study and also proposes few recommendations.

2.1 HISTORY OF EARTHQUAKE STUDIES

2.1.1 CAUSES OF EARTHQUAKES

The study of earthquakes is comparatively new. Until perhaps the 18th century, the actual cause of earthquakes was little understood. That tectonics play a major role in causing an earthquake is now well established. The causes derived by earthquake researchers, a hundred years ago seem to be fanciful today. As mentioned by Hemmady (1996), as per an Indian legend, the earth is supported on the head of 'shesh nag' (mighty snake, a devotee of God Vishnu) and whenever he changes his position an earthquake occurs. Inhabitants of Kamchatka peninsula believed that shocks were due to a giant dog named Kosei. Whenever Kosei shakes the snow off his fur an earthquake occurs. Ancient Japanese attribute the cause of an earthquake to the movement of a giant spider, which carries the earth on its back. The great Greek philosopher Pythagorus thought that earthquakes occurred when the dead fought amongst themselves, whereas another Greek philosopher had been more modern to his ideas and believed that air masses escaping from the interior of the earth caused earthquakes. Religious fundamentalists believed that an earthquake was punishment from God whenever people committed sin or the splitting of the earth was manifestations of God's wrath whenever someone rose against Moses.

It is now understood that the earth's surface can be thought to be composed of about a dozen large plates that move relative to one another at speeds of about 1 - 12 cm per year. This theory known as the 'plate tectonics' theory has developed some 30 years from now. Tectonics imply to the deformation on the earth's crust, the forces producing such deformation, and the geologic and structural features that result. The rigid plates, whose average thickness in the continents is about 30 to 80 kilometers and in oceans is about 10 km, are spreading apart (causing divergent plate margin), sliding past each other

(generating transform faults), or colliding with each other (causing converging boundary and subduction zones) in slow motion on top of the Earth's hot, pliable interior. Most spreading zones are found in oceans. The North American and Eurasian plates are spreading apart along the mid-Atlantic ridge. Spreading zones usually have earthquakes at shallow depths (within 30 kilometers of the surface) (http://pubs.usgs.gov/gip/earthq1/where.html). Volcanoes generally tend to form where plates collide or spread apart (http://vulcan.wr.usgs.gov/Volcanoes/JuanDeFucaRidge/description_juan_de_fuca.html). A typical example of a transform-fault plate boundary is the San Andreas Fault, along the coast of California and northwestern Mexico. Earthquakes at transform faults tend to occur at shallow depths and form fairly straight linear patterns. A typical example of a subduction zone is found along where the Indian plate is being subducted beneath the Eurasian plate along where the mighty Himalayas are rising. Subduction zones are characterized by deep-ocean trenches, shallow to deep earthquakes, and mountain ranges containing active volcanoes.

The current major continental and oceanic plates include: the Eurasian plate, Australian-Indian plate, Philippines plate, Pacific plate, Juan de Fuca plate, Nazca plate, Cocos plate, North American plate, Caribbean plate, South American plate, African plate, Arabian plate, the Antarctic plate, and the Scotia plate (figure 2.1). These plates consist of smaller sub-plates.

Most earthquakes of the world occur at these plate margins. In fact, the locations of earthquakes and the kinds of ruptures they produce help scientists define the plate boundaries. Earthquakes can also occur within plates, although plate-boundary earthquakes are much more common. Less than 10 percent of all earthquakes occur within plate interiors. As plates continue to move and plate boundaries change over geologic time, weakened boundary regions become part of the interiors of the plates. These zones of weakness within the continents can cause earthquakes in response to stresses that originate at the edges of the plate or in the deeper crust (http://pubs.usgs.gov/gip/earthq1/where.html).

2.1.2 HISTORICAL SEISMICITY

The earliest earthquake for which there is descriptive information is perhaps the China earthquake in 1177 B. C. China, in the next thousand years that followed, have described several large earthquakes. In Europe, earthquakes have been mentioned as early as 580 B. C., but the earliest earthquake for which there is some descriptive information occurred in the mid-16th century. The earliest known earthquakes in the Americas were in Mexico in the late 14th century and in Peru in 1471, but descriptions of the effects were not well documented. A series of three earthquakes in New Madrid, starting from 16 December 1811, second on 23 January 1812 and a third on 7 February 1812 rocked North America. The aftershocks continued for a long time. The magnitude 8.0 earthquake was felt as far as Boston and Denver, but luckily could not cause much damage as the region was sparsely populated. The San Francisco earthquake of 1906 claimed the lives of 700 people and was one of the most destructive earthquakes in history of North America. The earthquake and the fire that followed killed nearly 700 people and left the city in ruins. The Alaska earthquake of 27 March 1964 was of greater magnitude than the San Francisco earthquake. Though this earthquake released twice more energy than the San Francisco earthquake the loss of property and life was less since Alaska was sparsely populated. Table 2.1 gives a few most destructive earthquakes in history. Table 2.2 gives the major earthquakes in India (http://neic.usgs.gov/neis/eqlists/eqsmosde.html).

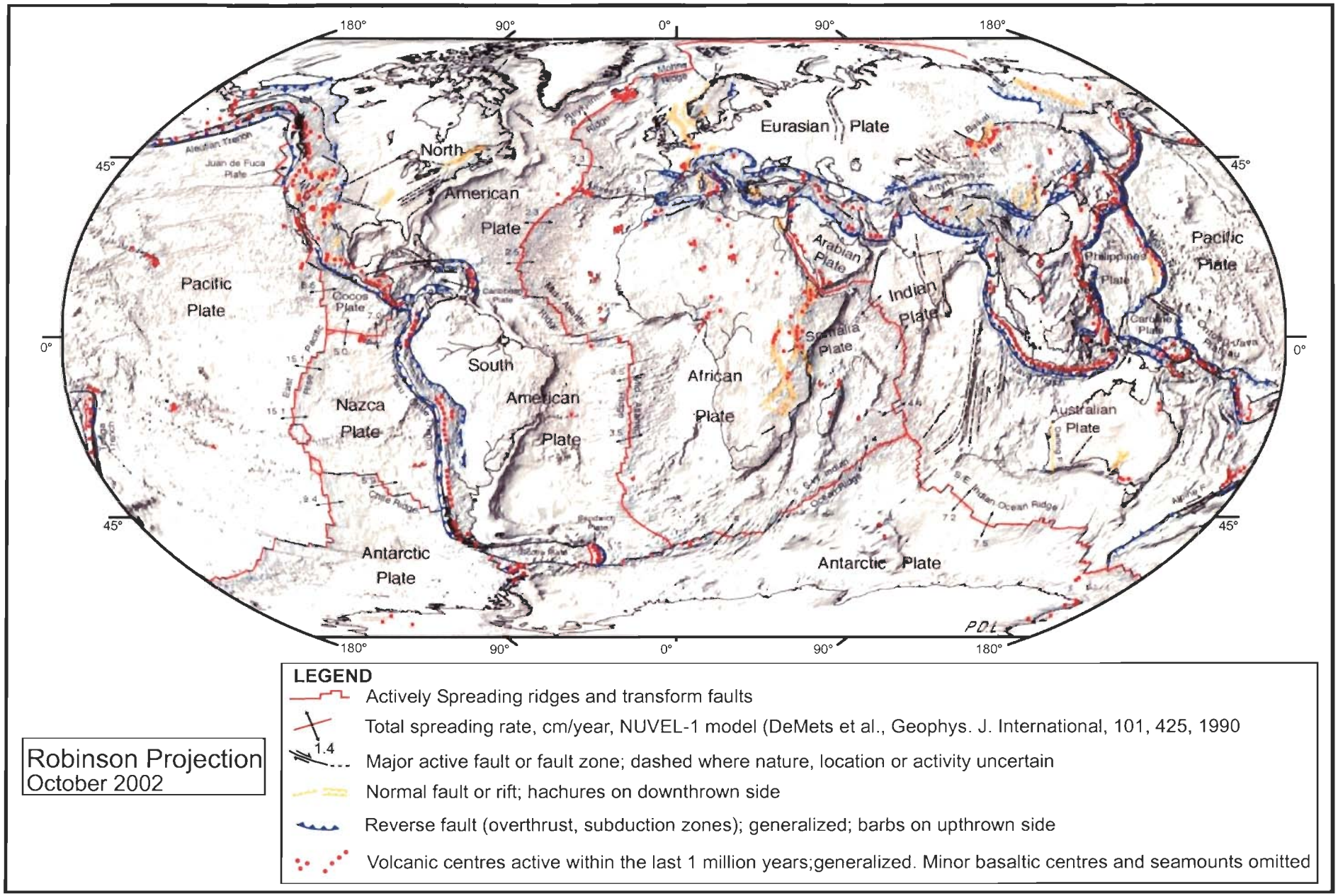

Figure 2.1: Tectonic Activity Map of the Earth showing tectonism and volcanism of the last 1 million years (Source: http://www2.umt.edu/geology/faculty/sheriff/437-Seismology_Magnetics/Images/Tectonic_Map_World.jpg).

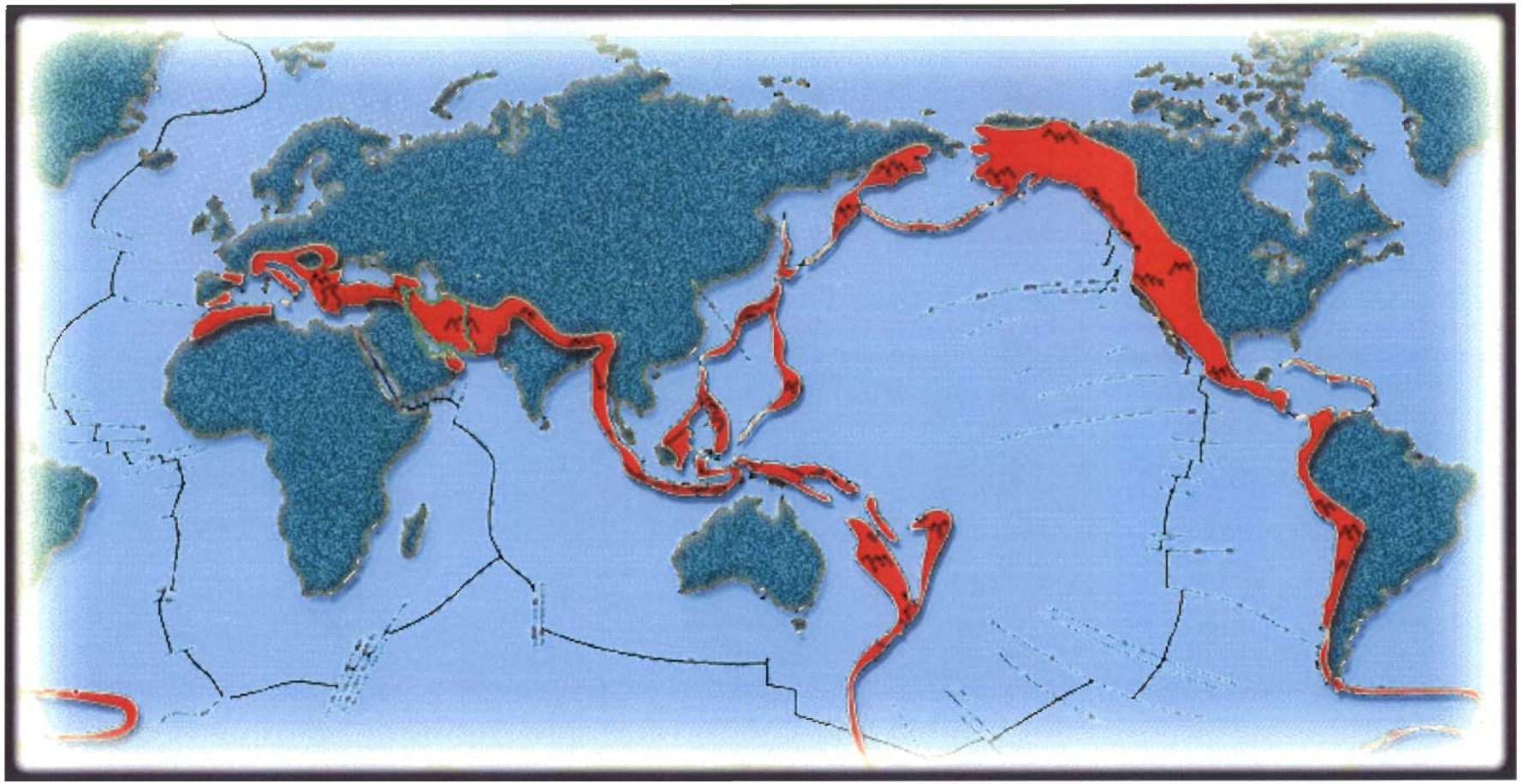

Figure 2.2: Highly seismically active regions of the world (http://www.iiees.ac.ir/English/Publicedu/seismic%20world.htm).

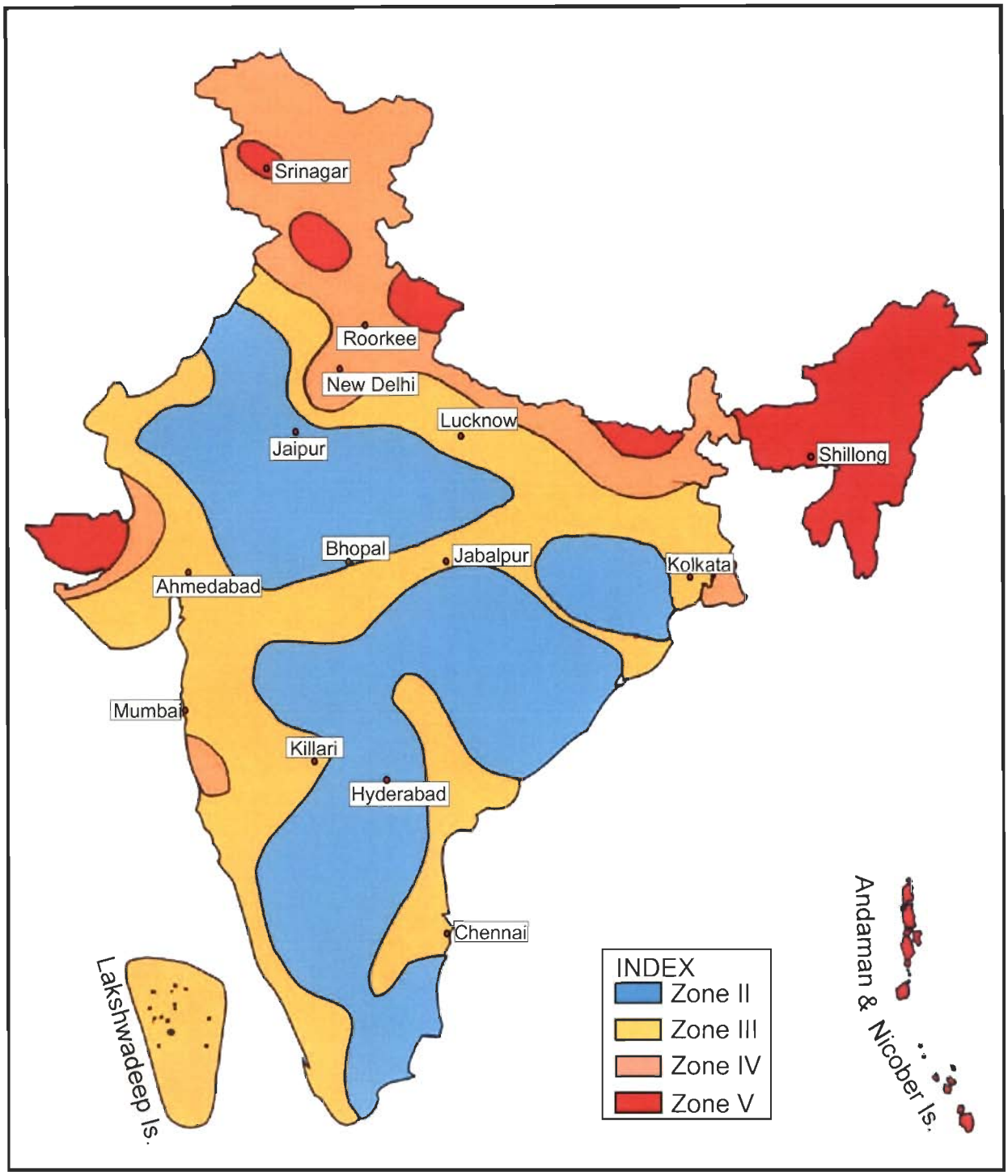

Figure 2.3: Seismic Zones of India (Source: http://asc-india.org/maps/seisindia.jpg). In the latest map released by Bureau of Indian Standards (BIS), Zone I and II have been merged as one.

Table 2.1: Most deadly historical earthquakes recorded in the world (http://neic.usgs.gov/neis/eqlists/eqsmosde.html)

Date	Location	Magnitude (USGS)	Deaths	Comments
22 December 856+	Iran, Damghan	-	200,000	-
23 March 893+	Iran, Ardabil		150,000	
9 August 1138	Syria, Aleppo	-	230,000	-
September 1290	China, Chihli	-	100,000	-
1268	Asia Minor, Silicia	-	60,000	-
23 January 1556	China, Shansi	~8	830,000	-
November 1667	Caucasia, Shemakha	-	80,000	-
11 January 1693	Italy, Sicily	-	60,000	-
18 November 1727	Iran, Tabriz	-	77,000	-
1 November 1755	Portugal, Lisbon	8.7	70,000	Great tsunami
4 February 1783	Italy, Calabria	-	50,000	-
28 December 1908	Italy, Messina	7.2	70,000 to 100,000 (estimated)	Deaths from earthquake and tsunami
16 December 1920	China, Gansu	8.6	200,000	Major fractures, landslides
1 September 1923	Japan, Kwanto	7.9	143,000	Great Tokyo fire
22 May 1927	China, near Xinjiang	7.9	200,000	Large fractures
25 December 1932	China, Gansu	7.6	70,000	-
30 May 1935	Pakistan, Quetta	7.5	30,000 to 60,000	Quetta almost completely destroyed
5 October 1948	USSR (Turkmenistan, Ashgabat)	7.3	110,000	-
31 May 1970	Peru	7.9	66,000	$530,000 damage, rock slides, floods
27 July 1976	China, Tangshan	7.5	255,000 (official)	Estimated death toll as high as 655,000
20 June 1990	Iran	7.7	50,000	Landslides

Table 2.2: Location of Past Major Earthquakes in India (http://www.imd.ernet.in/section/seismo/static/signif.htm). The magnitudes are as provided by India Meteorological Department (IMD)

Date	Location of Epicenter		Place	Magnitude (M_w) (IMD)
	Latitude (°N)	Longitude (°E)		
16 Jun 1819	23.6	68.6	Kutch, Gujarat	8.0
10 Jan 1869	25	93	Near Cachar, Assam	7.5
30 May 1885	34.1	74.6	Sopor, J & K	7.0
12 Jun 1897	26	91	Shillong Plateau	8.7
04 Apr 1905	32.3	76.3	Kangra, H. P.	8.0
08 Jul 1918	24.5	91.0	Srimangal, Assam	7.6
02 Jul 1930	25.8	90.2	Dhubri, Assam	7.1
15 Jan 1934	26.6	86.8	Bihar-Nepal Border	8.3
26 Jun 1941	12.4	92.5	Andaman Islands	8.1
23 Oct 1943	26.8	94.0	Assam	7.2
15 Aug 1950	28.5	96.7	Arunachal Pradesh-China Border	8.5
21Jul 1956	23.3	70.0	Anjar, Gujarat	7.0
10 Dec 1967	17.37	73.75	Koyna, Maharashtra	6.5
19 Jan 1975	32.38	78.49	Kinnaur, H. P.	6.2
06 Aug 1988	25.13	95.15	Manipur-Myanmar Border	6.6
21 Aug 1988	26.72	86.63	Bihar-Nepal Border	6.4
20 Oct 1991	30.75	78.86	Uttarkashi, U. P. Hills	6.6
30 Sept 1993	18.07	76.62	Latur-Osmanabad, Maharashtra	6.3
22 May 1997	23.08	80.06	Jabalpur, M. P.	6.0
29 Mar 1999	30.41	79.42	Chamoli District, U. P.	6.8

2.2 SEISMIC ZONES AROUND THE WORLD

Analyzing past earthquakes, it is obvious that though earthquakes can occur anywhere, but they are mainly concentrated in major seismic zones of the world (figure 2.2). The Circum-Pacific Belt stretches along the coast of the Pacific Ocean beginning from Chile, northward along the South American coast through Central America, Mexico, the West Coast of the United States, and the southern part of Alaska, through the Aleutian Islands to Japan, the Philippine Islands, New Guinea, the island groups of the Southwest Pacific, and to New Zealand. This belt accounts for around 81% of the world's major earthquakes. The second belt, namely, the Alpine Belt extends from Java to Sumatra through the Himalayas on

the northern boundary of India, the Mediterranean, and out into the Atlantic and accounts for 17% of the major earthquakes of the world. The third major belt runs along the submerged Mid-Atlantic Ridge in the Atlantic Ocean (http://earthquake.usgs.gov/faq/hist.html). These are areas of active earth tectonism, where mountain chains, ocean trenches and ridges are developing.

Apart from these linear belts of active seismic activity around the world, earthquakes do occur in other parts of the world induced by tectonics, volcanoes, etc.

2.3 SEISMIC ZONES IN INDIA

The idea of a seismic zoning map in India was to classify the area of the country into a number of zones in which one may reasonably expect earthquake shocks of more or less same intensity in future (Hemmady, 1996). Seismic zoning in India started in 1956, when a three zone map was prepared based on a broad concept of earthquake distribution and geotectonics in the plate boundary region which included the Himalayan Frontal Arc in the North, the Chaman fault region in the northwest and the Indo-Burma border region in the north east in the severe earthquake hazard zone; the lower hazard zone is confined to Indian shield region in the south and the moderate hazard zone confined to the transitional zone in between the two (http://www.asc-india.org/info/seisindia.htm). In 1962, the Indian Standards Institution (now renamed as Bureau of Indian Standards, BIS) prepared a six-zoned map of seismic hazards in India. The map underwent revisions in 1966, 1970, 1975 and 1984. Later, five seismic zones were delineated in India. Zone V is the most severe seismic zone which is vulnerable to earthquakes of more than intensity IX and above in the Modified Mercalli Intensity Scale and of magnitude 7 or more in the Richter scale. This zone is therefore referred to as Very High Damage Risk Zone. This region included the Andaman & Nicobar Islands, all of North-Eastern India, parts of north-western Bihar, eastern sections of Uttaranchal, the Kangra Valley in Himachal Pradesh, near the Srinagar area in Jammu & Kashmir and the Rann of Kutchh in Gujarat. Zone IV is referred to as High Damage Risk Zone and is liable to earthquakes of intensity VIII. New Delhi lies in this zone, along with major part

of Jammu and Kashmir, northern part of Uttar Pradesh, Sikkim, some part of Gujarat and Maharastra. Zone III is regarded as Moderate Damage Risk Zone. Mumbai lies in this zone with associated intensity VII. Zone II has a probable intensity of VI and is referred to as Low Damage Risk Zone. Chennai lies in this zone. Zone I is termed as Very Low Damage Risk Zone and is liable to earthquakes of intensity V. Almost the whole of peninsular India lies in zones I and II (http://gujarat-earthquake.gov.in/final/seismic.html) (figure 2.3).

In 2000, BIS revised the Five Zoning Map of earthquake risk in India. Zone I and Zone II have been merged into a single zone and new regions have been included in Zone III such as the Marathwada region of Maharashtra and the Chennai area in Tamil Nadu (http://asc-india.org/info/seisindia.htm). Zoning undergoes revision as and when necessary.

2.4 HISTORY OF THERMAL REMOTE SENSING IN EARTHQUAKE STUDIES

The history of the application of thermal remote sensing in natural resources perhaps started in Russia in the nineteen sixties. Thermal data in seismic studies was first put to application in Russia in 1985 (Tronin 2000) and the results were published in 1988 (Gorny et al., 1988). The use of thermal data from satellites in application to earthquake studies along with other studies like permafrost phenomenon, monitoring leakages from major gas and oil pipelines, urban heating pipelines, etc. was experimented upon in Russia (Gorny and Shilin, 1992). Case studies on earthquakes were carried out in Russia, Japan and China. This realization that earth's surface temperature is significantly related to the earth's physical processes has led to the development of an interesting trend of earthquake research.

Gorny and Shilin (1992) noted that within a 500 km radius from the epicenter of an earthquake there are sites within the earth's crust that change their characteristics before an earthquake. Stations for analysis can be located within such zones. Statistical analysis of data for medium range earthquakes gave a probability of earthquake prediction as 0.87, for the ratio of the period of

seismic alarm in days to the total number of days as 0.38 (Gorny et al., 1992). Positive thermal anomalies at a regional scale was observed with the examination of around 9000 thermal images for the Middle Asia earthquake which was attributed to the green house effect which was caused before the earthquake by an increase in gases like CO_2, CH_4 etc.

Depending on the advantages of thermal infrared data of meteosat, such as data accuracy, large area coverage, large amount of dynamic variation of temperature before earthquakes, the Chinese tried to predict the 18 October 1989 Datong Earthquake in Shanxi province (Zu-ji et al., 1991). The temperature was seen to increase four days before the earthquake and spread along valleys. It was a trial for determining an idea and method for an impending earthquake prediction.

A new theory of charge generation in rocks prior to earthquakes is given by Friedmann Freund (Freund, 2002 and Freund, 2003). This theory keeps parity with laboratory experiments (Zu ji et al., 1997, Ouzounov and Freund, 2004) and also supports the appearance of thermal anomalies related to earthquakes. Thermal infrared emission under application of enormous pressure has been experimented upon by NASA researchers (http://science.nasa.gov/headlines/y2003/11aug_earthquakes.htm). A 20-year plan to deploy a network of satellites - the Global Earthquake Satellite System (GESS) - using InSAR to monitor fault zones around the world has been thought upon, and eventually use the InSAR data to infer when stresses in the earth's crust have reached a dangerous level, issuing a monthly "hazard assessment" for a given fault and forecasters can report that the likelihood of having a major quake on, say, the San Andreas fault during the coming month is 2%, or 10%, or 50%. NASA believes that InSAR is one way to forecast quakes, but perhaps not the only one.

In an experiment carried out at NASA laboratories, pressure of 1,500 ton (like that which exists below the earth) was applied on red granite blocks. A sensitive camera developed at NASA's laboratories JPL and GSFC monitored the rock and detected infrared emissions. There was also voltage built up on the

block. This leads Freund to believe the cause might be electrical. The explanation thus given by Freund is that ordinary rocks are insulators. However, rocks placed under great stress, sometimes act like semiconductors. Freund believes that, before a quake, pairs of positive charges called 'defect electrons' or 'positive holes' split up and migrate to the surface of stressed rocks. There they recombine with each other and, in the process, release infrared radiation (http://science.nasa.gov/headlines/y2003/11aug_earthquakes.htm). This theory is supported experimentally. However, the analysis is very recent and is still on going.

Visible remote sensing in the field of earthquake studies had been used extensively all along for earthquake damage estimation and in aiding of relief operations and rehabilitations. Use of thermal remote sensing started in Russia in the nineteen sixties and the application of thermal remote sensing in earthquake studies started in Russia in 1985 (Tronin 2000). The results were published in 1988 (Gorny et al., 1988). The advent of thermal remote sensing widened many new avenues in the field of earthquake studies. Thermal infrared sensors like Advanced Very High Resolution Radiometer (AVHRR) on board the National Oceanic and Atmospheric Administration (NOAA) - series of satellites, Multi-spectral Visible and Infrared Radiometer (MVISR) on board the Chinese series of Feng Yun (FY) satellites, Moderate Resolution Imaging Spectroradiometer (MODIS) on board Terra and Aqua satellites, Enhanced Thematic Mapper (ETM+) on Landsat, Advanced Spaceborne Thermal Emission and Reflection Radiometer (ASTER) on board NASA's satellite Terra, and also passive microwave sensors like the Special Sensor Microwave Imager (SSM/I) on board Defense Meteorological Satellite Program (DMSP) series of satellites can detect the earth's emissivity at any time over any region. These sensors can be used to study any thermal anomaly developing on the land surface.

3.1 DATA USED

The earth's surface and atmosphere radiates thermal energy owing to the heating by solar irradiation and internal heat flow (very minor contribution). Sensors, sensing in the thermal infrared / microwave sections of the electromagnetic spectrum (figure 3.1) record this emitted energy and provide very useful information for various applications. The basis for thermal remote sensing is the Planck's law (i). The frequency or wavelength of EMR is a function of the energy of the electromagnetic quanta. The relationship (Planck's law) is as follows:

$$E = \nu h = ch / \lambda \qquad \text{(i)}$$

where, E = energy

ν = frequency of electromagnetic fields

h = Planck's constant (= 6.62 x 10^{-34} Js)

c = velocity of EMR in vacuum

λ = wavelength

The shorter the wavelength or higher the frequency of EMR, the greater is the energy of each quantum (Drury, 1987).

Beyond about 4 μm in the EM spectrum energy from the earth's surface is almost due to radiant emission from natural materials. The energy emitted (ii) is governed by the fourth power of the absolute temperature of the material (Stefan-Boltzmann Law) given by the following relation:

$$H = \sigma T^4 \qquad \text{(ii)}$$

where, H = total radiant emittance

σ = Stefan's Boltzmann constant

T = absolute temperature

The main windows for thermal sensors are between 8-14 μm. Narrow wave bands highlight distinctive features in remote sensing. The advantage of thermal infrared remote sensing is that images can be acquired day and night. The earth's surface is always above absolute zero, and thus it emits thermal radiation day and night equally. In fact, at nighttime the effect of solar heating and partial sun illumination is overcomed. As discussed above sensors like AVHRR on board NOAA series of satellites, MODIS on board satellites Terra and Aqua, etc. have been successfully sensing the earth's emissivity and providing useful information for studies like forest fire, volcanic, climate, snow cover mapping etc.

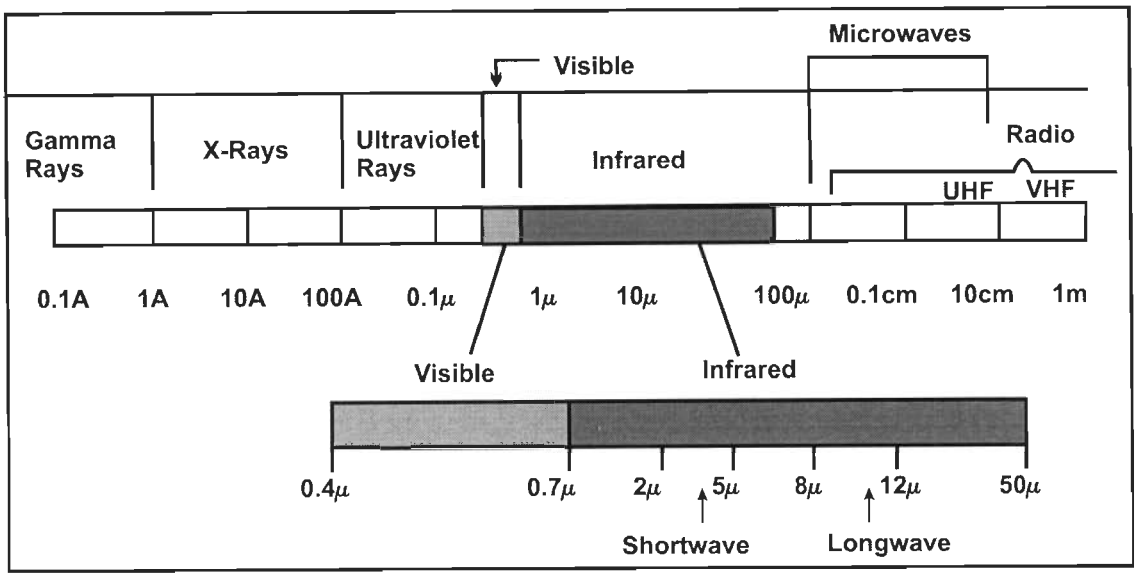

Figure 3.1: Electromagnetic Spectrum, showing infrared and microwave wavelengths.

While infrared sensors retrieve thermal data from the earth's surface only through areas of clear sky (since infrared radiation does not penetrate clouds), therefore the only limitation for thermal infrared remote sensing is the presence of clouds. Clouds appearing between the satellite and the earth's surface will lead to erroneous calculation of land surface temperature (LST) because the sensor will be measuring the temperature of cloud tops and not the actual emissivity of the earth. Thus cloud cover can sometimes stand as a disadvantage.

However, the passive microwave radiometer SSM/I on board DMSP has the advantage of being more transparent to clouds and therefore has an all weather advantage (apart from being capable to provide data day and night).

Microwave Remote Sensing provides data in two formats: passive remote sensing (sensing radiation in the 8-14 μm range, which is emitted by the earth's surface) and active remote sensing (by generating microwave beam and then sensing the back scatter). Passive microwave radiometers like SSM/I provide opportunity to study the thermal scenario of the earth. However, resolution of a passive microwave antenna is inversely proportional to its diameter. Apart from suffering from coarser resolution, passive microwave images contain all the geometric distortions of a line scan system (Drury, 1987).

For the present study, NOAA-HRPT-AVHRR data has been used for analysis of the thermal regime before and after the earthquakes in Bhuj (India), Boumerdes (Algeria) and Bam (Iran) (table 1.1). The earthquakes in Zarand (Iran) and the Southeast Iran earthquakes along with the cluster of smaller quakes in Iran and the Banda-Aceh (Sumatra) earthquake have been studied using NOAA-GAC-AVHRR data sets (table 1.1). The earthquakes in Xinjiang and Zhangbei (China), Izmit / Kocaeli (Turkey), two earthquakes in Hindukush (Afghanistan) and Kalat (Pakistan) have been studied with SSM/I data sets.

3.1.1 ADVANCED VERY HIGH RESOLUTION RADIOMETER (AVHRR)

The NOAA sun-synchronous, polar orbiting operational environmental satellite program evolved over many years of experiments and operational satellite programs after the launch of their first satellite TIROS 1 on 1 April 1960. The subsequent generations were enhanced further in terms of sensors and machines. They carried additional payloads, including independent search and rescue facilities (http://www.stvincent.ac.uk/Resources/Weather/NOAA/systeminfo.html) and enhancement of channels in the sensors came into being. In 1970, an infrared sensor was added and the first NOAA was launched. In the year 1978, a new generation satellites (TIROS-N or NOAA-6 and 7) with greater capabilities were developed, which were replaced in 1983 by Advanced TIROS-N or NOAA-8. The last in this series, NOAA-14, was launched in 1994. The KLM series of NOAA satellites (NOAA-15, 16 and 17) were launched to introduce a new era of improved environmental monitoring, for meteorology, hydrology, climate research and agriculture. The latest NOAA satellite (NOAA-N, renamed after launch as NOAA-18) was launched very recently (on 20 May 2005). The launch dates and frequencies of transmission of the NOAA satellites are given in table 3.1. Data from NOAA-14, 16 and 17 has been used in the present study.

Polar orbiting satellites provide daily global data for land, ocean and atmospheric studies. In a polar satellite, the number of near-polar orbits per day is not an integer (NOAA-satellites make about 14.1 orbits per day), therefore the sub-orbital tracks do not repeat on a daily basis although the local solar time of

each satellite pass remains the same for a particular place. Each polar satellite provides at least two daytime and two nighttime scenes. This makes possible regular and continuous monitoring of the earth.

Table 3.1: Launch dates and transmission frequencies of NOAA-series of satellites

Satellite	Launch Date	Transmission Frequencies (MHz)
NOAA-14 (J)	30 December 1994	HRPT-1707.0
NOAA-15 (K)	13 May 1998	HRPT-1702.5
NOAA-16 (L)	21 September 2000	HRPT-1698.0
NOAA-17 (M)	24 June 2002	HRPT-1707.0
NOAA-18 (N)	20 May 2005	HRPT-1698.0

The AVHRR on board the NOAA-series of satellites is an optical instrument, which provides multi-spectral imaging by sensing reflected sunlight and thermal emissions. It is a five- to six-channeled radiometer (depending on the NOAA satellite) providing data in visible, near infrared and thermal infrared for a wide range of applications. The thermal channels 4 and 5 are the windows in the range of 10.3-11.3 and 11.5-12.5 μm. AVHRR has a spatial resolution of 1.1 km (table 3.2).

The image taken by each satellite is broadcast directly continually by the satellite to earth, which is received by different earth stations, as well as tape-recorded onboard the satellite for readout at a NOAA receiving centre. The direct broadcasting of the images by the satellite is also known as the Direct Readout Service. This readout service distributes the raw or minimally processed data, which can be received by various earth stations all over the world.

Table 3.2: General specifications of the NOAA-series of satellites

S. N.	Parameter	NOAA-Specifications
1	Orbit	Sun synchronous satellites
2	Sensor	AVHRR Sensor onboard NOAA
3	Channels	5 (AVHRR/2 till NOAA-14) or 6 (AVHRR/3, NOAA 15 onwards)
4	Telemetry	HRPT (High Resolution Picture Transmission)
5	Altitude	850 (+/- 30) km
6	Spatial resolution	1.1 km
7	Temporal resolution	4 images daily per satellite
8	Temperature resolution	0.12 – 0.5°C
9	Swath width	2800 km
10	Instantaneous Field of View (IFOV)	1.3 μr
11	Inclination	98.70°
12	Period	102.301 minutes (makes 14.1 orbits per day)
13	Scan Angle	± 55°
14	Scan rate	6 scan lines per seconds

AVHRR data is broadcast in the four following formats (http://www2.ncdc.noaa.gov/docs/klm/html/c3/sec3-1.htm):

(a) Automatic Picture Transmission (APT) Services

(b) High Resolution Picture Transmission (HRPT) Services

(c) Local Area Coverage (LAC) Services

(d) Global Area Coverage (GAC) Services

(a) Automatic Picture Transmission (APT) Services:

ATP services were initially developed to broadcast Direct Readout Satellite images to the receiving low cost satellite earth station (SES) equipments. APT data are acquired about 4 times per day, whenever the satellite is within the range of the antenna of any earth station. The station's latitude control the number of satellite overpass. A high latitude SES can receive more than 4 passes in 24 hours. Any two of the six AVHRR/3 channels can be command-selected for processing. It undergoes resolution reduction by using every third scan line of AHVRR data, geometric correction to reduce the perspective effect due to the Earth's curvature and the satellite altitude. The data also undergoes digital to analog conversion (http://www2.ncdc.noaa.gov/docs/klm/html/c3/sec3-1.htm).

Table 3.3: NOAA-AVHRR channels specifications and typical use

NOAA-16/17-AVHRR Channels		**Typical Use**
Channel	**Bandwidth (μm)**	
1	0.58-0.68 (Visible)	Daytime cloud, ice and snow, vegetation
2	0.73-1.10 (Near Infrared)	Daytime cloud, vegetation
3A	1.58-1.64 (Infrared)	Soil humidity, ice/snow distinguishing (operates only at daytime)
3B	3.55-3.93 (Near Infrared)	Heat source, night cloud (operates only at nighttime)
4	10.3-11.3 (Thermal Infrared)	SST, LST, day/night cloud
5	11.5-12.5 (Thermal Infrared)	SST, LST, day/night cloud

(b) High Resolution Picture Transmission (HRPT) Services:

The HRPT digital data include all the 5 transmitted channels of AVHRR data (out of the six channels in AVHRR/3, only five works at any time. At

nighttime, channel 3A is switched off). HRPT data are directly transmitted to the earth stations as soon as the satellite collects them. The HRPT data has a spatial resolution of 1.1 km. HRPT data sets received by Indian Institute of Technology Roorkee - Satellite Earth Station (IITR-SES) and other stations have been used extensively in this study.

(c) Local Area Coverage (LAC) Services:

The LAC data of 1.1 km spatial resolution are not transmitted at the time of acquisition. These data are collected in a recorder onboard and are transmitted to the special earth stations of NOAA during overpass.

(d) **Global Area Coverage (GAC) Services:**

GAC data has 4 km spatial resolution. It is derived on board the NOAA satellite by sub-sampling and averaging the nominal 1.1 km resolution AVHRR data. It provides daily global coverage, which is recorded on a satellite tape recorder and then transmitted to a ground station administered by NOAA authority. 115 minutes of these lower resolution scenes can be stored on an onboard recorder, which is enough for covering the whole orbit of data acquisition. GAC data can only be obtained from NOAA's National Environmental Satellite, Data and Information Service (NOAA-NESDIS) in GAC format (http://ceocat.ccrs.nrcan.gc.ca/client_acc/guides/avhrr/ch3.html). GAC data has been used in the present study for a few earthquakes.

The Indian Institute of Technology Roorkee - Satellite Earth Station (IITR-SES) is the only operational satellite earth station in any educational institute in India. IITR-SES [sponsored by Department of Science and Technology (DST), New Delhi] became fully operational on 24 October 2002. Feng Yun data acquisition facilities were added on 10 June 2004. This NOAA–HRPT & FY–CHRPT (Chinese High Resolution Picture Transmission) satellite earth station acquires AVHRR (Advanced Very High Resolution Radiometer) and MVISR (Multi-spectral Visible and Infrared Radiometer) data (almost 12-16 scenes per day) from NOAA and FY series of satellites. IITR-SES is a fully computerized and

automatic satellite data acquisition system and works day and night. It has external rotating parabolic 1.2 m diameter antenna. It has a vast coverage of >3000 km radius, which not only includes India but also many neighboring countries like Nepal, Bangladesh, Bhutan, Myanmar, Thailand, Laos, Sri Lanka, Oman, Parts of Saudi Arabia, UAE, Iran, Turkmenistan, Uzbekistan, Kazakhstan, Kyrgyzstan, Afghanistan, Pakistan, parts of Mongolia, China and Russia (http://drarunsaraf.tripod.com/iitr-ses.htm) (figure 3.2). The IITR-SES is also equipped with a fixed GPS receiver and provides its own location and GPS satellite based highly accurate timings at any instant of time (all GPS satellites have highly accurate atomic clocks within them).

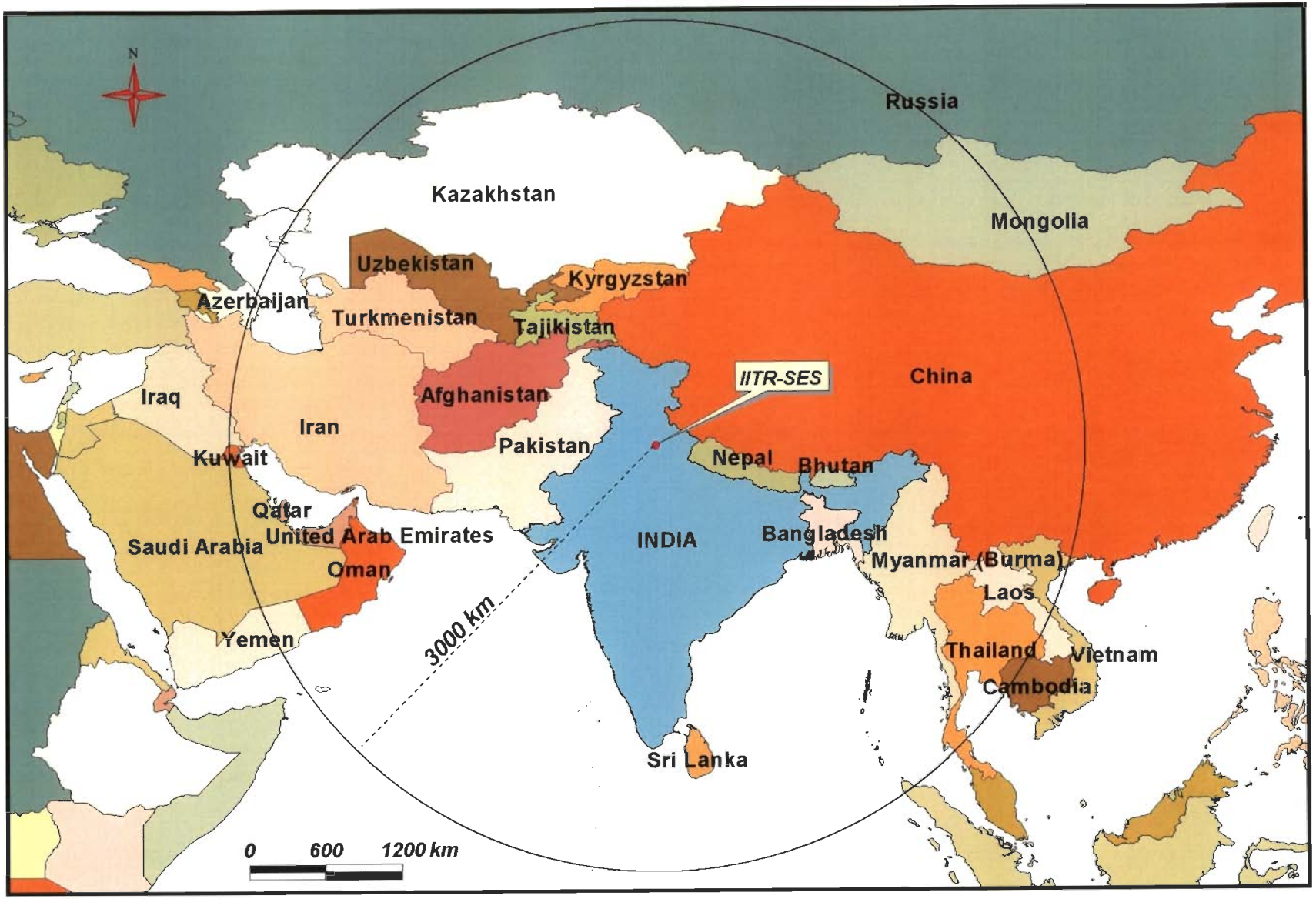

Figure 3.2: Coverage Area of Indian Institute of Technology Roorkee-Satellite Earth Station (IITR-SES). IITR-SES has been operating since October 2002, and acquring day and night data from NOAA and FY series of satellites for important tectonic locations in and around India, which has been used for the present study.

3.1.2 PREPARATION OF LAND SURFACE TEMPERATURE (LST) MAPS

NOAA-AVHRR data for around two months before the earthquake and one month after the earthquakes (depending on the availability of scenes with minimum or no cloud cover) were used to study the thermal conditions around the epicenter of the earthquakes. First a visual analysis of the thermal channels of the data was carried out and later detailed analysis of images showing appearance and disappearance of thermal anomaly was done. The digital data sets used were tried best to keep a consistency in the time of acquisition of all scenes.

For the preparation of time series LST maps, the data was treated uniformly. For the earthquakes in Bhuj, Iran and Sumatra, LST calculation had been done using the radiance value of channel 4 only. This calculation was done using HRPT Reader software and is based on algorithm given at http://perigee.ncdc.noaa.gov/docs/podug/html/c1/sec1-410.htm. A user specified range of temperature, which was consistent for all the scenes of a particular earthquake, was used. The temperature was calculated within a continuous colour range for point thermal data calculation of the image and the area outside this range was masked. Cloud covers were also delineated and avoided for any temperature calculation. For the Boumerdes earthquake in Algeria daily nighttime average NOAA-AVHRR data composites were obtained from German Aerospace Center (DLR), Koln, Germany (http://www.dlr.de/dlr). DLR maintains monthly, weekly and daily daytime and nighttime LST composites. Three daytime or nighttime NOAA-16-AVHRR images are averaged for a nighttime LST composite map. The generation of LST maps is based on the Becker and Li (1990) split window algorithm, which uses the differential absorption effects in channels 4 and 5 of NOAA-AVHRR for correcting atmospheric attenuation mainly caused by water vapour absorption. For estimating surface emissivity the relationship given by Van de Griend and Owe (1993) is applied. Thresholds of cloud detection scheme for nighttime LST synthesis maps are based on AVHRR channels 3, 4 and 5. The climate zone in the lower latitude is also taken into account. Any pixel identified as cloud are excluded from LST calculation and shown as white areas in all LST maps. The data are remapped into a stereographic projection with a

given resolution of 1.12 km at the centre. The nearest neighbour technique is applied to resample the pixels into the map.

3.1.3 SPATIAL SENSOR MICROWAVE IMAGER (SSM/I)

The DMSP is a United States' Department of Defense (DoD) program run by the Air Force Space and Missile Systems Center (SMC) (http://dmsp.ngdc.noaa.gov/dmsp.html). The DMSP system began with the launch of the first satellite on 16 September 1966. The principal instrument was the Operational Linescan System (OLS), which sensed in the visible and thermal infrared regions. Later, DMSPs also carried the Special Sensor Microwave Imager (SSM/I), vertically- and horizontally-polarized radiation at four frequencies, namely, 19.36, 22.23, and 85.5 GHz and measures the surface/atmospheric microwave brightness temperature of the earth's surface. SSM/I data used operationally are archived by the National Climatic Data Center and are available from the Satellite Data Services Division.

SSM/I is a seven-channeled radiometer. All frequencies, except the 22.235 GHz are of dual polarization (vertical and horizontal). These measurements have become available to various communities since 1987. The DMSP orbit is near circular, sun-synchronous, near polar, with an orbital altitude of 860 km and 1394 km wide swath. The orbital period is 102.4 minutes and provides complete coverage of the earth, except for two circular sectors of 2.4° centered on the North and South poles. The SSM/I data provided feasibility of study of earthquakes all over the world because of its global coverage and easy availability.

3.1.4 PREPARATION OF TEMPERATURE ANOMALY MAPS

SSM/I Image Products are available at National Climatic Data Center, for users, as both weekly and monthly values since 1988 to the latest available week, for 11 regions around the world. The temperature product is available as anomalies from the mean climatological values. Anomalies are derived from the 1988 - 2002 base period. For, weekly products, the first week always begins on 01 January,

regardless of the day (Sunday, Monday, etc.) the year begins. Composite maps of seven days of satellite observation are prepared as a weekly derivative. For monthly products, the average value of each week is independently derived. The spatial resolution is 30 km for all the products. This is a disadvantage in some remote sensing applications and reduces many atmospheric corrections.

The SSM/I data used to study the seven earthquakes (in India, Turkey, China, Afghanistan and Pakistan) was weekly average temperature anomaly data for the study region. The weekly anomaly was calculated with reference to 14 years mean climatological data. The temperature scale, therefore, actually represents thermal difference in degree Celsius with respect to the base period of 14 years. A value of +1 on the temperature scale will represent an increase of temperature of 1° C with respect to the base for that particular week on an average, i.e., the region was 1° C warmer in that year than the usual in all 14 years.

3.1.5 AIR TEMPERATURE DATA

Meteorological data (maximum and minimum temperature, rainfall, sunshine hours, humidity, cloudiness etc.) from ground meteorological stations located around the epicentral area were collected for the earthquakes in Bhuj (India), Zarand and Southeast Iran earthquakes.

The daily air temperature data were analyzed to see the trend of temperature change before and after the earthquake events.

For the Bhuj earthquake, daily temperature data collected by 16 meteorological stations (Deesa, Bhuj, Viramgarh, Ahmedabad, Dahod, Vasad, Baroda, V. V. Nagar, Surat, Bhavnagar, Rajkot, Junagarh, Porbandar, Dhari, Kasod and Veraval) of India Meteorological Department (IMD) in the state of Gujarat in India for the year 2001 (the year in which the earthquake occurred), was obtained. Apart from the daily data, weekly average temperature data for the past 30 years (1951-1980) was also obtained. Weekly average temperature graphs for the data available were constructed and the trend of change of

temperature for the year 2001 (in which the earthquake occurred) was analyzed. Further, the trend of temperature variations in the 30 years average data was also analyzed.

For the earthquakes in Iran, temperature data from 21 stations (Ardebil, Tabriz, Maragheh, Zanjan, Rasht, Ghazvin, Tehran-Mehrabad, Kermanshah, Semnan, Sharud, Esfahan, Mashhad, Sirjan, Shiraj, Kerman, Bam, Birjand, Iranshar, Chahbahar, Zahedan and Bandarabbas) located around the epicenters was obtained. The meteorological stations in Iran are maintained by Islamic Republic of Iran Meteorological Department (IRIMO). This data is made available by Russia's Weather Server, developed and maintained by Hydro-Meteorological Center of Russian Federation and Satellite Monitoring Technologies Department of Space Research Institute with the support from Russian Foundation for Basic Research (http://meteo.infospace.ru). Maximum and minimum air temperature data collected by 7 stations (Sirjan, Kerman, Bam, Birjand, Iranshar, Chahbahar and Zahedan) was obtained for 10 years (1996-2005) available in the site http://www.wunderground.com/global/Region/A2/Temperature.html. Normals were constructed by averaging the data for 9 years (1996-2004) (excluding the year 2005 in which the earthquakes occurred in calculation of the normals) and were compared with the temperature variations in the year 2005 for the 7 stations.

Air temperature data collected by meteorological stations differ from land surface temperature (LST) calculated from thermal satellite data in that the ground meteorological stations usually have temperature measuring instruments located in instrument shelters placed about 1.5 m above ground, whereas LST is actually the temperature of the land surface. The shelters in a meteorological station act as a protection of the instruments from exposure to direct sunrays, precipitation and condensation. Air temperature data is point data at each station, whereas LST is a spatial data with a continuous coverage at continental scale. A comparison has shown that the difference of LST and air temperature is within +/- 1° C.

Information on earthquakes (as regards to location of epicenter, focal depth, magnitude, time of event, casualty, faults and tectonism etc.) was obtained from reliable sources or refereed journals and articles. The United States Geological Survey (USGS) (http://www.usgs.gov/), National Earthquake Information Center (NEIC) (http://neic.usgs.gov/), Amateur Seismic Center (ASC) (http://www.asc-india.org/) etc. have catered information for the study. Geology, tectonic settings, climatological conditions of the regions where the earthquakes have occurred was also studied.

3.2 THE CONCEPT OF THERMAL ANOMALIES RELATED TO EARTHQUAKES

The identification of a correlation between short duration temporal thermal anomalies and earthquakes has been validated by the observation of the phenomenon prior to 12 past major earthquakes around the world [Saraf and Choudhury, 2003 (a) and (b); Saraf and Choudhury, 2004 (a) and (b); Saraf and Choudhury, 2005 (a) and (b); Saraf et al. 2005 (a) and (b)]. It has been observed in all these earthquakes there was a rise in the LST around the epicentral region before the earthquakes. These short-duration thermal anomalies went away along with the earthquake events.

It has been discovered that there are sites in the earth's crust near or around the epicenter of the impending earthquake, which most intensively change their characteristics with the processes preceding the earthquake, e.g., strain build up over an extended area. Such processes are known to be the cause of a number of observable effects, e.g., load uplift, changes in electrical properties of rocks, radon emission etc. These phenomena are known as *earthquake precursors*. Recognition of thermal anomalies associated with earthquakes can lead to the identification of areas of increased seismic risk.

Prior to an earthquake, crustal deformation is due to a stress field. It is a known fact that increases in pressure leads to an increase in temperature. Due to the acting stress field in tectonically active regions, sub-surface pressure increases with the consequent increase in temperature. Such deviation from

normal in the thermal regime can pose to be an interesting observation in earthquake studies. It is also known that increase of stress might lead to release of green house gases like CO_2, CH_4, N_2, etc., trapped in the pore spaces of the rocks, which escape to the lower atmosphere and create a localized green house effect and thus augment the LST of the region (figure 3.3).

The crust disrupts under stress field prior to an earthquake (Red Swelling Theory) and the existing gases in the crust such as CH_4 are emitted above the ground or water surface (Zu ji et al., 1999). Meanwhile, due to abrupt movement of underground electric water, electric particles transmit to the surface resulting in the mutation of the transient electric field. Gases like N_2, CO_2 obtain energy from the electric field, change energy grade and release heat, thus creating impending earthquake precursors. Such study on temperature increasing mechanism is called Gas-thermal Theory (Zu Ji et al., 1999). Thermal changes due to stress fields have also been determined in laboratory studies of materials (Brady and Rowell, 1986; Zu ji et al., 1997).

A new theory of charge generation in rocks prior to earthquakes is given by Friedmann Freund (Freund, 2002 and Freund, 2003). This theory keeps parity with laboratory experiments (Qiang, 1997, Ouzounov and Freund, 2004) and also supports other explanations of pre-earthquake thermal anomalies and other unusual geophysical phenomena as well.

Electronic charge carriers can be free electrons or sites of electron-deficiency in crystal structure, the latter known as p-holes. Crystallographically, rock-forming mineral-structures practically are three-dimensional array of oxygen; where it is tacitly assumed that oxygen always occur in O^{2-} oxidation state. Using different techniques (spectroscopically and using electrical conductivity, magnetic susceptibility, dielectric polarisation measurements etc.), presence of oxygen as O^- state in silicate and oxide minerals has been confirmed (Freund, 2002 and Freund, 2003).

An O^- is an anion or radical (also written as $O\cdot$) with an incomplete valence shell, 7 electrons instead of the usual 8. If the O^- is part of a XO_4^{4+}

polygon (usually tetrahedron) ($X=Si^{4+}$, Al^{3+}, etc.), it might be written either as XO_4^{3+} or as $O_3X/^{O\cdot}$. Being unstable radicals, O^- or $O\cdot$ and XO_4^{3+} or $O_3X/^{O\cdot}$ form pairs, generating a positive hole pair (PHP), chemically equivalent to a peroxy anion, $O^- + O^- = O_2^{2-}$ or a peroxy link as follows:

$$O_3X/^{O\cdot} + {}_{\cdot O}/XO_3 = O_3X/^{OO}\backslash XO_3$$

A PHP is devoid of any charge, as outer shells of both of the two O- atoms are filled. Such peroxy links can be thermodynamically stable, if they are associated with certain defect sites in the host crystal structure (Freund, 2002 and Freund, 2003). Introduction of PHPs in minerals during rock-genesis and alteration has been explained by Freund (2002).

Interestingly, O^-–O^- bond-distance (1.5Å) is almost half of O^{2-}–O^{2-} bond distance (2.8–3.0Å). It implies that the peroxy-bound O^- has a small partial molar volume, thus having a tendency to be favoured by high pressure. Being dissociated under high-accumulated stress a PHP introduces two holes (charge deficiencies) into the valence bond, causing the insulator to become a p-type semiconductor. Positive holes propagate though an oxide or silicate structure by electron hopping, whereby electrons from neighbouring O^{2-} can hop onto the O^- site. The estimated maximum speed at which a positive hole could propagate by hopping is in the order of 100–300 ms^{-1} (Freund, 2002). Since the positive holes travel via the O 2p-dominated valence bond, they can easily cross grain boundaries without being scattered or annihilated.

Laboratory experiments have proved the generation of heat and electric potentials on the surface of dry rock that is subjected to heavy stress (Ouzounov and Freund, 2004). Heat is especially generated along surfaces with maximum curvature, i.e., at the edges and corners. A thermal infrared camera can monitor the thermal emissions from the surface of the rock under stress. In rocks under high stress, PHPs dissociate into positively charged holes. In order to attain electrostatic stability, like any other movable charged particles, positive holes immediately rush towards the earth-surface with high speed as mentioned above (figure 3.4).

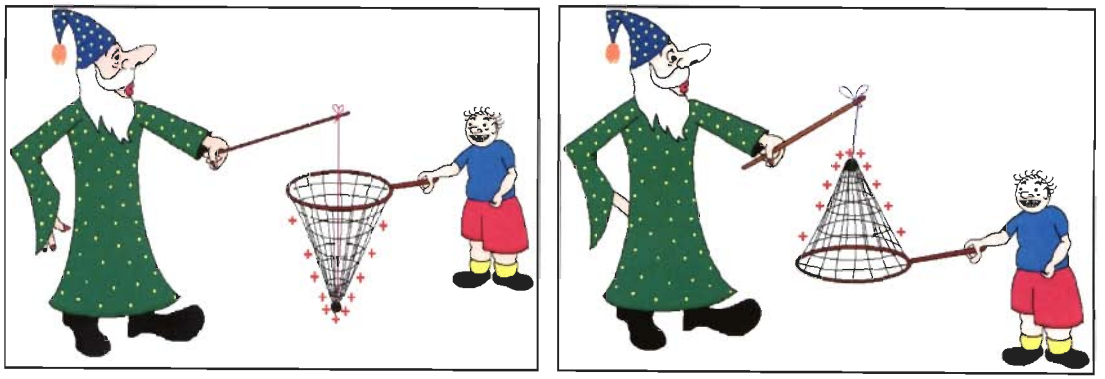

Figure 3.4: Concentration of positive charges (denoted by '+' sign) on the surface of butterfly net, especially at the apex (maximum positive curvature). If the net is inverted by pulling up the thread, charges have the tendency to move towards the new outer surface (Dasgupta, 2005).

Immediately after reaching a non-solid medium like atmosphere or water, a positive hole acquires an electron to become O^{2-} from O^{-}. The energy, therefore, emitted by this electron acquirement increases the surface temperature.

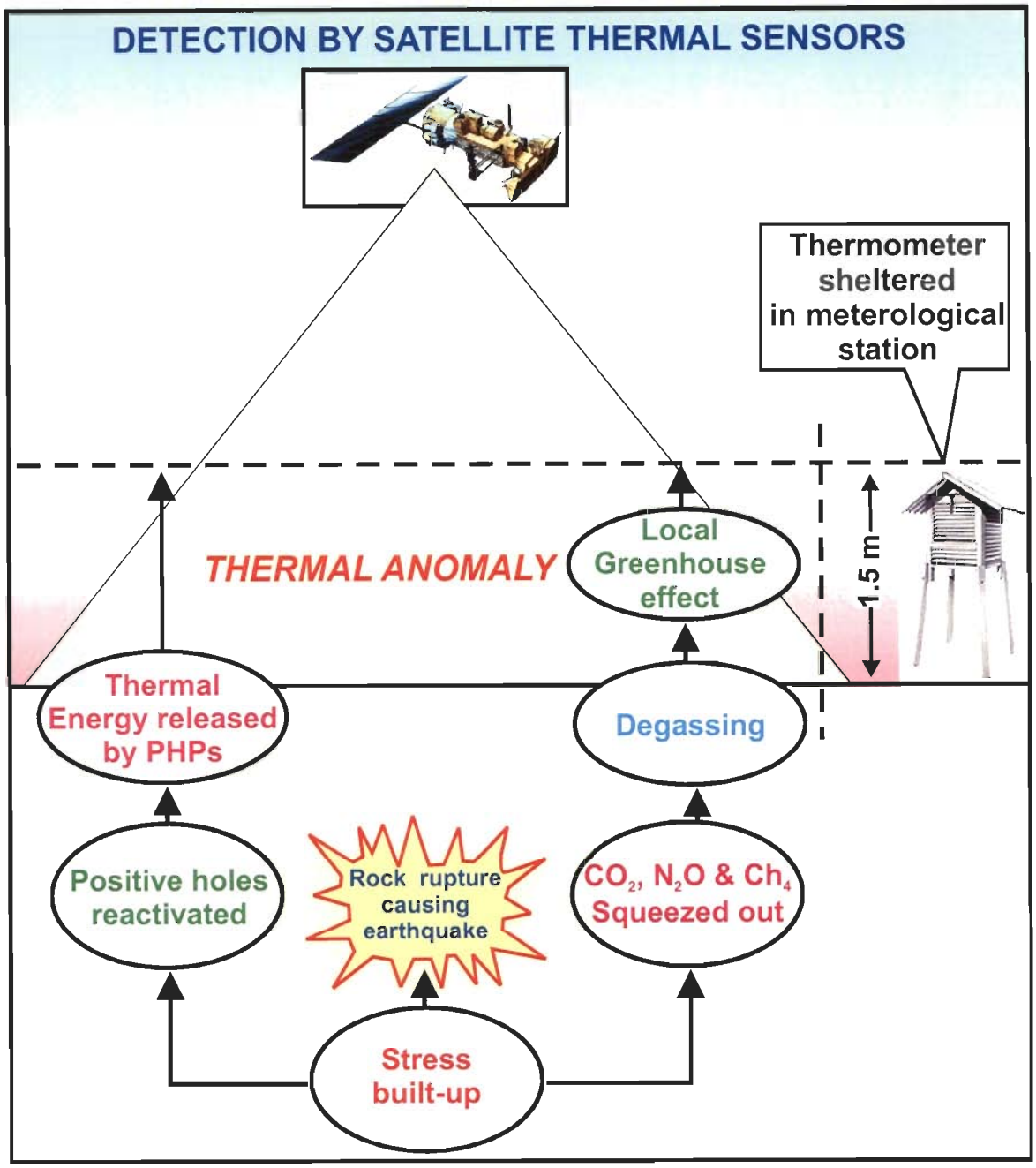

Figure 3.3: Schematic model showing the generation of pre-earthquake thermal anomaly and detection by thermal remote sensing & meteorological stations in the ground.

Before any earthquake event, stresses built up in rocks, which might bring near surface thermal anomalies and later a seismic activity. Satellite based thermal remote sensing exploits the thermal infrared part of the electromagnetic spectrum, which permits the monitoring of earth's thermal regime. Analysis of satellite data sensing the earth's emissivity for 12 past major earthquakes around the world have revealed the appearance of short-term thermal anomalies prior to the earthquakes. These anomalies came before the earthquakes and went away along with the earthquake events.

4.1 PRE-EARTHQUAKE THERMAL ANOMALY STUDY THROUGH NOAA-AVHRR DATA

The thermal channels 4 and 5 of NOAA-AVHRR have been successfully used to study the earthquake in Bhuj (India) on 26 January 2001, Boumerdes (Algeria) on 21 May 2003, Bam (Iran) on 26 December 2003, Zarand (Iran) on 22 February 2005 and also the great mega-thrust Banda-Aceh (Sumatra) on 26 December 2004 (table 1.1). All these earthquakes show definite built up of pre-earthquake thermal anomalies, which disappeared after the earthquakes. Air temperature data from meteorological stations (wherever available) were analyzed and the trend of variation of temperature was studied. Meteorological data conforms to the observations made through satellite data.

4.1.1 BHUJ EARTHQUAKE, INDIA

A powerful earthquake hit Bhuj in the state of Gujarat on 26 January 2001, with a USGS magnitude of 7.7, with its epicenter at 23.41° N latitude and 70.23° E longitude (figure 4.1) at 03:16 (UTC) [8:46 a.m. (IST)], while whole India was celebrating her 51st Republic Day. The death toll was estimated at 20,083 according to Gujarat Government figures and was accompanied by wide scale damage to property and economy of the state of Gujarat, India. Places like Bhuj,

Anjar, Bhachau and Rapar faced near total destruction and Gandhidham, Morvi, Rajkot and Jamnagar faced extensive damages to concrete structures (figure 4.1). Total of 7633 villages of 181 talukas of 11 districts were affected (Saraf et al., 2002).

The major affected region after the 26 January 2001 earthquake is seen to be located in and around major fault systems. The faults oriented around the epicenter of this earthquake are the Alla Bund Fault, the Katrol Hill Fault, the Kutch Mainland Fault, the Adhoi Fault, the Banni Fault and the Island Belt Fault embracing important places like Bhachau, Samakhiali, Rapar, Manfara, Chobari, Trambau, Vondh and Bhimasar (figure 4.2). These faults have history of periodic earth movements from time to time (Saraf et al., 2002). The earthquake of 26 January 2001 was the result of an east-west thrusting attributed by stresses due to the Indian plate pushing northward into the Eurasian plate. However, no surface rupture was observed after this earthquake.

4.1.1.1 ANALYSIS

NOAA-AVHRR data sets consisting of pre- and post-earthquake images (1 December 2000 - 15 February 2001) were studied. Detailed analysis of the data followed the first step of a visual analysis of thermal channels of three months. The digital datasets used were tried best to keep a consistency in the time of acquisition of all scenes used. Later, images significant for the analysis of thermal anomalies before the earthquake were delineated (table 4.1). Further, in order to obtain background thermal regime of the study area for comparison purposes, analysis of NOAA-AVHRR data sets of the year 2003 representing the same period (12 January 2003 to 29 January 2003) (table 4.2) were analyzed. This data was obtained from IITR-SES. The data of the year 2001 was acquired by the satellite NOAA-14. The data for the year 2003, used as a comparative study, is acquired by the satellite NOAA-16.

Table 4.1: Details of the NOAA-AVHRR data of the year 2001 used in the present study

S. No.	DATE	TIME (IST)
Scene 1	12.01.01	17:39
Scene 2	14.01.01	17:15
Scene 3	21.01.01	17:32
Scene 4	23.01.01	17:09
Scene 5	27.01.01	18:02
Scene 6	28.01.01	17:50
Scene 7	29.01.01	17:38

Table 4.2: Details of the NOAA-AVHRR data of the year 2003 used in the present study

S. No.	DATE	TIME (IST)
Scene 1	12.01.03	23:01
Scene 2	14.01.03	22:15
Scene 3	21.01.03	22:59
Scene 4	23.01.03	22:13
Scene 5	27.01.03	22:23
Scene 6	28.01.03	22:00
Scene 7	29.01.03	23:20

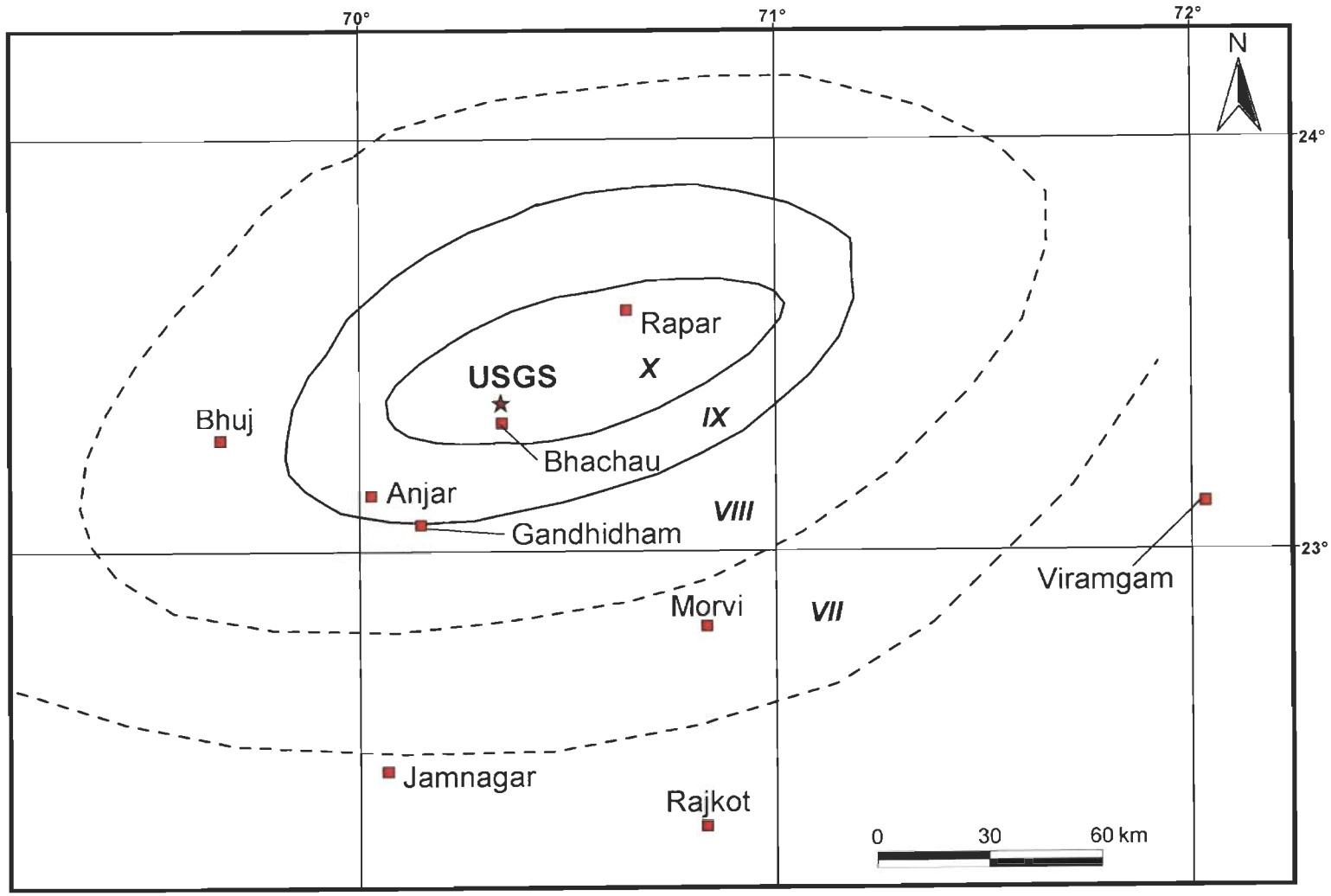

Figure 4.1: Isosiesmal map shows epicenter (USGS) and locations of some of the most earthquake-affected places after the devastating Bhuj Earthquake, India on 26 January 2001 (Saraf et al., 2001 and 2002).


CENTRAL LIBRARY
12109
14/10/05
I. I. T. ROORKEE

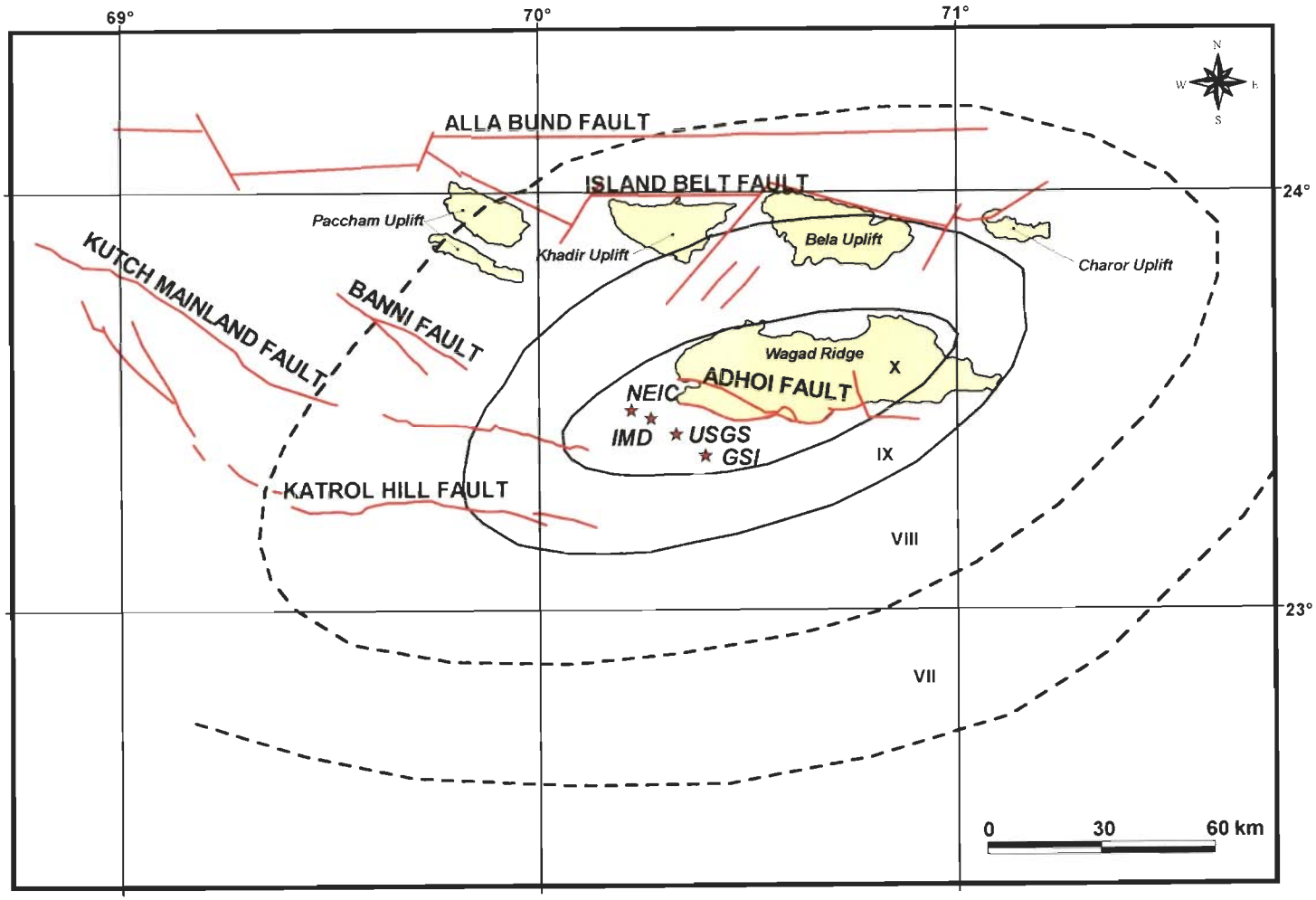

Figure 4.2: Isoseismal map (Sinvhal et al., 2001), major faults, uplifts and ridges (Peters et al., 2001) in and around the epicentre of the Bhuj Earthquake, India on 26 January 2001. Also shows epicentres from different organisations.

The AVHRR scenes were first checked against cloud cover. Calibration of data and calculation of temperature was done on raw data sets. LST calculation had been done using the radiance value of channel 4 only. This calculation is based on algorithm given at http://perigee.ncdc.noaa.gov/docs/podug/html/c1/sec1-410.htm. A user specified range of temperature between -40° C to 35° C was used. The temperature was calculated within a continuous colour range for every pixel thermal data calculation of the image. Cloud pixels were excluded from LST calculations.

Weekly average temperature data for a period from 1951 to 1980 (which was the only available past data) of the month of January were obtained from six IMD (India Meteorological Department) stations. Further weekly average temperature data collected by 14 IMD stations located around the epicenter (figure 4.3) in the state of Gujarat of the same month for the year 2001 were also obtained. The IMD station in Bhuj (the worst hit place by this earthquake) was totally destroyed and therefore could not collect data after 26 January 2001. The above two weekly average temperature data sets were analyzed and the trend of weekly variation of temperature for the period in which the earthquake occurred was obtained.

4.1.1.2 OBSERVATIONS

AVHRR data showed that on 14 January 2001, south-west Gujarat started to pick up an increase in temperature with respect to the surrounding region. Within a few days there was a spread and increase of the thermal anomaly and occupied an area of around 179,150 km^2. The area of this anomaly had spread in a NW-SE direction. On 23 January an intense anomaly was seen to develop with a temperature of about 31° C in the highly anomalous region (about 7° C higher than the normal temperature) covering an area of about 300 km^2, SE of the 26 January 2001 earthquake epicenter and about 28° C (about 5° C higher than usual) in the surrounding lesser anomalous region (figure 4.4). Succeeding this peak anomaly, the temperature started to decrease. On 28 January 2001, the anomaly disappeared and the region showed a normal temperature of around 24°

C. Analysis of thermal conditions using same dates satellite data from NOAA-AVHRR for the year 2003 (table 4.2) of the corresponding period (figure 4.5) showed that during that time in January 2003 the thermal regime of the study area was completely normal [Saraf and Choudhury 2003 (a) and 2005 (a)].

Using MODIS data, Ouzounov and Freund (2003), scientists in NASA have also reported a positive thermal change of around 4° C in the region before the Bhuj earthquake. They have observed that the temperature was definitely above normal before the earthquake and disappeared after the earthquake. However, the report presented MODIS data for only three days (6, 21 and 28 January 2001), and the closest date before the earthquake was of 21 January 2001. Whereas, analysis of continuous dates in the present study showed the maximum anomalous temperature on 23 January 2001 (5-7° C above normal). Experiments and observations in laboratory have also been performed and IR emissions under extreme crushing pressures in conditions that might prevail deep below the earth was done by NASA scientists.

Available weekly average air temperature data of past 30 years (between 1951-1980) clearly showed that in the third week, the temperature trend touches the lowest as compared to second and fourth weeks of the year (figure 4.6). The temperature trend of the year 2001 showed a peak in the third week (instead of the second or fourth weeks) (figure 4.7). This is in contrary to the observed trend for the past thirty years. This ground observation is in accord with the observed satellite thermal detection during January 2001.

4.1.2 BOUMERDES EARTHQUAKE, ALGERIA

On 21 May 2003, Algeria was hit by a powerful shallow focus (at 10 km) earthquake of magnitude M_w = 6.8 (http://neic.usgs.gov/neis/bulletin/03_EVENTS/eq_030521/) at 18:44 (UTC) (table 1.1), which led to the death of 2,276 lives, injured more than 11, 000 people and left 2,00,000 people homeless (http://www.reliefweb.int/w/rwb.nsf/6686f45896f15dbc852567ae00530132/b49cf0730dc7884149256d480021ee90?OpenDocument). The geographical location of

the epicenter was 36.90° N longitude and 3.71° E latitude (figure 4.8), just offshore from the province of Boumerdes, and about 60 km ENE of the capital city of Algiers.

The province of Boumerdes, including the coastal city of Boumerdes, Thenia, Rouiba and the eastern district of Algiers are among the heavily damaged regions by this earthquake (www.Reliefweb.int/w/rwb.Nsf/6686f45896f15dbc852567ae00530132/b342fd7d3ea5bb285256d4000671dce?OpenDocument). The earthquake has been named after the worst hit region 'Boumerdes' in Algeria. Notably large-scale concrete structure damage was witnessed in this 6.8 magnitude earthquake. Since Algeria's independence from France in 1962, the country has seen a rapid rise in urbanization. There was a growth in the building of concrete structures in the cities. The buildings heavily damaged, or which collapsed was built within the last decade, some just completed or in the process of completion. Widespread liquefaction, rock falls, landslides and ground cracks were reported in the earthquake-affected region. A tsunami generated with an estimated wave height of 2 m caused damage to boats and underwater telephonic cables off the Balearic Islands, Spain (http://neic.usgs.gov/neis/bulletin/03_EVENTS/eq_030521/).

This major earthquake was followed by a number of low intensity earthquakes (table 4.3), which continued till 29 May 2003. Minutes after the 6.8 magnitude earthquake played havoc in northern Algeria, a 5.7 M_w earthquake occurred at 18:51 (UTC) epicenter at 36.97° N latitude and 3.85° E longitude (http://neic.usgs.gov/neis/bulletin/03_EVENTS/eq_030527/neic_uhbj_m.html). Other aftershocks of magnitude greater than 5 (M_w) occurred on 22, 27 and 28 May 2003. More than 21 aftershocks (table 4.3) were reported within 9 days beginning from 21 May 2003, ranging in magnitude from 2.4 to 5.8 (M_w).

The North African country of Algeria is surrounded by the Mediterranean Sea to the north (about 1200 km of shoreline), by the countries Morocco and Western Sahara to the west, Tunisia and Libya to the east and Mauritania, Mali and Niger to the south. The development of the Mediterranean Alpine ranges in

the northern fringe of the African plate along with their Algerian section is the result of the rotation of the African continent with respect to the Eurasian continental plate. This rotation is a slow drifting of the continents towards one another (www.mem-algeria.org/hydrocarbons.htm).

Table 4.3: List and details of earthquake aftershocks after the 21 May 2003, 6.8 magnitude earthquake in Algeria

S. No.	Date	Magnitude (M_w)	Latitude (°N)	Longitude (°E)	Time (UTC)	Depth (km)
1	21.05.03	6.8	36.89	3.78	18:44	10
2	21.05.03	5.7	36.97	3.85	18:51	10
3	21.05.03	5.2	36.80	3.76	19:02	10
4	21.05.03	4.4	36.94	3.60	20:07	10
5	21.05.03	4.0	36.97	3.53	21:53	10
6	21.05.03	4.2	36.77	3.65	22:18	10
7	21.05.03	4.4	36.87	3.90	23:18	10
8	21.05.03	4.7	36.97	3.53	23:23	10
9	22.05.03	4.4	36.78	3.65	1:39	10
10	22.05.03	5.5	36.91	3.68	3:14	10
11	22.05.03	4.2	36.71	3.76	4:29	10
12	22.05.03	4.8	36.93	3.92	11:11	10
13	22.05.03	4.3	36.81	3.68	12:51	10
14	23.05.03	4.4	36.83	3.88	0:08	10
15	24.05.03	4.4	36.93	3.96	19:21	10
16	25.05.03	2.8	36.88	3.72	8:03	10
17	25.05.03	2.6	36.78	3.98	10:19	10
18	25.05.03	2.4	36.50	3.79	18:43	10
19	25.05.03	2.5	36.82	3.66	18:59	10
20	27.05.03	5.8	36.88	3.65	17:11	10
21	28.05.03	5.0	36.74	3.45	6:58	10
22	29.05.03	4.9	36.84	3.39	2:15	10

The African plate is moving northwest towards the Eurasian plate with a velocity of 6 mm per year. The relative plate motions create a compressional tectonic environment, which is manifested by a series of thrust-faulting and normal faulting (http://neic.usgs.gov/neis/eq_depot/2003/eq_030521/). The folded Paleozoic-Mesozoic sediments in the Atlas ranges extending from northern Tunisia through northern Algeria and Morocco are also an expression of this continent-continent convergence. This northern tectonic region of Africa therefore is seismically very active.

Examples of the manifestation of the compression due to the collision of the African-Eurasian plates are the east to west running South Atlas Fault (SAF) and the Middle Atlas Fault (MAF). The MAF runs parallel and lies to the north of the SAF. The overriding plate of both these thrust fault zones lie to the north (figures 4.9) (http://monitoring.llnl.gov/regionalization/tect_map.html). Both the SAF and the MAF are low angle thrusts and are parallel to the African-Eurasian plate margins, which sketch along the coastline of North Algeria. Relatively low focal depth of 10 km infers the origin of the earthquake on the SAF plane.

In the past, Algeria has experienced many destructive earthquakes. On 10 October, 1980, the city of El Asnam (now Ech-Cheliff) situated approximately 220 km to the west of the 21 May 2003 earthquake epicenter had been hit by a 7.1 magnitude earthquake that killed at least 5000 people. The same city as Orleansville was heavily damaged on 9 September 1954, by a 6.7 magnitude earthquake that killed over 1000 people. On 29 October 1989, a 5.9 magnitude earthquake struck about 110 km to the west of the 21 May 2003 earthquake epicenter and killed 30 people (http://neic.usgs.gov/neis/eq_depot/2003/eq_030521/). All these events have been located in the Tellian Atlas of Algeria where approximately all seismic zones of Algeria have been observed to be located (http://www.ictp.trieste.it/~attia/algeriaseis.htm).

4.1.2.1 ANALYSIS

Daily nighttime LST maps prepared from NOAA-16-AVHRR were analyzed for observing the thermal regime of Algeria before and after the 21 May 2003 earthquake. The channels 4 and 5 [based on Becker and Li (1990) 'split window' algorithm and Van de Griend and Owe (1993)] were used for the LST calculation (http://eoweb.dlr.de.8080/servlets/template/welcome/entryPage.vm). For estimating surface emissivity the relationship given by Van de Griend and Owe (1993) is applied. Channels 3, 4 and 5 were used for cloud detection and cloud masking (vide chapter 3, Section 3.1.2). The required region of interest was extracted from the nighttime composite maps. Nighttime LST maps from 13 – 30 May 2003, were used for studying the daily thermal scenario over Algeria (figure

4.10). Nighttime thermal data is advantageous in eliminating differential solar heating and partial sun illumination due to topographic effects and cloud shadow regions.

Structural features and tectonics of northern Algeria were studied to ascertain the relation between the structures of the region with the series of earthquakes in May 2003 in Algeria. Fault and thrust locations and trends of the region were delineated and their relation to the location of the focus and epicenter was observed. The cause of the earthquake on 21 May 2003 along with the aftershocks appears to be due to the tectonic conditions in northern Africa as was reported about the force behind many past major seismic events in Algeria.

4.1.2.2 OBSERVATIONS

Nighttime AVHRR derived LST composite maps of 13 May 2003 showed that a small area south of the epicenter of the Boumerdes earthquake developed a thermal anomaly as compared to the surrounding region (figure 4.10). This anomaly showed an intense rise on the night of 20 May 2003 covering in total an approximate area of 91,100 km^2. The temperature of the anomalous area was about 20-24° C, around 5-10° C higher than the surrounding area. The main shock struck Boumerdes province on 21 May 2003 at 18:44 (UTC). The anomaly decreased in intensity on the night of 21 May 2003. This less intense anomaly was perhaps a precursor to a 5.5 magnitude earthquake, which occurred on 22 May 2003. The anomaly disappeared on the night of 22 May 2003. Again since the night of 23 May 2003, a weak thermal anomaly appeared on the LST images and faded out with the low intensity aftershocks. Clouds, which covered the study area, hampered the study of the development of any anomaly for the 5.8 magnitude earthquake on 27 May 2003. A weak anomaly was again noticed on the night of 28 May 2003. An earthquake of magnitude 4.9 rocked Algeria on 29 May 2003 [Saraf and Choudhury 2003 (a), 2003 (b) and 2004 (a)].

The location of the thermal anomaly concur with the SAF (figure 4.9), which is a thrust running east to west in northern Algeria. The offshore location and shallow depth (10 km) of the epicenter indicates that the focus lies on the

thrust plane of the SAF. The coastline of northern Algeria along the Mediterranean Sea is the trace of a plate boundary, in which the African plate is subducted under the Eurasian plate. This compression leads to the creation of a series of thrusts and normal faults in northern Algeria. Therefore, the SAF, which is a part of such series of active structural features, may be regarded as the main cause of the 6.8 magnitude earthquake of 21 May 2003.

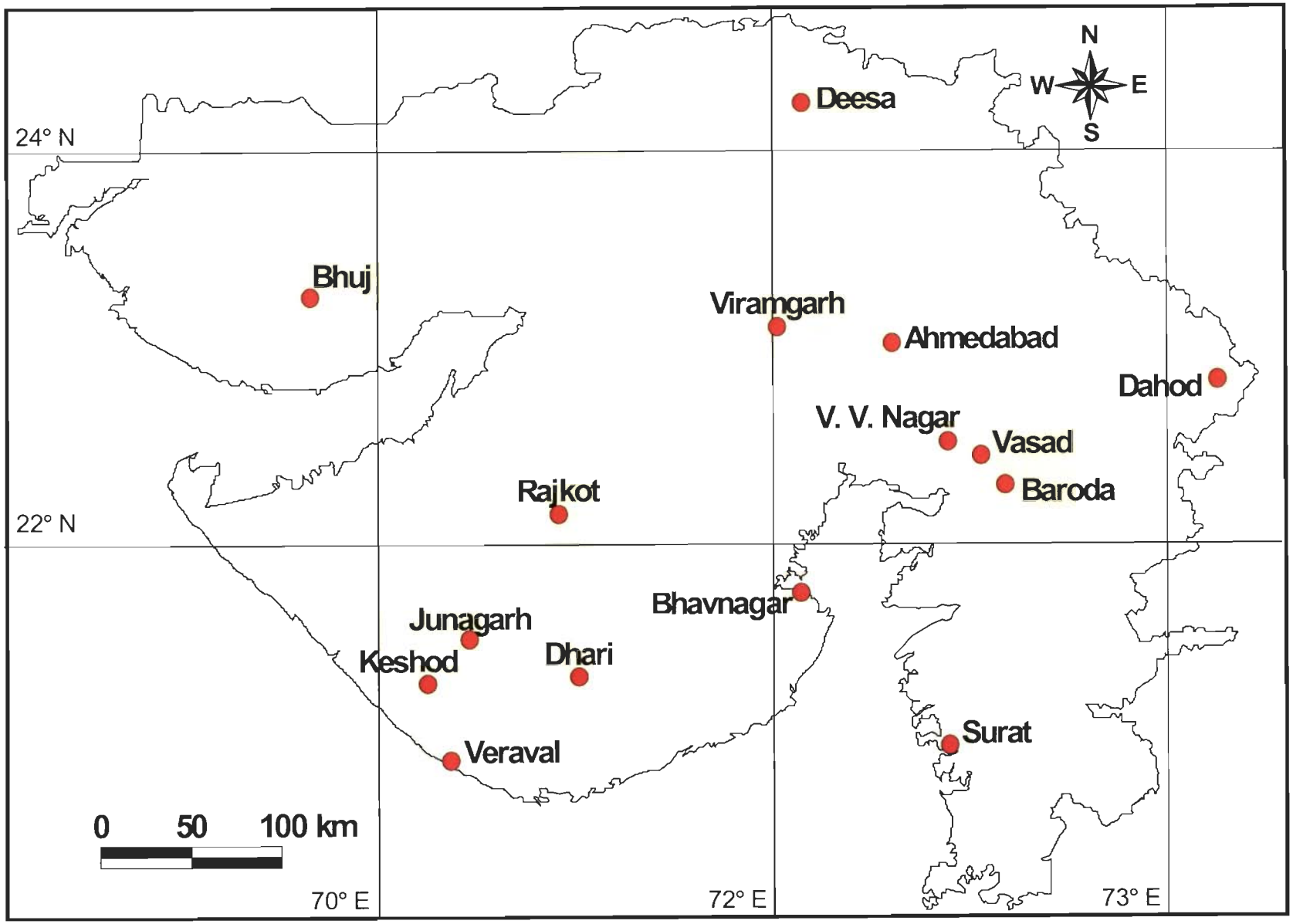

Figure 4.3: Location of the India Meteorological Department (IMD) stations in the state of Gujarat from which the air temperature data was collected for the year 2001.

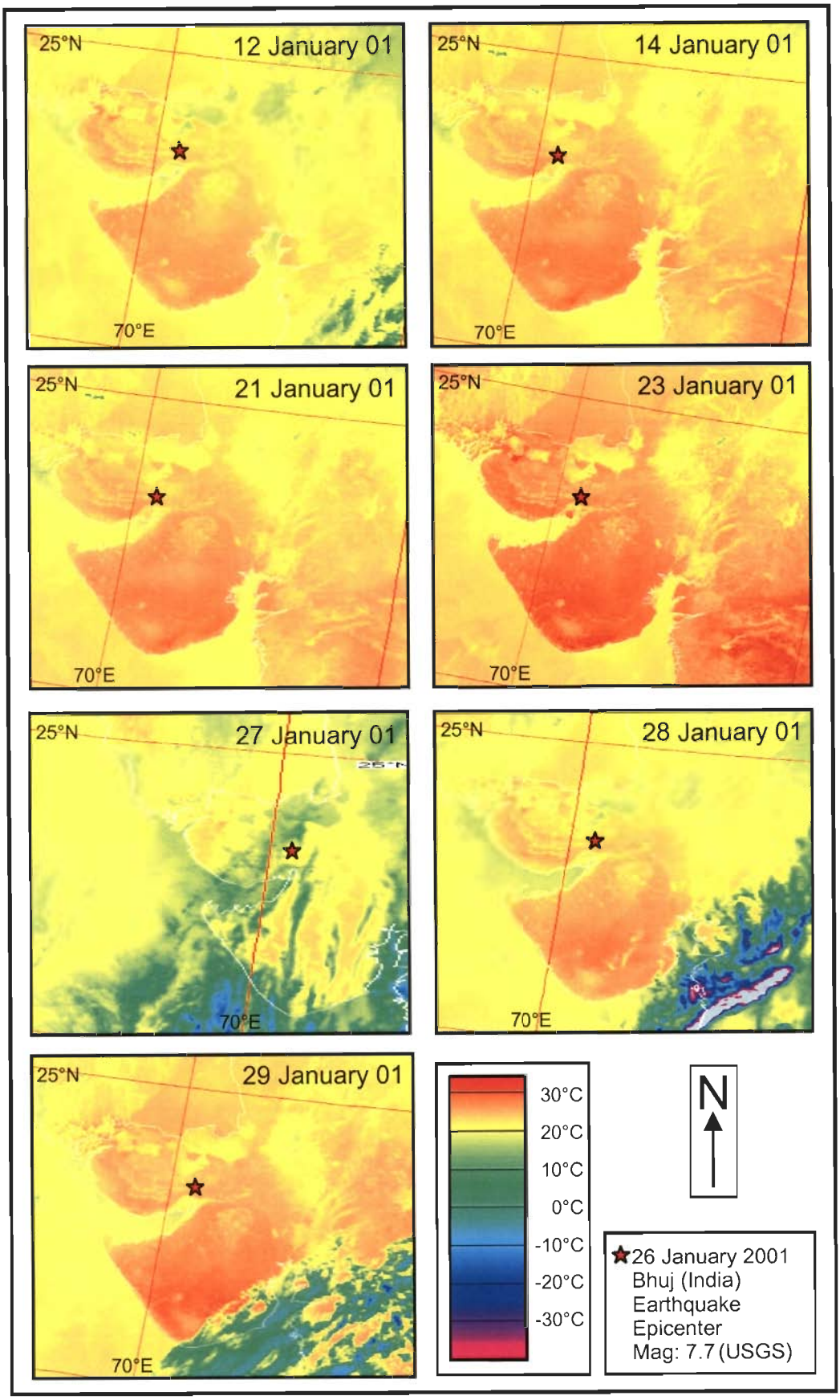

Figure 4.4: NOAA-AVHRR Land Surface Temperature (LST) time series maps before and after the Bhuj Earthquake. Temperature started rising from 14 January 2001, which escalated further to a maximum on 23 January 2001, three days before the earthquake. Post-earthquake images of 27 - 29 January 2001 show normal temperature.

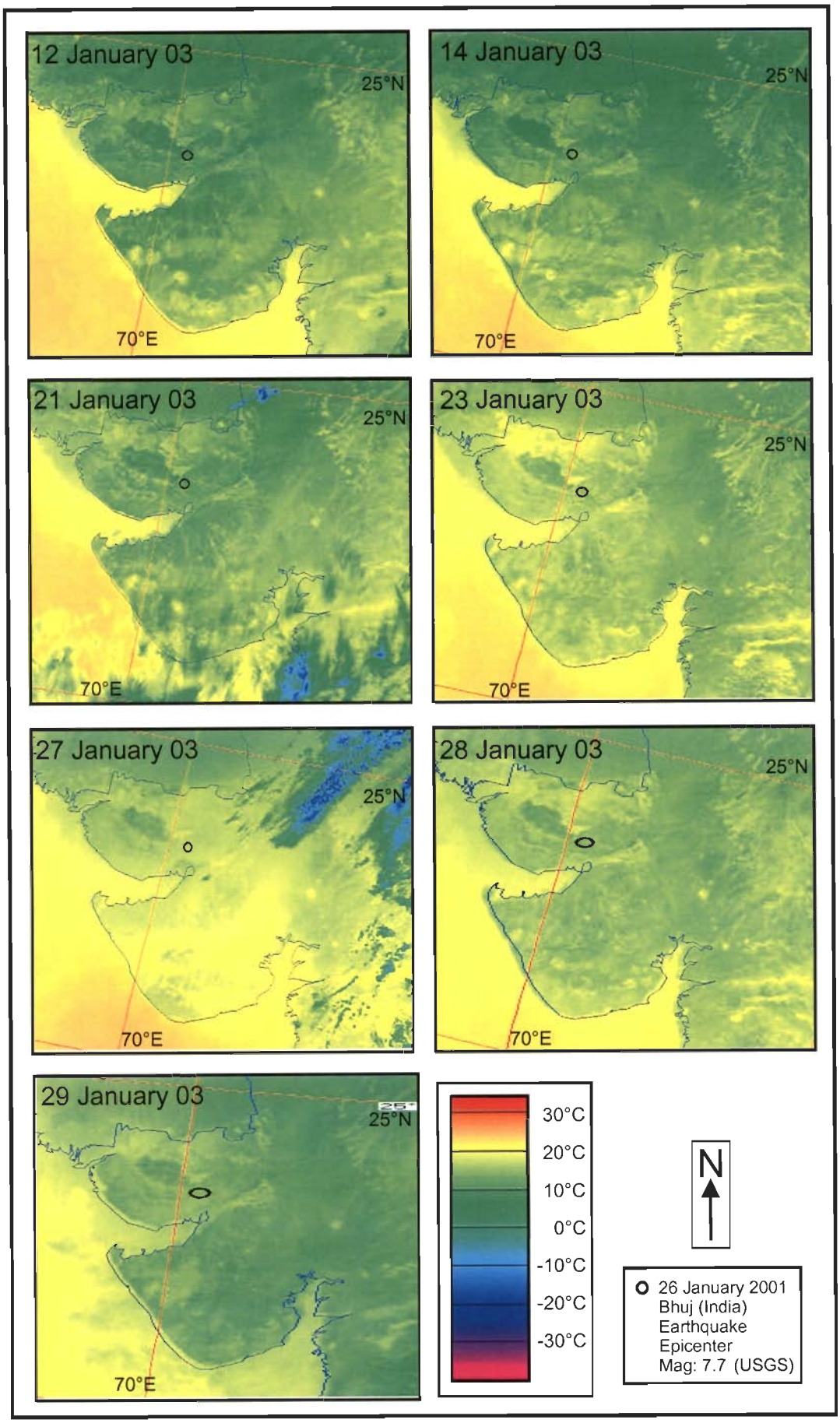

Figure 4.5: NOAA-AVHRR Land Surface Temperature (LST) time series maps January 2003, provides a comparison of the temperature scenario over the same dates in which anomalous rise of LST was observed before the earthquake of 26 January 2001. Scenes show almost unchanging temperature scenario over Gujarat in the month of January 2003.

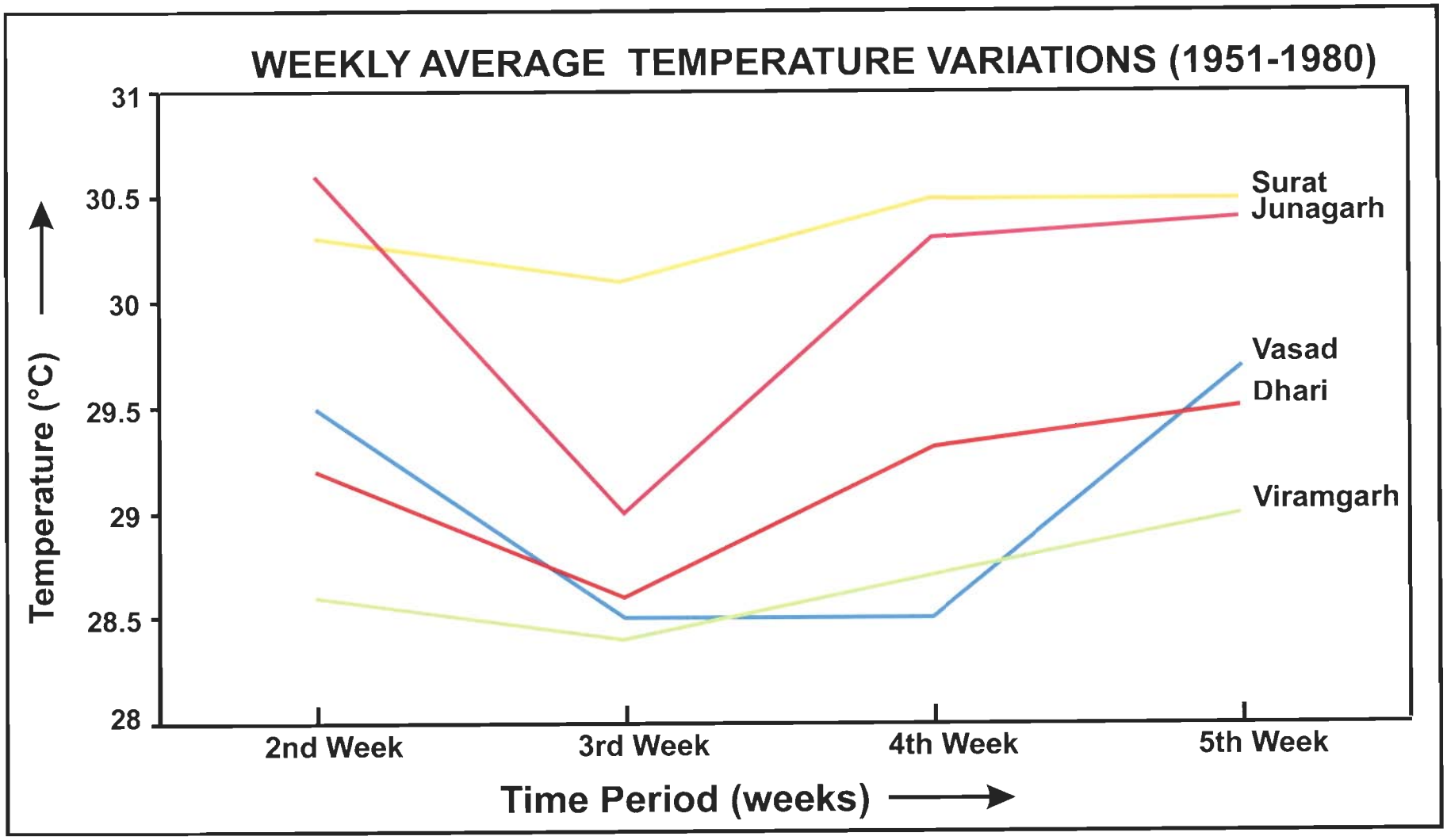

Figure 4.6: Weekly average air temperature variations in the second, third, fourth and fifth weeks (Julian weeks) over the years from 1951 to 1980 (data source: IMD, 1991).

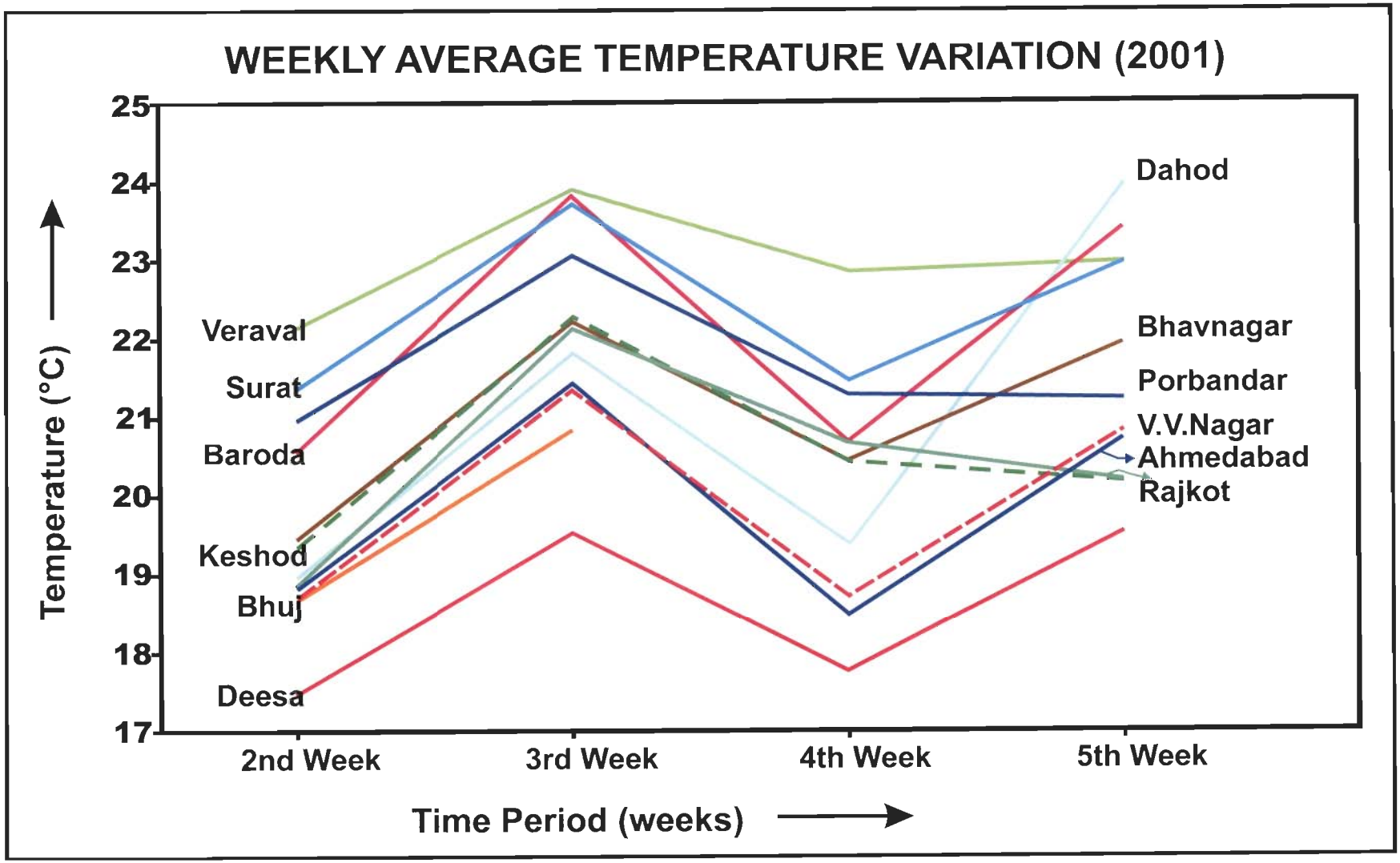

Figure 4.7: Weekly average air temperature variations in the second, third, fourth and fifth weeks (Julian weeks) of the year 2001.

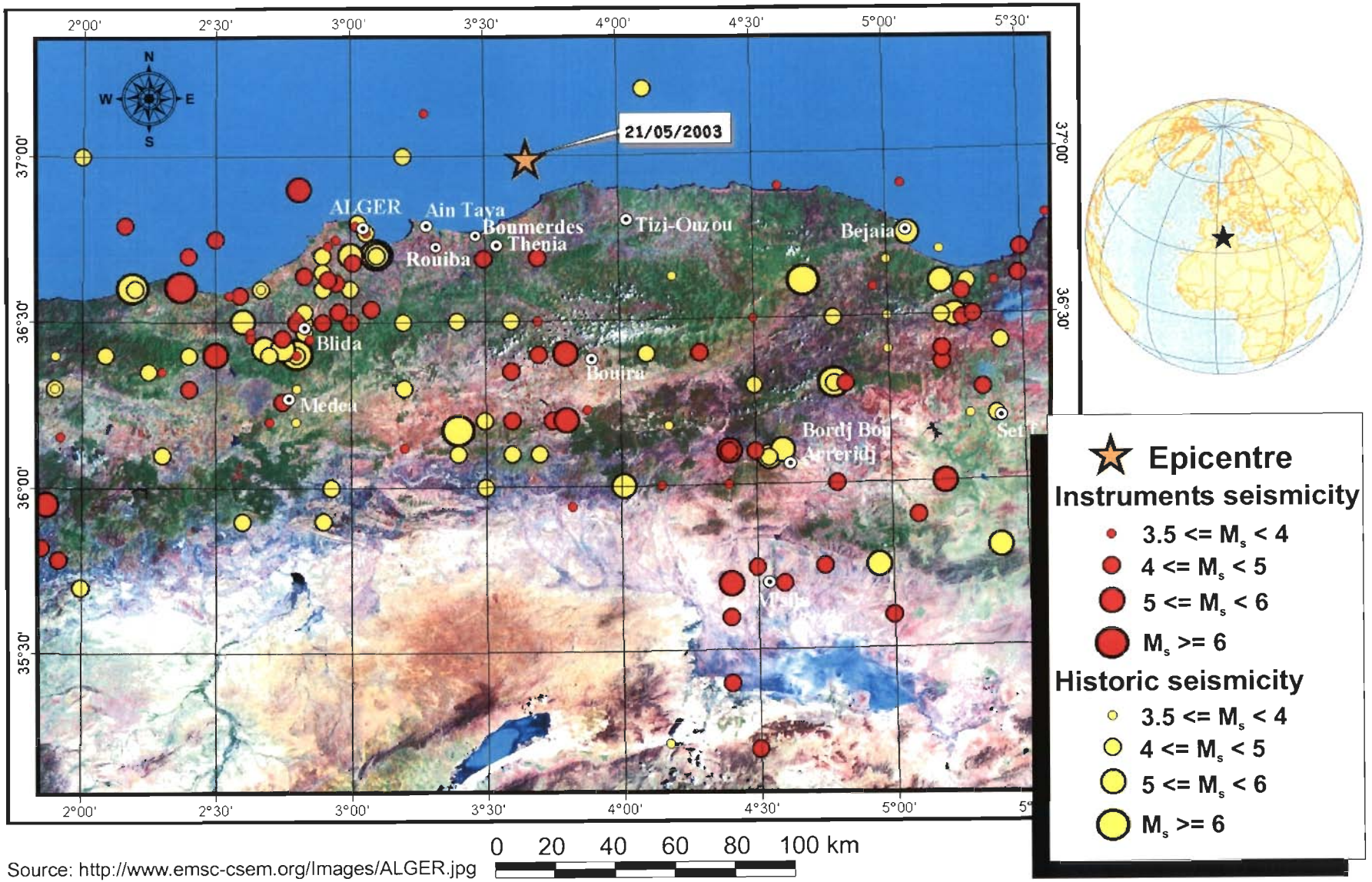

Source: http://www.emsc-csem.org/Images/ALGER.jpg

Figure 4.8: Location of Boumerdes earthquake in Algeria on 21 may 2003. Also shows locations of recorded seismicity and historic seismicity of the place.

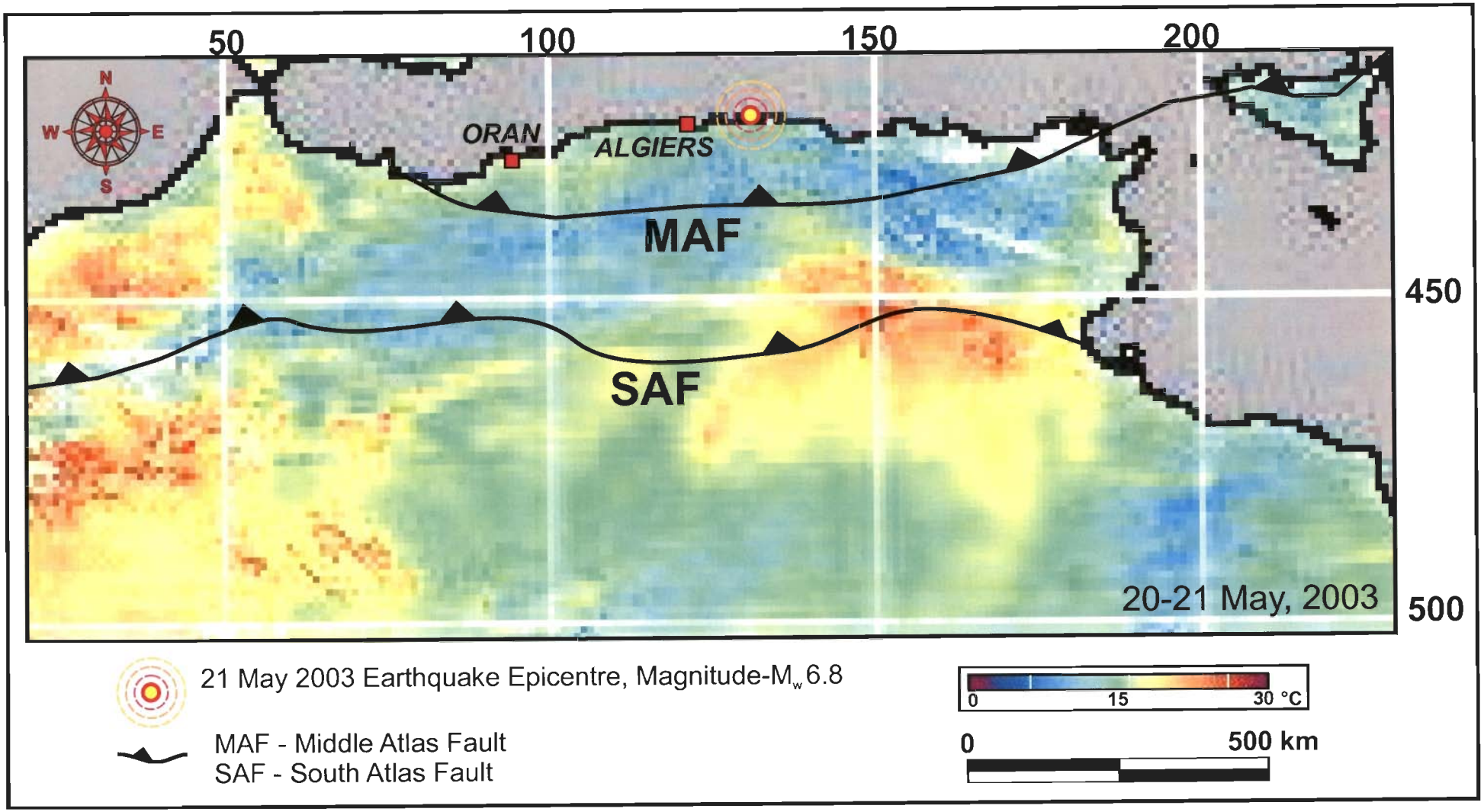

Figure 4.9: Location of 21 May 2003 Boumerdes earthquake epicentre and South Atlas Fault (SAF) and Middle Atlas Fault (MAF). The thermal anomaly appears to be just above the SAF fault (movement on which is reported to be the cause for the Boumerdes earthquake).

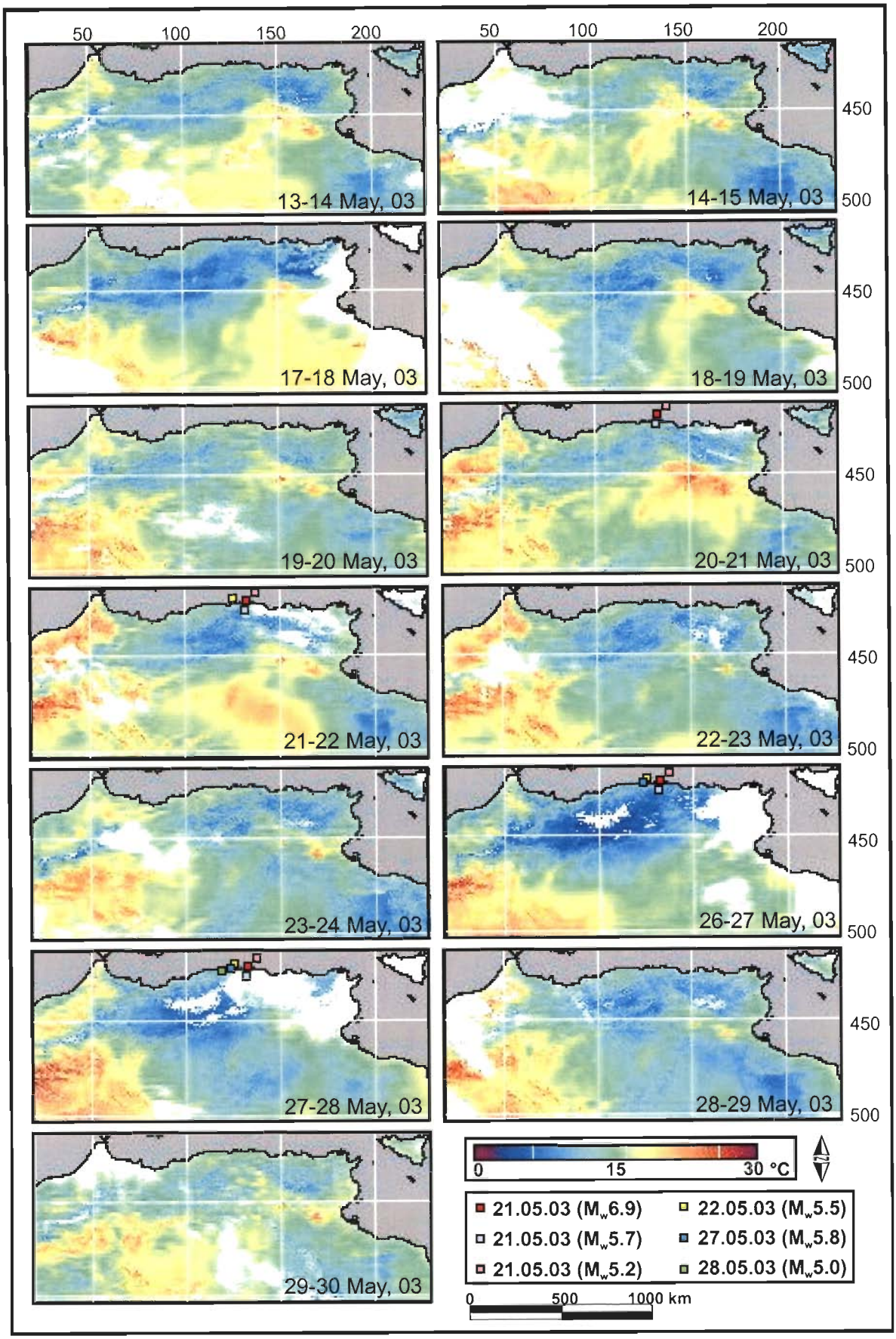

Figure 4.10: Time series nighttime Land Surface Temperature (LST) composite maps. The maximum thermal anomaly can be seen on 20-21 May 2003 night. Aftershock events occurred after the main shock is also marked and thermal anomaly associated with the aftershocks is observed. White areas show prevailing cloud conditions.

4.1.3 BAM, ZARAND, SOUTHEAST IRAN EARTHQUAKES

The Bam earthquake in Iran, of magnitude 6.6 (M_w), brought devastation over Southeast Iran on Boxing Day (26 December 2003), killing about 31,000 people, injuring 30,000, with around 75,600 homeless. Large-scale damage occurred to properties in the Bam area where an earthquake intensity of IX was felt (http://neic.usgs.gov/neis/eq_depot/2003/eq_031226/). The major damage was suffered by the historical mud-brick and clay citadel of Arg-e-Bam, which is more than 2000 year old. Numerous smaller aftershocks ranging in magnitude from 2 to 5 (M_s) continued in the Bam area till end of January 2004 (http://www.iiees.ac.ir/English/bank/Bam/Bam_report_english_aftershock.html). The location of the main shock was 29.00° N latitude and 58.34° E longitude (figure 4.11) in the Kerman province at a focal depth of 10 km.

In the year 2005, the months of February and March witnessed two major earthquakes of magnitude 6.4 (22 February 2005) in Central Iran and magnitude 6.0 (USGS, M_W) (13 March 2005) in Southeast Iran (http://earthquake.usgs.gov/eqinthenews/2005/usuvae/). The 22 February Zarand Earthquake caused the death of at least 627 people, injured more than 2000 and affected more than 20 villages. Two villages, namely, Daghuye and Gethukiye were totally destroyed (http://www.reliefweb.int/rw/rwb.nsf/db900SID/RMOI-6AQ9UK?OpenDocument). The epicentre was situated near Zarand in the province of Kerman (table 4.4) (figure 4.12), about 250 km northwest of Bam earthquake (http://neic.usgs.gov/neis/poster/2005/20050222.html). There were no confirmed reports of casualties in the 13 March 2005 earthquake of magnitude 6.0 in southeast of Iran near the Pakistan border (http://abcnews.go.com/International/wireStory?id=576069).

The Arabian Plate, which includes Saudi Arabia, Persian Gulf and the Zagros Ranges in Iran, converges towards the Eurasian Plate at a rate of approximately 3 cm / yr (http://neic.usgs.gov/neis/bulletin/neic_uvae_ts.html), a zone of deformation that generates both reverse and strike-slip faults in the region and thus causing earthquakes in entire Iran (http://neic.usgs.gov/neis/eq_depot/2003/eq_031226/neic_cvad_ts.html). The

Bam Earthquake of 26 December 2003 earthquake has been reported to be generated by right-lateral strike-slip motion on the North-South trending Bam fault. Around the location of the epicenter, several active faults have been mapped. The Gowk fault is oriented along the west of the Bam fault in a similar North-South trend (figure 4.13). Reverse strike-slip motion on this fault had generated the 11 June 1981 earthquake of magnitude 7.3 and the 28 July 1981 earthquake of magnitude 7.3. The Bam fault passes from the vicinity of the city of Bam and between the cities of Bam and Baravat in the province of Kerman.

The interior parts of Iran at the North of Zagros Thrust Zone (ZTZ) are included in Eurasian Plate as the Persian micro-plate. The ZTZ constitutes the boundary between the two colliding plates. Complex folding and fault movements (figure 4.13) in the Zagros Ranges are resulted due to the mechanical deformation by the collision of the two plates. As a result, earthquakes in Iran occur mainly in Zagros Ranges. A number of sub-parallel faults are also present to the North of the Zagros. However, in the interior parts of Iran in the North of the Zagros Ranges and in the South of the Alborz Ranges, deformation is mainly due to strike slip movements along complexly arranged intersecting faults (http://freethoughts.org/archives/000389.php). The 22 February Zarand Earthquake was caused by reverse slip on an East-North-East or East-striking fault (http://neic.usgs.gov/neis/bulletin/neic_uvae_ts.html).

4.1.3.1 ANALYSIS

Day and nighttime NOAA-AVHRR data acquired by the IITR-SES was used (table 4.4) to study the thermal scenario before and after the Bam earthquake in Iran on 26 December 2003. Time series maps were prepared for day and night scenes. Thermal channel 4 was used to calculate the LST of the study area. The LST calculation is based on the method provided in http://perigee.ncdc.noaa.gov/docs/klm/html/c7/sec7-1.htm#sec71-2. For the daytime scenes a user specified temperature range –30°C to 35°C was used. For the nighttime data, a user range of –70°C to 20°C was used for the data acquired around 03:00-04:00 IST hours. Temperature outside this range was masked. Cloud covers were delineated and avoided for any temperature calculation. For

the data acquired around 20:00-23:45 IST hours, the temperature range was fixed at –30°C to 20°C. On 19 and 20 December 2003, nighttime (03:00-04:00 hours) coverage of Iran was not available. Nighttime data acquired at 20:00-23:45 hours (with a difference of around 4 hours) on 18 and 19 December 2003 was analyzed for the two days. The NOAA-AVHRR data for 18 December doesn't actually substitute for the pre-dawn scene, but was used not to have a gap of more than 24 hours. Further, nighttime AVHRR data (table 4.5) for the year 2004, around the period when the earthquake occurred a year earlier was analyzed to compare the thermal scenario.

Table 4.4: Details of nighttime and daytime NOAA-AVHRR data [acquired by IITR-SES, Indian Standard Time (IST)] of the year 2003 used to prepare LST time series maps to study pre-earthquake thermal anomaly before the Bam Earthquake in Iran

S. N.	Date	Time of Acquisition (IST)		
		Nighttime		Daytime
		03:00-04:30 hours	22:00-23:45 hours	14:30-15:30 hours
1	18 December 2003	03:10	23:30	-
2	19 December 2003	-	23:06	-
3	20 December 2003	-	22:43	-
4	21 December 2003	04:20	-	-
5	22 December 2003	04:08	-	15:29
6	23 December 2003	03:55	-	15:16
7	24 December 2003	03:44	-	14:53
8	25 December 2003	03:32	-	14:41
9	26 December 2003	03:20	-	-
10	27 December 2003	03:09	-	-

Daytime NOAA-AVHRR Global Area Coverage (GAC) data [vide chapter 3, Section 3.1.1] with a consistency in the time of acquisition, from 10 February to 31 March 2005 (table 4.6), were analysed to observe the thermal regime of Iran before and after the major Zarand earthquake on 22 February 2005. A similar processing as was done with the HRPT data for the Bam earthquake was done on the GAC data. A user specified temperature range of temperature between –

50°C to 40°C was used. Due to occasional climatic disturbances (cloudy days) in Iran before the second large earthquake (i.e., the earthquake of magnitude 6.0 M_w on 13 March 2005, table 4.7), AVHRR data could not be exploited to detect any pre-earthquake thermal anomaly.

Table 4.5: Time of acquisition of nighttime NOAA-AVHRR data of the year 2004 used to compare the LST scenario around the same time as the Bam earthquake on 26 December 2003 (a year ago)

S. N.	Date	Time of Acquisition (IST) 22:30-23:30 hours
1	18 December 2004	23:09
2	19 December 2004	22:45
3	21 December 2004	23:42
4	22 December 2004	23:18
5	23 December 2004	22:54

Table 4.6: Time of acquisition of daytime NOAA-AVHRR GAC data for the year 2005 used to study the thermal scenario over Iran before the Zarand earthquake on 22 February 2005

S. N.	Date	Time of GAC Acquisition (UTC)
1	15 February 2005	06:48 to 08:34
2	16 February 2005	06:28 to 08:12
3	19 February 2005	06:57 to 08:43
4	20 February 2005	06:42 to 08:20
5	21 February 2005	06:12 to 07:57
6	22 February 2005	05:49 to 07:34
7	23 February 2005	07:06 to 08:52

Air temperature data of the year 2005 in the months of February and March, collected by 21 meteorological stations (Ardebil, Tabriz, Maragheh, Zanjan, Rasht, Ghazvin, Tehran-Mehrabad, Kermanshah, Semnan, Sharud, Esfahan, Mashhad, Sirjan, Shiraj, Kerman, Bam, Birjand, Iranshar, Chahbahar, Zahedan and Bandarabbas) across Iran, located across Iran (figure 4.14) was also analysed for all the earthquakes in 2005 mentioned in table 4.7. Thermal Variation Curves (TVC) were constructed from the data to analyze the air temperature trend for the earthquakes in 2005. Further, air temperature maximum and minimum were collected for 10 years (1996-2005) from 7

meteorological stations (Sirjan, Kerman, Bam, Birjand, Iranshar, Chahbahar and Zahedan) around the epicentre of the Zarand earthquake of 22 February 2005. Temperature normals were constructed by averaging the data for 9 years (1996-2004, the only available data for the past years) and TVCs were constructed for the stations. For the year 2005, TVCs were also constructed for the 7 stations. The 2005 TVCs were compared with the 9 years normals (as base period) to see the thermal anomalies with respect to the base before the 2005 earthquakes.

4.1.3.2 OBSERVATIONS

Both nighttime and daytime NOAA-AVHRR time series LST maps for the earthquake in Bam showed that there was definitely a thermal anomaly, which appeared before the devastating earthquake of 26 December 2003 [figures 4.15 (a), (b) and 4.16]. The temperature increase was about 5 - 7° C than the usual temperature of the region. At some places, the temperature was about 6 - 10° C higher than normal.

In the nighttime maps, it was seen that on 18 December 2003 there was a complete normal temperature regime in the region. The appearance of an intense thermal anomaly was seen around the earthquake epicenter near Bam on 21 December 2003 [figure 4.15 (a)] (data was not available on 19 and 20 December 2003 for the same time of acquisition, vide 4.1.3.1). If this rise had started earlier and then reached its peak on 21 December, it could not be ascertained through the gap in the data. To bring continuity to this gap, data acquired on 18 and 19 December 2003 night (table 4.4) at 22:00-23:45 IST hours (comparable to 19 and 20 December 2003), with a difference of four hours, was analyzed [figure 4.15 (b)]. A thermally anomalous region had developed near the epicenter on 19 December 2003, which rose to the maximum amplitude of thermal anomaly on 21 December 2003 [figure 4.15 (a)]. The normal temperature observed on 18 December 2003 was around –0.5-5° C. The temperature was around 7-13° C on 21 December 2003 (around 7-8° C higher than normal). On 22 December, the temperature was less than this boost. The temperature was normal again on 23 December. The earthquake came on 26 December, five days after this boost in LST.

Table 4.7: List and details of the earthquakes in Iran from 22 February to 2 April 2005 (http://neic.usgs.gov/neis/bulletin/bulletin.html and http://www.emsc-csem.org)

Date	Time (UTC)	Magnitude	Latitude (°N)	Longitude (°E)	Depth (km)
22 Feb 05	**02:25:22**	**6.4**	**30.74**	**56.901**	**14**
22 Feb 05	05:08:31	4.3	30.87	57.06	10
22 Feb 05	05:26:47	4.6	30.46	57.10	10
24 Feb 05	23:26:41	4.3	31.46	56.69	35
26 Feb 05	20:20:15	4.3	31.92	56.64	10
27 Feb 05	01:34:18	4.0	32.46	49.31	10
27 Feb 05	12:56:45	3.8	30.30	57.27	10
27 Feb 05	13:20:44	3.9	30.66	57.03	10
28 Feb 05	03:48:36	3.8	30.73	56.76	44
01 Mar 05	10:47:49	3.9	27.08	54.69	25
01 Mar 05	16:13:52	4.2	30.80	56.96	56
03 Mar 05	00:50:04	4.6	30.77	56.97	10
03 Mar 05	16:52:58	4.7	27.18	56.14	35
06 Mar 05	09:02:53	4.1	30.77	56.85	10
08 Mar 05*	19:07:57	4.6	27.63	54.48	58
13 Mar 05	**03:31:23**	**6.0**	**27.15**	**61.88**	**55**
14 Mar 05	12:32:15	3.7	37.91	44.20	26
19 Mar 05	01:29:55	3.8	30.60	56.71	10
22 Mar 05	17:27:34	4.4	27.86	52.74	45
25 Mar 05	12:48:56	4.5	34.89	50.03	17
25 Mar 05*	16:06:03	4.1	32.68	49.81	81
27 Mar 05*	02:54:33	3.2	38.08	47.91	4
27 Mar 05*	09:53:11	3.7	31.94	52.07	22
27 Mar 05*	15:09:11	3.0	31.99	50.04	10
28 Mar 05*	15:33:22	3.5	33.41	57.16	10
01 Apr 05*	04:58:33	3.1	30.66	56.59	10
01 Apr 05*	20:03:25	3.7	34.11	45.60	4
02 Apr 05*	19:09:25	3.3	27.55	53.82	10
02 Apr 05*	22:24:52	4.1	31.13	56.55	14

* European-Mediterranean Seismological Centre (EMSC)

A peculiar cloud pattern was also observed on 21 December 2003. The cloud appeared to originate from the epicenter itself (figure 4.17 (a). Post-earthquake linear cloud was also observed on 27 December 2003 through daytime data (figure 4.17 (b). The appearance of peculiar clouds was observed

on 21 December 2003. The cloud appeared to originate from the epicenter itself (figure 4.17 (a).

Daytime LST time series maps show that the rise in temperature started on 22 December 2003. The anomaly stayed on till 24 December 2003 (just two days before the earthquake) (figure 4.16). The normal temperature was around 22-25° C on 21 December 2003. On 24 December 2003, the temperature was around 29-32° C (about 7-10° C higher than usual).

Analysis and similar processing of nighttime 2004 NOAA-AVHRR data (table 4.5) acquired at around the same time and on the same days as the 2003 data, showed that there was no such abnormal behavior of the LST on those days in that year (figure 4.18).

The anomalous region in the nighttime data on 21 December 2003 occupied an area of 308,034 km^2 (figure 4.15) and in the daytime LST map of 24 December covered an area of 328,287 km^2 (figure 4.16). The area of the province of Kerman is 181,714 km^2.

In case of 22 February 2005 Zarand Earthquake, daytime NOAA-AVHRR LST time series maps (figure 4.19) show a build up of positive thermal anomaly near the epicentral region. The anomaly spread over an area of about 75 km diameter on 16 February 2005. This anomaly gradually increased till 21 February 2005. On 21 February 2005, the temperature was the highest (about 10°-12°C higher than the usual temperature observed in the region), with a large patch of intense anomalous region covering an area of about 75,600 km^2. The earthquake of magnitude 6.4 (Mw) occurred on 22 February 2005 at 02:25:22 UTC. Unfortunately, clouds covered the epicentral region, hindering observation of the change in the thermal anomaly on the day the earthquake occurred. On 23 February 2005, one day after the main earthquake event, the temperature was normal.

Series of tremors continued around the epicenter of the main shock (figure 4.12) in Iran as aftershocks following the main shock of 22 February 2005. The

continuous cloud cover over the entire region hindered further study of the thermal scenario of Iran through satellite data for any change brought by the aftershocks. The earthquake in Southeast Iran also could not be studied using satellite data due to continuous cloud cover. This earthquake, however, also showed abnormal thermal conditions in the TVC [Saraf et al., 2005 (e)].

A close observation of the TVC produced from the air temperature data for the earthquakes in 2005 show that before the two main earthquakes or cluster of aftershocks there are distinct spikes in the TVC. The spikes appeared about 1-5 days before the earthquake or a cluster of smaller quakes (Dasgupta, 2005). The occurrence of an earthquake after an anomalous spike and the amplitude of the spike depend upon the distances of the meteorological stations from the epicenter. The temperatures decreased after the event [figures 4.20 (a), (b), (c), (d), (e), (f), (g), (h), (I), (j), (k), (l), (m), (n) and (o)].

However, the TVC of Bandarabbas did not show any significant trend of thermal spike is probably as that Bandarabbas is a coastal city. The location of the city allows heat-exchange with the neighbouring Gulf of Oman and Persian Gulf through wind and water. Interestingly, Bandarabbas is the second nearest meteorological station from the epicentre of Zarand earthquake (figure 4.14).

Upon comparing TVCs of 7 stations constructed for the year 2005 for the days beginning from 15 February to 31 March 2005 with air temperature normals for 9 years (1996-2004), it was observed that there was a completely normal trend for the past 9 years, whereas distinct spikes were observed in the temperatures in the stations before the earthquakes [figures 20 (p), (q), (r), (s), (t), (u) and (v)].

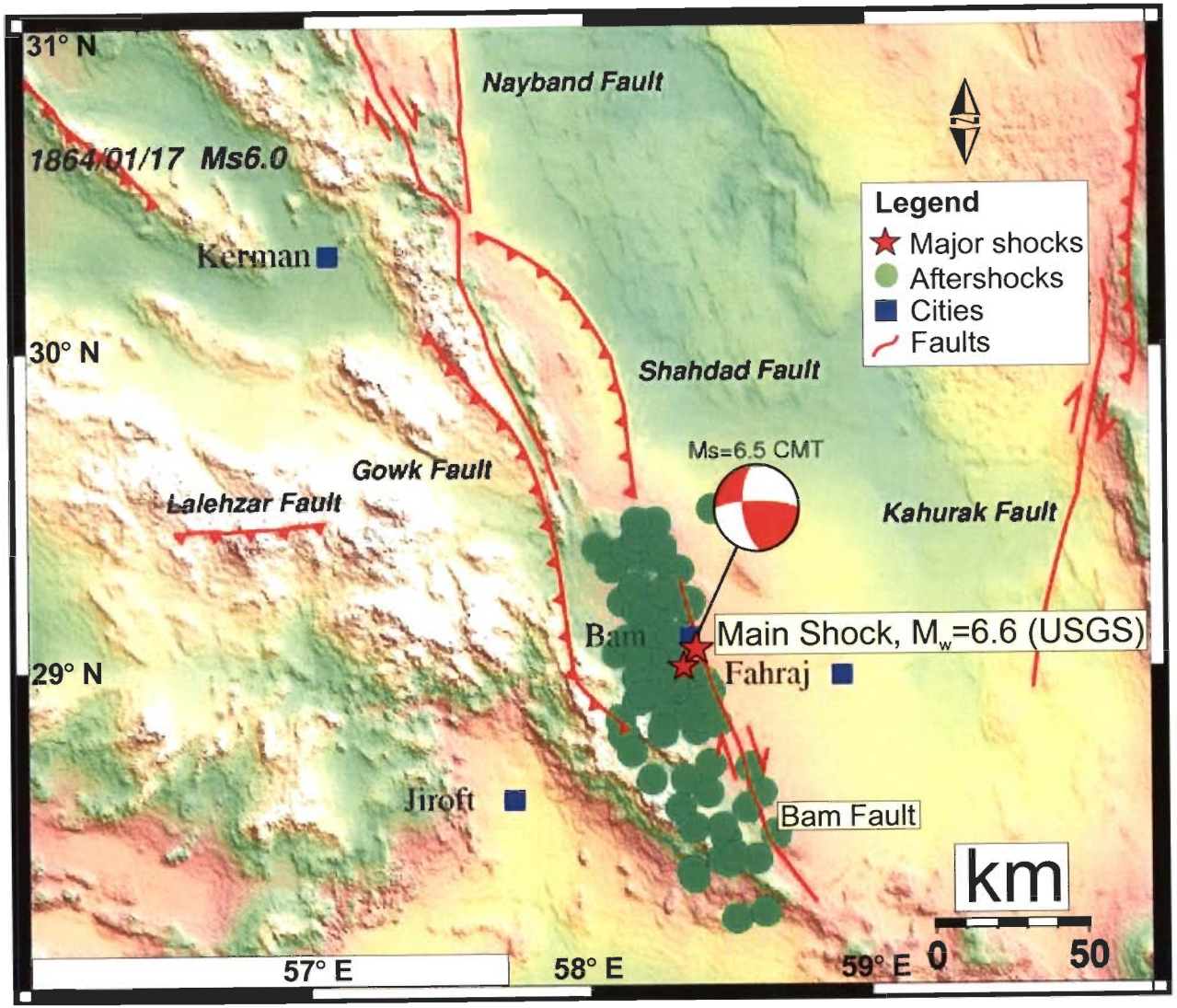

Figure 4.11: Location of the epicenter of the main event of the Bam earthquake (Iran), aftershocks and tectonics (faults) of the region. The Bam fault is reported to be responsible for the earthquake of 26 December 2003 (after http://www.iiees.ac.ir/English/bank/Bam/Bam_report_english_aftershock.html).

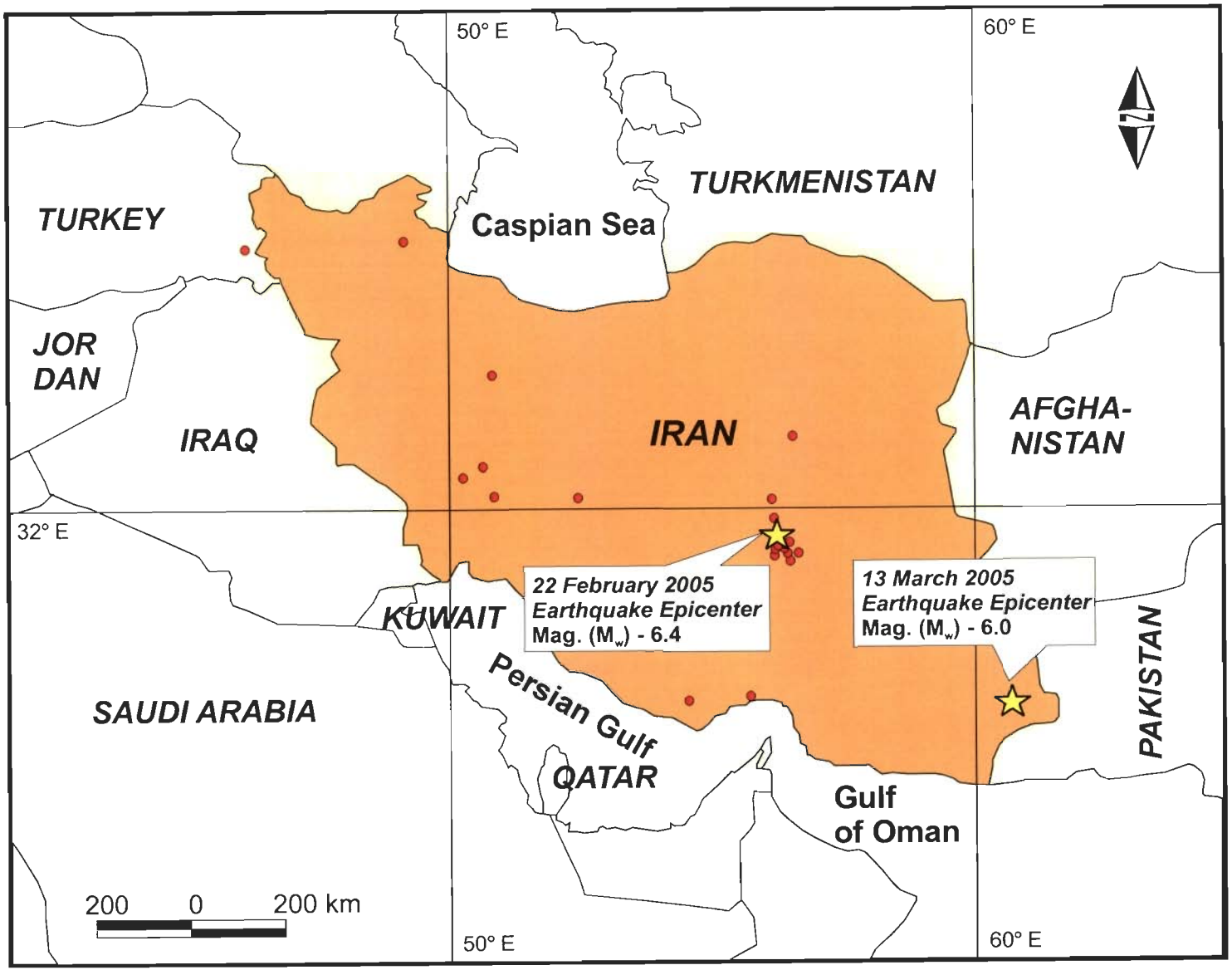

Figure 4.12: Locations of the Zarand Earthquake on 22 February 2005 and its aftershocks, the Southeast Iran Earthquake on 13 March 2005 and other small quakes in Iran in February-March 2005.

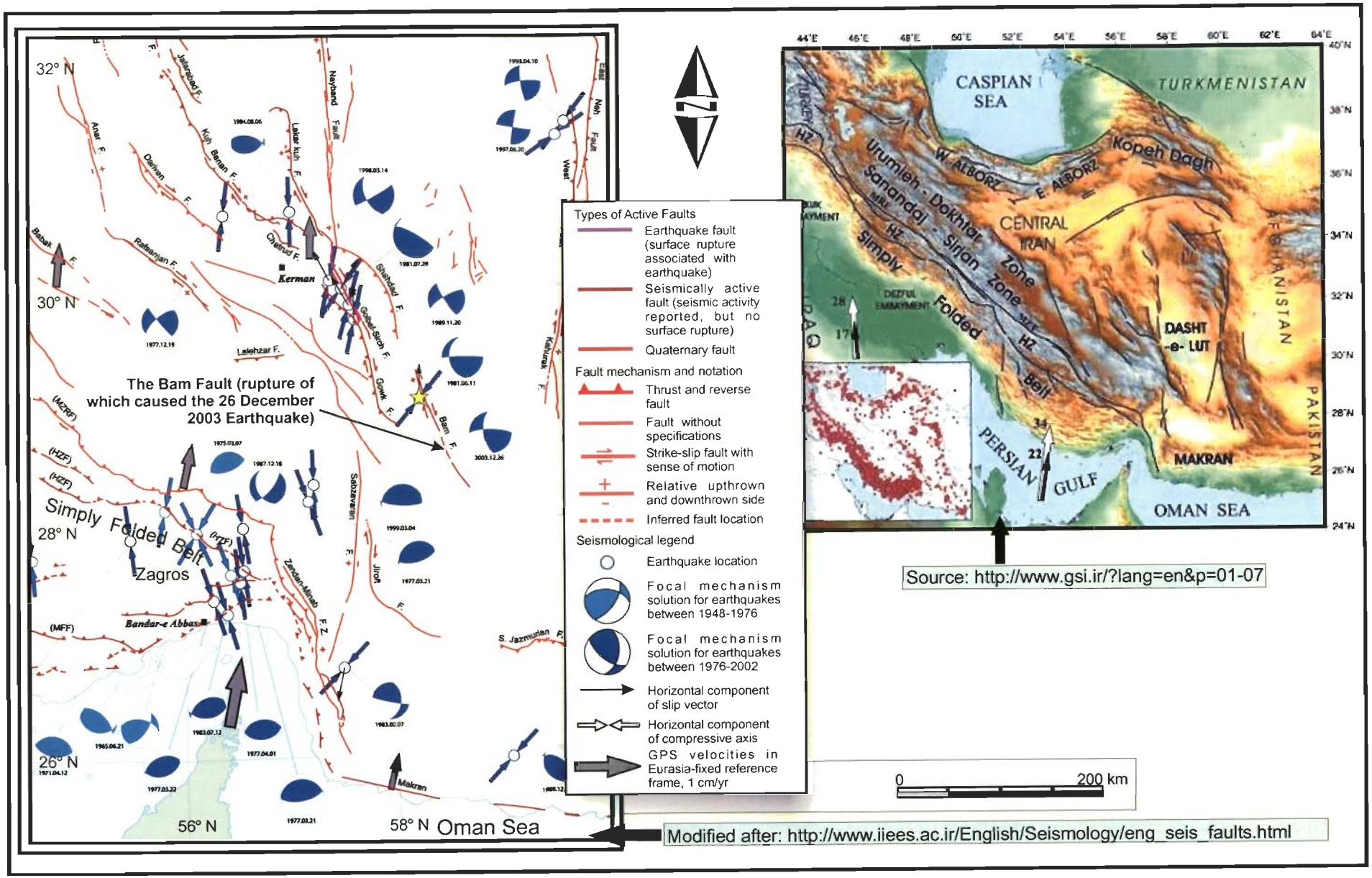

Figure 4.13: Main tectonics and active faults around the 26 December 2003 Bam earthquake epicentre in Iran.

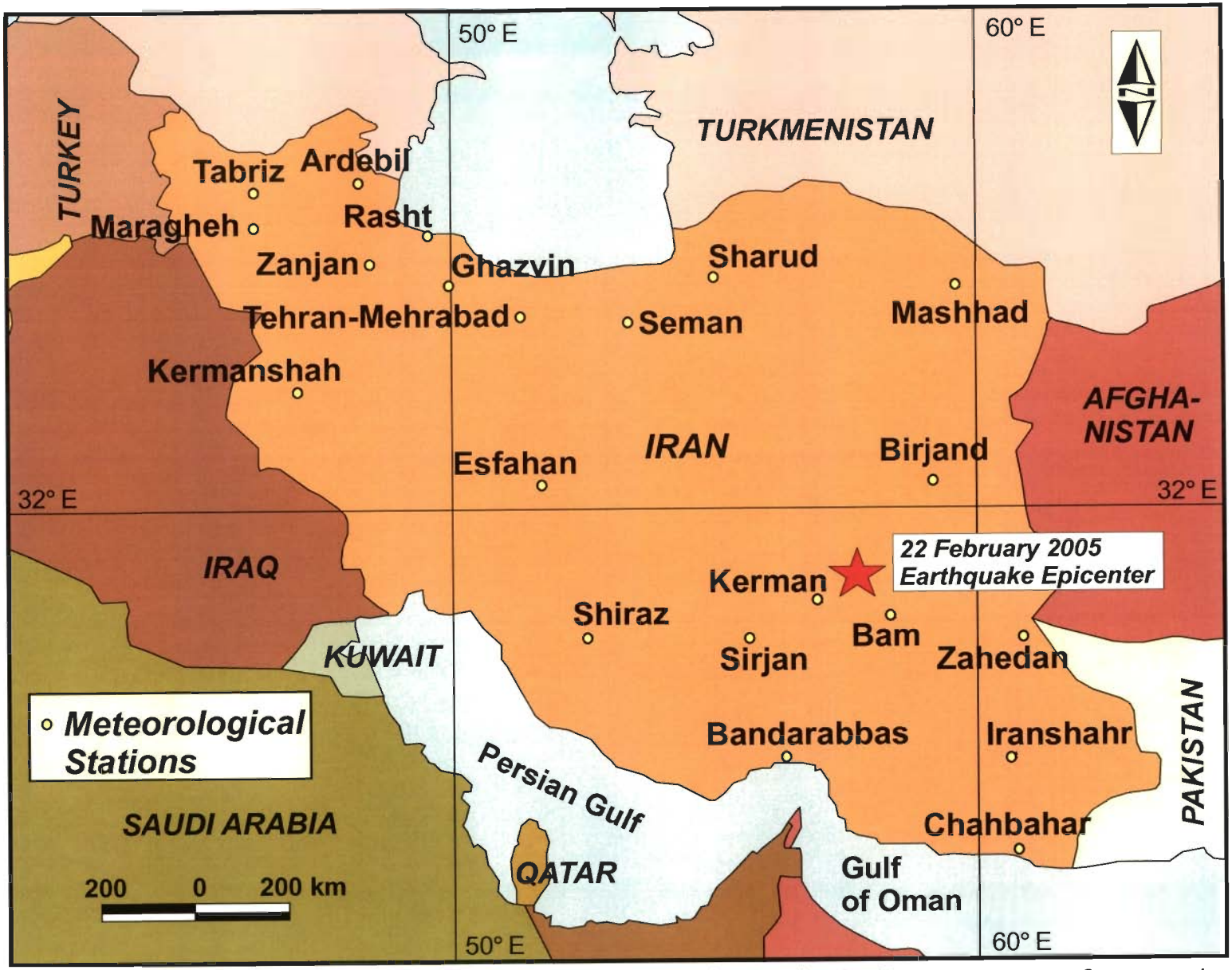

Figure 4.14: Locations of meteorological stations in Iran, provided online by Russian Weather Server and maintained by Islamic Republic of Iran Meteorological Department (IRIMO).

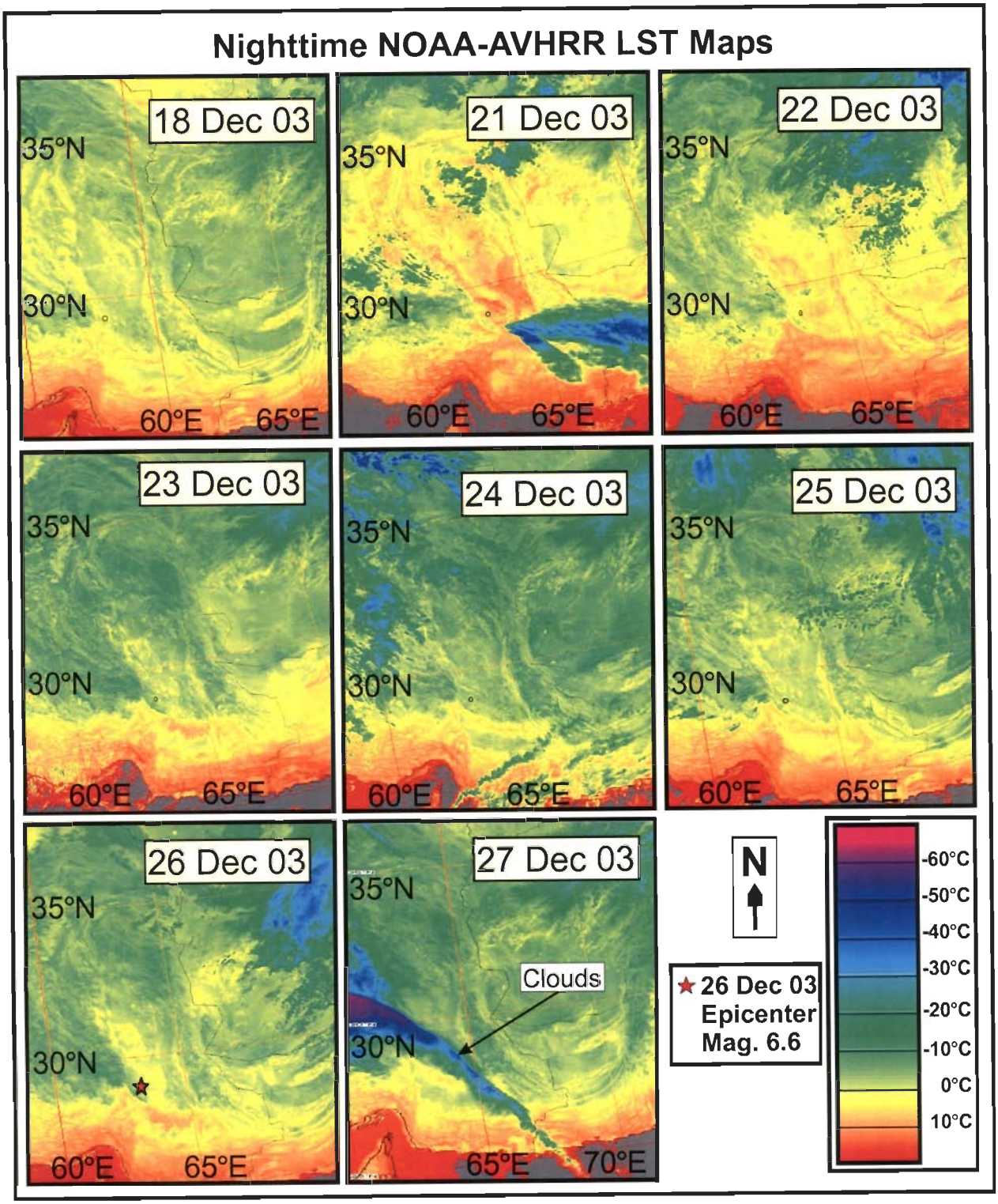

Figure 4.15 (a): Nighttime NOAA-AVHRR LST time series map of Iran before and after the earthquake in Bam, Iran on 26 December 2003.

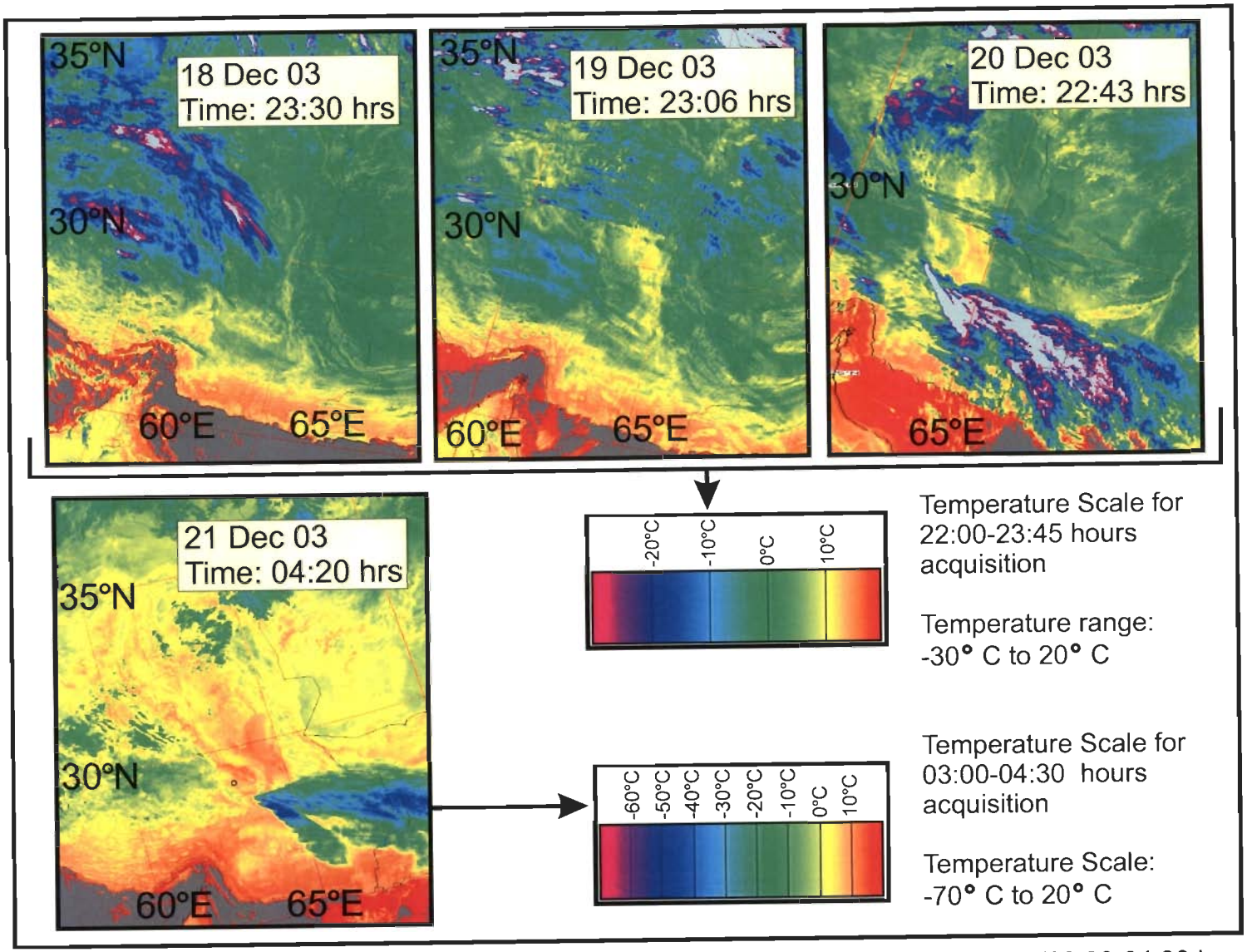

Figure 4.15 (b): Build up of thermal anomaly at nighttime. Since same time of acquisition (03:00-04:30 hours) of nighttime scenes were not available for 18-20 December 2003, data with 4 hours difference (22:00-23:45 hours) was used to see the thermal scenario on those days. It was seen that a thermal anomaly was also present on 19 and 20 December night.

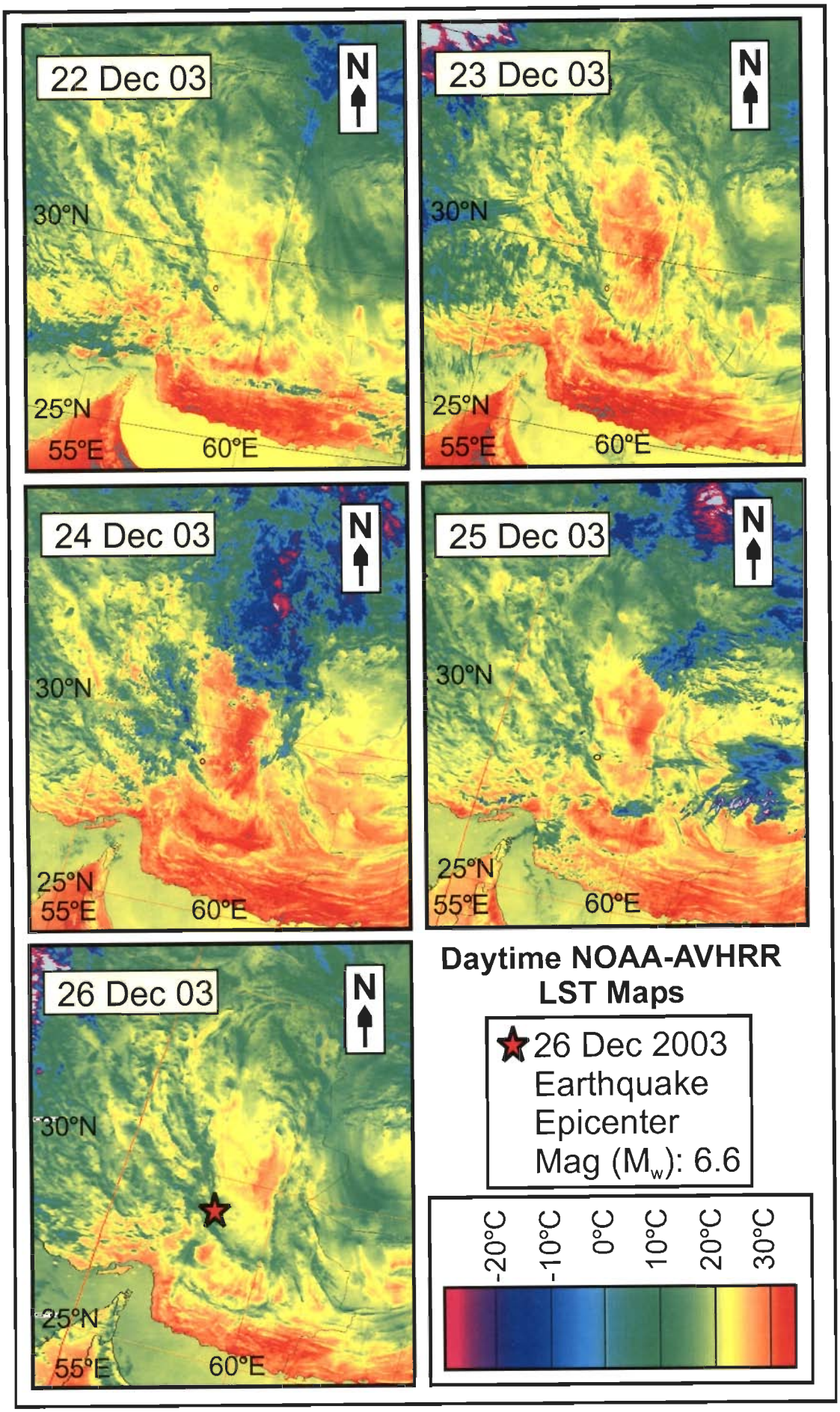

Figure 4.16: Daytime NOAA-AVHRR LST time series map of Iran before and after the earthquake in Bam, Iran on 26 December 2003. An intense thermal anomaly can be seen on 24 December 2003, two days before the earthquake.

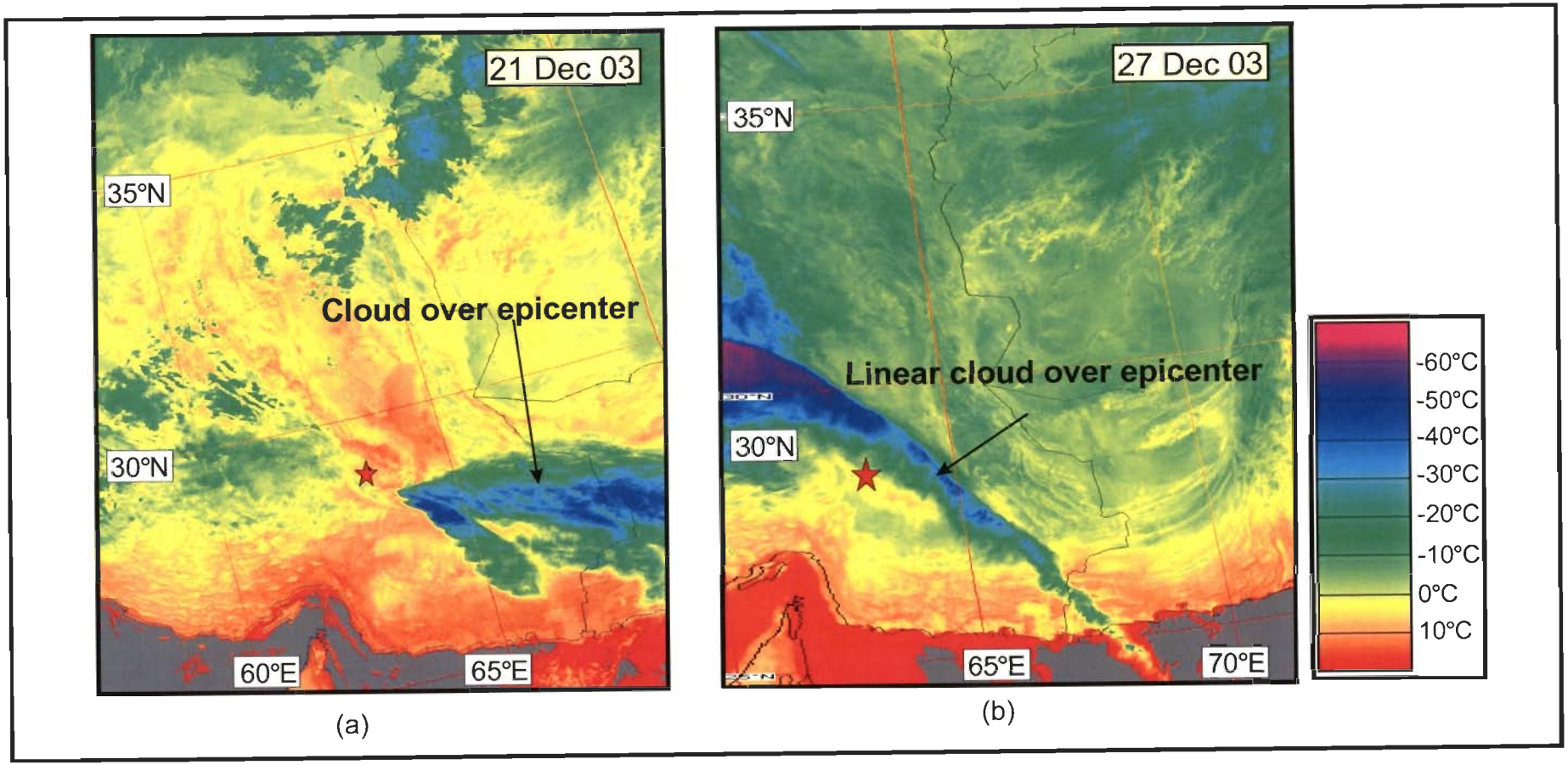

Figure 4.17: (a) Peculiar pattern of clouds seen as if to originate from the Bam earthquake epicenter on 21 December 2003. (b) Linear cloud over the epicentral area on 27 December 2003 (after the earthquake). Such earthquake clouds have been reported by different workers to be 'earthquake clouds', and sometimes also earthquake precursors.

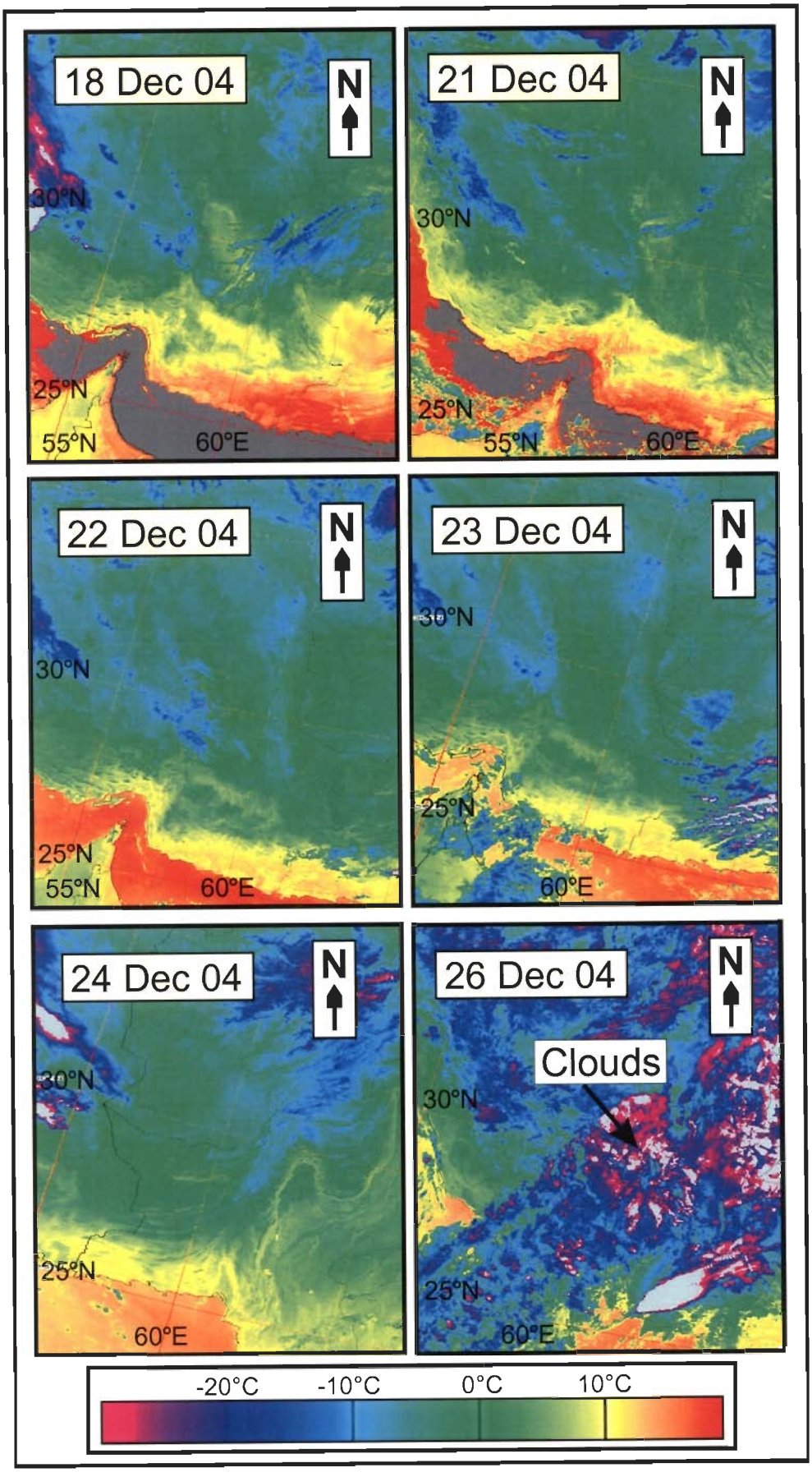

Figure 4.18: NOAA-AVHRR LST maps of the year 2004 of Iran around the same time in which the Bam earthquake occurred a year ago. It was observed that in the year 2004 there was no unusual variation in the LST maps around the 26 December 2003 earthquake in Bam.

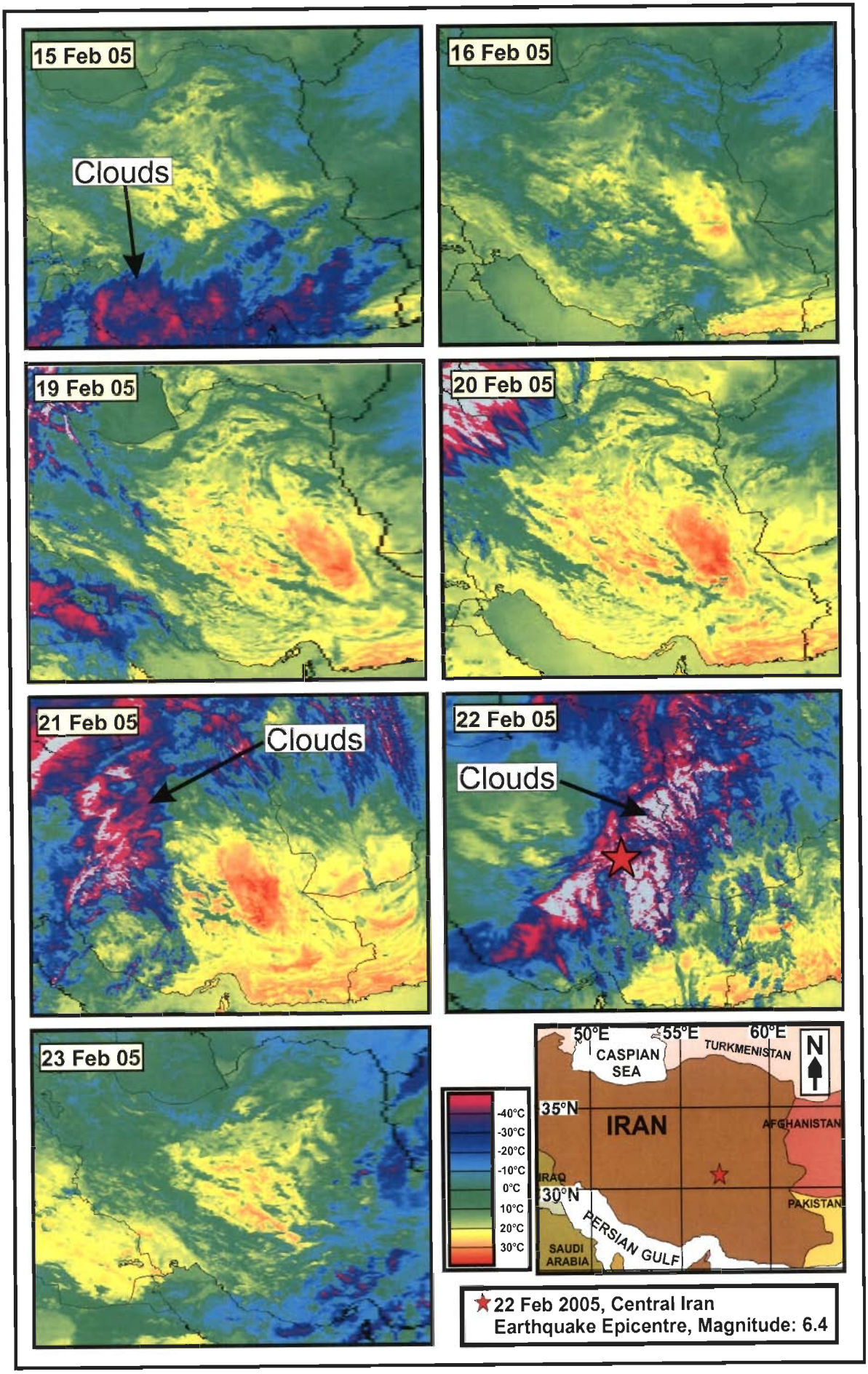

Figure 4.19: Daytime NOAA-AVHRR LST time series map of Iran before and after the earthquake in Zarand, Iran on 22 February 2005.

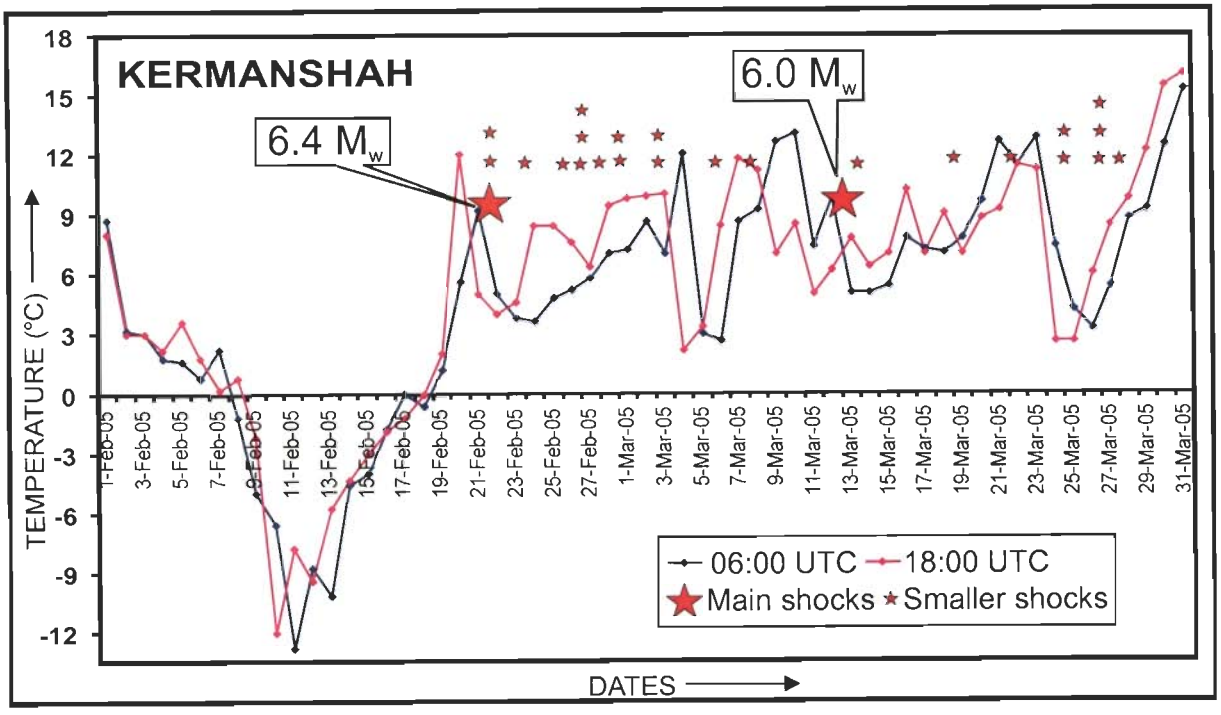

Figure 4.20 (a): Temperature Variation Curves (TVC), showing air temperature trend in the Kermanshah city in Iran around the time of the series of earthquakes in Iran in 2005.

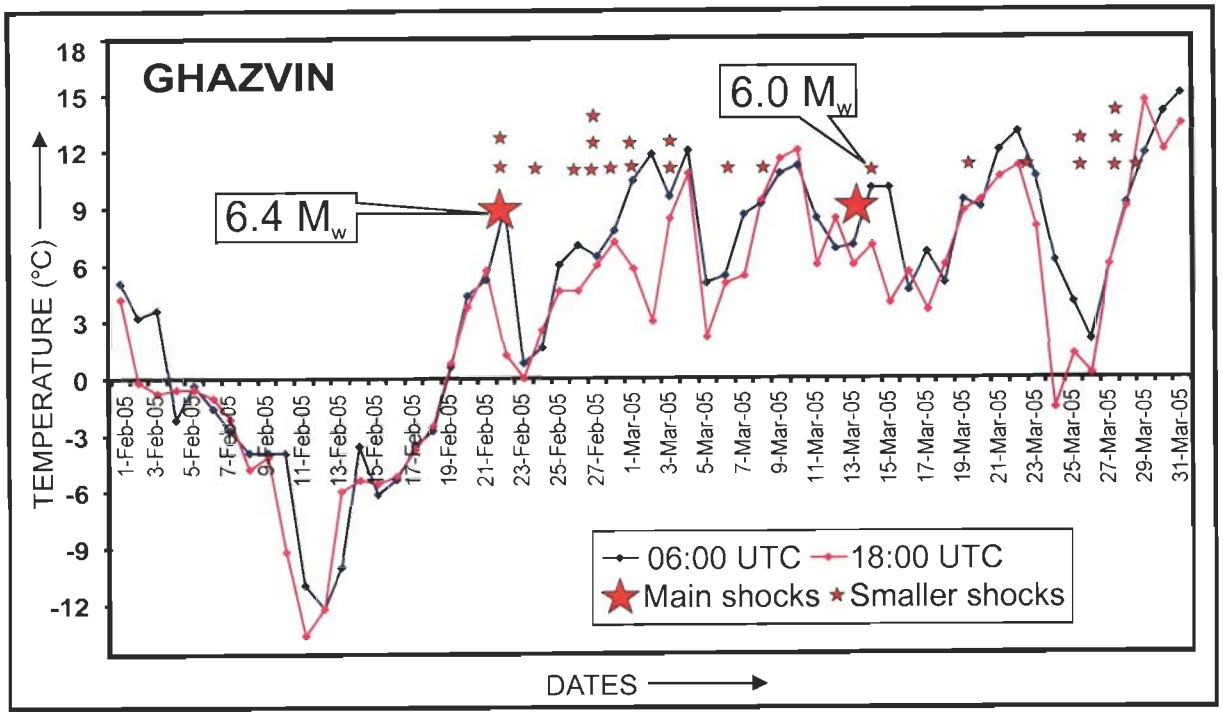

Figure 4.20 (b): Temperature Variation Curves (TVC), showing air temperature trend in the Ghazvin city in Iran around the time of the series of earthquakes in Iran in 2005.

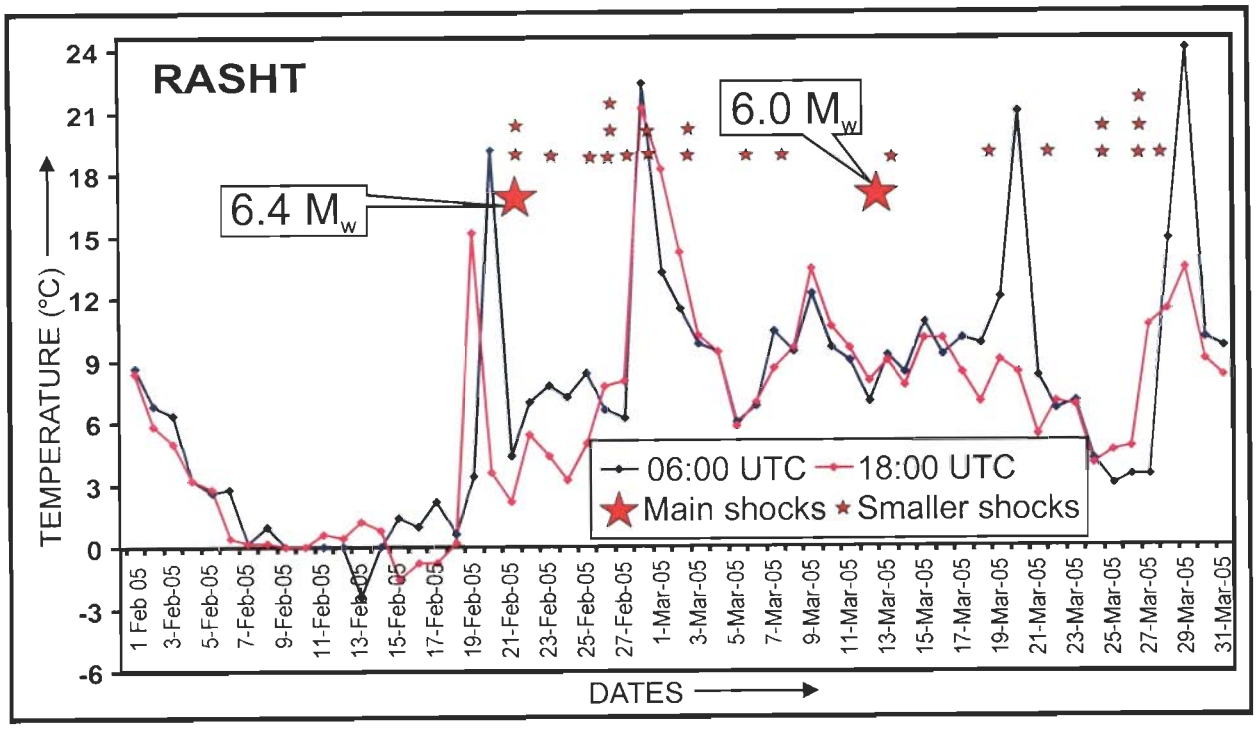

Figure 4.20 (c): Temperature Variation Curves (TVC), showing air temperature trend in the Rasht city in Iran around the time of the series of earthquakes in Iran in 2005.

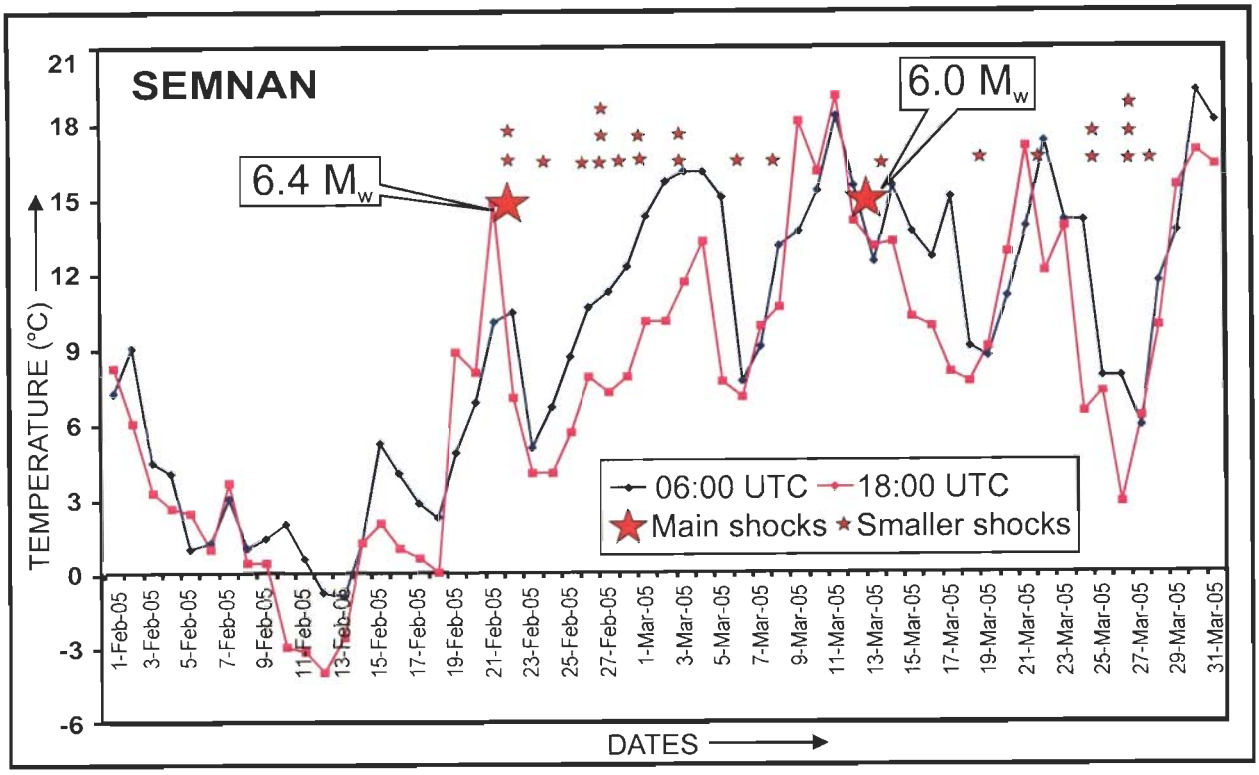

Figure 4.20 (d): Temperature Variation Curves (TVC), showing air temperature trend in the Semnan city in Iran around the time of the series of earthquakes in Iran in 2005.

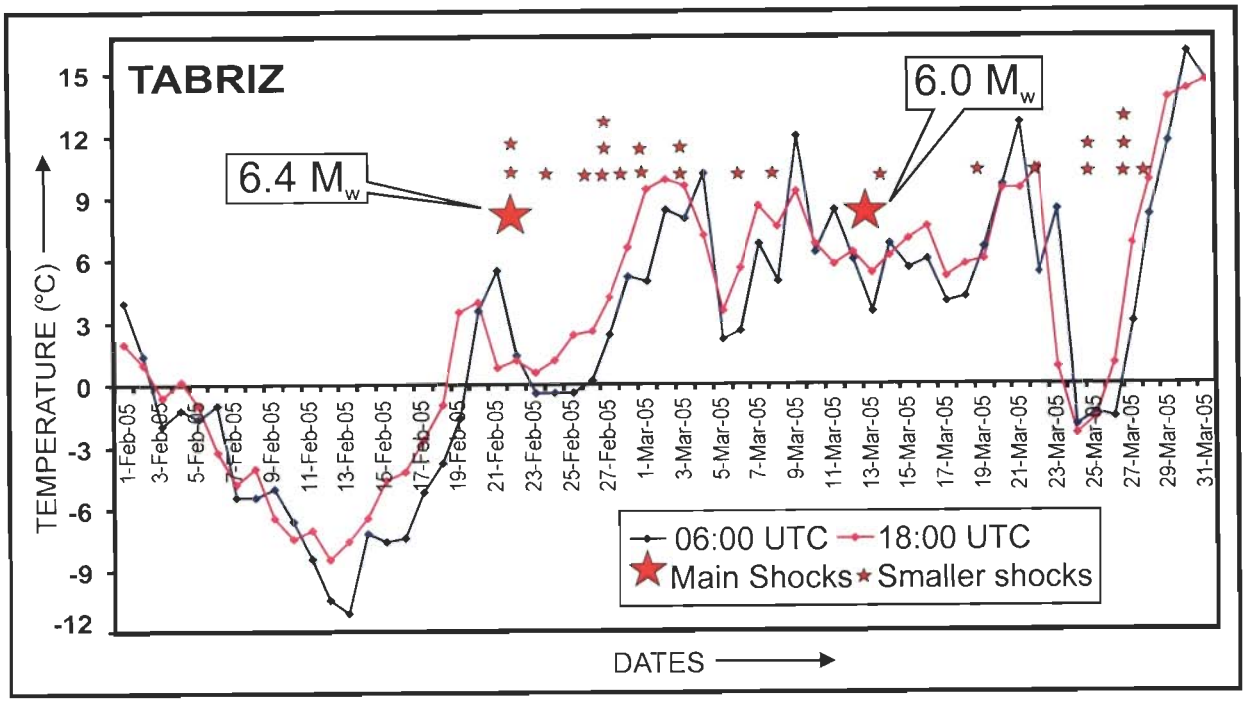

Figure 4.20 (e): Temperature Variation Curves (TVC), showing air temperature trend in the Tabriz city in Iran around the time of the series of earthquakes in Iran in 2005.

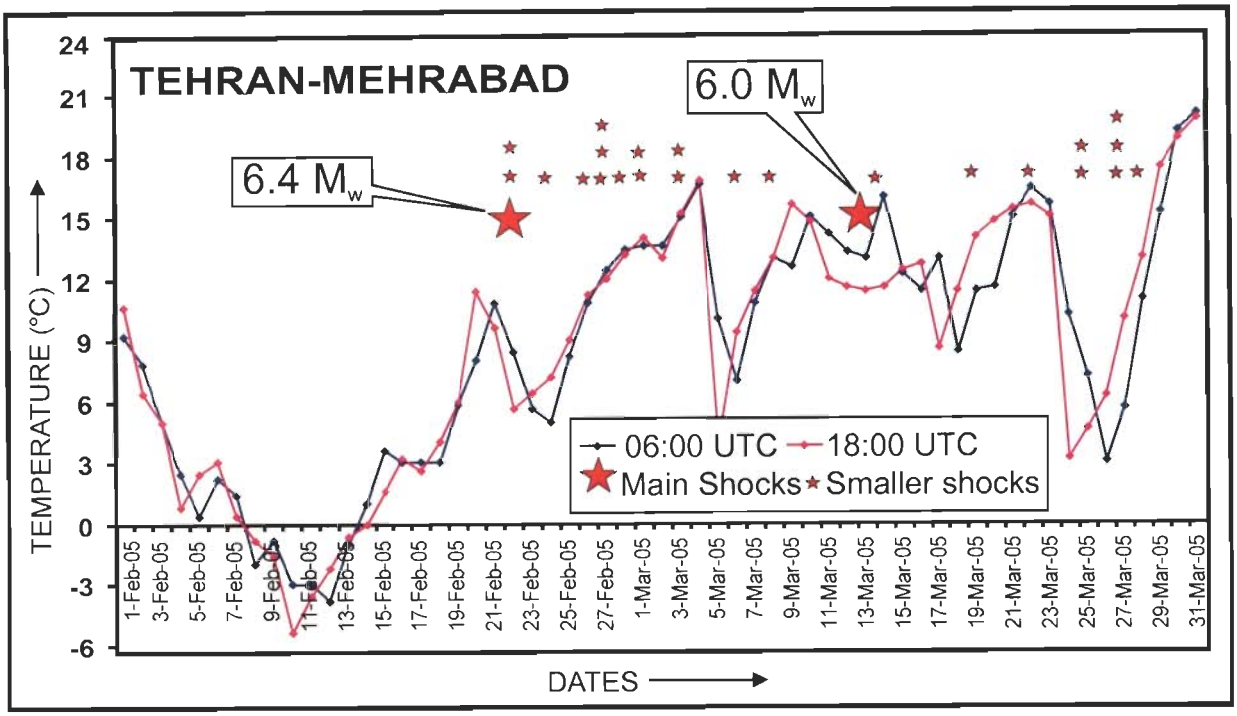

Figure 4.20 (f): Temperature Variation Curves (TVC), showing air temperature trend in the Tehran-Mehrabad city in Iran around the time of the series of earthquakes in Iran in 2005.

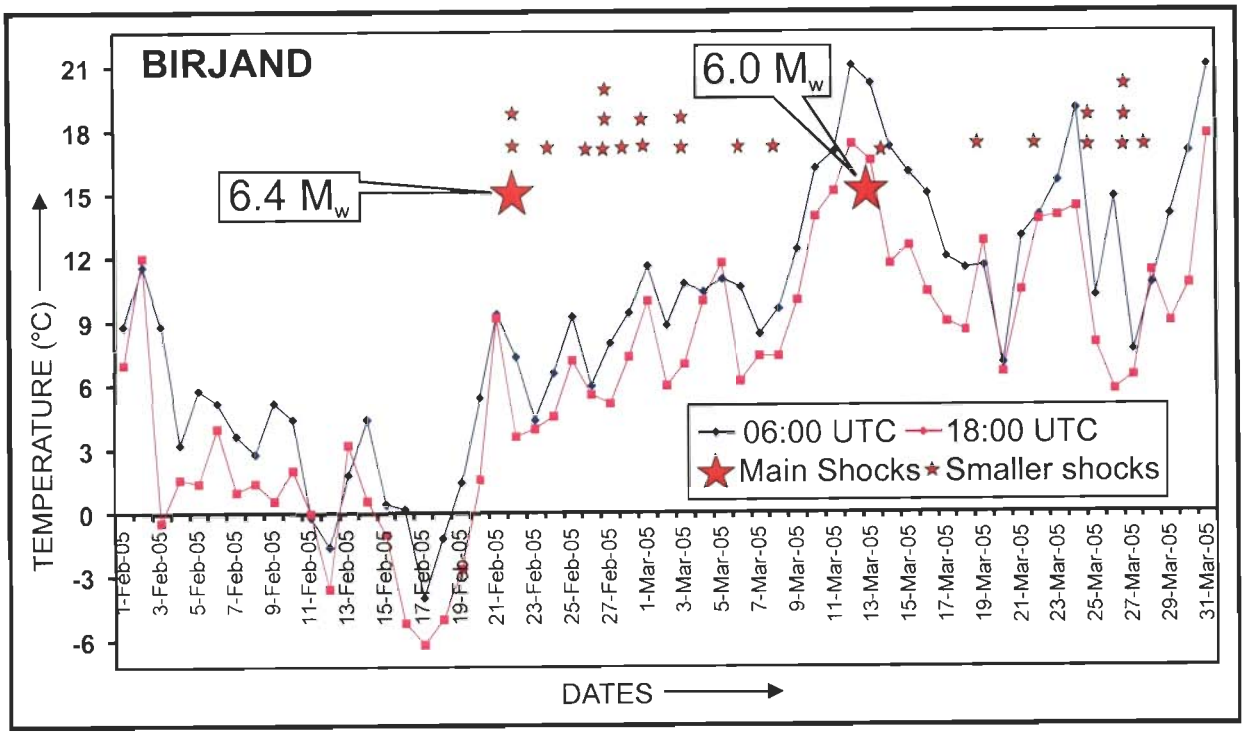

Figure 4.20 (g): Temperature Variation Curves (TVC), showing air temperature trend in the Birjand city in Iran around the time of the series of earthquakes in Iran in 2005.

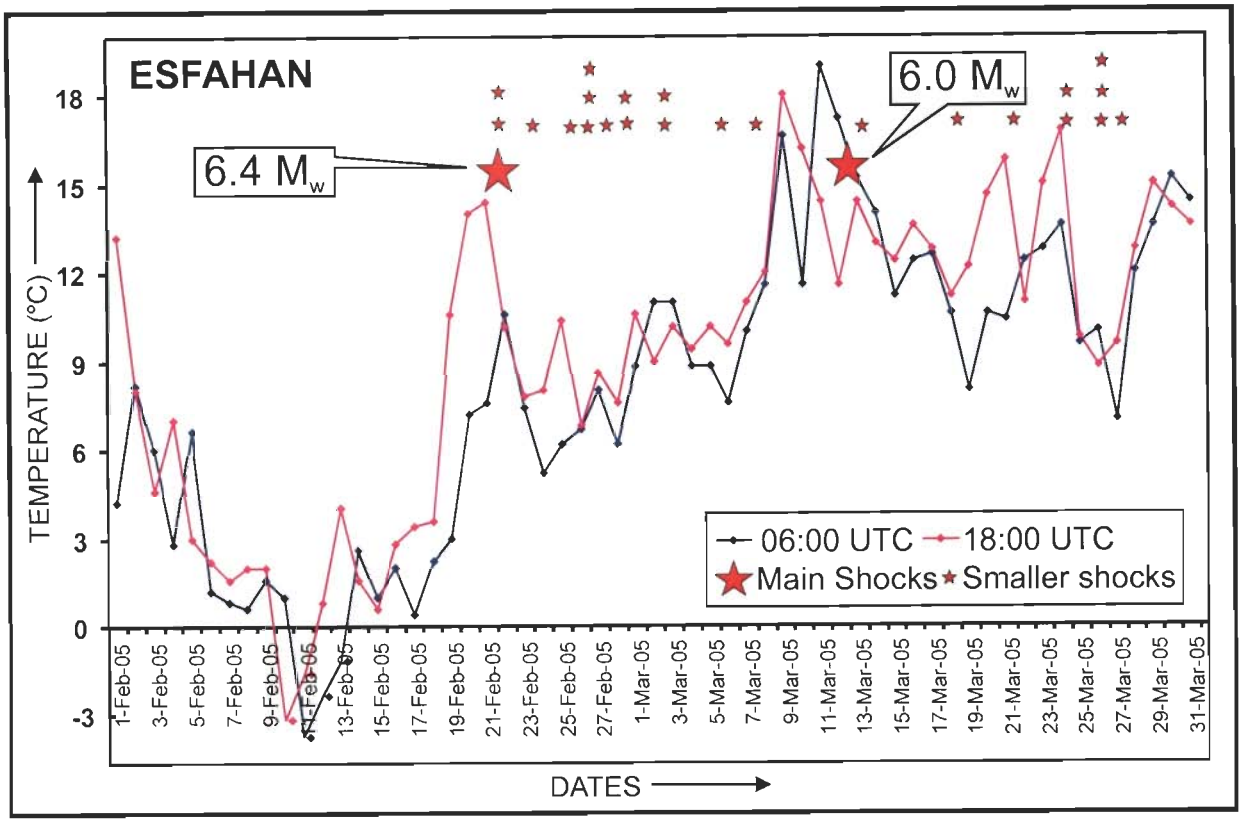

Figure 4.20 (h): Temperature Variation Curves (TVC), showing air temperature trend in the Esfahan city in Iran around the time of the series of earthquakes in Iran in 2005.

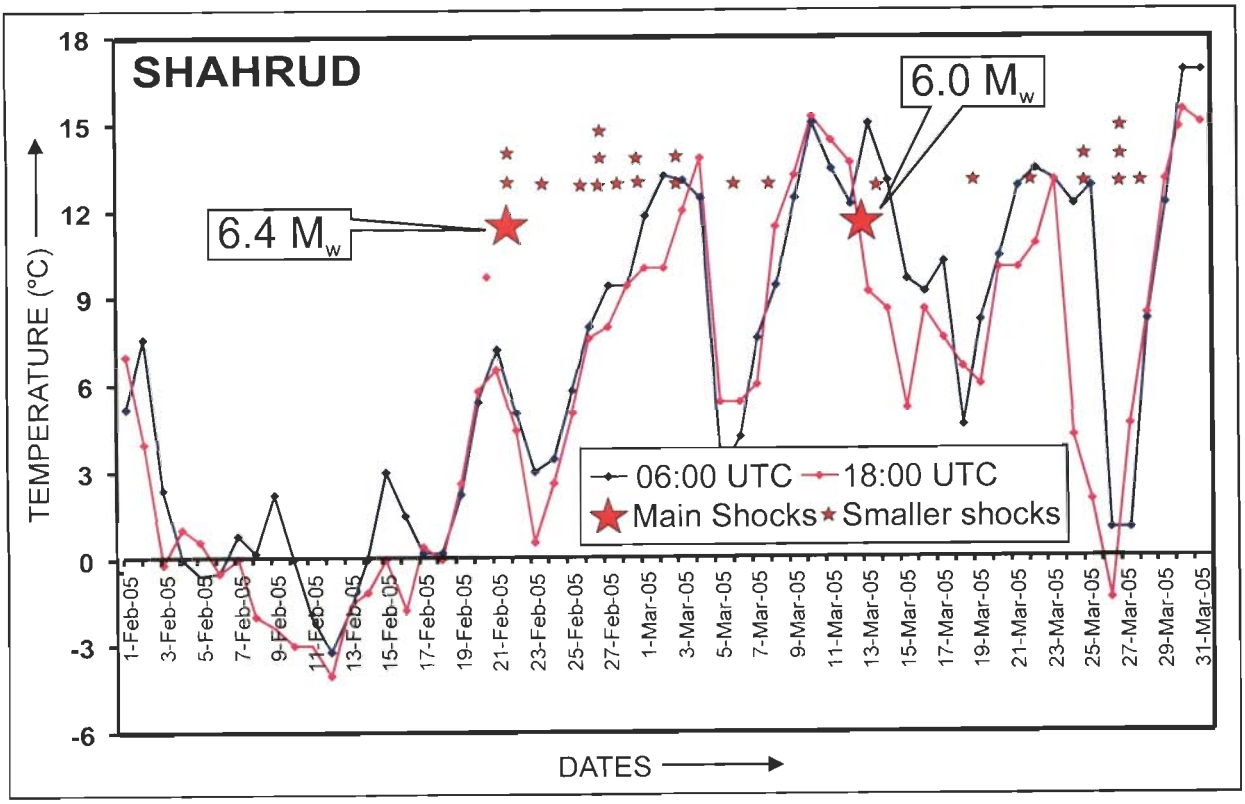

Figure 4.20 (i): Temperature Variation Curves (TVC), showing air temperature trend in the Shahrud city in Iran around the time of the series of earthquakes in Iran in 2005.

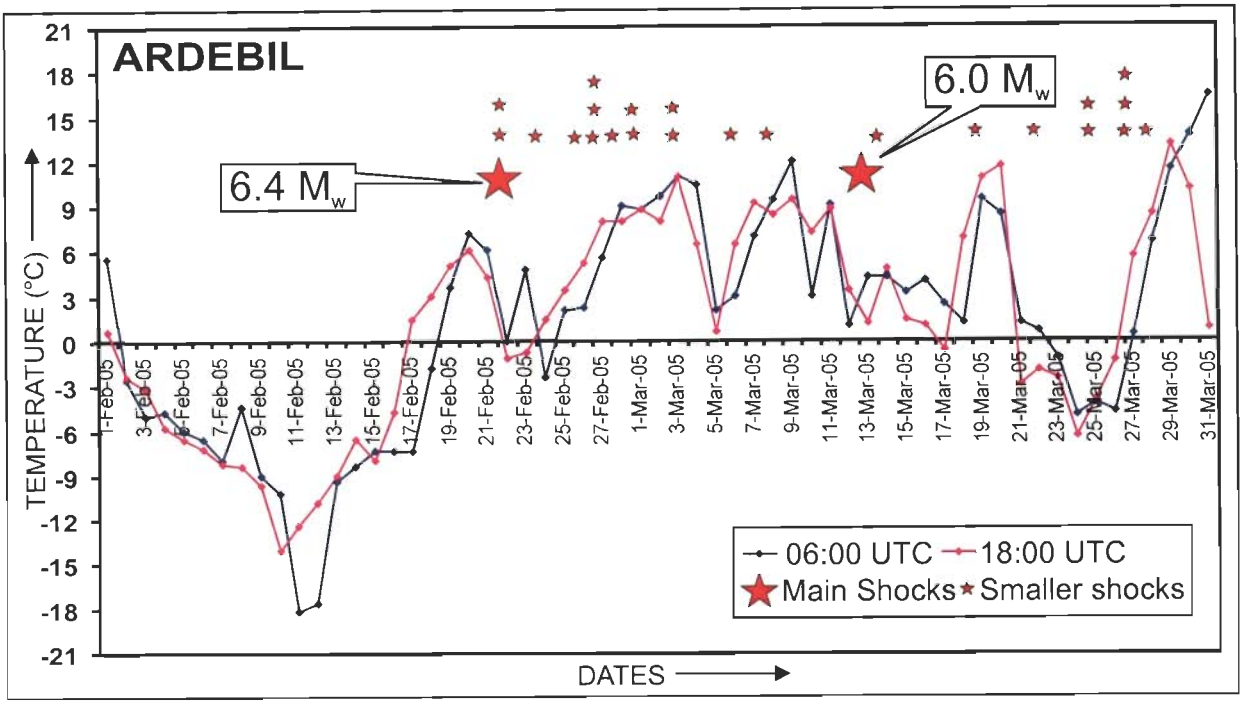

Figure 4.20 (j): Temperature Variation Curves (TVC), showing air temperature trend in the Ardebil city in Iran around the time of the series of earthquakes in Iran in 2005.

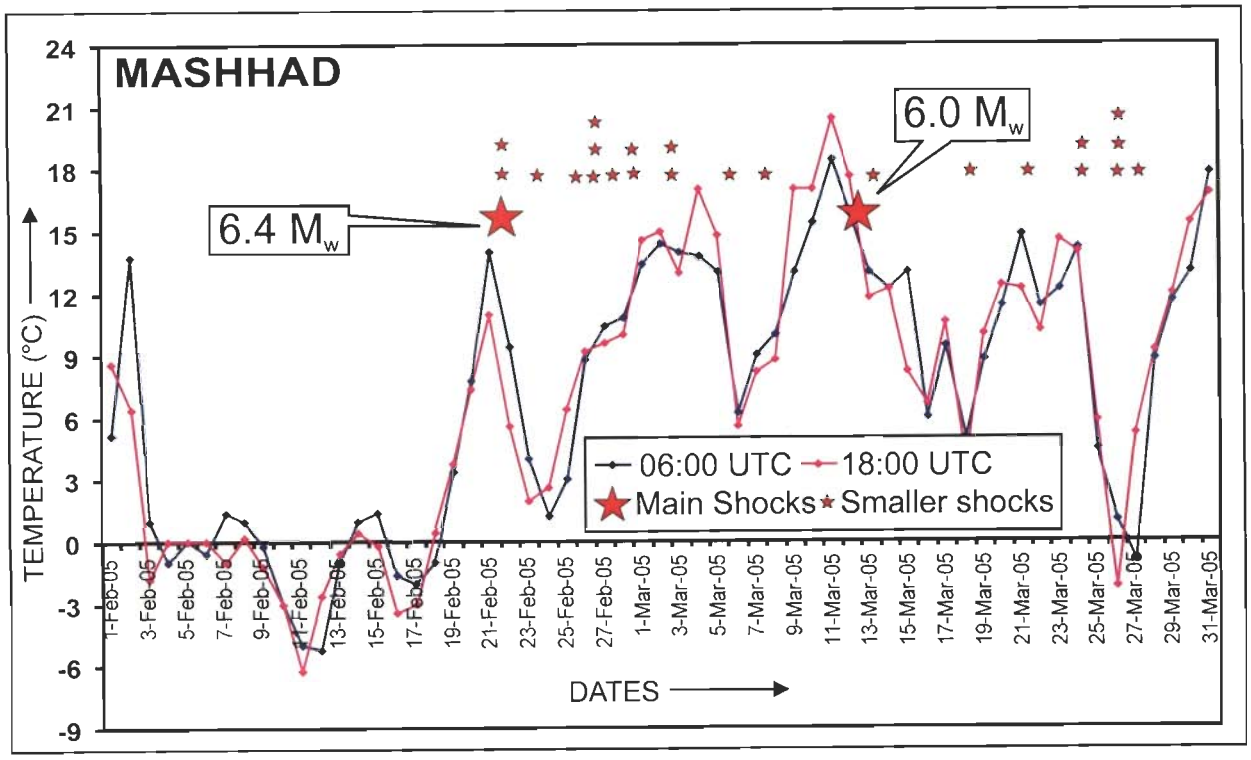

Figure 4.20 (k): Temperature Variation Curves (TVC), showing air temperature trend in the Mashad city in Iran around the time of the series of earthquakes in Iran in 2005.

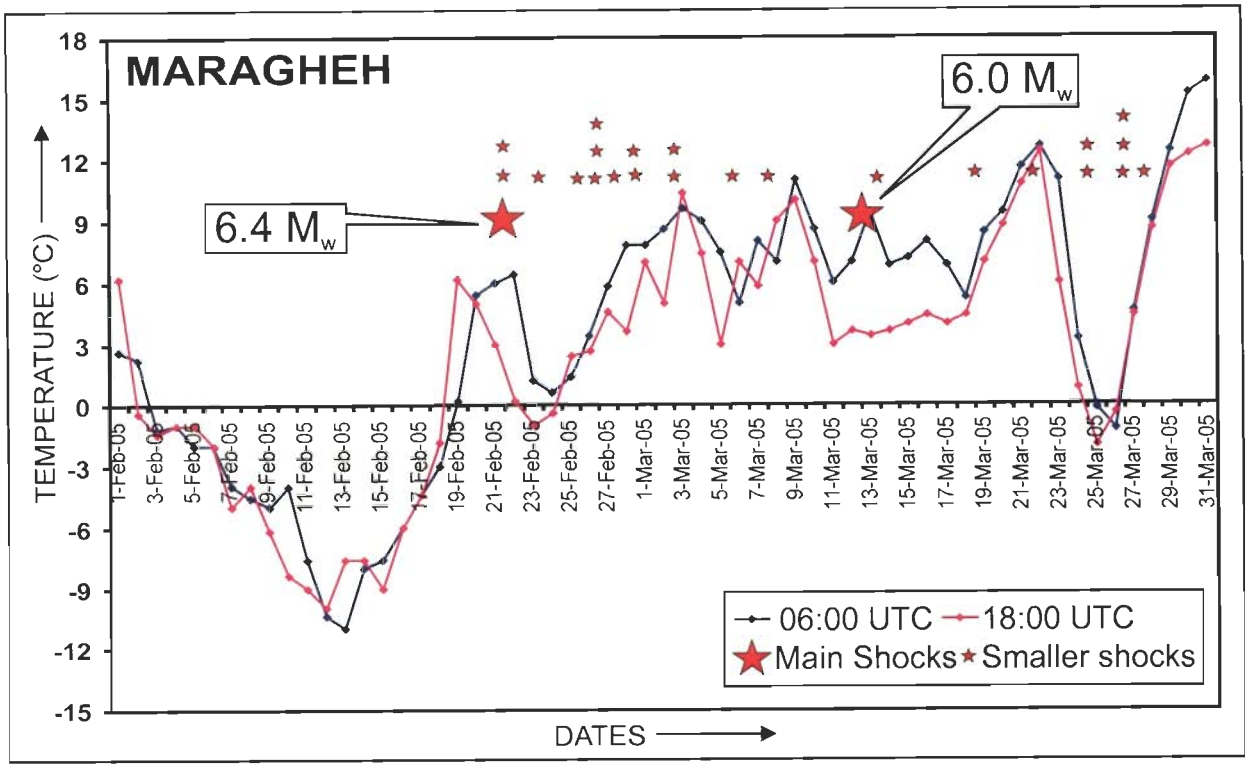

Figure 4.20 (l): Temperature Variation Curves (TVC), showing air temperature trend in the Maragheh city in Iran around the time of the series of earthquakes in Iran in 2005.

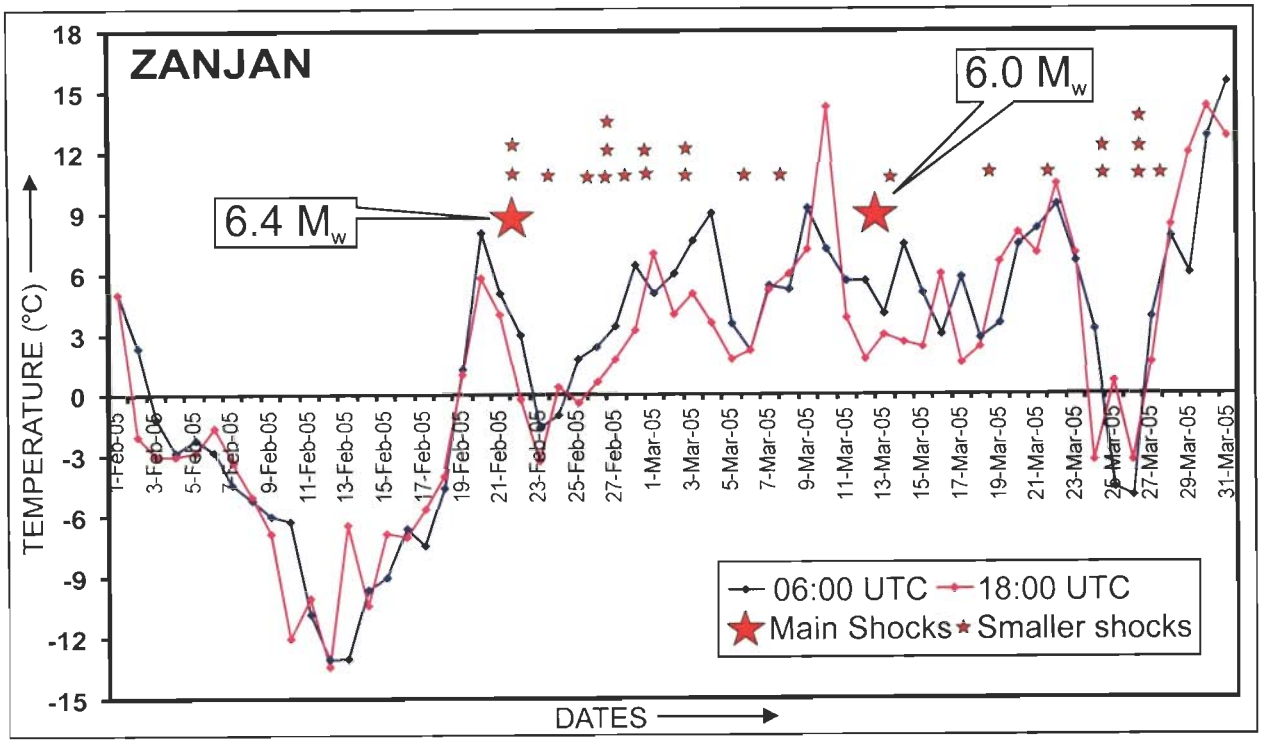

Figure 4.20 (m): Temperature Variation Curves (TVC), showing air temperature trend in the Zanjan city in Iran around the time of the series of earthquakes in Iran in 2005.

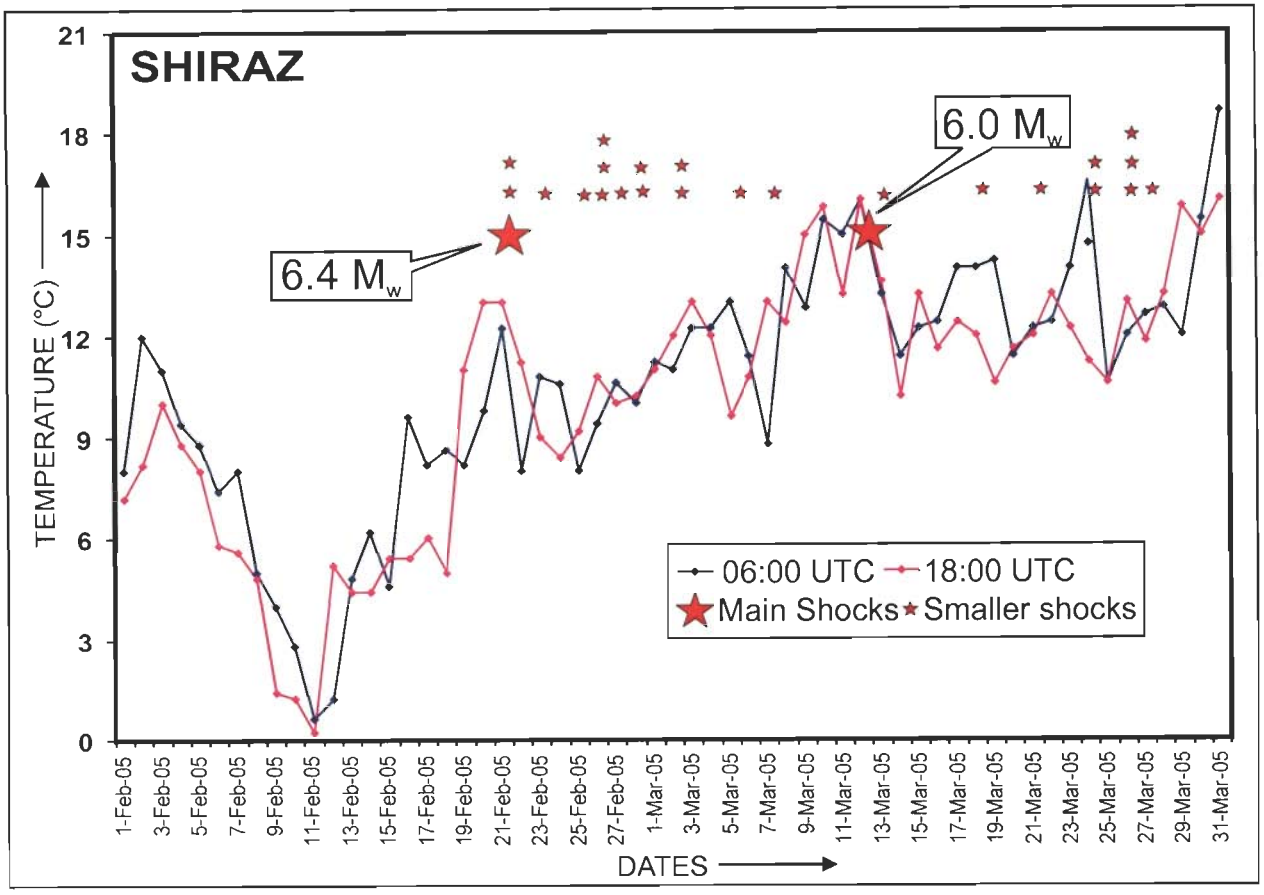

Figure 4.20 (n): Temperature Variation Curves (TVC), showing air temperature trend in the Shiraj city in Iran around the time of the series of earthquakes in Iran in 2005.

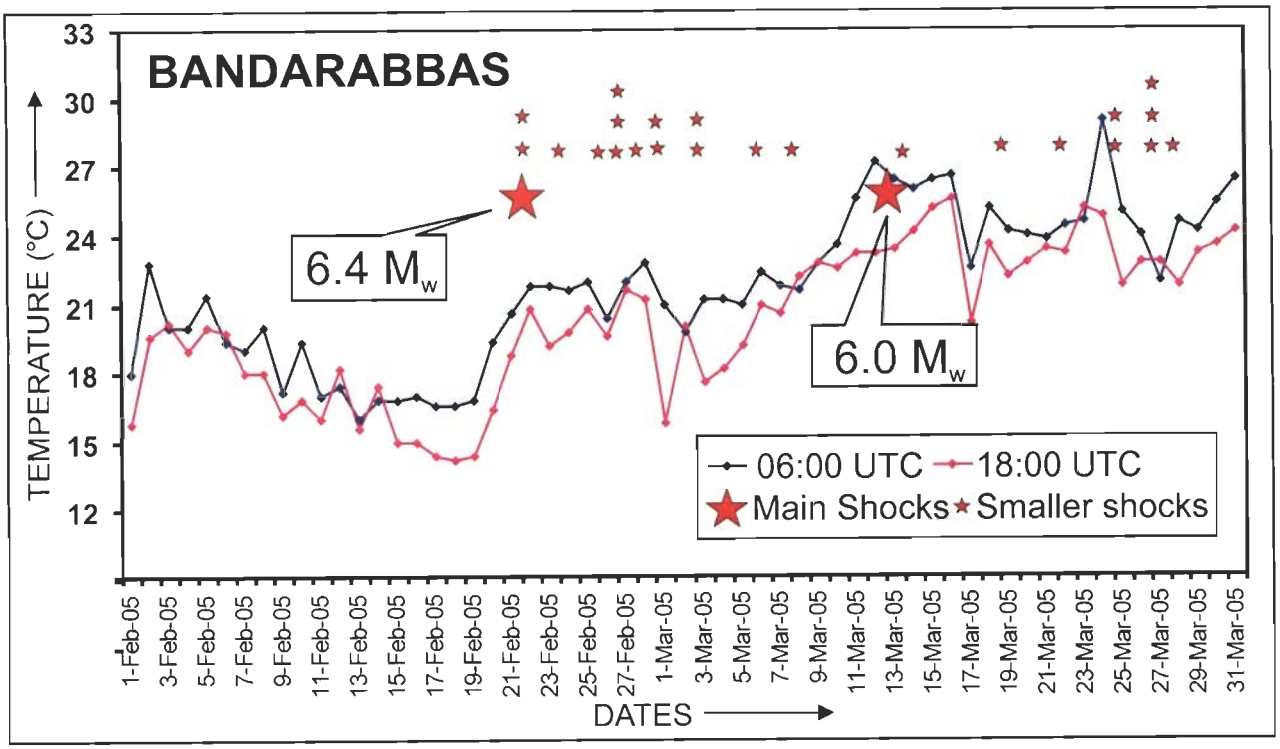

Figure 4.20 (o): Temperature Variation Curves (TVC), showing air temperature trend in the Bandarabbas city in Iran around the time of the series of earthquakes in Iran in 2005. Bandarabbas did not show any distinct trend in the change of air temperature before the earthquake, probably because Bandarabbas is a coastal city and is influenced by sea winds etc.

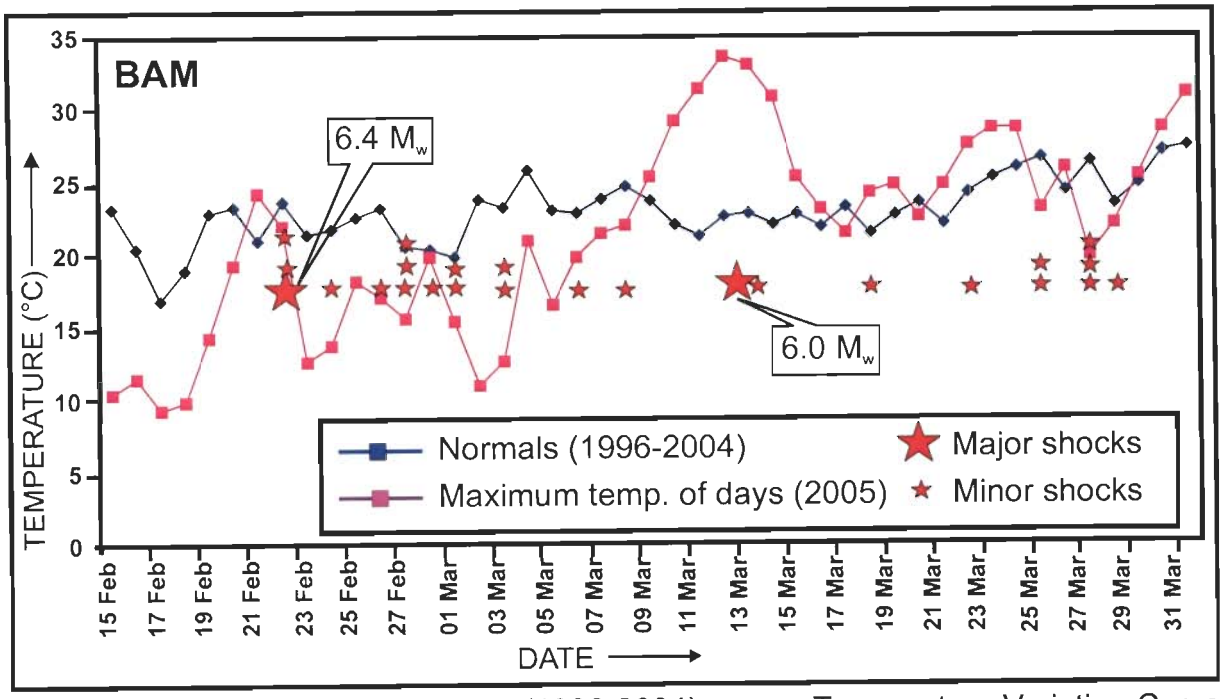

Figure 4.20 (p): Temperature normals (1996-2004) versus Temperature Variation Curves (TVC) of the year 2005 (around the time of the series of earthquakes in 2005) of the Bam city in Iran. It was observed that there was a normal trend in the 9 years, whereas in the year 2005 there were spikes of temperature rise before the earthquake events.

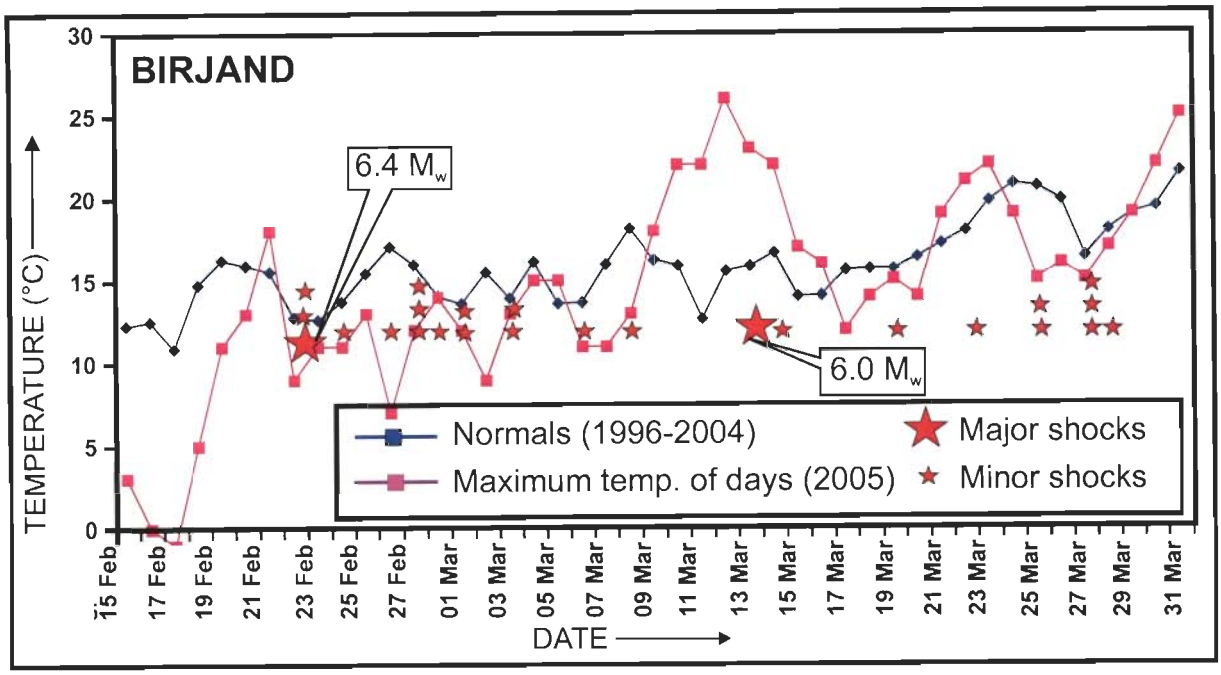

Figure 4.20 (q): Temperature normals (1996-2004) versus Temperature Variation Curves (TVC) of the year 2005 (around the time of the series of earthquakes in 2005) of the Birjand city in Iran. It was observed that there was a normal trend in the 9 years, whereas in the year 2005 there were spikes of temperature rise before the earthquake events.

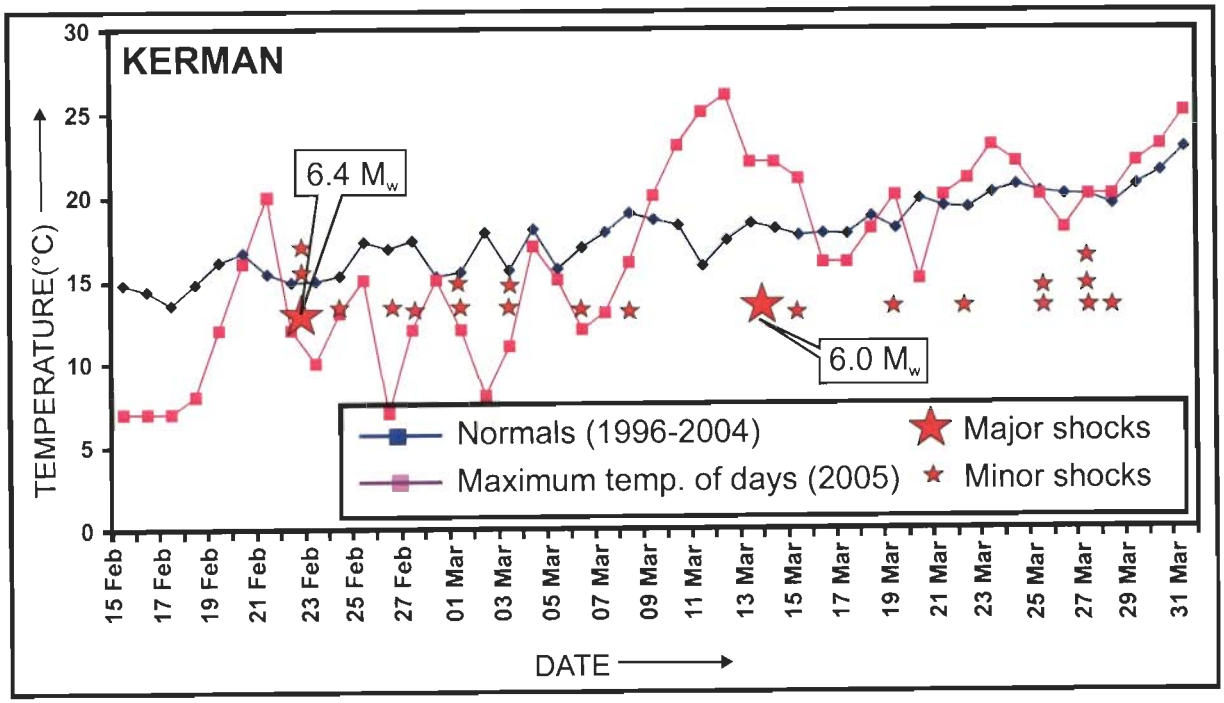

Figure 4.20 (r): Temperature normals (1996-2004) versus Temperature Variation Curves (TVC) of the year 2005 (around the time of the series of earthquakes in 2005) of the Kerman city in Iran. It was observed that there was a normal trend in the 9 years, whereas in the year 2005 there were spikes of temperature rise before the earthquake events.

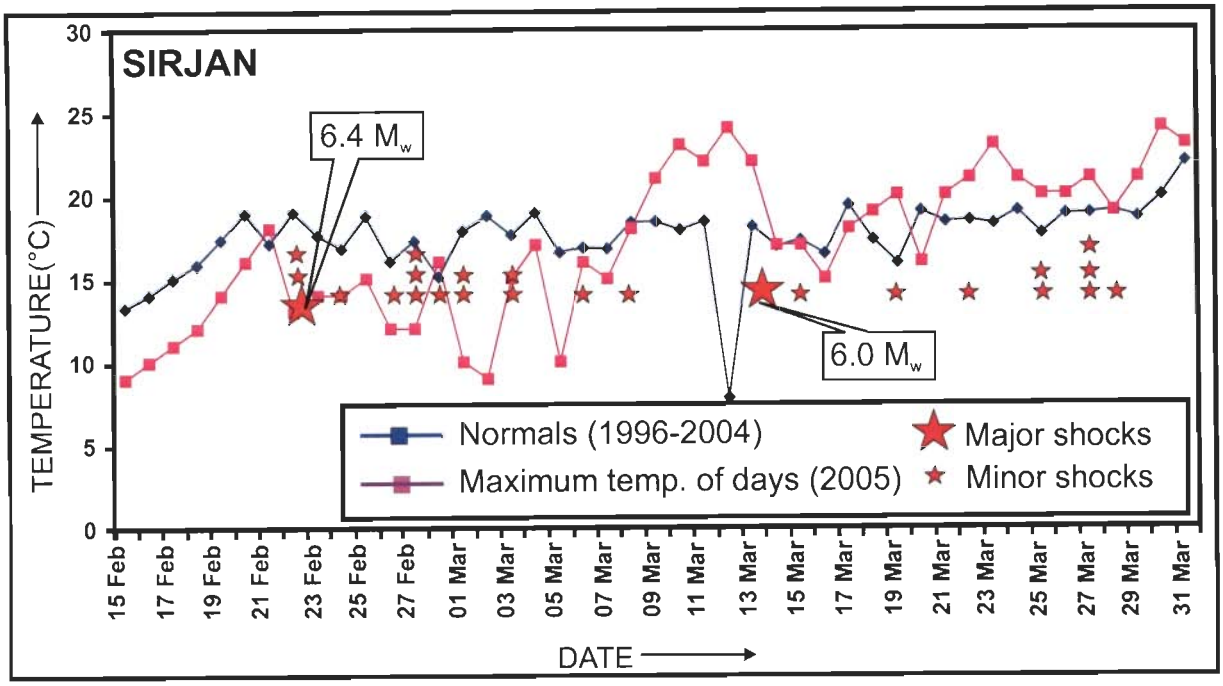

Figure 4.20 (s): Temperature normals (1996-2004) versus Temperature Variation Curves (TVC) of the year 2005 (around the time of the series of earthquakes in 2005) of the Sirjan city in Iran. It was observed that there was a normal trend in the 9 years, whereas in the year 2005 there were spikes of temperature rise before the earthquake events.

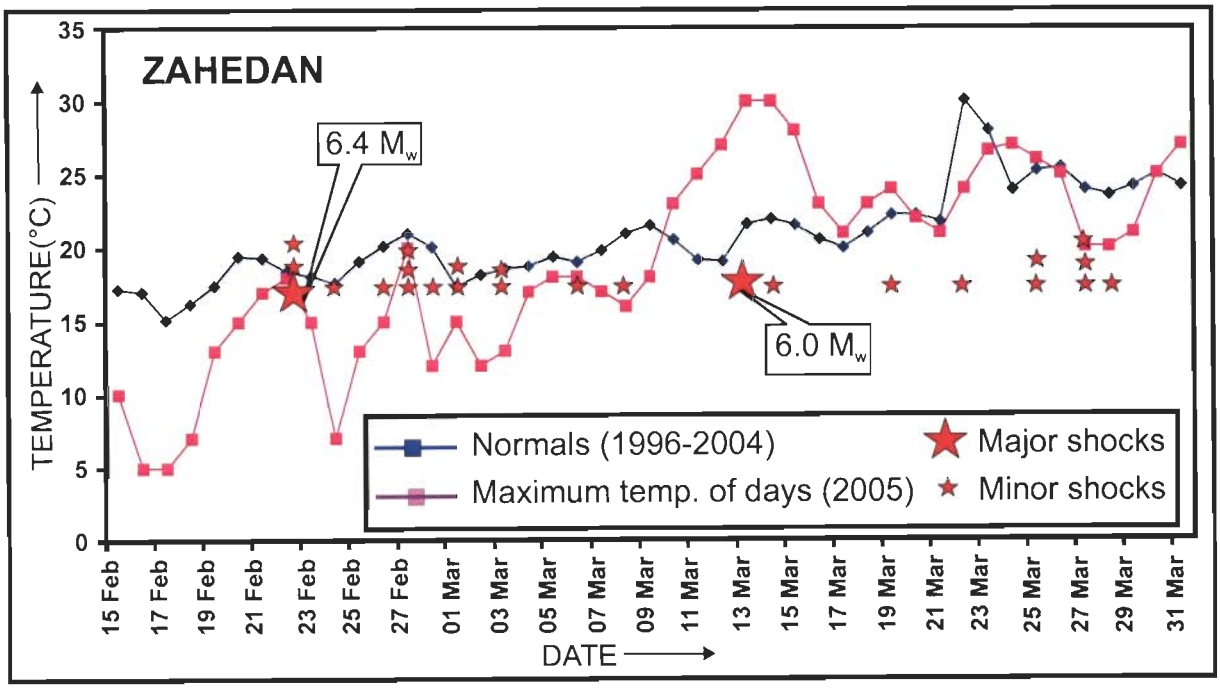

Figure 4.20 (t): Temperature normals (1996-2004) versus Temperature Variation Curves (TVC) of the year 2005 (around the time of the series of earthquakes in 2005) of the Zahedan city in Iran. It was observed that there was a normal trend in the 9 years, whereas in the year 2005 there were spikes of temperature rise before the earthquake events.

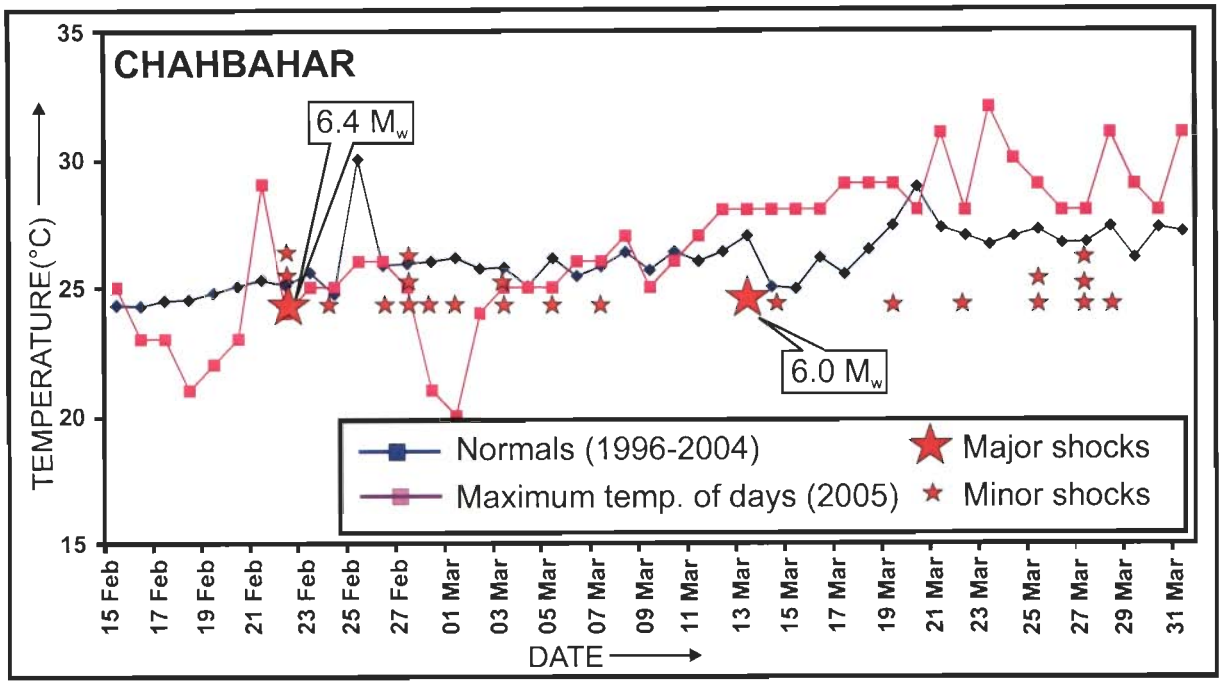

Figure 4.20 (u): Temperature normals (1996-2004) versus Temperature Variation Curves (TVC) of the year 2005 (around the time of the series of earthquakes in 2005) of the Chahbahar city in Iran. It was observed that there was a normal trend in the 9 years, whereas in the year 2005 there were spikes of temperature rise before the earthquake events.

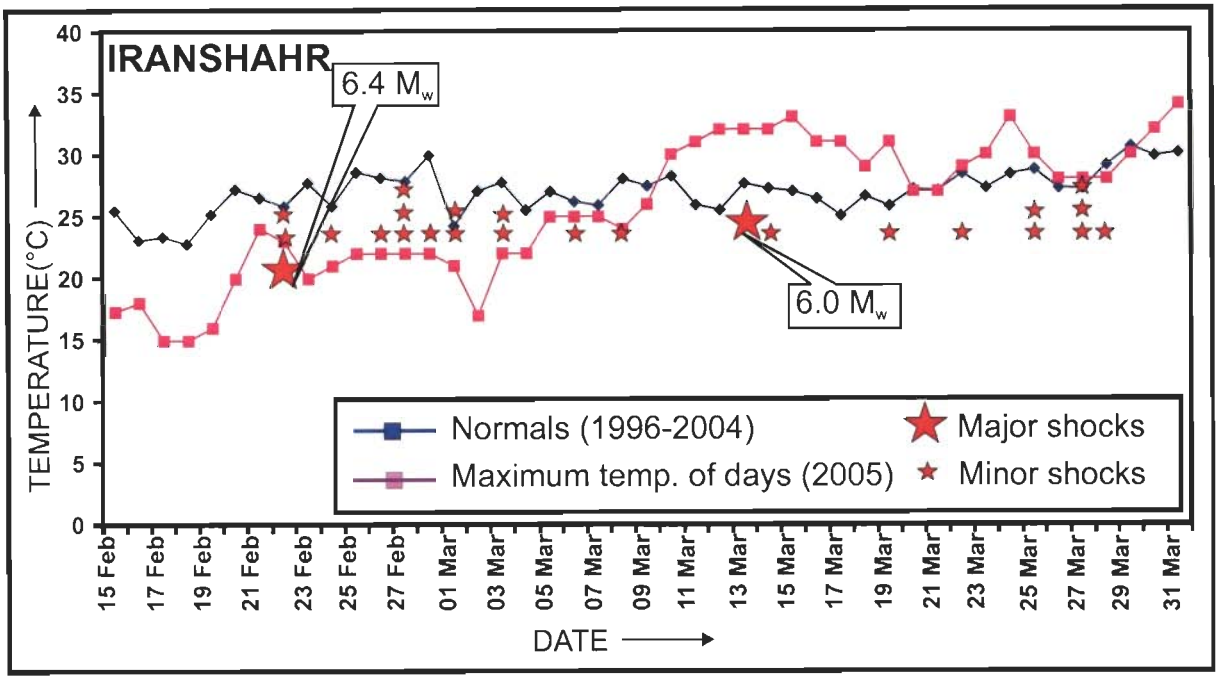

Figure 4.20 (v): Temperature normals (1996-2004) versus Temperature Variation Curves (TVC) of the year 2005 (around the time of the series of earthquakes in 2005) of the Iranshahr city in Iran. It was observed that there was a normal trend in the 9 years, whereas in the year 2005 there were spikes of temperature rise before the earthquake events.

4.1.4 BANDA ACEH EARTHQUAKE, SUMATRA

The violent earth's manifestation can be visualized in this century's fourth largest earthquake of magnitude (M_w) 9.0 in Sumatra on 26 December 2004 at 00:58 hours (UTC), which originated at a depth of about 30 km (epicenter at 3.32° N latitude and 95.85° E longitude, figure 4.21). The earthquake was felt at Banda-Aceh with intensity IX, at Meulaboh with intensity of VIII and at Medan, intensity IV, Sumatra and in parts of Bangladesh, India, Malaysia, Maldives, Myanmar, Singapore, Sri Lanka and Thailand with III-V intensity (http://neic.usgs.gov/neis/eq_depot/2004/eq_041226/). This megathrust earthquake generated a totally unexpected Tsunami in the Indian Ocean and Bay of Bengal whose fury left more than 283,100 people dead, 14,100 missing and more than 1,120,000 displaced in numerous countries; the effects of which were felt as far as East Africa. The Indian Ocean and the Bay of Bengal has rare records of Tsunamis in the past. This Tsunami is the direct consequence of about 1300 km long thrust faulting (figure 4.22), which ruptured undersea displacing huge volumes of water in the Indian Ocean and the Bay of Bengal. Numerous aftershocks ranging in magnitude (M_w) from 3 to > 7 rocked the region from Simeulue Island (Sumatra, Indonesia) in the south to near Landfall Island (North Andaman, India) in the north. Twenty-five aftershocks were of magnitude (M_w) 6.0 or greater, the strongest one being of magnitude 7.1 that occurred on 26 December 2004 at 04:21 hours (UTC) (epicenter at 6.91° N latitude and 92.96° E longitude, figure 4.21). This mega event was followed by another powerful earthquake of magnitude (M_w) 8.7 on 28 March 2005 at 16:09:36 (UTC). This earthquake killed more than 1000 people and brought about huge damage in Simeulue. Several strong aftershocks followed the main earthquake event, including a 6.0 magnitude earthquake at 16:38 UTC and a 6.1 shock at 18:30 UTC (http://asc-india.org/events/050328_bob.htm). An earthquake of such magnitude after the 9.0 magnitude (M_w) earthquake on Boxing Day, 2004 was unexpected. The 28 March 2005 earthquake was located at 2.07° N latitude and 97.01° E longitude, on a segment of the fault, 160 kilometers to the southeast of the rupture zone of the magnitude 9.0 (M_w) Sumatra earthquake (http://neic.usgs.gov/neis/eq_depot/2005/eq_050328/neic_weax_ts.html). This

earthquake is believed to be triggered by stress changes caused by the December 2004 earthquake.

The earthquake occurred in the plate boundary where the North-East moving Indian plate is subducting under the Burmese micro-plate with the Sunda trench as undersea surface expression (figure 4.23). The movement of the plate is almost at a rate of 6 cm/year (http://neic.usgs.gov/neis/eq_depot/2004/eq_041226/neic_slav_ts.html). The movement of the Indian/Australian plate towards Eurasia is oblique and this movement is partitioned into thrust-faulting and strike-slip faulting. The movement along the Sunda megathrust during the Sumatra earthquake has caused overriding of Burmese Plate over the Indian Plate. The rupture length (oriented parallel to the Sunda trench) of the thrust is estimated to be 1300 km, the width of the earthquake rupture measured perpendicular to the Sunda trench is about 150 km. The maximum displacement on the thrust plane is reported to be 20 m (http://neic.usgs.gov/neis/eq_depot/2004/eq_041226/neic_slav_ts.html).

4.1.4.1 ANALYSIS

Pre- and post-earthquake, daytime NOAA-AVHRR Global Area Coverage (GAC) data (table 4.8) have been used to study the thermal regime of the land region around the Sunda Trench and the tectonic zone extending up to Myanmar. The region was quite cloudy around the time of the earthquake. However, regions, which were free from clouds, were analyzed. Thermal channels 4 and 5 of NOAA-AVHRR were used to calculate the LST of the study area. The LST calculation is based on the method provided in http://perigee.ncdc.noaa.gov/docs/klm/html/c7/sec7-1.htm#sec71-2. User specified temperature range of –50° C to 35° C was used and temperature outside this range was masked. Cloud covers were delineated and avoided for any temperature calculation.

For studying the turbidity conditions of the seawater after the fault rupture undersea, visible channel 1 (5.8-6.8 μm) of NOAA-AVHRR GAC datasets (table 4.9) was used. This channel is best to measure the solar reflectance of the sea in

the orange–red part of electromagnetic spectrum. Visible channel data from Moderate Resolution Imaging Spectroradiometer (MODIS) on board Terra satellite (table 4.10) have been used to study the turbidity in seawater due to the devastating Tsunami generated by the earthquake.

Table 4.8: Time of acquisition of NOAA-AVHRR GAC data used to prepare LST time series maps to study pre-earthquake thermal anomaly

S. N.	Date	Time of GAC Acquisition (UTC)
1	16 December 2004	03:11 to 05:04
2	17 December 2004	02:46 to 04:41
3	20 December 2004	03:19 to 05:12
4	21 December 2004	02:55 to 04:49
5	25 December 2004	03:05 to 04:58
6	26 December 2004	02:41 to 04:36
7	28 December 2004	03:36 to 05:30

Table 4.9: Time of acquisition of NOAA-AVHRR GAC data, used for analysis of seismically induced turbidity in the seawater by the mega-thrust earthquake of 26 December 2004

S. N.	Date	Time of GAC Acquisition (UTC)
1	25 December 2004	03:05 to 04:58
2	26 December 2004	02:41 to 04:36
3	29 December 2004	03:13 to 05:07

Table 4.10: Time of acquisition of Terra-MODIS data, used for analysis of tsunami induced turbidity in the seawater by the mega-thrust earthquake of 26 December 2004

S. N.	Date	Time of Acquisition (UTC)
1	22 December 2004	04:00
2	27 December 2004	04:20
3	29 December 2004	04:05

The earthquake on 28 March 2005, three months later of magnitude 8.7 could not be studied using thermal remote sensing data as clouds covered the sky before and after this second mighty Sumatra earthquake and thus prevented a study of the thermal scenario over Sumatra and adjoining areas.

4.1.4.2 OBSERVATIONS

The time series maps show that LST was normal on 9 December 2004. A small anomaly was seen to develop on 13 December 2004. Upto 21 December the whole region was very cloudy. On 21 December 2004 (about five days prior to the main shock on 26 December 2004) temperature was seen to rise in parts of Thailand (figure 4.24). The temperature rose further on 25 December 2004 (one day prior to the main shock). Cloud covered the entire region on 27 December. But on 28 December, the temperature was seen to be normal again. The rise in temperature was about 6-12° C [Saraf et al., 2005 (f)].

The epicenter was offshore Banda-Aceh, Sumatra at a focal depth of 30 km and the surrounding region largely comprises of water bodies. The study of the behavior of Sea Surface Temperature (SST) before and after the earthquake was limited by the cloud covers all the time.

The violent earthquake of magnitude 9.0 and associated aftershocks was caused by the vertical movement of the seafloor (estimated up to 20 m) over a large area (up to 1300 km along the Sunda Trench, reaching up to Andamans Islands). Overriding of Burmese Plate over the Indian Plate has caused the deadly Tsunami. The vertical and horizontal displacements from this earthquake caused slumping of the sea floor (schematic diagram of the possible slumping is shown in figure 4.25). Turbidity in the seawater was observed by AVHRR data as well as MODIS data. There were two kinds of turbidity in the water: (a) that which is introduced by the underwater slumping [with increase of total suspended solids (TSS) with landslides] in the rupture zone, which is visible along the line in which, the Sunda trench passes (figure 4.26); and (b) that which is brought about by the tsunami and is visible in the region along the coastlines and the shallow sea of Sumatra (figure 4.27) and where ever the Tsunami hit.

Channel 1 of NOAA-AVHRR was used to study the turbidity conditions of the seawater because of the rupture and underwater slumping. The GAC acquisition time was around 03:00 to 05:00 UTC; their common area of coverage around that time range from 2° N to 18° N latitudes and 92° E to 104° E longitudes, thus providing coverage of the earthquake affected region just after the earthquake event. Cloud free scenes were analyzed for this study. The pre-earthquake scene (on 25 December 2004) shows that the seawater was clear before the earthquake (figure 4.26). Turbidity in the seawater was seen to appear on 26 December 2004 in images acquired after the earthquake (table 4.9). The clarity of the water was seen again on 29 December 2004.

Terra-MODIS data was used for analysis of the turbidity around the coast of Sumatra induced by Tsunami after the earthquake. Satellite data on 22 December 2004 of the coastline of Sumatra shows a clear coast and a serene sea. On 27 December the seacoast and seawater was rough and turbid with suspended materials after the tsunami picked up sediments from the coast (figure 4.27). Several coasts in the Indian Ocean were severely damaged, with human death and immense loss to properties. The suspended materials lessened, but stayed on till 29 December 2004

4.2 PRE-EARTHQUAKE THERMAL ANOMALY STUDY THROUGH DMSP-SSM/I DATA

The Special Sensor Microwave Imager (SSM/I) on board Defense Meteorological Satellite Program (DMSP) (vide Chapter 3, Section 3.2.1) has been successful to detect definite buildup of temperature prior to several major earthquakes, which occurred around the world (India, China, Afghanistan and Pakistan) over the past thirteen years (table 1.2). The SSM/I has the advantage of being transparent to clouds (but has a coarser resolution; 4 km spatial resolution). The SSM/I data available for the study was weekly average maps, which were constructed as temperature anomaly maps with respect to the base period of 14 years (1988-2002). Through the analysis of SSM/I data, pre-earthquake thermal anomaly was detected to occur prior to all the earthquakes in

table 1.2 in Chapter 1. The anomalies appeared around a week or a few days before the earthquakes [Saraf and Choudhury, 2005 (c)].

4.2.1 KALAT EARTHQUAKE, PAKISTAN

On 4 March 1990 a shallow focus earthquake of magnitude 6.1, hit the Kalat region of the province of Balochistan in Pakistan (figure 4.28) (epicenter at 28.92° N latitude and 66.33° E longitude, and focal depth 10 km) at 19:46:19 (UTC) (table 1.2). The earthquake led to 11 deaths, injury to 40, and damage to structures and homes, especially in the Kalat area. The earthquake was also felt at Quetta and Mastung (http://neic.usgs.gov/neis/eqlists/sig_1990.html).

To the north and western sections of Pakistan lies the boundary of the Indian and the Iranian plates along with the Afghan micro plates. The Indian and the Eurasian plates are converging towards each other at a rate of 5 cm per year (http://asc-india.org/menu/seismi.htm). This convergence generates complex stresses in the region resulting from both subduction and rotation of continental blocks. Earthquakes especially occur in this region due to this plate activity and the associated faulting. The Chaman fault runs along Pakistan's western frontier with Afghanistan from Kalat, in the northern Makran range, past Quetta and then to Kabul (http://asc-india.org/seismic/pakistan.htm).

4.2.1.1 OBSERVATIONS

SSM/I weekly average temperature anomaly maps for the Kalat Earthquake showed that a small anomaly started appearing in the epicentral area two weeks before the earthquake hit the Kalat region in Pakistan [figure 4.29 (a)]. In the next week between 19 and 25 February 1990, the anomaly intensified to a maximum with around 2-10°C difference of temperature than the usual temperature for the base period of 14 years in the anomaly maps. The anomaly remained for over a week and occupied a small area like a linear arch around the epicenter [figure 4.29 (a)]. This anomalous rise was seen to disappear in the week from 26 February - 4 March 1990, just before the earthquake. Similar weekly surface temperature maps were also constructed for the year 1989 for the

same weeks as for 1990, for a comparison of the thermal conditions of the region in 1989. The region showed no such unusual variation in temperature around that time in 1989 [figure 4.29 (b)].

4.2.2 ZHANGBEI EARTHQUAKE, CHINA

An earthquake of magnitude 6.2 (M_L), occurred in the Zhangbei region in the Hebei province, about 180 km northwest of Beijing on 10 January 1998 (table 1.2), with its epicenter located at 41.08 N and 114.50 E longitude (figure 4.30). The earthquake left 70 dead, about 11,500 injured, 44,000 families homeless, along with extensive damage to concrete structures in the Shangyi-Zhangbei region. In and around the epicenter an area of 500 km^2 was rocked by numerous aftershocks, the largest of them being of magnitude 4.6. Around 90% of the houses have been damaged in Zhangbei alone (http://www.cnn.com/WORLD/9801/10/china.quake.update/mackinnon.30.aiff). Even damage to the Great Wall of China was reported in northwestern Hebei Province (http://neic.usgs.gov/neis/eqlists/sig_1998.html). The earthquake was felt strongly at Zhangjiakou and as far as Beijing. Past seismic history reports the experience of very few earthquakes by this region.

Geological structures in and around the Zhangbei epicenter (capable of generating moderate earthquakes) were not marked before and after the earthquake. But two conjugate surface features trending NNE-NE and NNW–WNW have been discovered by field investigation (www.cosis.net/abstracts/EAE03/08814/EAE03-J-08814.pdf). The structure attributing to this shock, however, can be regarded as a N10-20° E striking fault with right lateral reverse slip and tectonically driven compressional stresses (www.cosis.net/abstracts/EAE03/08814/EAE03-J-08814.pdf).

4.2.2.1 OBSERVATIONS

Anomaly for the Zhangbei earthquake appeared almost three weeks before the earthquake. The week beginning from 17 up to 24 December 1997, started to pick up a thermal anomaly with an increase of temperature of about 1-

4° C as compared to the normal temperature of the area towards the northeast of the epicenter. In the next week, from 25 - 31 December 1997 an area to the south of the epicenter also showed an increase in temperature of about 4-8° C than the temperature in the base map for 14 years. This anomaly covered a large area, covering all southeast provinces like Guangxi, Guangdong, Fujiyan, Jiangxi, Henan and Hubei in the east amongst others. Guangxi and Guangdong experienced an increase of temperature of about 10° C. This anomaly was the most intense two weeks before the earthquake, i. e., in the week beginning from 25 up to 31 December 1997 (figure 4.31). The anomaly disappeared after the earthquake.

Similar observations were also reported in China and increase of temperature about 14 days prior to the earthquake was seen (www.gisdevelopment.net/aars/acrs/1999/ps6/ps61179a.shtml). The analysis of NOAA-AVHRR datasets by Chengyu et al. (1999) gives the location and magnitude of the thermal anomaly similar to that observed by the SSM/I data in the present study.

4.2.3 IZMIT EARTHQUAKE, TURKEY

The Izmit or Kocaeli Earthquake, which struck Turkey on 17 August 1999 (table 1.2) with a magnitude of 7.6 at 00:01:39 (UTC) was centered at 40.74° N latitude and 29.86° E longitude (figure 4.32), 90 km east of Istanbul and was felt as far as Ankara, about 320 km from the epicenter. The devastating main shock lasted for 37 seconds. The quake killed about 18,000 people, injured around 50,000, with thousands of people missing, left about 500,000 people homeless (http://neic.usgs.gov/neis/eq_depot/2003/eq_030501/) and caused a damage amounting to 3 to 6.5 billion U.S. dollars in Istanbul, Kocaeli and Sakarya Provinces. The shock was felt also in the neighbouring places of Anapa, Russia; Chisinau, Moldova; Simferopol and on the south coast of Crimea, Ukraine. Various districts of Istanbul and the provinces of Izmit (Kocaeli), Adapazari (Sakarya), Yalova, Bursa, Eskishir, and Bolu have been affected. This earthquake was located on a rupture on the Anatolian Fault on a seismic gap

between the 1967 Mudurnu Valley earthquake of magnitude 7.1 and the 1963 Yalova earthquake of magnitude 6.4.

The earthquake originated at a shallow depth of about 17 km and generated strong ground motion (and moderate to high accelerations) in the region of the Gulf of Izmit of the Sea of Marmara up to east of Adapazari. It occurred along the northernmost strands of the 1300 km long North Anatolian fault system with a right-lateral strike-slip movement on the fault (figure 4.32). This fault which is similar to the San Andreas Fault of America is one of the most seismically active faults of the world and has produced eleven earthquakes with magnitudes greater than 6.7 since 1939. Earthquakes in Turkey are generated by the movement of the Arabian plate towards the Eurasian plate and the associated fault system. A block of continental crust almost the size of Turkey, called the Anatolian block, is being squeezed to the west. The block is bounded to the north by the North Anatolian Fault and to the south-east by the East Anatolian fault. Initial field observations indicate that the earthquake produced at least 60 km of surface rupture and right-lateral offsets as large as 2.7 m along a 120-km zone of the North Anatolian Fault between Karamursel and Golyaka. Rupture proceeded from west to east in two sub-events (http://neic.usgs.gov/neis/eqlists/sig_1999.html). The Izmit earthquake is one of the events in a largely westward progression of the large earthquakes along the North Anatolian fault.

4.2.3.1 OBSERVATIONS

The SSM/I derived weekly anomaly maps for the Izmit earthquake clearly showed an increase in temperature of the region before the deadly event. The anomaly was centered on the epicenter, but spread around over a vast area over Western Turkey. The anomaly started building up in the week beginning from 6 August 1999. The anomaly map of this week showed a difference in temperature of 2-6° C in the region (figure 4.33). The next week witnessed a boost of temperature with an increase of 6-10° C with respect to the base period of 14 years. This anomaly disappeared in the week right after the 19 August 1999

earthquake and since 20 August 1999 showed similar temperature values as normal.

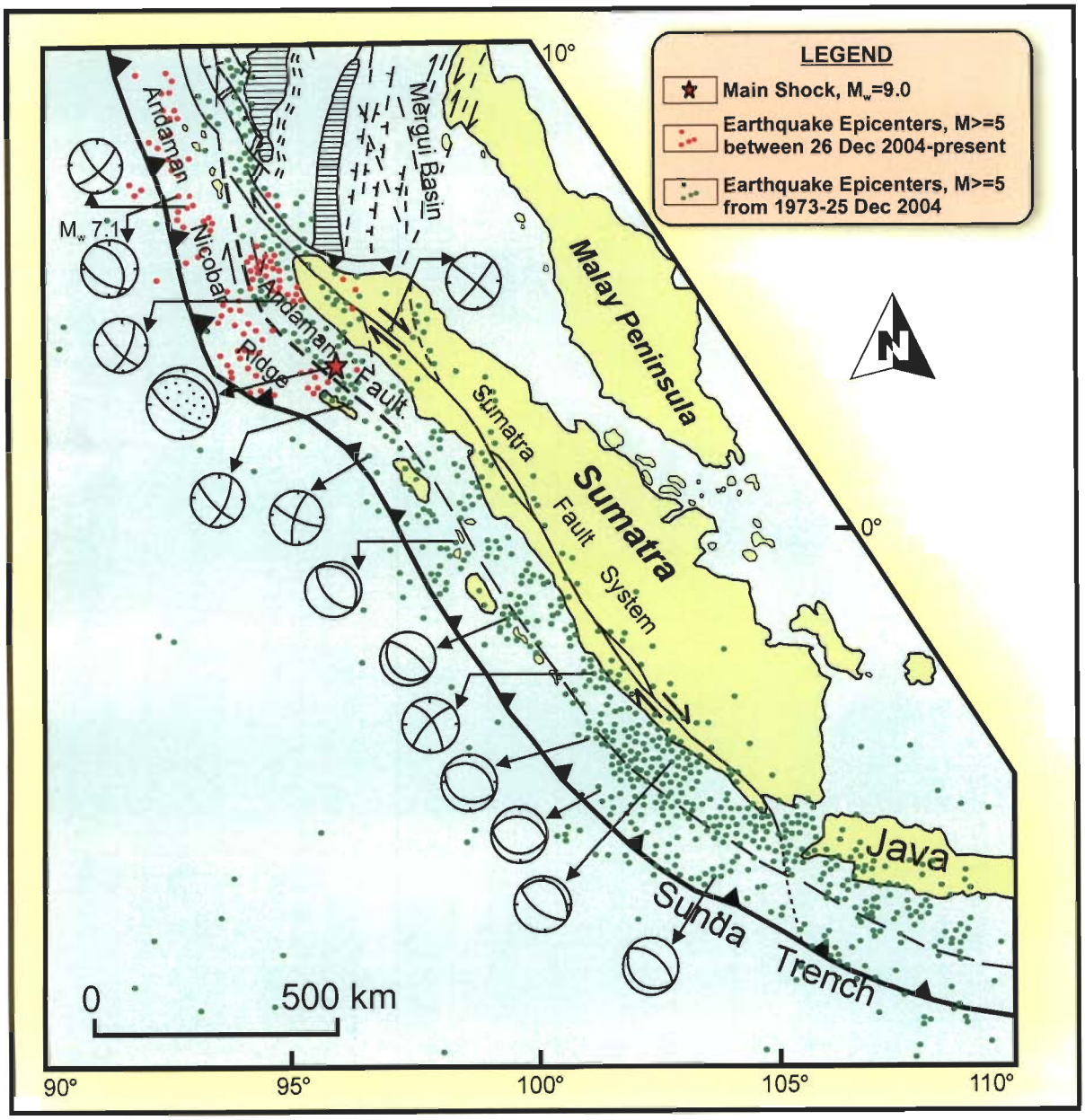

Figure 4.21: Location of the megathrust Great Sumatra Earthquake of 26 December 2004, along with locations of aftershocks around the main shock and focal mechanism of major shocks and aftershocks (Das et al., 2005). Figure also shows the locations of shocks from 1973 to present in the region. Locations obtained from USGS site (http://neic.usgs.gov/).

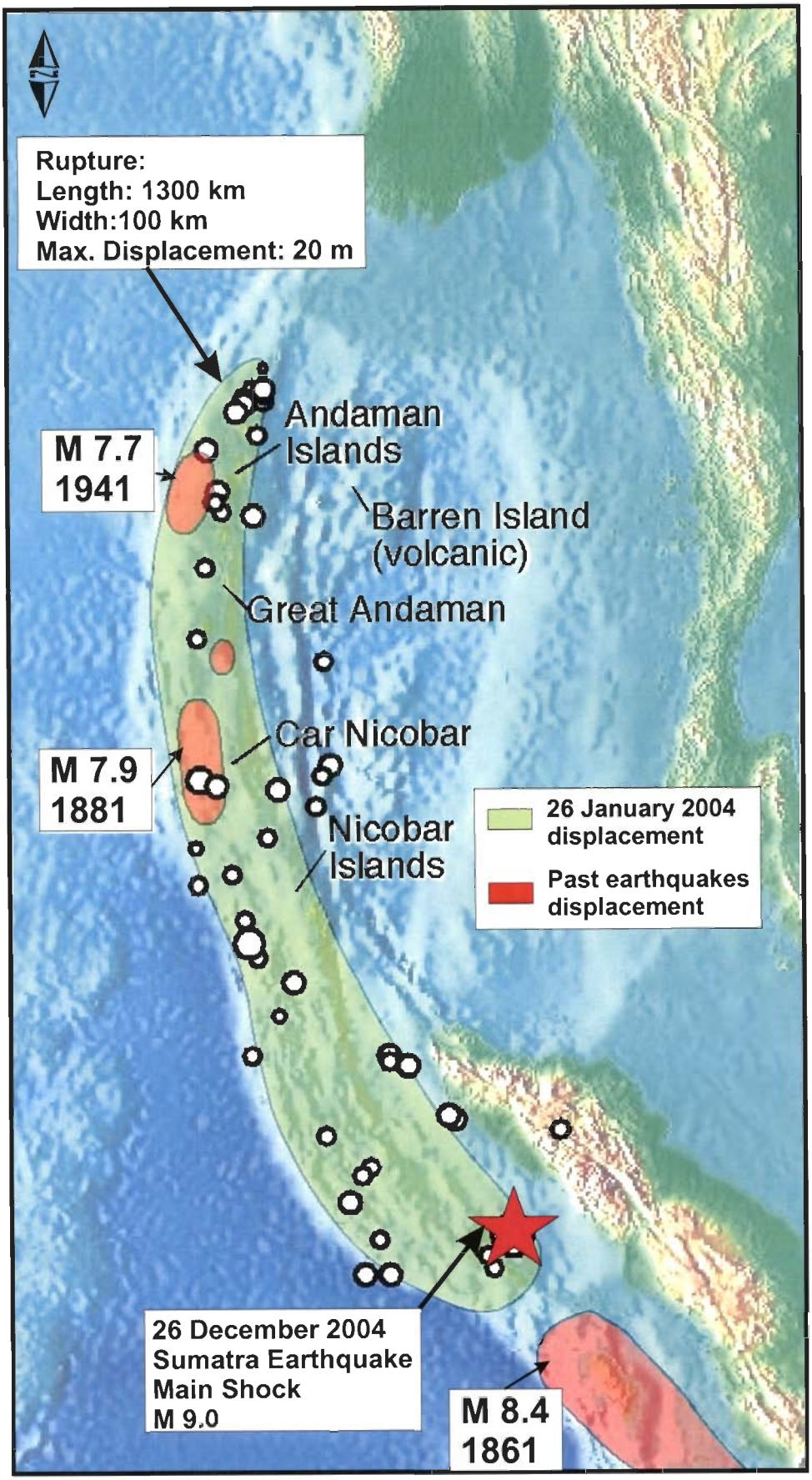

Figure 4.22: Rupture length associated with the great Sumatra earthquake of 26 December 2004, in comparison to other important earthquakes of the past (Source: Bilham, http://cires.colorado.edu/~bilham/IndonesiAndaman2004_files/).

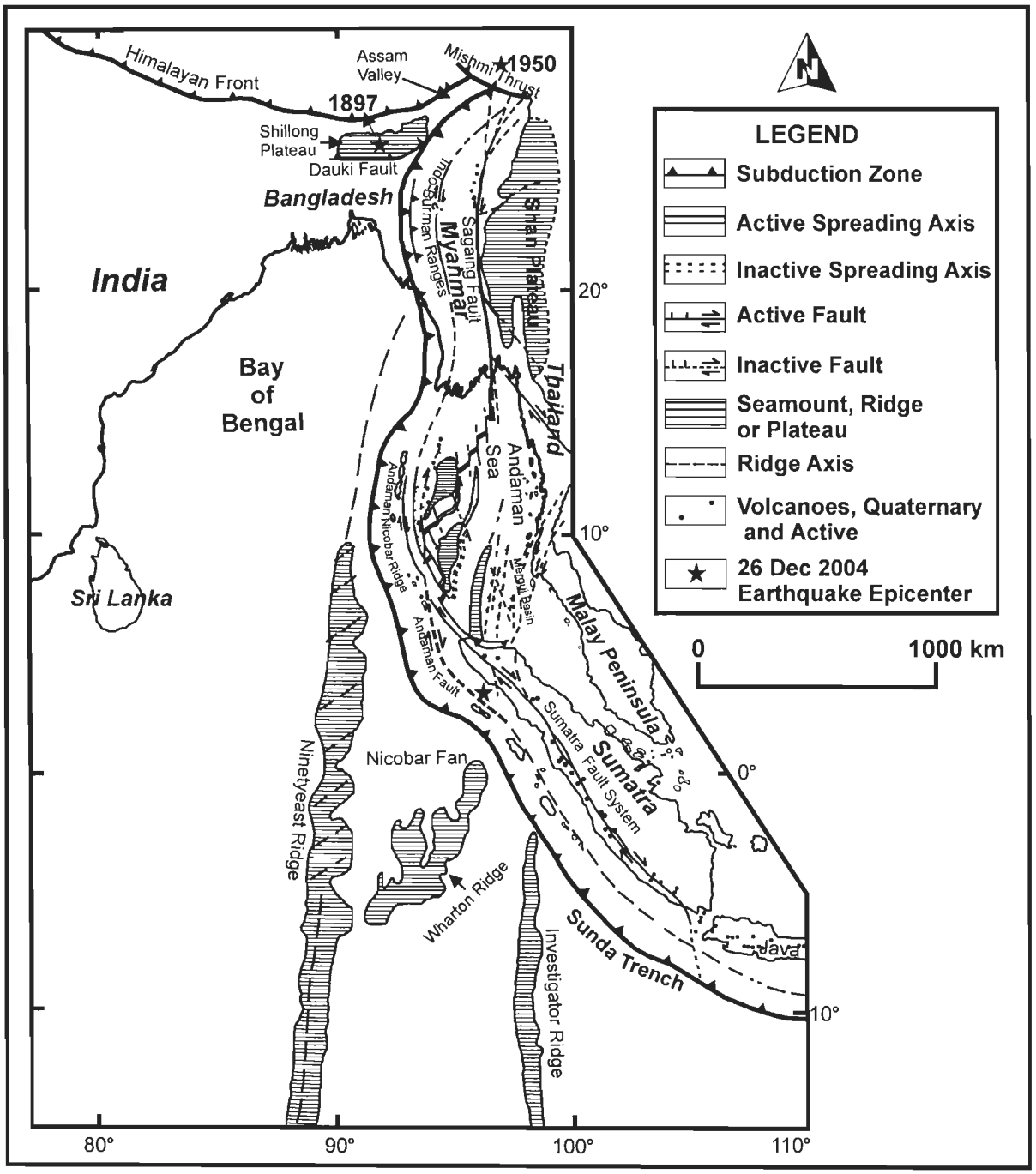

Figure 4.23: Tectonic features of Sumatra and the Andaman-Nicobar region, plate movement on which led to the great mega-thrust earthquake on 26 December 2004 (after, J. R. Curray, 1991 and Das et al., 2005).

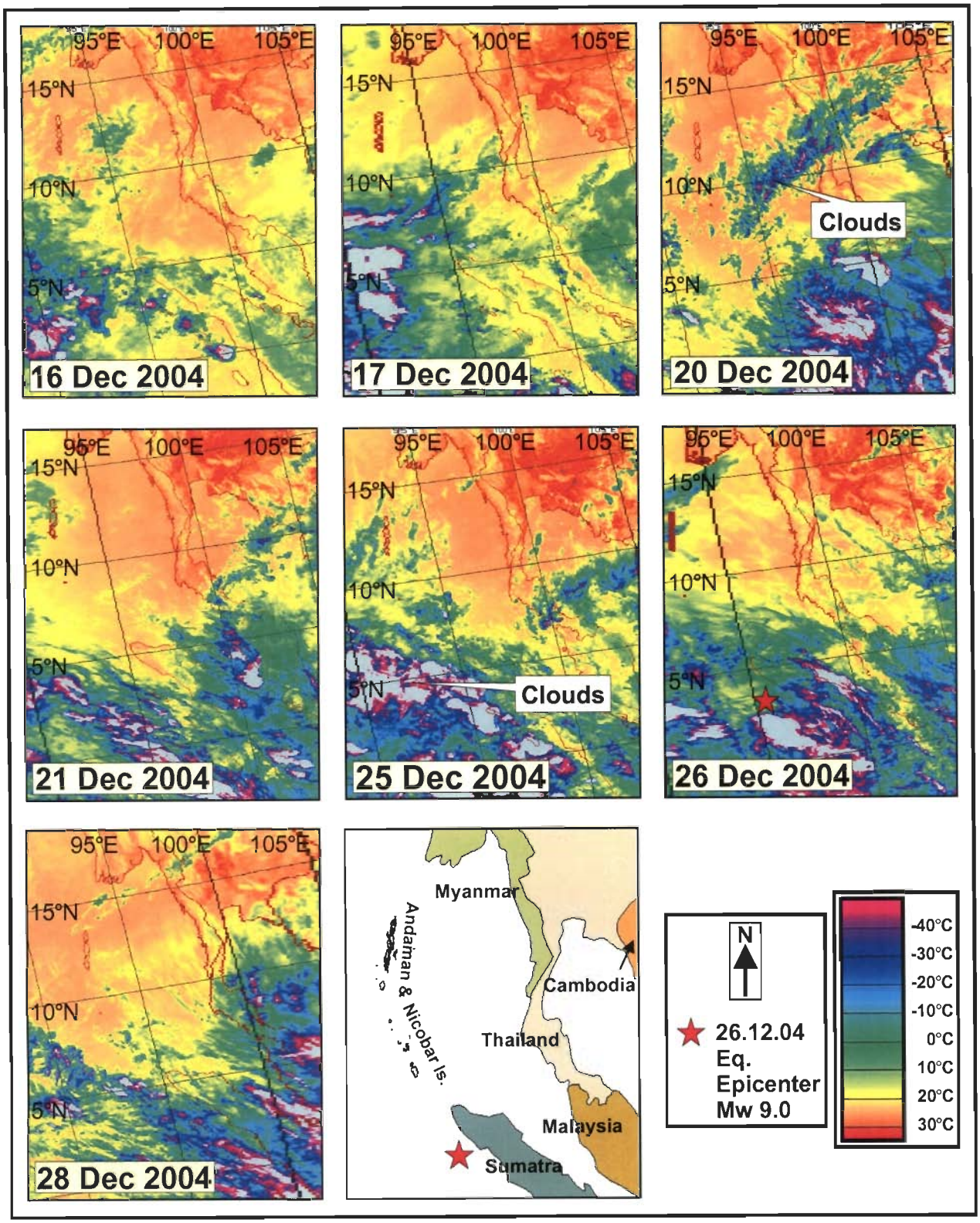

Figure 4.24: NOAA-AVHRR Time Series LST Map of the megathrust earthquake in Banda-Aceh (Sumatra). Clouds covered almost the entire region around the epicenter on the days before and after the earthquake. However, a thermal anomaly appeared to be at its peak on 25 December 2004 (just one day before the earthquake) in the Myanmar-Thailand region.

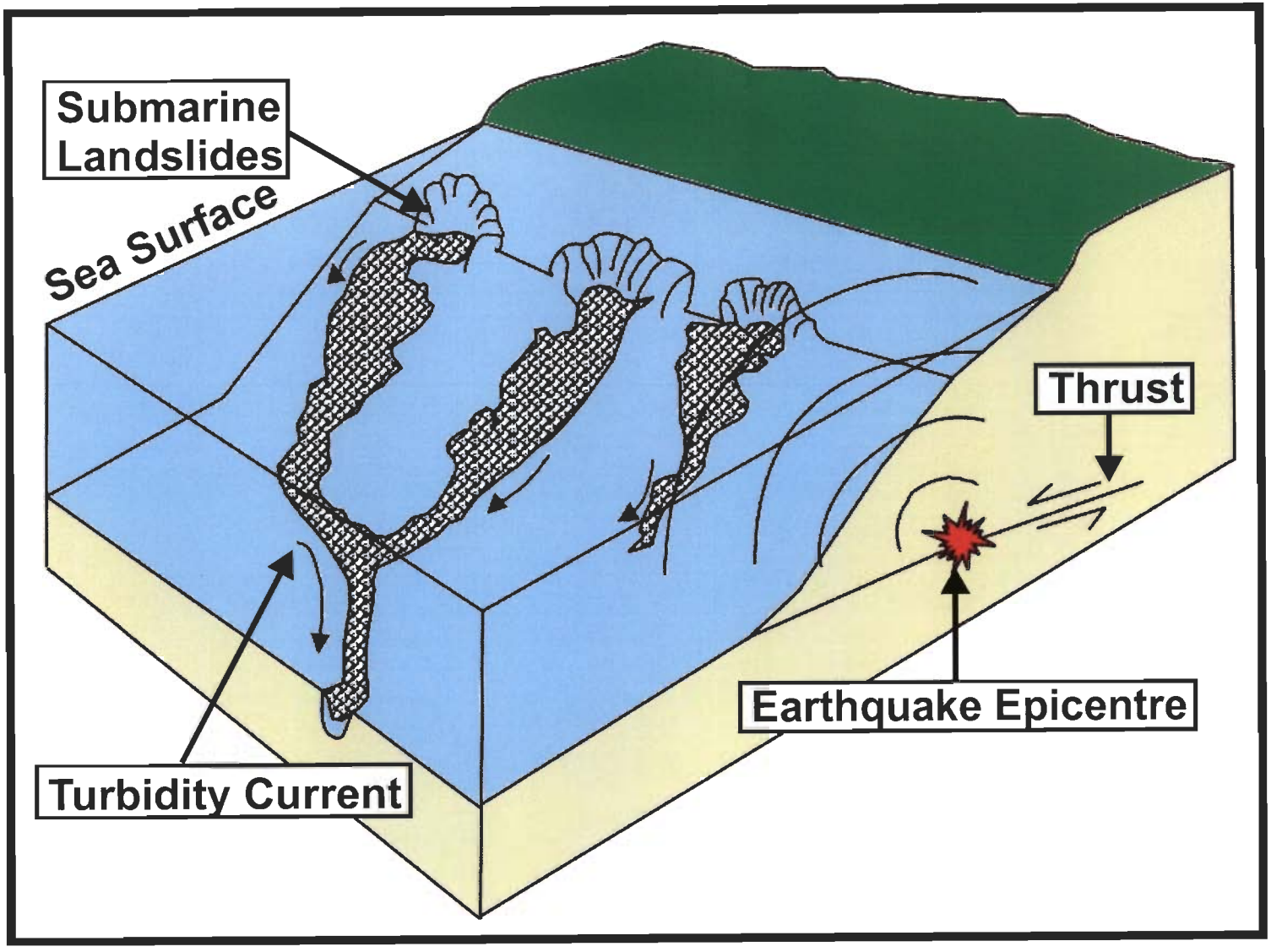

Figure 4.25: Schematic diagram showing slumping and landslide underwater brought about by earthquake rupture under the sea, similar to the one that occurred during the great Sumatra earthquake on 26 December 2004, which brought about a rupture of the length of 1300 km.

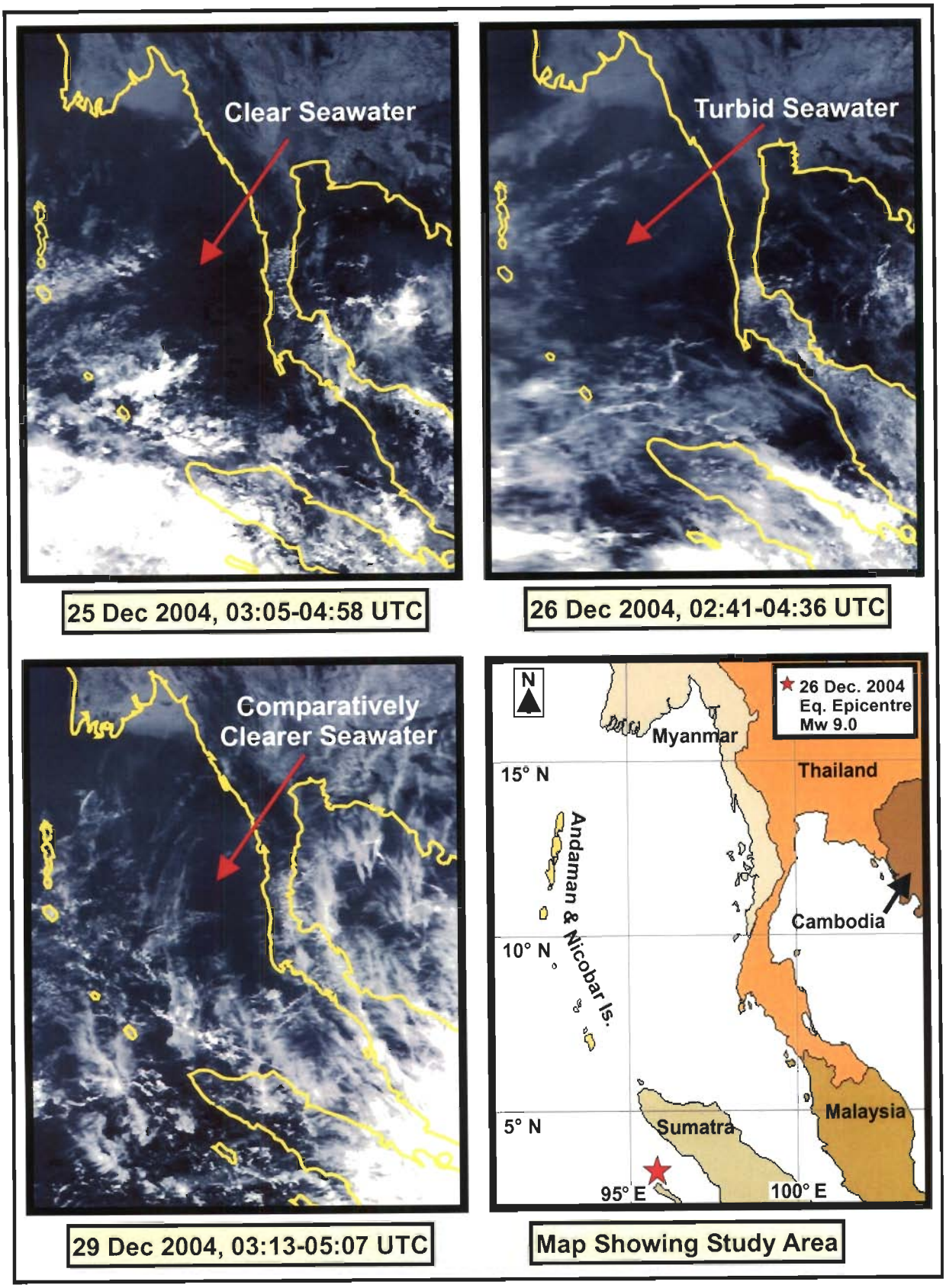

Figure 4.26: NOAA-AVHRR (channel 1) data shows turbidity in the sea caused by underwater slumping due to the rupture associated with the great Sumatra earthquake on 26 December 2004.

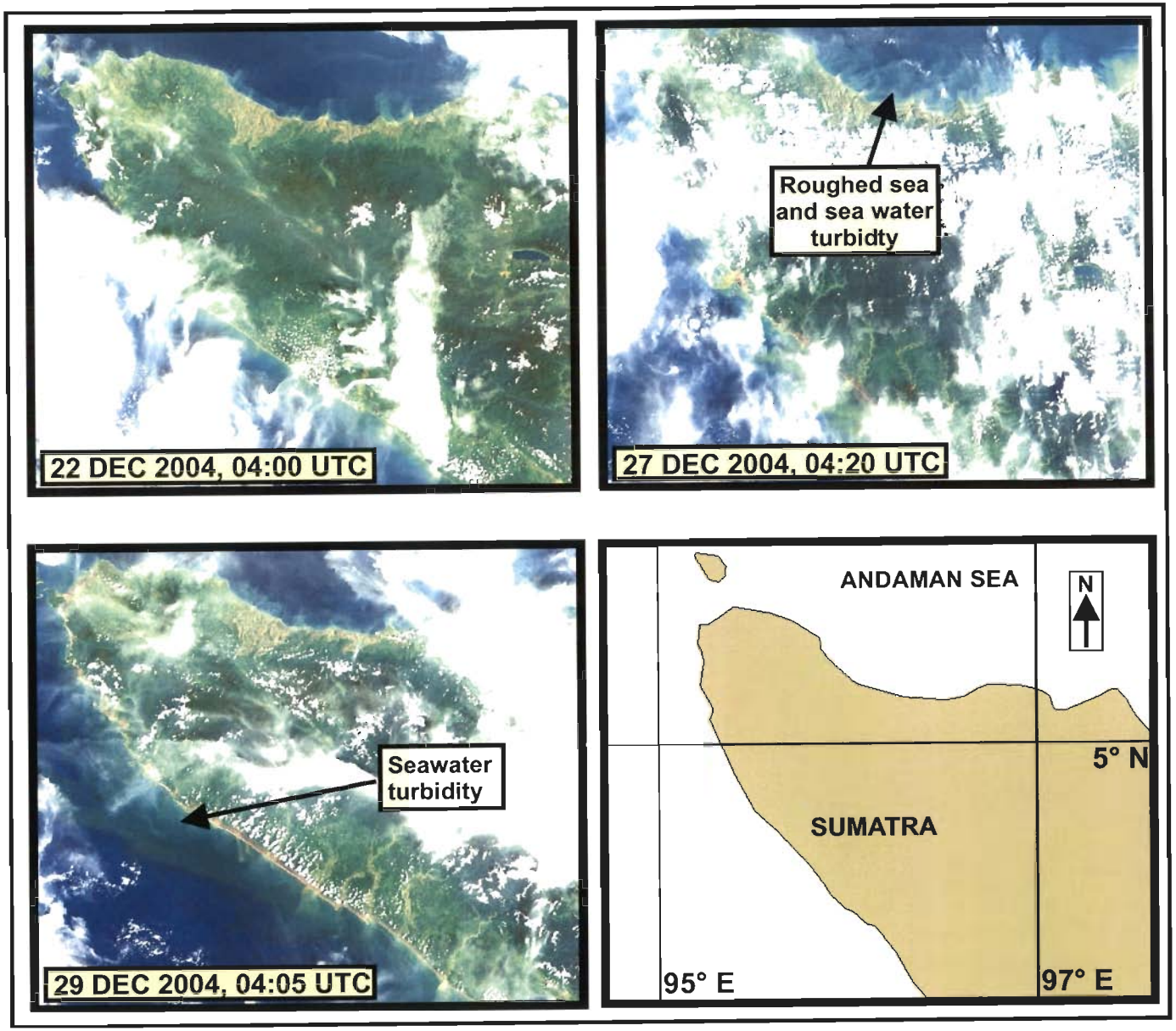

Figure 4.27: MODIS Visible channel shows turbidity in the seawater (induced by the deadly Tsunami) along the coast after the great Sumatra earthquake on 26 December 2004.

Figure 4.28: Location of the 4 March 1990 Kalat Earthquake in Pakistan.

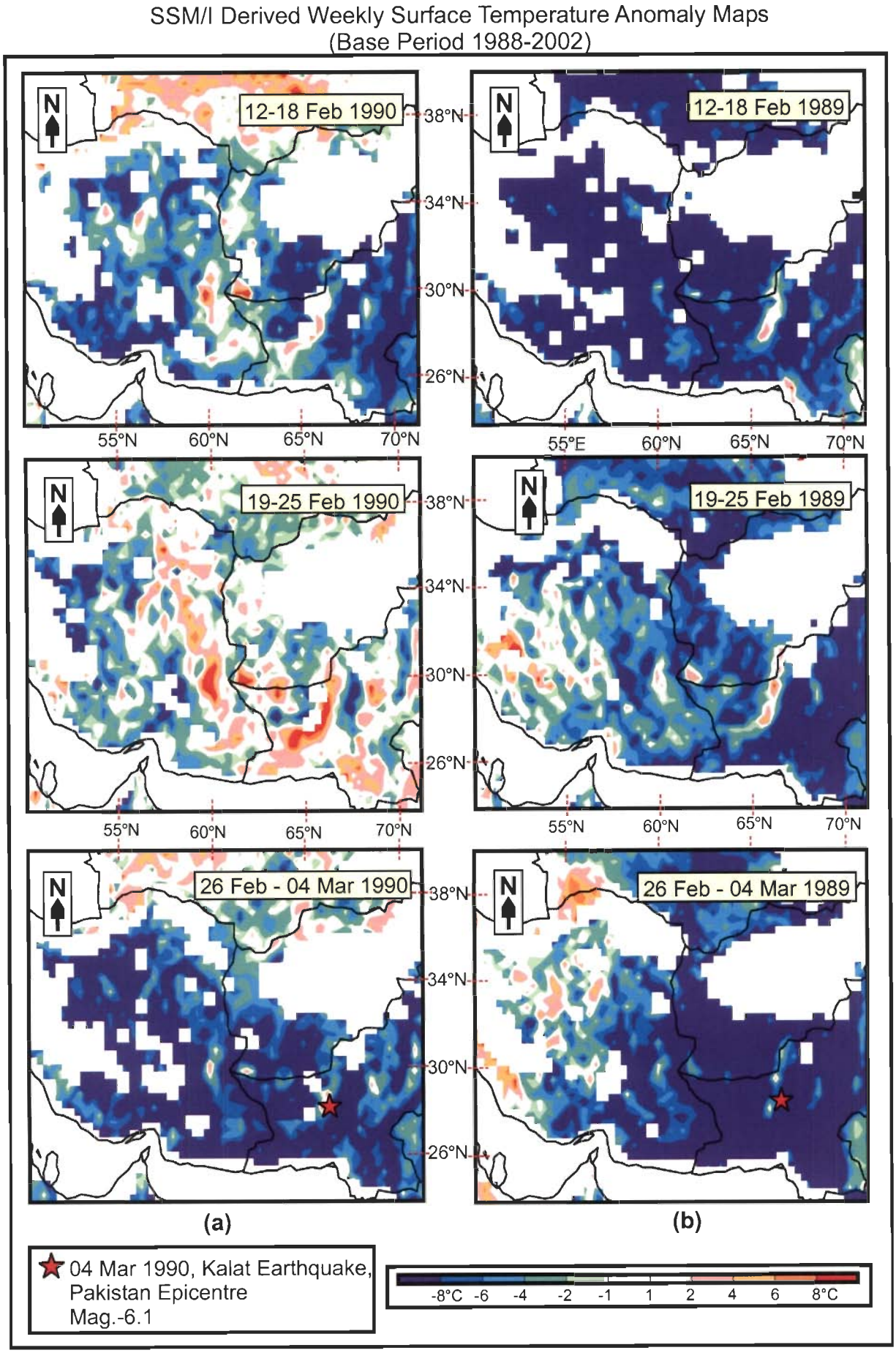

Figure 4.29: Temperature anomaly maps of the region around the epicenter of the Kalat earthquake in Pakistan (a) of the year 1990, in which the earthquake occurred, and (b) 1989, one year prior to the earthquake. A thermal anomaly was observed before the Kalat earthquake. Time series maps in 1989 showed normal thermal scenario.

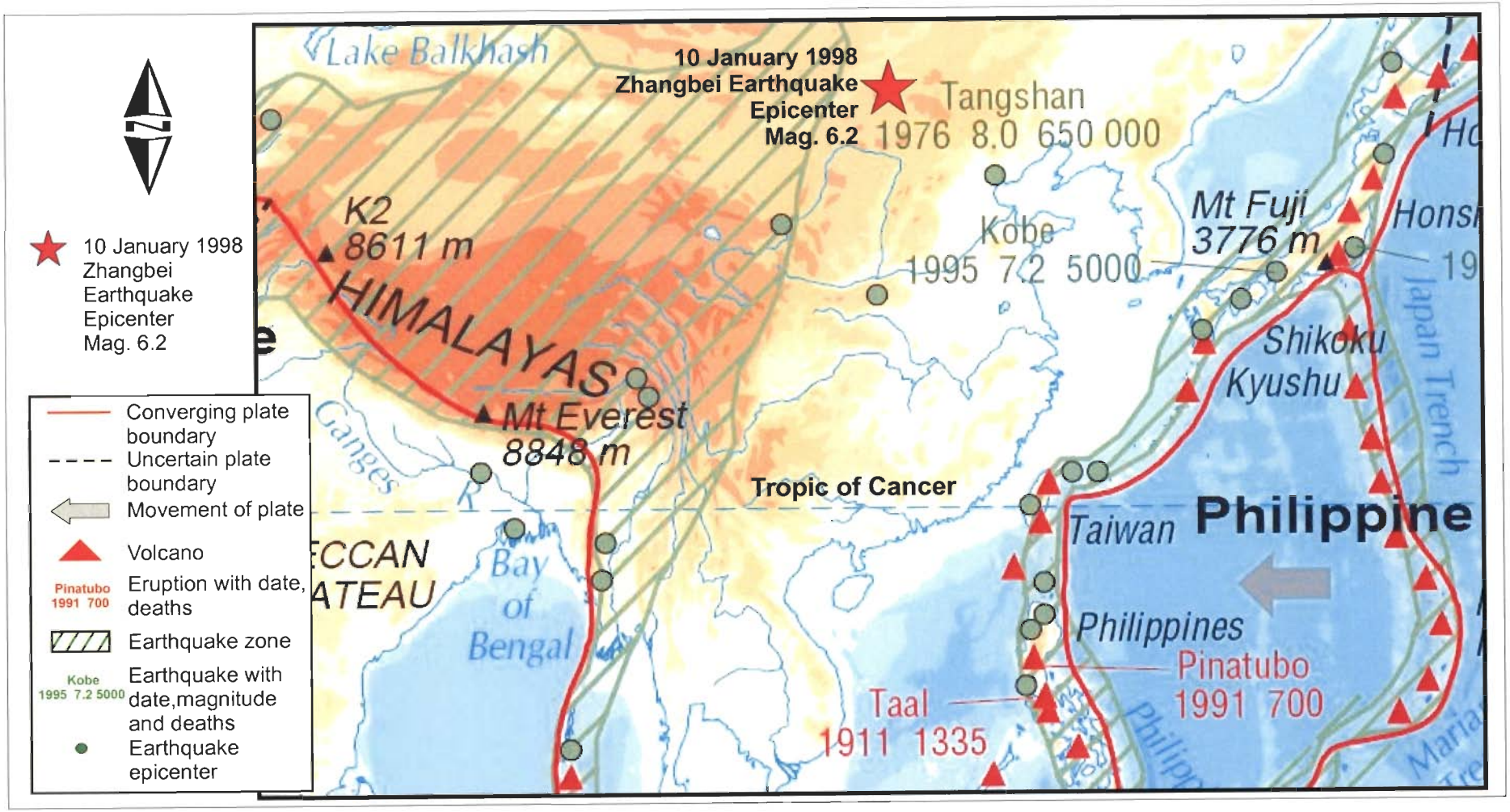

Figure 4.30: Location of the epicenter of the Zhangbei earthquake on 10 January 1998 in China. Also shows tectonics, past major seismicity and volcanism around the region (after http://www.jaconline.com.au/jacatlas5e/downloads/samplepages/activeearth.pdf).

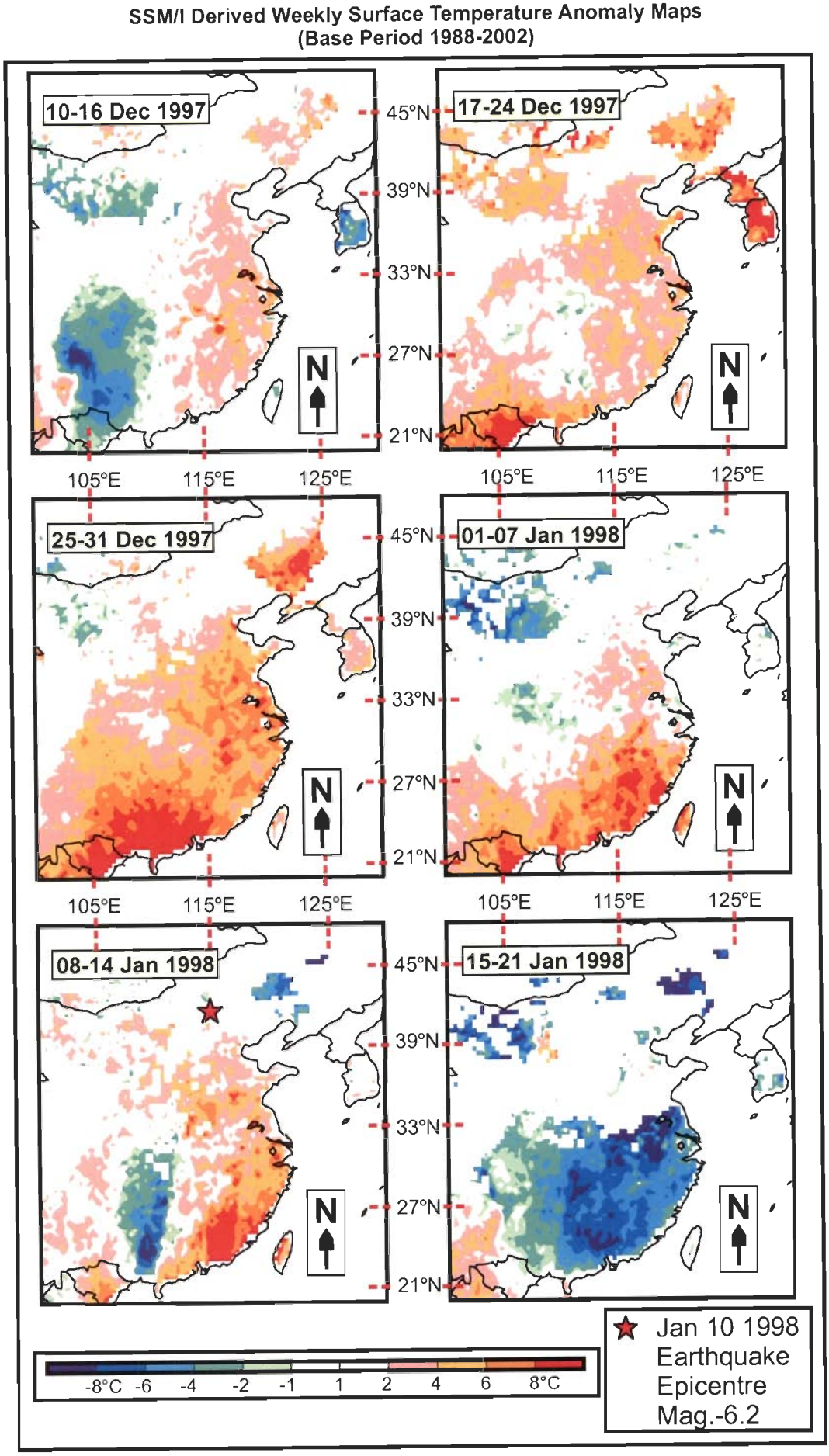

Figure 4.31: Anomaly maps of the region around the Zhangbei earthquake epicenter. A thermal anomaly appeared around three weeks before the earthquake and was maximum in the week beginning from 25 December 1998. The anomaly went away along with the earthquake.

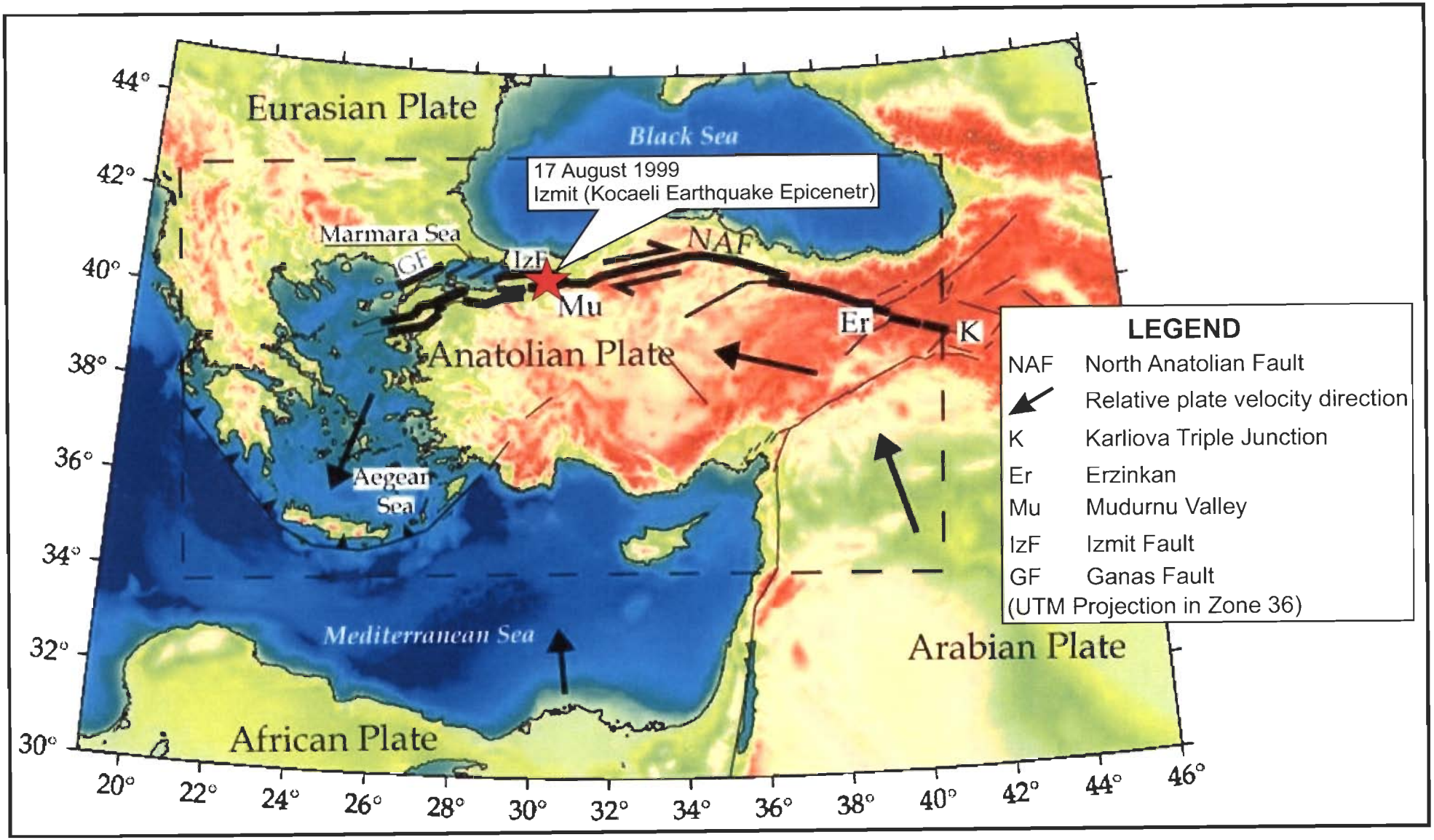

Figure 4.32: Location of the great Izmit (Kocaeli) earthquake of 17 August 1999. Figure also shows the active tectonics and the right lateral strike-slip Anatolian fault, movement on which has produced numerous earthquakes in Turkey (after A-S Provost et al., 2003, http://www.isteem.univ-montp2.fr/PERSO/chery/Adeli_web/web_expe/NAF/PLOT/Image_naf_setup.jpg).

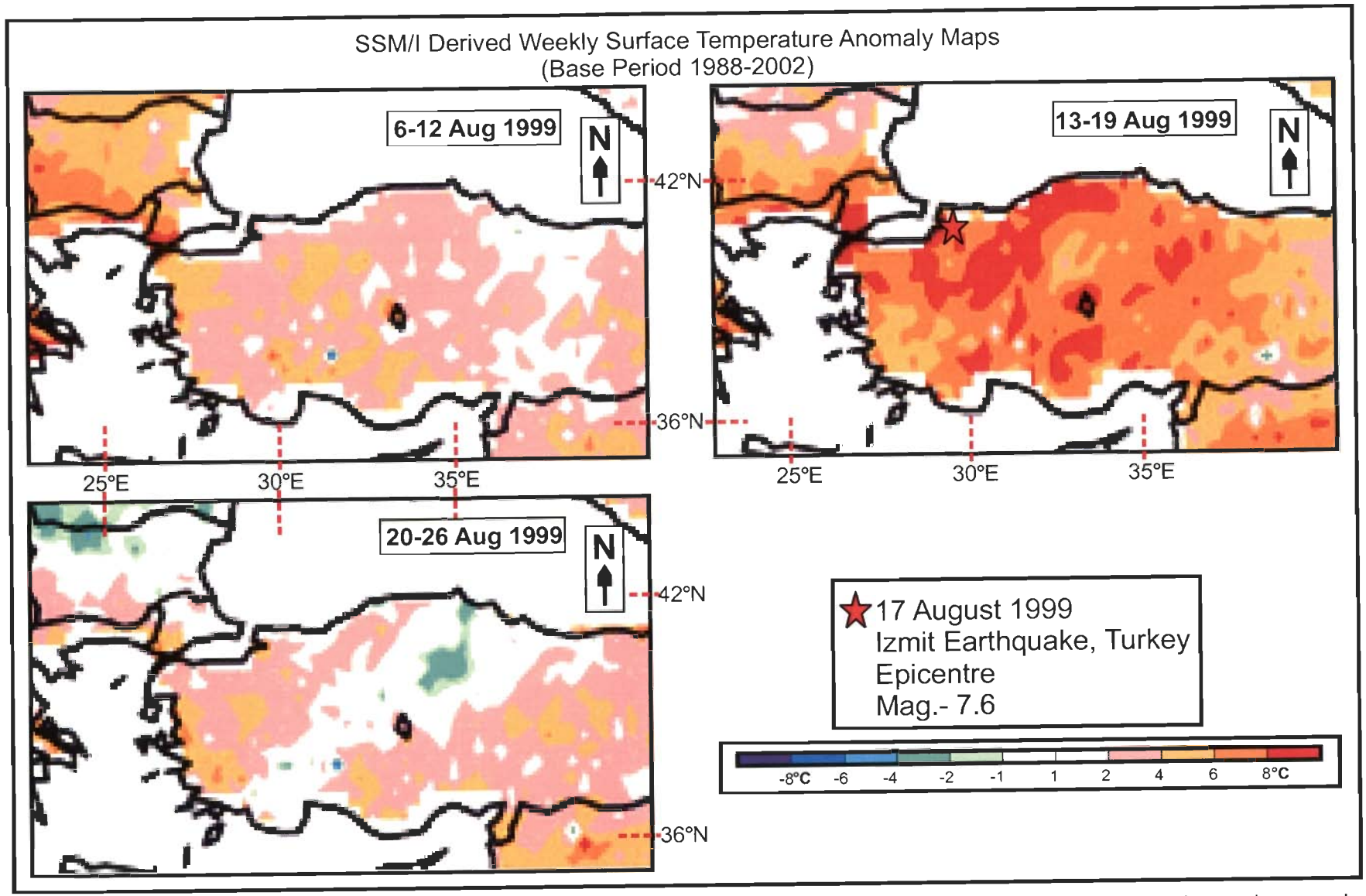

Figure 4.33: Anomaly maps for the Izmit earthquake. The week beginning from 13 August 1999, showed a thermal anomaly developing around the epicenter of the 17 August 1999 earthquake.

4.2.4 BHUJ EARTHQUAKE, INDIA

The earthquake in Bhuj, India on 26 January 2001 of magnitude 7.7 was also studied through NOAA-AVHRR datasets (vide Section 4.1.1).

4.2.4.1 OBSERVATIONS

Similar to the analysis through NOAA-AVHRR datasets of the Bhuj earthquake, SSM/I data also shows anomalous behavior of surface temperature before the earthquake around the same period. The rise of temperature was about 4-8° C in the region with respect to the average temperature for a base period of 14 years. The anomaly map of the week starting from 15 up to 21 January 2001 showed the maximum thermal anomaly in the region close to the epicenter (figure 4.34) in the landmass.

4.2.5 HINDUKUSH EARTHQUAKES, AFGHANISTAN

Two consecutive earthquakes in Hindukush (Afghanistan) hit the Badakhshan Province on 3 March 2002. The first 6.2 magnitude shock occurred at 12:08:12 UTC and was followed by the main shock with a magnitude of 7.4 just 10 seconds later at 12:08:12 UTC (table 1.2). Both these earthquakes are associated with the deformation belt created by the collision of the Indian plate with the Eurasian plate. The location of the 7.4 magnitude mainshock epicenter is 36.54° N latitude and 70.42° E longitude (http://orfeus.knmi.nl/newsletter/vol4no2/afghan.html) (figure 4.35). The earthquake was felt in Pakistan, Tajikistan, Uzbekistan, Khazakstan, Kyrgyzstan, India and China. Highest casualty and damage was reported from the Samanghan Province. A landslide incurred by this earthquake in the Samangham Province flooded the Surkundara valley and killed around 150 people, injured several and damaged around 400 houses. Deaths were also reported in Kabul, Rustaq, Bajaua in Pakistan and caused damage to Badakhshan and Takhar Provinces (http://neic.usgs.gov/neis/eq_depot/2002/eq_020303/)

On 25 March 2002, just 135 km southwest of the double earthquakes of 3 March 2002, an earthquake of magnitude 6.1 hit the Pamir-Hindukush region at 14:56:37 UTC. This earthquake originated at a shallow depth of 33 km, epicenter at 35.97° N latitude and 69.18° E longitude (table 1.2) (http://www.geotimes.org/mar02/WebExtra0326.html) (figure 4.35). The 25 March earthquake was more devastating than the 3 March earthquake. Shallow earthquakes cause more damage than intermediate and deep ones since the energy generated by the shallow events is released closer to the ground surface and therefore produces stronger shaking and intensity than is generated by quakes that are deeper within the Earth. The more-destructive earthquake on 25 March actually produced about 95 times less energy than the event on 3 March, but it had caused much more damage (http://neic.usgs.gov/neis/bulletin/02_EVENTS/EQ_020325/). The earthquake killed around 1000 people in the Baghlan Province of Afghanistan, hundreds were injured and several thousands were rendered homeless. Large damage to concrete structures occurred in Nahrin (around 1500 houses were damaged) and in Baghlan Provinces. Landslides blocked many roads in and around the area near the epicenter. The earthquake was felt strongly in much of northern Afghanistan, and was felt as far as Islamabad-Peshawar area in Pakistan and at Dushanbe in Tajikistan. More than 20 aftershocks continued to hit the region, with the strongest one with a magnitude of 6.0 on 12 April 2002.

There was a similar seismic event in history in the same location as these earthquakes, in which a deep focus earthquake preceded a shallow earthquake. The deep earthquake occurred at 16:04:52 UTC on 3 May 1981, epicenter at 36.30° N latitude and 71.20° E longitude with a magnitude of 6.2. This was followed by a shallow earthquake at 00:40:48 UTC on 16 December 1982 with a magnitude of 6.3. The location of the epicenter was 36.15° N latitude and 69.01° E longitude and focal origin at a depth of 36 km. The earthquake had killed around 450 people in Baghlan Province, Afghanistan and caused considerable damage (http://orfeus.knmi.nl/newsletter/vol4no2/afghan.html). At least five earthquakes with magnitude 5 or larger occur per year within 150 km of the 25 March 2002 earthquake epicenter.

These earthquakes in the Pamir-Hindukush regions are manifestations of active earth tectonics in these parts of the world, where the Indian plate is colliding with the Eurasian plate thus causing the uplift of the Himalayas and the Karokoram Ranges. The seismicity here is dominated by earthquakes ranging in depths between near-surface to 330 km. The compressional stresses generated by this subduction and rotation of the two major plates along this Himalayan Arch give rise to active faults and thrusts like the Darvaz-Karakul fault (DKF), the Main-Karakoram thrust (MKT) (figure 4.35), the Harat fault, the Chaman fault etc.

The 25 March 2002 earthquake can be considered to have occurred due to movement on southern branch of the left lateral strike slip DKF (figure 4.35) (http://orfeus.knmi.nl/newsletter/vol4no2/afghan.html). Several faults have been mapped in this region having orientations similar to the DKF.

4.2.5.1 OBSERVATIONS

The beginning of the thermal anomaly was observed in the week beginning from 19 February 2002 for the 3 March 2002 earthquakes. This anomaly intensified in the next week beginning from 26 February 2002, just one, or maybe hours to five days before the earthquake (figure 4.36). The increase in temperature was around 4-10° C higher than that of the base period of 14 years. The anomaly spread over a large area. The week after the earthquake hit Hindukush Mountains saw normal temperatures again.

An unusual observation was made in case of the 6.1 magnitude earthquake of 25 March 2002. The thermal anomaly, which appeared just one week (12 - 18 March 2002) before the earthquake was seen to persist even in the week after the earthquake. The intense anomaly, which spread over a vast area, finally disappeared after 2 April 2002 (figure 4.37).

4.2.6 SOUTHERN XINJIANG, CHINA

A destructive earthquake of magnitude 6.4 hit Southern Xinjiang, China at 02:03:41 (UTC) on 24 February 2003. The epicenter was located at 39.61° N

latitude and 77.24° E longitude and the focal depth at 11 km (table 1.2) (figure 4.38). The earthquake killed more then 250 people and injured around 4,000. Damage was extensive in the Bachu county area and around 38,259 head of livestock was killed (http://neic.usgs.gov/neis/eq_depot/2003/eq_030224/).

The earthquake occurred near the boundary between the Tarim Basin and the Tien Shan Mountain range in the north-west Tarim Basin. This region has been seismically very active and has produced many deadly earthquakes in the past decade. The most destructive one was of a magnitude 6.3 on 19 March 1996. This remote, flat and featureless area of western China known as the Tarim Basin, lies on the Eurasian plate and remains flat while it is being squeezed by the motion of the Indian plate, which is about 1000 km away. As mentioned earlier, the Indian plate is moving at a rate of about 4.6 cm per year towards the Eurasian plate, generating massive mountain ranges like the Himalayas and causing the uplift of the Tibetan plateau. The Tarim Basin, instead of deforming into belts of mountain ranges, is transmitting force applied by the Indian Plate to the interior of Asia, where the Tien Shan Mountains are rising (http://earthobservatory.nasa.gov/Newsroom/NewImages/images.php3?img_id=10933).

4.2.6.1 OBSERVATIONS

The anomaly observed in the Xinjiang Earthquake is well situated over and around the epicenter (figure 4.39). The anomaly was not very strong with the increase in temperature of about 4-6° C than the average temperature in the base period of 14 years. The rise started one to five days before the earthquake and stayed for not more than a week.

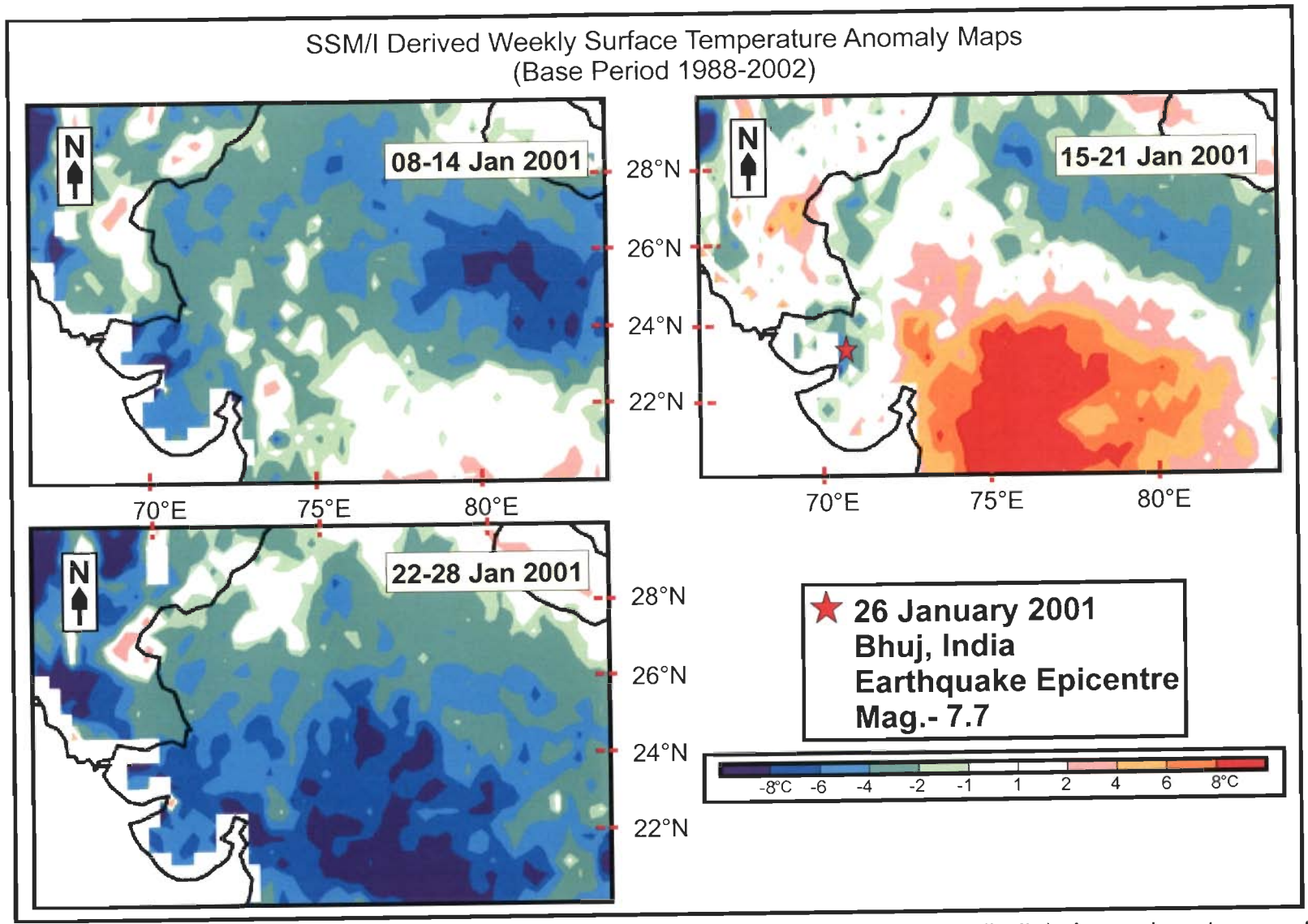

Figure 4.34: Anomaly maps around the 26 January 2001 earthquake in Bhuj, Gujarat (India). Anomalous temperature is seen in the week beginning from 15 January 2001. This thermal anomaly was seen to go away after the earthquake.

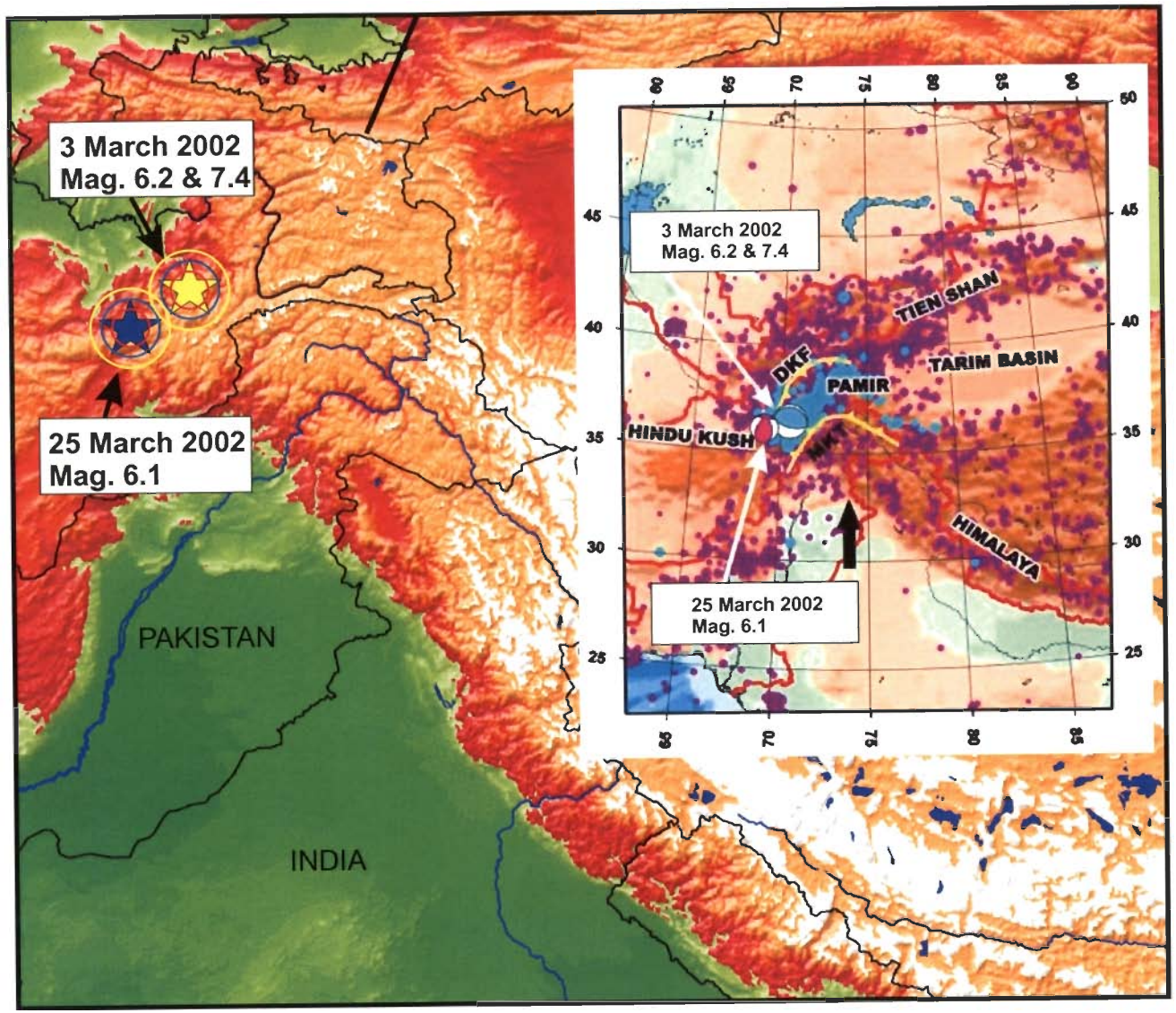

Figure 4.35: Location of the doubles earthquakes on 3 March 2002 (Mag. 6.2 and 7.4) and on 25 March 2002 (Mag. 6.1) in Hindukush, Afghanistan (Source: http://activetectonics.asu.edu/Pamir/PamirPhotos/). The fault (DKF) responsible for the 25 March 2002 earthquakes is shown in the inset (Source: http://orfeus.knmi.nl/newsletter/vol4no2/afghan.html).

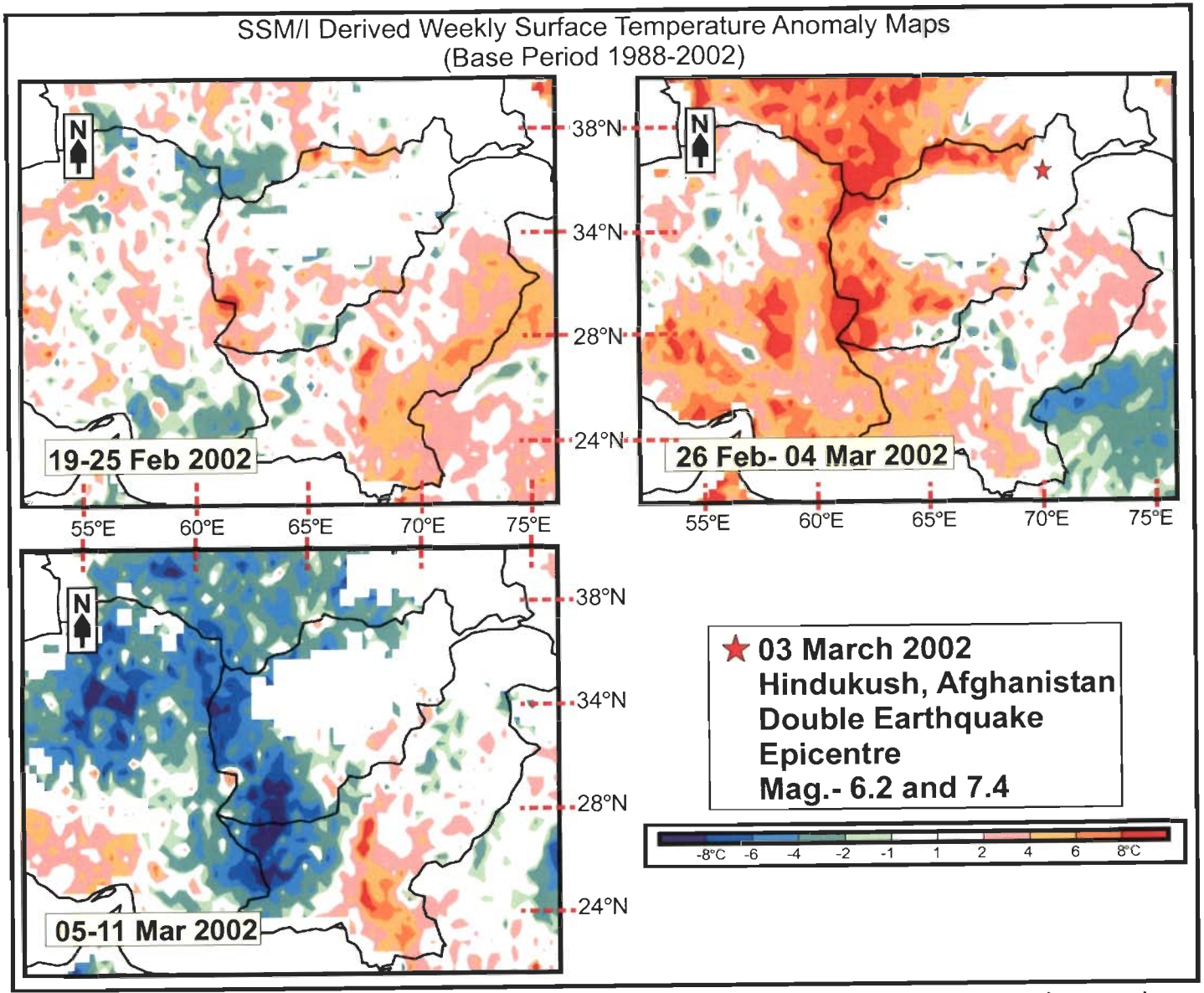

Figure 4.36: Anomaly maps for the double Hindukush earthquake in Afghanistan. A thermal anomaly was seen beginning from 26 February 2002 near the epicenter of the earthquake. The anomaly went away along with the earthquake.

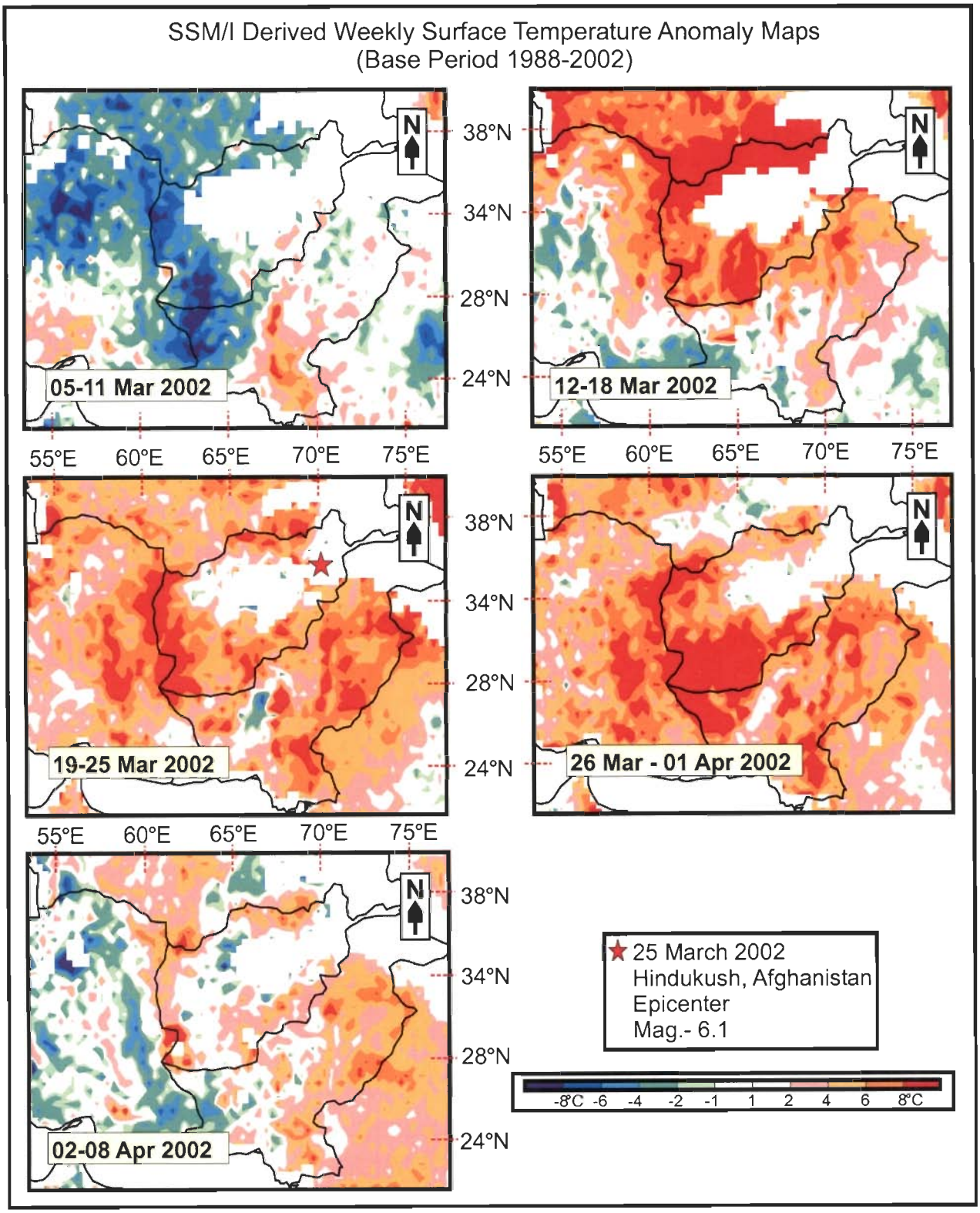

Figure 4.37: Anomaly maps for the 25 March 2002, Hindukush earthquake in Afghanistan. Thermal anomaly was observed in the week preceding the earthquake, which stayed on even after the earthquake. The thermal anomaly finally went away in the week beginning from 2 April 2002.

Figure 4.38: Location of the 24 February 2003 earthquake epicenter in Xinjiang,China. The epicenter is loacted south of the tectonically active Tien shan ranges in the Tarim basin.

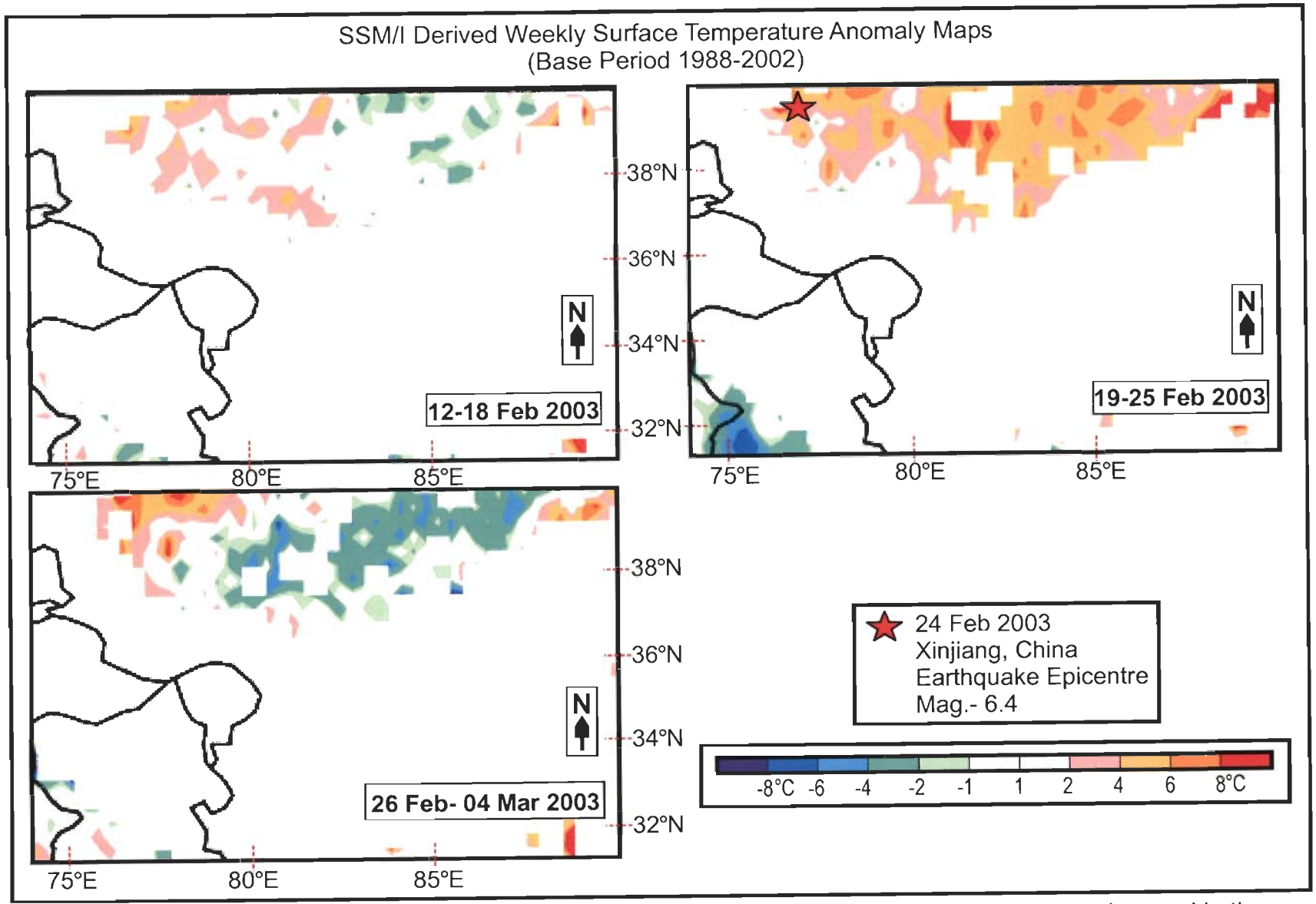

Figure 4.39: Anomaly map for the Xinjiang earthquake on 23 February 2003. Thermal anomaly was observed in the week beginning from 19 February 2003.

4.3 DISCUSSIONS

The thermal anomalies observed in all the 12 earthquakes appeared from three weeks to even hours before the earthquakes (tables 4.11 and 4.12). The number of days prior to which the thermal anomalies appeared varied from earthquake to earthquake. Few earthquakes [e.g., the Bhuj earthquake of 26 January 2001 (M_w 7.7), the great Sumatra earthquake of 26 December 2004 (M_w 9.0) and the Zarand earthquake of 22 February 2005 (M_w 6.4)], varying in magnitudes, showed varying spatial extent of anomalies (tables 1.1 and 4.11, figures 4.4, 4.24 and 4.19 respectively). The earthquakes in Bhuj and Sumatra were of large magnitudes as compared to the earthquake in Zarand. The temperature rose by 5-7° C for the Bhuj earthquake, 6-12° C for the Sumatra earthquake, but 10-12° C for the Zarand earthquake. It was observed that the thermal anomalies for the earthquakes in Bhuj and Sumatra occupied vast areas, whereas, the Zarand earthquake anomaly was of a relatively lesser spatial extent. The rise of temperature for the two bigger earthquakes started around 12 days and more than 15 days (for Bhuj and Sumatra respectively). The temperature started rising around 5 days prior to the Zarand earthquake (table 4.11). The reason for the relatively higher rise of LST for the Zarand earthquake was probably because the anomaly was confined within the lesser spatial extent. The time duration of the presence of thermal anomaly for the Zarand earthquake was also short (5 days). The processes of development of thermal anomaly happened within this time span and probably gave a more intense anomaly. This less spread but intense thermal anomaly for the Zarand earthquake might also be due to prevailing tectonic settings and proximity to active faults. Further, the larger spread of thermal anomaly for the Bhuj and Sumatra earthquake gave a lesser intense anomaly as compared to the Zarand earthquake (table 4.11).

The increase in temperature in all the earthquakes in general ranged from about 5° to even 13° C in some places (tables 4.11 and 4.12). It was observed that the anomalies appeared around the epicenter or near the epicenter.

Table 4.11: List of earthquakes studied through NOAA-AVHRR datasets and specifications of the number of days prior to the earthquake in which the thermal anomaly was seen to occur and reach the maximum amplitude

S. N.	Earthquake	Magnitude (M_w)	Focal Depth (km)	Pre-earthquake thermal anomaly (before the earthquake)		Intensity of thermal rise
				Rise started	Maximum rise observed	
1	Bhuj, India 26 Jan 01	7.7	16	12 days	3 days	5-7° C
2	Boumerdes, Algeria 21 May 03	6.8	10	7 days	Few hours	5-10° C
3	Bam, Iran 26 Dec 03	6.6	10	7 days (nighttime data), 4 days (daytime data)	5 days (nighttime data), 2 days (daytime data)	7-13° C (nighttime) 7-10° C (daytime)
4	Zarand, Iran 22 Mar 05	6.4	14	5 days	1 day	10-12° C
5	Banda-Aceh Earthquake, Sumatra 26 Dec 04	9.0	30	>15 days (whole region was very cloudy)	1 day	6-12° C

An offset was observed between the thermal anomaly and the epicenter in the case of the Boumerdes earthquake in Algeria on 21 May 2003 (table 1.1, figures 4.8 and 4.10). The thermal anomaly was observed to be in a linear orientation over the South Atlas Fault (SAF) (movement on which is reported to be responsible for the Boumerdes earthquake) tracing E-W towards the south of the epicenter (figure 4.9). The offshore location and shallow depth (10 km) of the epicenter indicates that the focus lies on the thrust plane of the SAF (figure 4.40). Escape of gases from pore spaces of rocks due to stresses developing prior to an earthquake has been reported by Zu ji et al. to be the cause of localized greenhouse effect in the lower atmosphere (Zu ji et al., 1991). These greenhouse gases augment the LST conditions of the earth's surface and might be pre-cursors to an impending earthquake. The energy and gases while moving to the earth's surface will escape through the weaker zones like fault planes. The

anomaly of the Boumerdes earthquake thus can be seen oriented over the fault trace of the SAF (south to the earthquake epicenter) (figures 4.9 and 4.40).

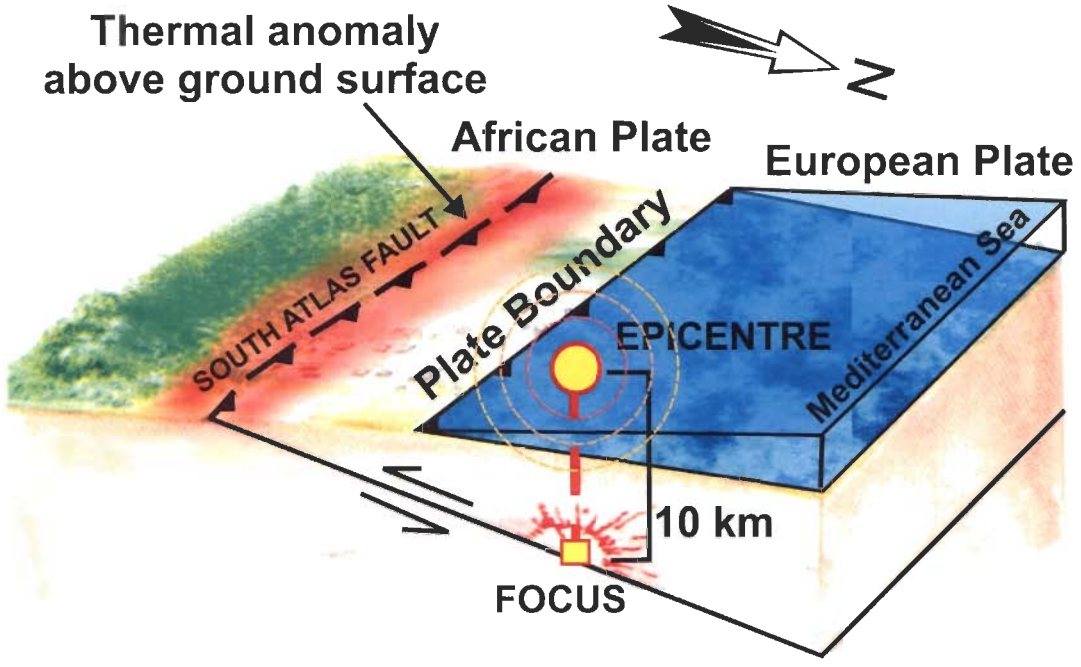

Figure 4.40: Schematic 3-D model showing the location of the focus of the 21 May 2003 earthquake the epicenter and the trace of South Atlas Fault (SAF). The thermal anomaly as shown in the figure was oriented along the surface trace of the SAF.

The anomaly for the Bam earthquake in Iran was conspicuously more spread in area as observed through the daytime data than in the nighttime data. Further, the anomaly in the nighttime data appeared earlier and went away earlier as compared to the anomaly observed through the daytime LST maps. The amplitude of rise of temperature was higher during daytime than at nighttime [figures 15 (a) and 4.16].

Table 4.12: List of earthquakes studied through weekly average DMSP-SSM/I datasets and specifications of the number of days prior to the earthquake in which the thermal anomaly was seen to occur and reach the maximum amplitude

S. N.	Earthquake	Magnitude (M_w)	Focal Depth (km)	Thermal anomaly before the earthquake (weekly SSM/I data used)	Intensity of thermal rise
1	Kalat, Pakistan 04.03.90	6.1	10	2 weeks	2-10° C
2	Zhangbei, China 10.01.98	6.2	30	3 weeks	4-8° C
3	Izmit, Turkey 17.08.99	7.6	17	1 week	6-10° C
4	Bhuj, India 26.01.01	7.7	16	1 week	4-8° C
5	Double earthquakes in Hindukush, Afghanistan 03.03.02	6.2 and 7.4	195	Few days to a week	4-10° C
6	Hindukush, Afghanistan 25.03.02	6.1	33	2 weeks	6-10° C
7	Xinjiang, China 24.02.03	6.4	11	Less than a week	4-6° C

Generally, the maximum temperature of a region is around pre-dusk and the minimum temperature is around pre-dawn. During afternoon solar heating is at its peak. Around 15:00 hours, the earth is heated up well enough and exhibits the maximum temperature during that time. At nighttime, the earth emits the received heat at infrared wavelengths at a rate that depends strongly upon the surface temperature. Warmer ground radiates significantly more energy than colder ground. By pre-dawn, the earth cools down to emit the minimum radiation and thus the minimum temperature is observed around this time of the day. But the presence of clouds can affect the reception or emission of energy during the day or night respectively, and thus influence the diurnal temperature of a place. Clouds, more than a few hundred meters thick reflect sunlight efficiently, about as well as new fallen snow, thereby reducing the solar energy reaching the ground. This lowers the maximum temperature that would have been attained if the sky

were clear. At nighttime, clouds absorb infrared radiation very effectively and re-radiate it back toward the ground at a rate dependent upon the cloud temperature and thus increase the nighttime temperature. However, high clouds tend to be colder than low clouds; thus they do not reduce the diurnal temperature range as much. Even when the sky is clear, water vapor reduces the diurnal temperature range. Along with other gases in the air such as carbon dioxide and ozone, water vapor absorbs infrared radiation and then re-radiates the energy in all directions (including downward) at a rate that is temperature dependent. Even when the sky is clear, water vapor (along with other gases) reduces the diurnal temperature range. When the sky is clear, atmospheric moisture elevates the overnight minimum temperature because the water vapor in the atmosphere absorbs some of the infrared radiation from the ground and re-radiates a portion of the absorbed energy back toward the ground. In a dry atmosphere, more infrared radiation would pass to space, and thus surface cooling would be more pronounced. The combined effects of soil moisture and atmospheric water vapour influence the diurnal temperatures in a dry climate. The diurnal temperature range is significantly higher where it's dry (http://www.weatherwise.org/qr/qry.diurnaltemp.html). The above-mentioned meteorological influence is very significant in climates, like that of Iran. During the period in which the thermal regime was studied for the Bam earthquake, the meteorological parameters must have influenced the thermal conditions of Iran differently at day and night. Cloudiness might bring a hot day but a cooler night. On the other hand, on a clear day (in a climate like that of Iran), the days are hot with comparatively much cooler nights. Therefore, the peak of increase of the LST anomaly at daytime and nighttime may not coincide. There may be difference in the intensity of thermal anomaly induced by the earthquake as meteorological conditions may influence the thermal regime of any place all the time. Similar trends have also been observed in the TVCs of the air temperature data for the earthquake in Zarand, Southeast Iran and the cluster of smaller quakes in Iran in the year 2005 [figures 4.20 (a) to 4.20 (m)].

The disadvantages of AVHRR could be felt in areas of cloudiness. The thermal infrared channels of AVHRR on NOAA series of satellites retrieve thermal data from the earth's surface only through areas of clear sky, since

infrared radiation does not penetrate clouds. Clouds appearing between the satellite and the earth's surface will lead to erroneous calculation of land surface temperature because the sensor will be measuring the temperature of cloud tops and not the actual emissivity of the earth. Thus cloud cover can stand as a disadvantage for remote sensing based geothermic studies for earthquakes since there are often areas of cloudiness. While calculating the LST of a place in the present study, cloud masking had been done.

The passive microwave radiometer, SSM/I, flown aboard the DMSP series of satellites has the advantage of being more transparent to clouds and therefore has an all weather advantage (though the spatial resolution is low). However, sensors like AVHRR have their advantages. AVHRR is multispectral scanner and has a comparatively better spatial resolution. The temporal resolution of NOAA-AVHRR is very good. Operating as a series, the NOAA satellites ensure that the data is not more than few hours old. Global coverage of NOAA-AVHRR is also an advantage. Seismic regions of the world (figures 2.1 and 2.2) are spread across the globe. NOAA-AVHRR enables regular real time monitoring of the thermal regime of any region.

Under what conditions the intensity and spatial extent of anomaly varies imbibes interest. There was an interesting observation in the Hindukush earthquake of 25 March 2002, magnitude 6.1, and the Kalat earthquake of 4 March 1990, of the same magnitude but which had different focal depths (tables 1.2 and 4.12). The Hindukush earthquake had a focus, which rested at a depth of 33 km and the focus for the Kalat earthquake was located at a depth of 10 km. These two earthquakes are located in similar tectonic regions in the vicinity of plate margins where the Indian plate is colliding with the Eurasian plate at a rate of 4.6 cm per year and buckling its topography with folded mountains. The significant observation in these earthquakes was that the thermal anomaly showed varying spatial extent (figure 4.41), although the other variables (magnitude and location) are similar. The Hindukush earthquake showed a thermal anomaly, which was spread over a larger area as compared to the thermal anomaly developed before the Kalat earthquake.

This relation between varying focal depths and differing spatial extent of thermal anomalies before two similar magnitude earthquakes can be explained by assuming two 3-D subsurface cones with the vertices located at the foci for the two earthquakes. The cone with the vertex at the deeper depth, i. e., the Hindukush earthquake will have a surface expression of the cone spatially spread more and with a bigger radius than the Pakistan earthquake whose focus is at a shallower depth (figure 4.42). The cone beginning from the focus of the deeper depth earthquake will traverse a larger area all along its trace to the surface. The processes of stresses developing subsurfacially before an earthquake, which can generate heat and electric potentials has been reported by scientists (Freund, 2002 and 2003). Electronic charge carriers can be free electrons or sites of electron-deficiency in crystal structure (p-holes). Positive holes propagate though an oxide or silicate structure by electron hopping, whereby electrons from neighbouring O^{2-} can hop onto the O^{-} site (an anion or radical with an incomplete valence shell) (vide Chapter 3, Section 3.2). The estimated maximum speed at which a positive hole could propagate by hopping is in the order of 100–300 ms^{-1} (Freund, 2002). The positive hole pairs (PHP) dissociating into positive charged holes rush towards the earth's surface to attain electronic stability. Immediately after reaching a non-solid medium like atmosphere or water, a positive hole acquires an electron to become stable. The energy emitted by this electron acquirement increases the LST of a region before an earthquake. In an earthquake with a comparatively deeper focus, the process of PHP are spread a bigger subsurface area (and ultimately a larger surface expression) while rushing to the surface to attain stability from the zone of stress. Thus the earthquake in Hindukush, with same magnitude and in same tectonic location developed a greater spatial extent and area of thermal anomaly (figure 4.41).

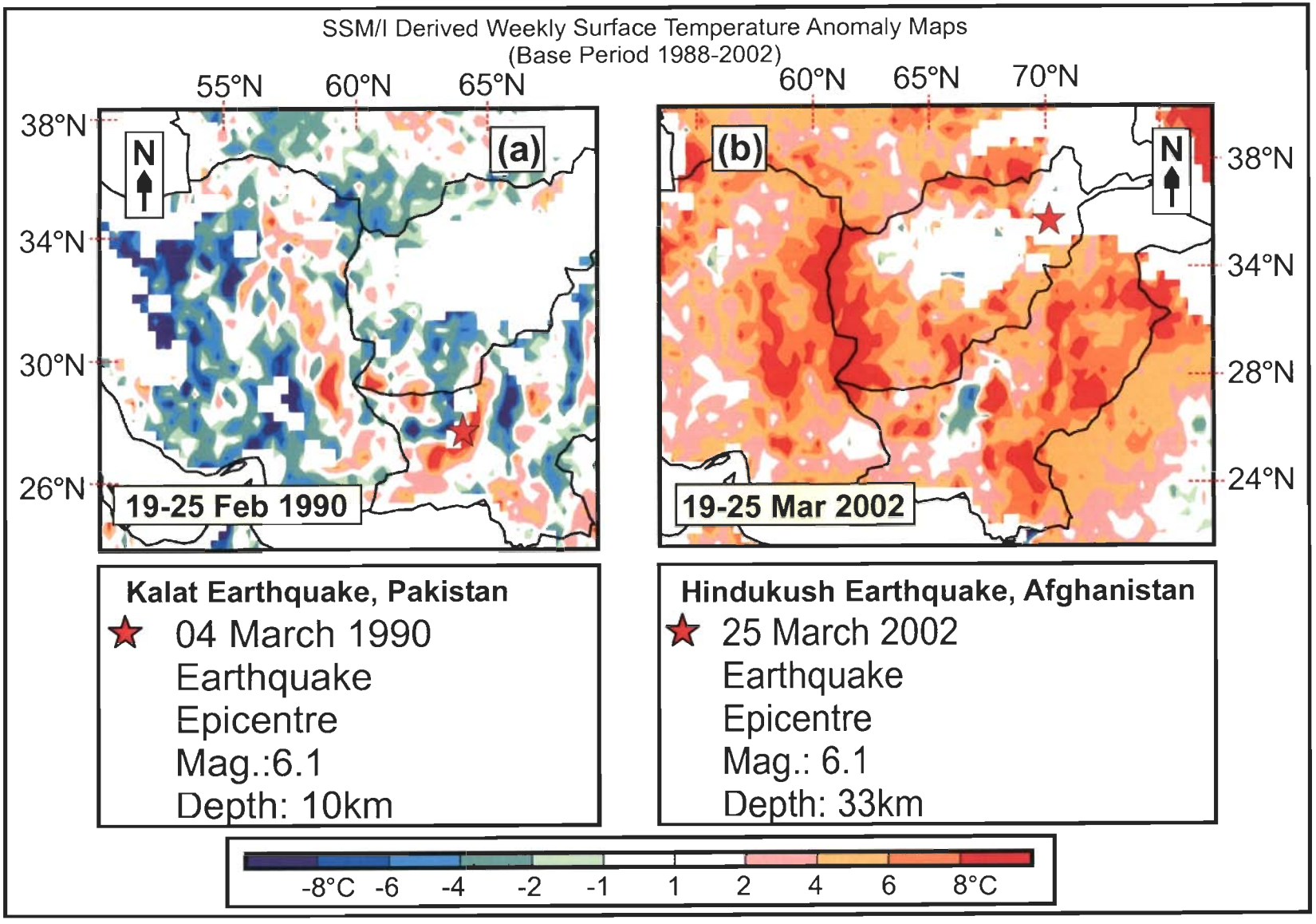

Figure 4.41: SSM/I thermal anomaly maps showing different spatial extents of anomalies of two earthquakes (Kalat Earthquake and the Hindukush Earthquake). Both these earthquakes have the same magnitude and are located in the same terrain conditions but have different focal depths. The spatial extent of the Hindukush earthquake (with deeper focus) was more than the Kalat earthquake. However, the anomaly for the Kalat earthquake stayed longer than the Hindukush earthquake.

Earthquakes with exactly equal magnitude and satisfying the similarity of other conditions like terrain, meteorological conditions etc. are hard to find. Such comparisons thus are difficult. If the magnitude of an earthquake differs by one unit, the comparison will be entirely wrong because even unit variation in magnitude means a ten-fold increase in released energy (the magnitude scale being logarithmic).

Thermal remote sensing data can provide totally unbiased recordings of the LST conditions of the earth's surface. Air temperature data collected by reliable meteorological stations can provide support to the satellite data analysis. Though, air temperature data is point data, if the stations are located close to one another, a better perspective of the ground thermal scenario can be had. This study imbibes similar analytical approach for all the earthquakes studied wherever possible.

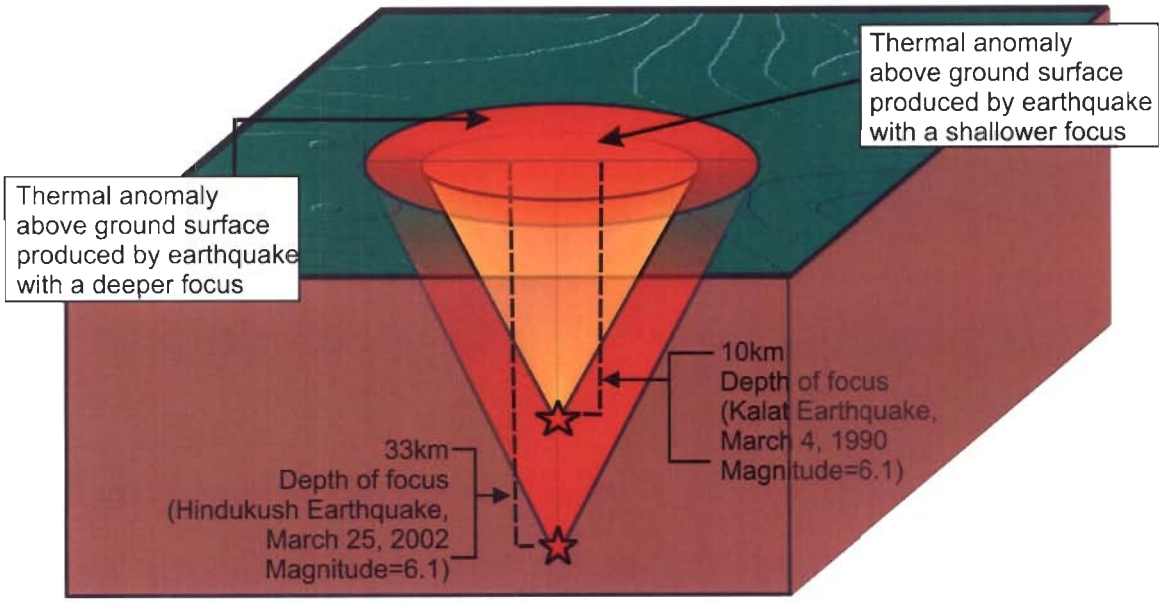

Figure 4.42: Schematic sketch showing focus of two earthquakes located at different depths and their associated areas of thermal anomalies on the ground surface. An earthquake with a shallow focal depth will have a surface expression of the thermal anomaly with a lesser spatial extent but more intense and vice-versa for a deeper focal depth.

Earthquakes are powerful, devastating and is one of the most unfathomable mysteries of nature. It has now been established that earthquakes are more prone to occur in active belts around the world, which are plate margins for this mobile earth. The plate margins of the world have produced some of most destructive and mightiest earthquakes.

It is now very clear where earthquakes are prone to occur. The seismic zones of the world fall in three distinct belts, namely, the Circum-Pacific Belt, the Alpine Belt and the third Atlantic Belt. The earthquakes studied in this work fall on important tectonic locations/plate margins around the earth and are associated with major fault systems.

Predictions for earthquakes have instilled interests in many seismologists around the world. Geller et al. (1997) have even declared, "Earthquakes cannot be predicted", providing more, challenges to earth scientists for earthquake studies. It is, however, rightly said, "to understand earthquakes further, we need more earthquakes". But if earthquakes forewarn us before they strike, it is of utmost importance that we understand and pick up the clues. Now thermal remote sensing studies and detection of satellite derived land surface temperature (LST) anomaly related to an earthquake is an important breakthrough for earthquake research. Satellite based radiometers, which can sense the thermal emission originating from the earth's surface and the intervening atmosphere, can be used to study any thermal anomaly developing near surface of the earth.

5.1 SUMMARY

The concept that prior to major earthquakes, the LST increases has been validated by the study of 12 major earthquakes around the world. LST maps using thermal NOAA-AVHRR datasets have been prepared and used to study the

thermal scenario for the earthquakes in Bhuj (India), Boumerdes (Algeria), Bam and Zarand in Iran and Banda-Aceh (Sumatra). The earthquakes in Xinjiang and Zhangbei (China), Izmit / Kocaeli (Turkey), two earthquakes in Hindukush (Afghanistan) and Kalat (Pakistan) have been studied using passive microwave SSM/I datasets. The Bhuj earthquake (India) has been analyzed using both by AVHRR and SSM/I data sets.

In tectonically active regions, stresses may build up. These stresses may augment the land surface temperature (LST) of the near earth's surface. Further, these stresses may also bring about sub-surface degassing. These gases upon their escape to the atmosphere may create a localized greenhouse effect and increase the temperature of the region, thus creating a thermal anomaly in the surrounding region. An earthquake may follow this anomaly if the acting stresses are released. Charge carriers in the ground carry electric charges and release electromagnetic radiations. Upon induced pressure (as generated before an earthquake) free radicals release heat and electric potential and is manifested as LST anomaly prior to an earthquake event.

It has been observed that for all the above earthquakes studied, there were decipherable short-term temporal anomalies in the LST maps before the earthquakes. This thermal anomaly went away along with the earthquake events. The anomalies appeared a few days to a few hours preceding the earthquakes. The increase in temperature varied from 2-13° C than the usual temperature of the region around the epicentral area and varied from earthquake to earthquake. Air temperature data collected by meteorological stations located around the epicenter also succeeded in showing thermal spikes before the earthquake events for the Bhuj earthquake in India and the Iran earthquakes.

The anomaly for the Bhuj earthquake in India on 26 January 2001 (M_w 7.7) had started 12 days before the earthquake (i. e., on 14 January 2001). The anomaly covered an area of 179,150 km^2 (about the whole state of Gujarat). This anomaly reached its peak 3 days before the earthquake (i. e., on 23 January 2001). An intense anomaly was seen to cover an area of 300 km^2, with an increase of temperature of around 5-7° C around the epicentral region. Weekly

averaged air temperature graphs were prepared for the year 2001. It was seen that there was a peak in the third week of the year in which the earthquake occurred, while average weekly air temperature data for the past 30 years show a low in the third week of the year.

The thermal anomaly for the Boumerdes earthquake in Algeria on 21 May 2003 (M_w 6.8) appeared on 13 May 2003 (7 days before the earthquake). The anomaly intensified on the night of 20 May 2003 (just hours before the earthquake). The increase of temperature was seen to be around 5-10° C on 20 May 2003. The anomaly covered an area of approximately 91,100 km^2. The anomaly lessened in intensity and went away finally along with aftershocks.

Interesting observation has been seen in the case of the Bam earthquake on 26 December 2003 (M_w 6.6). On analysis of both daytime and nighttime data, it was observed that the peak of the thermal anomaly did not occur on the same day. Nighttime data showed the appearance of a thermal anomaly on 19 December 2003 (7 days prior to the earthquake), which reached to a maximum anomaly (increase of about 10-12° C) on 21 December 2003. The daytime data showed the rise of temperature started on 22 December 2003, which reached to a peak on 24 December 2003 (just 2 days before the earthquake). The anomalous area on the night of 21 December 2003 was 308,034 km^2 and the area covered by the thermal anomaly on 24 December 2003 was 328,287 km^2 (maximum increase of temperature of around 10-13° C). The diurnal temperature of a place is influenced by the meteorological conditions. Presence of clouds lessens the daytime temperature. But clouds forbid the escape of the heat from the earth's surface at night and can give a much hotter night. On occasions when there are no clouds, the days are hot and the nights comparatively cooler.

The thermal anomaly for the recent Zarand Earthquake (Iran) on 22 February 2005 (M_w 6.4) appeared six days before the earthquake (i. e., 16 February 2005) and reached to a maximum just one day prior to the earthquake (i. e., on 21 February 2005). The increase in temperature was about 10-12° C. The anomaly covered an area of around 75,600 km^2. Air temperature data collected from various meteorological stations around the epicenter of a few

earthquakes in Iran (the Zarand earthquake, the Southeast Iran earthquake and a number of smaller quakes in different locations in Iran) also showed thermal spikes before the earthquakes. Air temperature normals for the years 1996-2004 (as base period), for 7 stations showed a normal temperature trend for all these years. Whereas in the year 2005, the TVCs from meteorological stations show that there were thermal peaks 1-5 days before the earthquakes.

The sky over Sumatra and the Indian Ocean was depressingly cloudy before and after the great megathrust earthquake in Banda-Aceh (Sumatra), which struck with might on 26 December 2004 (M_w 9.0). Yet, with whatever clear AVHRR data was available over land areas, was studied for detecting any thermal anomaly over Sumatra and adjoining areas before the earthquake. A thermal anomaly was seen to develop on 21 December 2004. The maximum built up of temperature was seen on 25 December 2004 (just one day before the earthquake), with an increase of temperature of about 6-12° C. On 26 December the LST map shows normal temperature again. The anomaly spread over a large region, and was seen as far as Thailand and Myanmar.

Though AVHRR data cannot penetrate clouds, it has an advantage over spatial resolution. The spatial resolution of AVHRR is 1.1 km for all channels, whereas, SSM/I data available to us for our study offers a resolution of 30 km. SSM/I has the advantage of being able to penetrate clouds. Weekly average thermal anomaly maps (prepared with respect to the base period between 1988-2002) were used for studying the thermal change for 7 earthquakes as mentioned above.

The Kalat earthquake in Pakistan on 4 March 1990 (M_w 6.1), showed a thermal anomaly 2 weeks before the week in which the earthquake occurred. The rise in temperature was around 2-10° C higher than the average temperature for 14 years.

The anomaly for the Zhangbei earthquake on 10 January 1998 (M_w 6.2) appeared three weeks before the week in which the earthquake occurred. The rise of temperature was observed to be around 4-8° C with respect to the base

period of 14 years. The anomaly occupied a vast area south of the epicenter of the earthquake.

The famous Izmit earthquake in Turkey occurred on 17 August 1999 (M_w 7.7). The thermal anomaly for this earthquake was observed 1 week before the week in which the earthquake occurred. The increase of temperature was around 6-10° C with respect to the base.

On 3 March 2002, there were two simultaneous big earthquakes of magnitudes 6.2 and 7.4 hit Hindukush Mountains. The double earthquakes were able to generate a thermal anomaly around a few days to a week before the earthquake. The week starting from 19 February showed a rise of temperature of about 6-10° C higher than the average temperature of a period of 14 years (used to prepare the anomaly maps) of the region. The temperature went away along with the earthquake events. A few days later (25 March 2002) another earthquake of magnitude 6.1 hit Hindukush. The thermal anomaly, which was generated by this earthquake, remained for two weeks. The anomaly showed a rise of temperature of about 6-10° C.

The Xinjiang earthquake occurred on 24 February 2003 (M_w 6.4) in the Tarim Basin in China. The earthquake developed an anomaly few days prior to the earthquake. Weekly anomaly maps showed the anomaly in the week in which the earthquake occurred. The rise of temperature was about 4-6° C than the average temperature for the base period of 14 years.

5.2 CONCLUSIONS

It was observed that prior to all the above earthquakes short-term thermal anomalies appeared and the anomalies disappeared along with the earthquake events. It was seen that the increase in temperature was between 2-13° C. This anomaly appeared around the epicenter or near the epicenter. There might be a pre-earthquake thermal anomaly, which is offset from the epicenter of the earthquake. This is probably because the weaker zones of the earth permit the escape of gases into the lower atmosphere. Therefore the anomaly forms over a

fault, movements on which is responsible for the earthquake. The development of thermal anomaly, the intensity and the spatial extent of the anomaly are all dependent on the magnitude of the earthquake, the focal depth, terrain conditions, meteorological conditions and proximity to the sea. An earthquake of higher magnitude will have an earthquake with an intense anomaly, which is spread over a larger areal extent. However, in two earthquakes, with same magnitude located in similar tectonic settings, but with different focal depths, the earthquake with the deeper focus will have an anomaly with a larger spatial extent than the earthquake with the shallower focus. Terrain conditions significantly influence the thermal anomaly. Terrain conditions are basically interlinked with other factors like hydrological conditions, meteorological conditions, vegetative cover etc. The extent and numbers of interconnected structural discontinuities spread the spatial extent of thermal anomaly. That is why anomalous thermal signature of the Great Sumatra earthquake could be observed even in Northern Thailand and Laos and similarly development of anomalous spikes in thermal variation curves (TVCs) were observed even for Ardebil, Tabriz and Maragheh in case of Iran, though these meteorological stations are located far from the epicenter for the Iran earthquakes. It has also been observed that air humidity and soil moisture are other important influencing factors towards the development of pre-earthquake thermal anomalies. Dry terrain and air are suitable conditions for the development of intense pre-earthquake thermal anomaly. That is why thermal anomalies in Iran with dry condition are more prominent. Further, diurnal temperature of a place is influenced by meteorological conditions like cloudiness, moisture content etc. The maximum and minimum temperatures of a place may not be conformable to each other. Therefore, pre-earthquake thermal anomaly analyzed through nighttime data may appear and disappear earlier than in the daytime data, or vice versa. Pre-earthquake thermal anomalies occurring in coastal regions (e.g. Bandarabbas in Iran) may not always develop, as there can be heat-exchange with the neighbouring sea through wind and water.

5.3 RECOMMENDATIONS FOR FUTURE WORK

The present study is a post-event attempt in identifying the correlation between short duration temporal thermal anomalies and earthquakes. This attempt is towards developing knowledge about the appearance of thermal anomalies prior to the earthquake studied and their detection by thermal remote sensing technique. This work is not intended towards forecasting or prediction of earthquakes. However, with regular monitoring and integrated approach based on other precursors, this might lead towards the same. This technique complements in great measure to other techniques in earthquake research to gather clues for a future earthquakes. The results of the study for 12 recent past earthquakes for pre-earthquake thermal anomalies prior to the events are now in public domain. Regular, near real-time monitoring and intensive analysis on an operational basis should be done regularly for tectonically and seismic regions around the world for early detection of temporal pre-earthquake thermal anomalies before the earthquakes actually strike.

BIBLIOGRAPHY

Becker, F. and LI, Z.L., 1990, *Towards a local split window method over land surface. Int. J. Remote Sensing*, Vol. 11, No. 3, pp. 369-393.

Brady, B. T. and Rowell, G. A., 1986, Laboratory investigation of the electrodynamics of the rock fracture, *Nature*, Vol. 321, pp. 488-492.

Cracknell, A. P. and Hayes, L., 1991, Introduction to Remote Sensing, Taylor & Francis, London, pages 304.

Cracknell, A. P., 1997, Advanced Very High Resolution Radiometer AVHRR, Taylor & Francis Books Ltd., London, pages 968.

Cracknell, A. P., 1998, Synergy in remote sensing – what's in a pixel?, *International Journal of Remote Sensing*, Vol. 19, No. 11, pp. 2025 – 2047.

Dai, F. C., Lee, C. F., Wang, S. J., 2003, Characterization of rainfall-induced landslides, *International Journal of Remote Sensing*, Vol. 24, No. 23, pp. 4817 – 4834.

Dai F. C. and Lee C. F, 2002, Landslide characteristics and slope instability modelling using GIS, Lantau Island, *Hong Kong Geomorphology*; Vol. 42, pp.212-228.

Dasgupta, 2005, *Satellite Geothermic Techniques in Earthquake Studies*, M. Tech. Dissertation, Department of Earth Sciences, Indian Institute of Technology Roorkee (unpublished).

Das, J. D., Choudhury, S., Saraf, A. K. and Panda, S. K., 2005, Megathrust Sumatra earthquake and the issue of evident earthquake risk in seismically active Northeastern part of India being affected by the same northward moving Indian Plate, Current Science (submitted).

Drury, S. A., 1987, Image Interpretation in Geology, London: Allen and Unwin Ltd, pages 242.

Freund, F., 2002, Charge Generation and Propagation in Rocks, *Journal of Geodynamics,* Vol. 33, pp. 545–572.

Freund, Friedemann, 2003, Rocks That Crackle and Sparkle and Glow: Strange Pre-Earthquake Phenomena, *Journal of Scientific Exploration*, Vol. 17, No. 1, pp. 37–71.

Geller, Robert. J., Jacksn, David D., Kagan, Yan Y. and Mulargia, Francesco, 1997, Enhanced: Earthquakes Cannot be Predicted, *Science*, 275, pp.1616-1617.

Gorny, V. I., Salman, A. G., Tronin, A. A. and Shilin, B. B., 1988, The earth outgoing IR Radiation of the Earth as an Indicator of Seismic Activity. *Proceeding of the Academy of Sciences of the USSR*, Vol 301, 67-69.

Gorny, V. I. and Shilin, B. V., 1992, Thermal method of remote sensing for study of natural resources, *Proceedings of the 18th Annual Conference of the Remote Sensing Society*, 1992, University of Dundee, 15-17th September 1992 (edited by A. P. Cracknell and R. A. Vaughan), pp.245-263.

Gupta, Alok, 2000, Information Technology and Natural Disaster Management in India, http://www.gisdevelopment.net/aars/acrs/2000/ts8/hami0001pf.htm, last accessed: 1 April, 2005.

Hemmady, A. K. R., 1996, Earthquake, National Book Trust of India, New Delhi.

India Meteorological Department, 1991, Normals of Agroclimatic Observatories in India, Division of Agricultural Meteorology, India Meteorological Department, Pune, 106p.

Kamal and Chabak, S. K., 2002. Chamoli Aftershocks: A view from the nearest Seismic Observatory. *Him. Geol.*, Vol. 23, No. 1&2, pp. 63-69.

Mahajan A. K., Kumar, Sushil & Kamal, 2004. Macroseismic field observations of January 26th 2001 Kachch Earthquake and its Seismotectonics. Asian *J. Earth Sci.*, Vol. 23, No. 1, pp. 17-23.

Marcal, A. R. S., B. Triebfurst, C. Schneider, R. A. Vaughan, 2000, Compression of NOAA/AVHRR data with a wavelet transform, *International Journal of Remote Sensing*, Vol. 21, No. 3, pp. 595-610.

Ouzonov, D., and Freund, F., 2003, http://science.nasa.gov/headlines/y2003/11aug_earthquakes.htm.

Ouzounov, D. and Freund, F., 2004, Mid-infrared emission prior to strong earthquakes analysed by remote sensing data, *Advances in Space Research*, Vol. 33, pp. 268–273.

Parrinello, T. and Vaughan, R. A., 2002, Multifractal analysis and feature extraction in satellite imagery, *International Journal of Remote Sensing*, Vol. 23, No. 9, pp. 1799-1825.

Peters, J., Rana, M. S., Kumar, S. and Bhoj, R. (2001), Kachchh earthquake of 26th January, 2001: Geological Implications of Relocating Anjar Town, Kachchh District, Gujrat, *ONGC Report*, March 2001, DehraDun.

Provost, A-S, Chery, Jean and Hassani, Riad, 2003, 3D mechanical modeling of the GPS velocity field along the North Anatolian fault, *Earth and Planetary Science Letters*, Vol. 209, pp. 361-377.

Saraf, A. K., Sinhval, A., and Sinhval, H., 2001, The Kutch earthquake of January 26th 2001: Satellite data reveals earthquake induced ground changes and appearance of water bodies. *Proceedings of Workshop on Recent Earthquakes of Chamoli and Bhuj*, 22-23 May, 2001, Department of

Earthquake Engineering, University of Roorkee (Roorkee, India: Indian Society of Earthquake Technology), pp. 207-216.

Saraf, A. K., Sinvhal, A., Sinvhal, H, Ghosh, P. and Sarma, B., 2002, Satellite data reveals 26 January 2001 Kutch earthquake-induced ground changes and appearance of water bodies, *Int. J. Remote Sensing*, Vol. 23, No. 9, pp. 1749-1756.

Saraf, A. K. and Choudhury, S., 2003 (a), Earthquakes and thermal anomalies, *Geospatial Today*, Vol. 2, No. 2, pp.18-20.

Saraf, A. K. and Choudhury, S., 2003 (b), Satellite detects surface thermal anomalies associated with the Algerian earthquakes of May 2003, *International Journal of Remote Sensing*, (in press).

Saraf, A. K. and Choudhury, S., 2004 (a), Satellite Detects Pre-earthquake Thermal Anomalies Associated with Past Major Earthquakes, *Proceedings of Map Asia 2004 Conference held at Beijing*, China, between 26-29 August 2004,pp.40, http://www.gisdevelopment.net/application/natural_hazards/earthquakes/pdf/ma04198.pdf

Saraf, A. K. and Choudhury, S., 2004 (b), Thermal Remote Sensing Technique in the Study of Pre-earthquake Thermal Anomalies, *Proceedings of the IGU Conference to be held at NGRI*, Hyderabad, India between 29-31 December 2004, pp. 5.

Saraf, A. K. and Choudhury, S., 2005 (a), NOAA-AVHRR detects thermal anomaly associated with 26 January, 2001 Bhuj Earthquake, Gujarat, India, *International Journal of Remote Sensing*, Vol. 26, No. 6, pp. 1065-1073.

Saraf, A. K. and Choudhury, S., 2005 (b), Thermal Remote Sensing Technique in the Study of Pre-earthquake Thermal Anomalies, *Journal of Indian Geophysical Union*, Vol. 9, No. 2, pp. 193-202.

Saraf, A. K. and Choudhury, S., 2005 (c), SSM/I Applications in Studies of Thermal Anomalies Associated with Earthquakes, *International Journal of Geoinformatics* (submitted).

Saraf, A. K., Dasgupta, S. and Choudhury, S., 2005 (b), Satellite Detects Pre-Earthquake Thermal Anomalies In Iran, Proceedings of the Symposium on Seismic Hazard Analysis and Microzonation, Dept. of Earthquake Engineering, Indian Institute of Technology Roorkee, India, to be held in November (accepted).

Saraf, A. K., Choudhury, S., and Dasgupta, S., 2005 (a), Thermal Remote Sensing Applications in Earthquake Studies, a Chapter in the book, edited by Alok Gupta (accepted).

Singh, S.K., Bansal, B.K., Bhattacharya, S.N., Dattatrayam, R.S., Pacheco, J., Suresh, G., Ordaz, M., Gupta, G.D., Kamal & Hough, S.E., 2003. Estimation of Ground Motion from Bhuj earthquake of January 26, 2001 (Mw 7.6) and Future earthquakes in India. *Bull. Seismol. Soc. America*, Vol. 90, No.1, pp. 353-370.

Sinvhal, A., Bose, P. R., V. Prakash, Bose, A., Saraf, A. K. and Sinvhal, H. (2001), damage, seismotectonics and isoseismals for the Kutch earthquake of 26th January, 2001, *Proceedings of Workshop on Recent Earthquakes of Chamoli and Bhuj*, held between 22-23 May, 2001, Department of Earthquake Engineering, University of Roorkee, pp. 61-70.

Sundaram, R.M., 1998, Integrated GIS studies for delineation of earthquake-induced hazard zones in parts of Garhwal Himalayas, unpublished Ph. D. Thesis, Indian Institute of Technology Roorkee.

Tripathi, N. K., Siddiqi, M. U. and Gokhale, K. V. G. K., 2000, "Directional morphological image transforms for lineament extraction from remotely sensed images", *International Journal of Remote Sensing*, Vol. 21, No. 17, pp 3281-3292.

Tripathi, N. K. and Singh, P., 2000, Integrated GIS and Remote Sensing Approach to Map Pollution in Upper Lake, Bhopal, India", *Geocarto International*, Vol. 15, No. 4, pp. 49-55.

Tronin, A. A., 1996, Satellite thermal survey-a new tool for the study of seismoactive regions, *Int. J. Remote Sensing*, Vol. 17, No. 8, pp. 1439-1455.

Tronin, A. A., 2000, Thermal IR satellite sensor data application for earthquake research in China, *Int. J. Remote Sensing*, Vol. 21, No. 16; pp. 3169-3177.

Van de Griend, A. A., and Owe, M., 1993, On the relationship between thermal emissivity and the normalized difference vegetation index for natural surfaces, *Int. J. Remote Sensing.*, Vol. 14, pp. 1119-1137.

Vaughan, R., Cuthbert, I. and Slater, M., 1999, Cover Page, *International Journal of Remote Sensing*, 1999, Vol. 20, No. 14, pp. 2689-2691.

Zu-ji, Qiang, Xiu-Deng, XU and Chang-Gong, DIAN, 1991, Thermal infrared anomaly – precursor of impending earthquakes, *Chinese Science Bulletin*, Vol. 36, No. 4; pp. 319-323.

Zu-ji, Qiang, Kong, Ling-Chang, Zheng, Lan-Zhe, Guo, Muan-Hong, Wang, Ge-Ping and Zhao, Yong, 1997, An Experimental Study on Temperature Increasing Mechanism of Satellite Thermo-infrared, *Acta Seismologica Sinica*, Vol. 10, No. 2, pp. 247-252.

Zu-ji, Qiang, Chang-gong, Dian, Lingzhi, LI, Min, XU, Fengsha GE, Tao, LIU, Yong, ZHAO and Manhong, GUO, 1999, Satellite thermal infrared

brightness temperature anomaly image – short-term and impending earthquake precursors, *Science in China*, Vol. 42, No. 3, pp. 313-324.

URL Links:

1. http://pubs.usgs.gov/gip/earthq1/where.html

2. http://vulcan.wr.usgs.gov/Volcanoes/JuanDeFucaRidge/description_juan_de_fuca.html

3. http://neic.usgs.gov/neis/eqlists/eqsmosde.html

4. http://www.imd.ernet.in/section/seismo/static/signif.htm

5. http://earthquake.usgs.gov/faq/hist.html

6. http://www.asc-india.org/info/seisindia.htm

7. http://gujarat-earthquake.gov.in/final/seismic.html

8. http://asc-india.org/info/seisindia.htm

9. http://science.nasa.gov/headlines/y2003/11aug_earthquakes.htm

10. http://www.stvincent.ac.uk/Resources/Weather/NOAA/systeminfo.html

11. http://www2.ncdc.noaa.gov/docs/klm/html/c3/sec3-1.htm

12. http://ceocat.ccrs.nrcan.gc.ca/client_acc/guides/avhrr/ch3.html

13. http://drarunsaraf.tripod.com/iitr-ses.htm

14. http://perigee.ncdc.noaa.gov/docs/podug/html/c1/sec1-410.htm

15. http://www.dlr.de/dlr

16. http://dmsp.ngdc.noaa.gov/dmsp.html

17. http://meteo.infospace.ru

18. http://www.wunderground.com/global/Region/A2/Temperature.html

19. http://www.usgs.gov/

20. http://www.asc-india.org/

21. http://neic.usgs.gov/neis/eq_depot/2003/eq_030521/

22. http://www.reliefweb.int/w/rwb.nsf/6686f45896f15dbc852567ae00530132/b49cf0730dc7884149256d480021ee90?OpenDocument

23. http://neic.usgs.gov/neis/bulletin/03_EVENTS /eq_030521/

24. http://neic.usgs.gov/neis/bulletin/03_EVENTS/eq_030527/neic_uhbj_m.html

25. http://monitoring.llnl.gov/regionalization/tect_map.html

26. http://neic.usgs.gov/neis/eq_depot/2003/eq_030521/

27. http://www.ictp.trieste.it/~attia/algeriaseis.htm

28. http://eoweb.dlr.de.8080/servlets/template/welcome/entryPage.vm

29. http://neic.usgs.gov/neis/eq_depot/2003/eq_031226/

30. http://www.iiees.ac.ir/English/bank/Bam/Bam_report_english_aftershock.html

31. http://earthquake.usgs.gov/eqinthenews/2005/usuvae/

32. http://www.reliefweb.int/rw/rwb.nsf/db900SID/RMOI-6AQ9UK?OpenDocument

33. http://neic.usgs.gov/neis/poster/2005/20050222.html

34. http://abcnews.go.com/International/wireStory?id=576069

35. http://neic.usgs.gov/neis/bulletin/neic_uvae_ts.html

36. http://neic.usgs.gov/neis/eq_depot/2003/eq_031226/neic_cvad_ts.html

37. http://freethoughts.org/archives/000389.php

38. http://perigee.ncdc.noaa.gov/docs/klm/html/c7/sec7-1.htm#sec71-2

39. http://quake.exit.com/

40. http://www.gisdevelopment.net/proceedings/tehran/p_session2/bama.htm

41. http://www.terraresearch.net/articles/earthquakeclouds_article1.htm

42. http://neic.usgs.gov/neis/bulletin/bulletin.html

43. http://www.emsc-csem.org

44. http://neic.usgs.gov/neis/eq_depot/2004/eq_041226/

45. http://asc-india.org/events/050328_bob.htm

46. http://rapidfire.sci.gsfc.nasa.gov/

47. http://neic.usgs.gov/neis/eq_depot/2005/eq_050328/neic_weax_ts.html

48. http://neic.usgs.gov/neis/eq_depot/2004/eq_041226/neic_slav_ts.html

49. http://neic.usgs.gov/neis/eqlists/sig_1990.html

50. http://asc-india.org/menu/seismi.htm

51. http://asc-india.org/seismic/pakistan.htm

52. http://www.cnn.com/WORLD/9801/10/china.quake.update/mackinnon.30.aiff

53. http://neic.usgs.gov/neis/eqlists/sig_1998.html

54. http://neic.usgs.gov/neis/eq_depot/2003/eq_030501/

55. http://neic.usgs.gov/neis/eqlists/sig_1999.html

56. http://orfeus.knmi.nl/newsletter/vol4no2/afghan.html

57. http://neic.usgs.gov/neis/eq_depot/2002/eq_020303/

58. http://www.geotimes.org/mar02/WebExtra0326.html

59. http://neic.usgs.gov/neis/bulletin/02_EVENTS/EQ_020325/

60. http://neic.usgs.gov/neis/eq_depot/2003/eq_030224/

61. http://earthobservatory.nasa.gov/Newsroom/NewImages/images.php3?img_id=10933

62. http://www.weatherwise.org/qr/qry.diurnaltemp.html

63. www.Reliefweb.int/w/rwb.Nsf/6686f45896f15dbc852567ae00530132/b342fd7d3ea5bb285256d4000671dce?OpenDocument

64. www.mem-algeria.org/hydrocarbons.htm

65. www.cosis.net/abstracts/EAE03/08814/EAE03-J-08814.pdf

66. www.gisdevelopment.net/aars/acrs/1999/ps6/ps61179a.shtml

ANNEXURE – I

LIST OF PUBLICATIONS OUT OF THE RESEARCH WORK

International Journals:

1. Saraf, A. K. and **S. Choudhury**, 2005, NOAA-AVHRR detects thermal anomaly associated with 26 January, 2001 Bhuj Earthquake, Gujarat, India, *International Journal of Remote Sensing*, Vol. 26, No. 6, pp. 1065-1073.

2. Saraf, A. K. and **S. Choudhury**, 2005, Satellite detects surface thermal anomalies associated with the Algerian earthquakes of May 2003, *International Journal of Remote Sensing*, (in press).

3. Saraf, A. K. and **S. Choudhury**, 2005, SSM/I Applications in Studies of Thermal Anomalies Associated with Earthquakes, *International Journal of Geoinformatics* (submitted).

4. Saraf, A. K., **S. Choudhury** and S. Dasgupta, 2005, Satellite observations of the great mega thrust Sumatra earthquake activities, *International Journal of Geoinformatics* (submitted).

National Journals:

5. Saraf, A. K. and **Swapnamita Choudhury**, 2003, Earthquakes and thermal anomalies, *Geospatial Today*, Vol. 2, No. 2, pp.18-20.

6. Saraf, A. K. and **Swapnamita Choudhury**, 2004, Thermal Remote Sensing Technique in the Study of Pre-earthquake Thermal Anomalies, Journal of Indian Geophysical Union, Vol. 9, No. 3, pp. 197-207.

7. Das, J. D., **S. Choudhury**, A. K. Saraf and S. Panda, (2005), Megathrust Sumatra earthquake and the issue of evident earthquake risk in seismically active Northeastern part of India being affected by the same northward moving Indian Plate, Current Science (submitted).

Chapters in Books:

8. Saraf, A. K., **Swapnamita Choudhury** and Sudipta Dasgupta, 2004, Thermal Remote Sensing Applications in Earthquake Studies, a Chapter in the book, edited by Alok Gupta (accepted).

International Conference:

8. Saraf, A. K. and **Swapnamita Choudhury**, 2004, Satellite Detects Pre-earthquake Thermal Anomalies Associated with Past Major Earthquakes, *Proceedings of Map Asia 2004 Conference held at Beijing, China*, between 26-29 August 2004, pp. 40 (available online at: http://www.gisdevelopment.net/application/natural_hazards/earthquakes/pdf/ma04198.pdf)

   This paper was awarded 'The Best Paper'.

National Conferences:

10. Saraf, A. K. and **Swapnamita Choudhury**, 2004, Thermal Remote Sensing Technique in the Study of Pre-earthquake Thermal Anomalies, Proceedings of the IGU Conference to be held at NGRI, Hyderabad, India between 29-31 December 2004, pp. 5 (abstract only, full paper will come in IGU Journal).

11. Saraf, A. K., Sudipta Dasgupta and **Swapnamita Choudhury**, Satellite Detects Pre-Earthquake Thermal Anomalies In Iran, Proceedings of the Symposium on Seismic Hazard Analysis and Microzonation, Department of Earthquake Engineering, Indian Institute of Technology Roorkee, India, to be held in September 23-24.

ANNEXURE – II

REPRINTS / PRE-PRINTS OF FEW SELECTED PUBLICATIONS

International Journal of Remote Sensing
Vol. 26, No. 6, 20 March 2005, 1065–1073

Taylor & Francis
Taylor & Francis Group

Cover

NOAA-AVHRR detects thermal anomaly associated with the 26 January 2001 Bhuj earthquake, Gujarat, India

A. K. SARAF and S. CHOUDHURY
Department of Earth Sciences, Indian Institute of Technology, Roorkee, Roorkee–247667, India; e-mail: saraffes@iitr.ernet.in

1. Introduction

The earthquake of 26 January 2001, USGS magnitude M_s=7.9 and epicentre at 23°23′57″ latitude and 70°18′51″ longitude (figure 1), struck the state of Gujarat at 8:46 a.m. (IST) while India was celebrating her 51st Republic Day. The death toll was estimated at 20 083 according to Gujarat Government figures and was accompanied by wide scale damage to the property and economy of the state of Gujarat. Places like Bhuj, Anjar, Bhachau and Rapar faced near total destruction and Gandhidham, Morvi, Rajkot and Jamnagar faced extensive damage to concrete structures. A total of 7633 villages of 181 talukas in 11 districts were affected (Saraf *et al.* 2002).

Thermal channels (4 and 5) of AVHRR onboard the NOAA series of satellites can be used to monitor the Earth's thermal regime. Prior to an earthquake, crustal

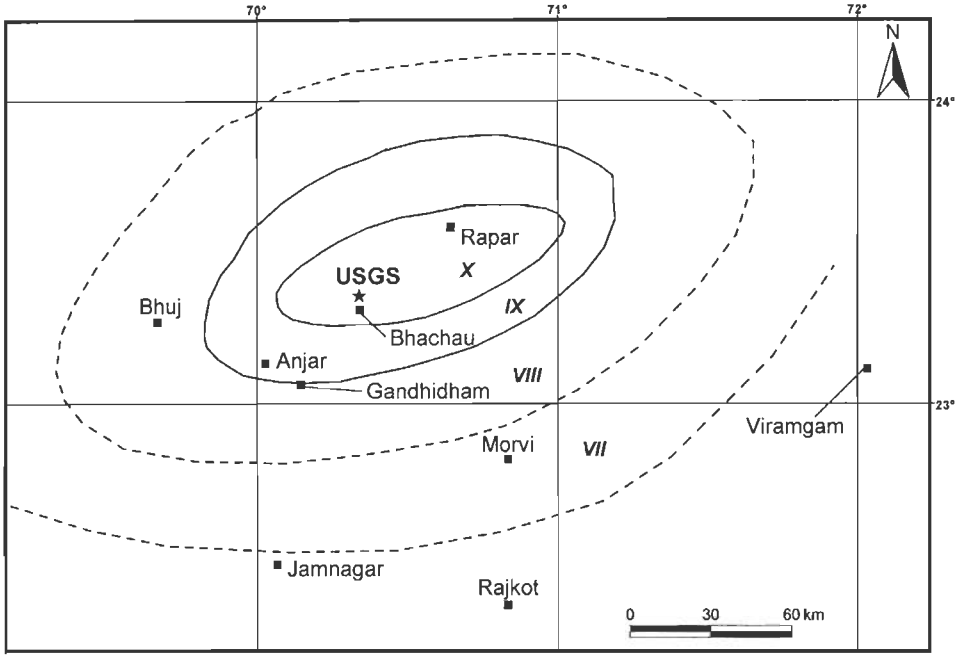

Figure 1. Isosiesmal map shows epicentre (USGS—United States Geological Survey) and locations of some of the most affected places (after Saraf *et al.* 2001, 2002).

International Journal of Remote Sensing
ISSN 0143-1161 print/ISSN 1366-5901 online © 2005 Taylor & Francis Ltd
http://www.tandf.co.uk/journals
DOI: 10.1080/01431160310001642368

deformation occurs due to stress fields. It is well-known that an increase in pressure leads to an increase in temperature. Due to the acting stress field, sub-surface pressure increases, with a consequent increase in temperature. Such deviation from the normal in the thermal regime can provide interesting observations in earthquake studies. It is also known that an increase of stress may lead to release of green house gases like CO_2, CH_4, N_2, etc, trapped in the pore spaces of the rocks. These gases escape to the lower atmosphere and create a localized green house effect and thus augment the land surface temperature of the area (figure 2; Qiang *et al.* 1999). An abnormality in the thermal properties of the Earth's surface, detected by thermal channels like AVHRR, can prove to be a valuable indicator of an impending earthquake.

In Gujarat, the major area affected after the 26 January 2001 earthquake is located in and around major fault systems. The faults oriented around the epicentre of this earthquake are the Alla Bund Fault, the Katrol Hill Fault, the Kutch Mainland Fault, the Adhoi Fault, the Banni Fault and the Island Belt Fault embracing important places like Bhachau, Samakhiali, Rapar, Manfara, Chobari, Trambau, Vondh and Bhimasar (figure 3). These faults have histories of periodic earth movements from time to time (Saraf *et al.* 2002).

NOAA-AVHRR thermal images studied with this view over a period of three months during December 2000 to February 2001 (pre- and post-earthquake), provided interesting observations. There was a thermal anomaly that was seen to show up around three days prior to the occurrence of the major earthquake event.

2. Data and methodology

2.1 *Data*

NOAA-AVHRR digital datasets consisting of pre- and post-earthquake images (1 December 2000–15 February 2001) were studied. This study followed two data analysis steps. First a visual analysis of the thermal channels of the 3-month dataset was carried out, and later a detailed analysis of images (table 1) was completed, showing the appearance and disappearance of the thermal anomaly (figure 4 and cover). It was attempted to keep the time of acquisition of all scenes relatively

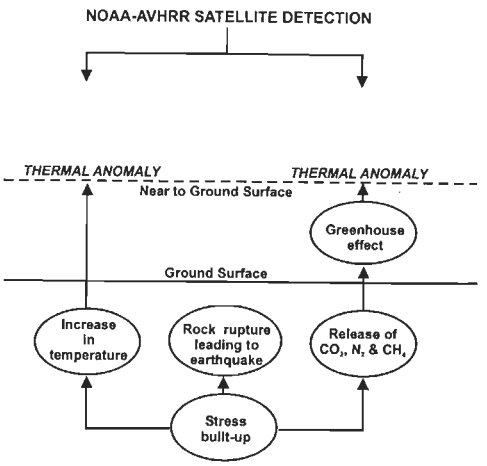

Figure 2. Proposed model behind the generation of pre-earthquake thermal anomaly.

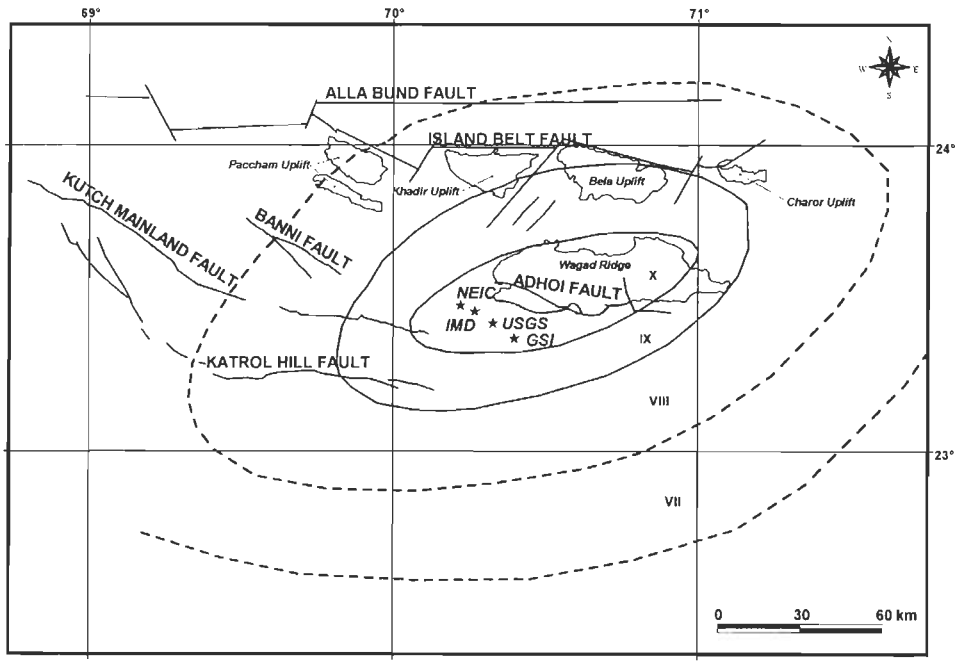

Figure 3. Isoseismal map (Sinvhal *et al.* 2001), major faults, uplifts and ridges (Peters *et al.* 2001). Also shows epicentres from different organisations.

consistent (table 1). Further, in order to obtain a background thermal regime of the study area for comparison purposes, analysis of NOAA-AVHRR datasets of the year 2003 representing the same period (12 January 2003 to 29 January 2003) (table 2) were analysed (figure 5). These data were obtained from IITR-SES (Indian Institute of Technology Roorkee Satellite Earth Station). AVHRR on board NOAA-14 is a 5-channel multispectral scanner with a spatial resolution of 1.1 km. Channels 4 and 5 of the AVHRR sensor are thermal infrared channels.

Scenes obtained from NOAA-14 were first checked against cloud cover. Calibration of data and calculation of temperature was done on raw datasets. Georeferencing of both pre- and post-earthquake images was done using AVHRR georeferencing techniques (available in ENVI software). Land Surface Temperature (LST) calculation was done using the radiance value of channel 4 only. This calculation is based on the algorithm given at http://perigee.ncdc.noaa.gov/docs/podug/html/cl/sec1-410.htm. A user-specified temperature range between −40°C

Table 1. Details of the NOAA-AVHRR digital datasets used in the present study.

Scene number	Date	Time (IST)
Scene 1	12 January 2001	17:39
Scene 2	14 January 2001	17:15
Scene 3	21 January 2001	17:32
Scene 4	23 January 2001	17:09
Scene 5	27 January 2001	18:02
Scene 6	28 January 2001	17:50
Scene 7	29 January 2001	17:38

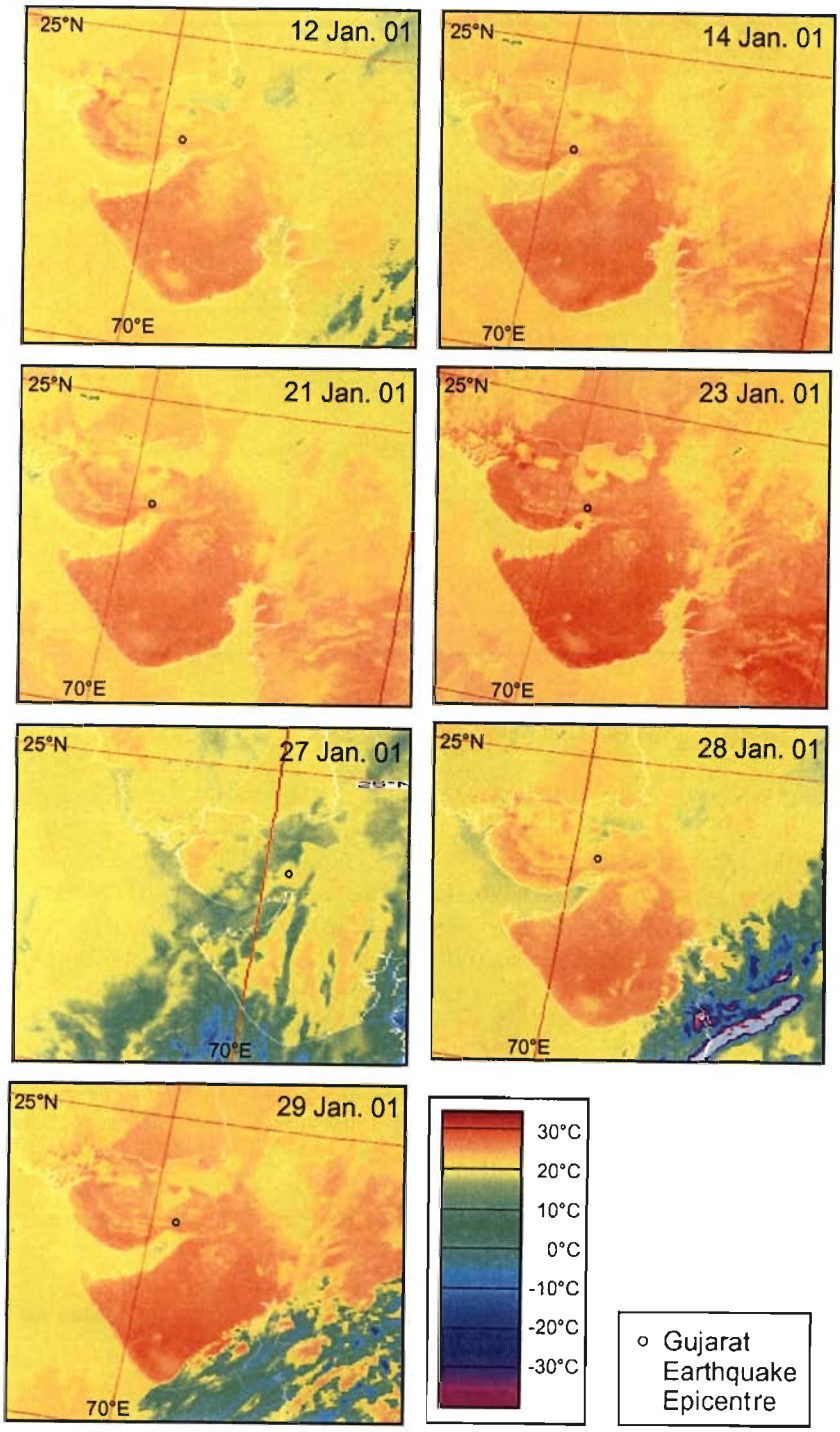

Figure 4. Pre- and post-earthquake Land Surface Temperature (LST) images of Gujarat derived from the thermal channel 4 of NOAA-14 AVHRR data. The earthquake occurred on 26 January 2001. Temperature intensification started from 14 January 2001, which escalated further to a maximum on 23 January 2001, three days before the earthquake. Post-earthquake images of 27, 28 and 29 January 2001 show normal temperature.

Table 2. Details of the NOAA-AVHRR digital datasets used in the present study.

Scene number	Date	Time (IST)
Scene 1	12 January 2003	23:01
Scene 2	14 January 2003	22:15
Scene 3	21 January 2003	22:59
Scene 4	23 January 2003	22:13
Scene 5	27 January 2003	22:23
Scene 6	28 January 2003	22:00
Scene 7	29 January 2003	23:20

and 35°C was used. The temperature was calculated within a continuous colour range for point thermal data calculation of the image.

Weekly average temperature data for a period from 1951 to 1980 (which were the only available past data) of the month of January were obtained from six IMD (India Meteorological Department) stations (figure 6). Further weekly average temperature data of 14 IMD stations of the same month for the year 2001 (figure 6) were also obtained. The above two weekly average temperature datasets were analysed and the trend of weekly variation of temperature for the period in which the earthquake occurred was obtained (figures 7 and 8).

3. Observations

On 14 January 2001, south-west Gujarat started to show an increase in temperature, with respect to the surrounding region. Within a few days, due to the extension of cracks and probably with further release of entrapped gases, there was a spread and increase of the thermal anomaly. The area experiencing this anomaly had spread in a NW–SE direction. On 23 January 2001 there developed an anomaly with an area of around 300 km^2, SE of the 26 January 2001 earthquake epicentre (figure 3). Succeeding this boost, the increase started to wane out, probably with the closing of micro-cracks after 23 January 2001, just three days before the earthquake of 26 January 2001. On 23 January, the temperature was at a maximum between 28°C and 31°C in the anomalous region (about 5–7°C higher than the normal temperature). On 28 January 2001, the anomaly disappeared and the region showed a normal temperature of around 24°C. In order to ascertain that the thermal anomaly discussed above was induced by the 26 January 2001 earthquake, same period satellite data from NOAA-AVHRR for the year 2003 (table 2) of the same area were analysed (figure 5). Further, it was observed that during the January 2003 the thermal regime of the study area shows completely normal pattern.

Available weekly average temperature data (between 1951 and 1980) of the epicentral area and the surrounding region clearly shows that the temperature trend reaches a minimum in the third week, compared to the second and fourth weeks (figure 7). However, in 2001, a peak was observed in the third week instead of in the second or fourth weeks (figure 8). This is in contrary to the observed trend for the past 30 years. This ground observation is in accord with the observed satellite thermal detection during January 2001.

4. Discussion and conclusion

The idea that the thermal anomalies may be connected with seismic activity was put to application in China, Russia and Japan (Qiang *et al.* 1991., 1999, Gorny and

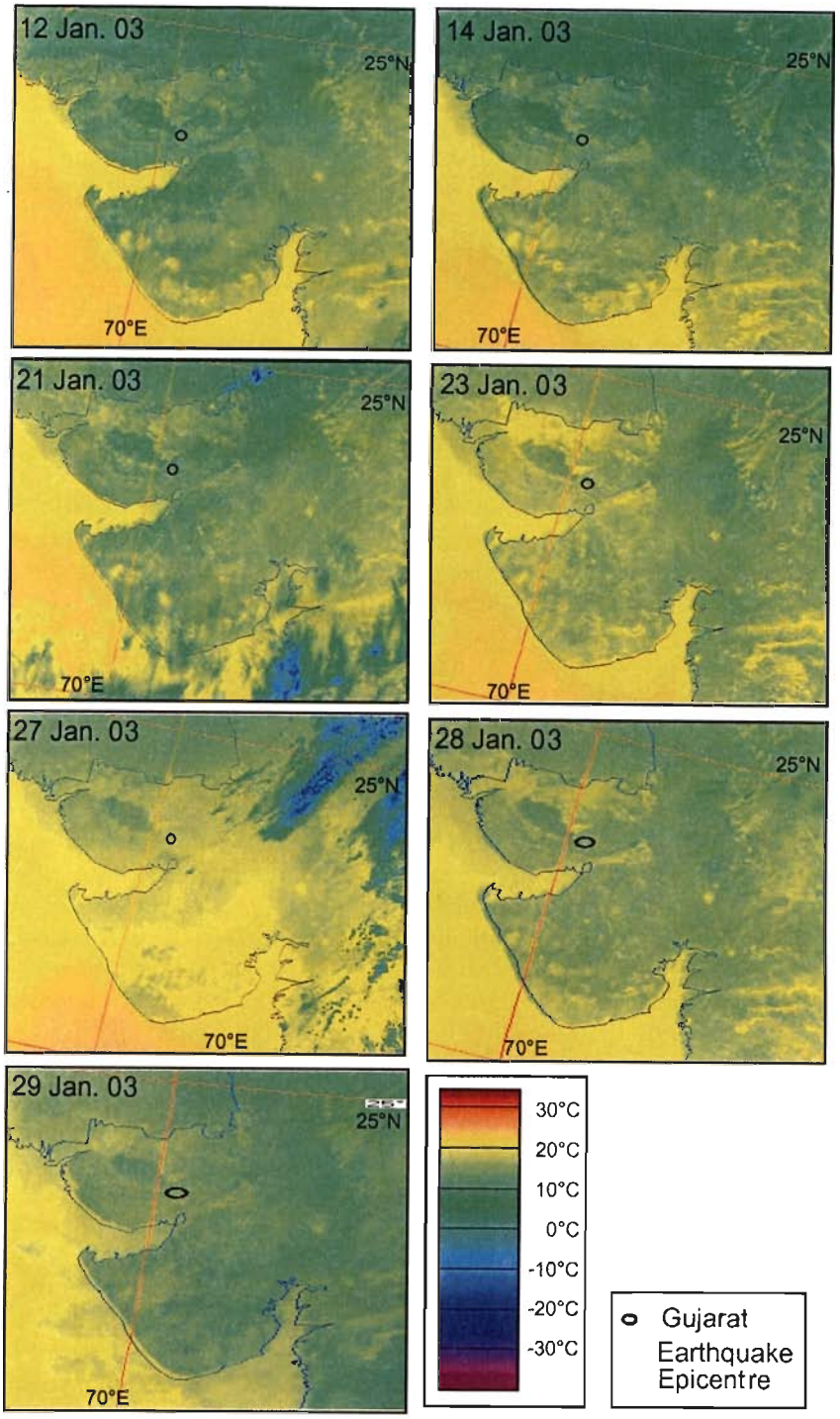

Figure 5. LST images of Gujarat of January 2003, providing a comparison of the temperature scenario over the same dates in which anomalous rise of LST was observed before the earthquake of 26 January 2001. Scenes show a calm and almost unchanging temperature scenario over Gujarat in the month of January 2003.

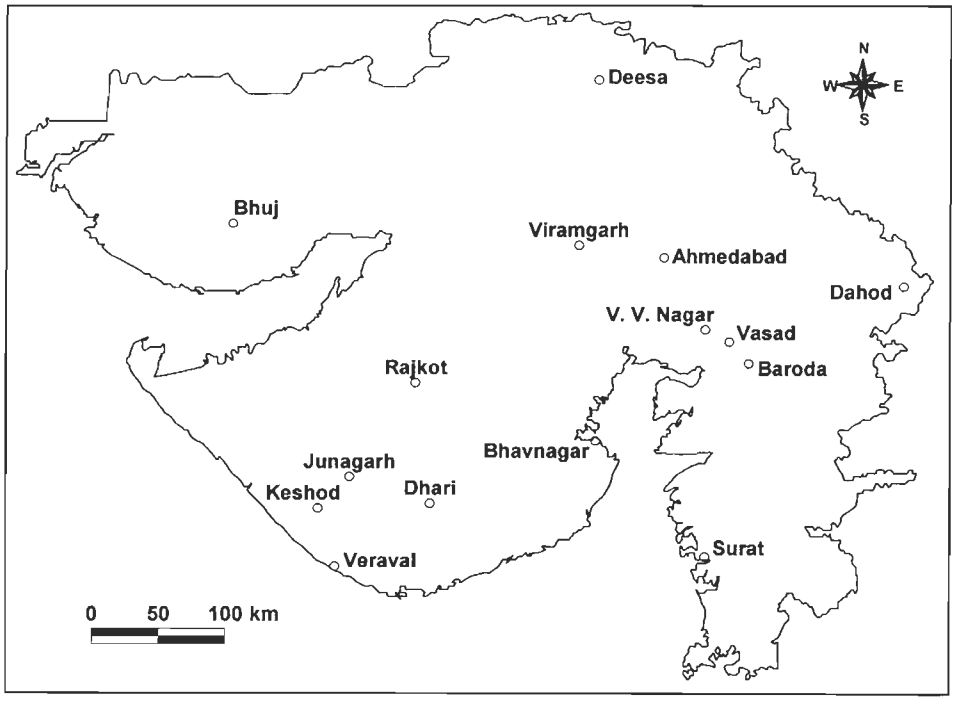

Figure 6. Location of the IMD stations in the state of Gujarat from which the ground temperature data were collected and analysed.

Shilin 1992, Tronin 1996, 2000). An interesting study is that of the Datong earthquake (M_s=6.1, epicenter=39°57′N, 113°43′E) of 18 October 1989 in Shaxi Province of China (Qiang *et al.* 1991). The study of such changes in the thermal behaviour of the area induced by an earthquake is also supported by the analysis

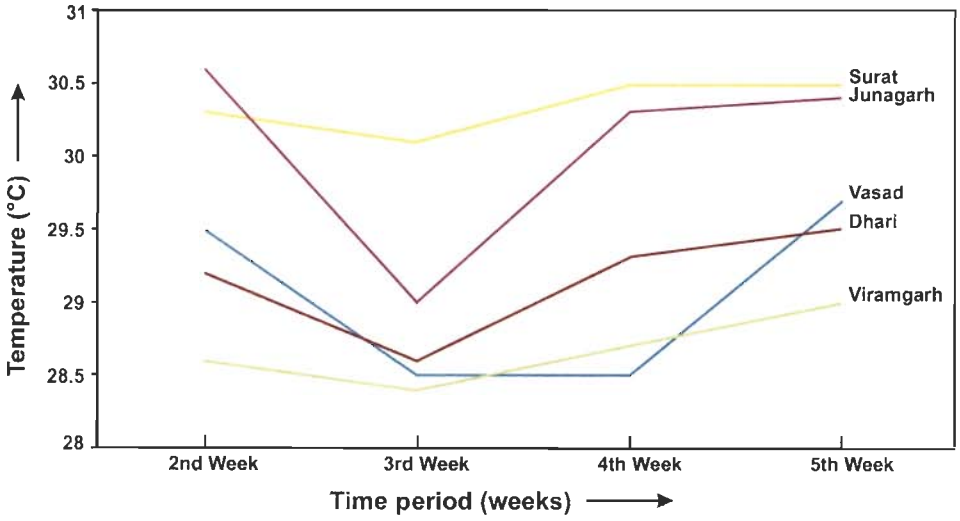

Figure 7. Weekly average temperature variations in the second, third, fourth and fifth weeks (Julian weeks) over the years from 1951 to 1980 (data source: IMD 1991).

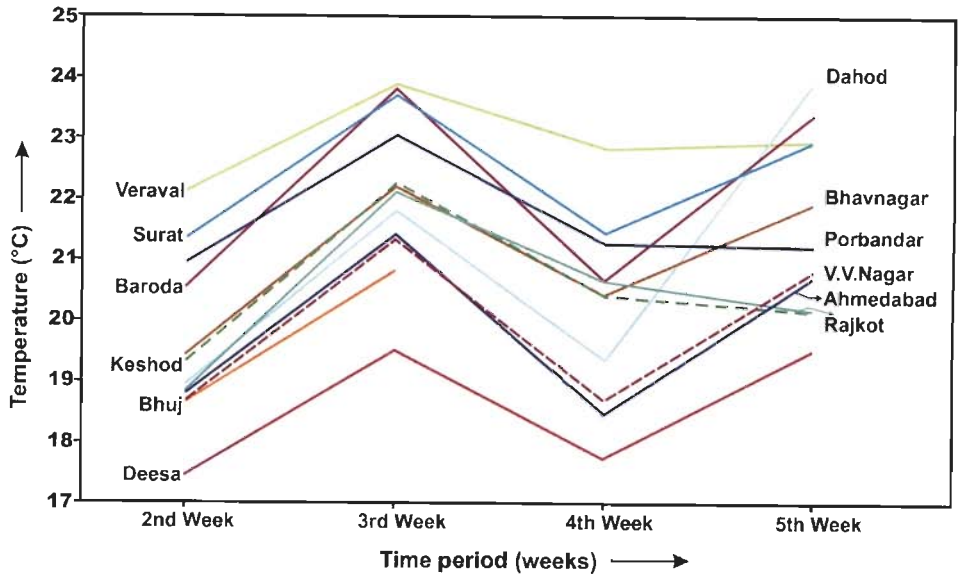

Figure 8. Weekly average temperature variations in the second, third, fourth and fifth weeks (Julian weeks) of the year 2001.

of+ MODIS data (http://amesnews.arc.nasa.gov/releases/2002/02images/quakes/earthquakes.html).

Series of NOAA operational satellites provide the great advantage that AVHRR data can be used to monitor an area on regular and frequent basis. The phenomenon of the occurrence of such thermal earthquake precursors recognises that earth degassing is behind the creation of a localized greenhouse effect. It is not clear under what circumstances will the escape of gases to the atmosphere be successful. Whether topography and the thickness of the earth crust play roles in permitting the escape, and the thicker the crust, the lower the capacity for the gases to reach the lower atmosphere, has not yet been ascertained. It seems that these changes in thermal regime can be more extensively used to forecast earthquakes rather than limiting them to post-earthquake phase studies.

Acknowledgment

We are greatly indebted to the Department of Science and Technology (DST), New Delhi for financial assistance, the National Institute of Oceanography (NIO), Goa, and India Meteorological Department (IMD), Ahmedabad for providing valuable data for this study.

References

GORNY, V.I. and SHILIN, B.V., 1992, Thermal method of remote sensing for study of natural resources. *Proceedings of the 18th Annual Conference of the Remote Sensing Society*, 1992, University of Dundee, 15–17 September 1992, edited by A.P. Cracknell and R.A. Vaughan, pp. 245–263.

INDIA METEOROLOGICAL DEPARTMENT, 1991, Normals of Agroclimatic Observatories in India, Division of Agricultural Meteorology, India Meteorological Department, Pune, 106 p.

PETERS, J., RANA, M.S., KUMAR, S. and BHOJ, R., 2001, Kachchh earthquake of 26th January, 2001: Geological Implications of Relocating Anjar Town, Kachchh District, Gujrat, ONGC Report, DehraDun, March 2001.

SARAF, A.K., SINHVAL, A. and SINHVAL, H., 2001, The Kutch earthquake of January 26th 2001: Satellite data reveals earthquake-induced ground changes and appearance of water bodies. *Proceedings of Workshop on Recent Earthquakes of Chamoli and Bhuj*, Department of Earthquake Engineering, University of Roorkee 22–23 May 2001, edited by H.R. Wason, A.K. Pachauri and V. Prakash (Roorkee, India: Indian Society of Earthquake Technology), pp. 207–216.

SARAF, A.K., SINVHAL, A., SINVHAL, H., GHOSH, P. and SARMA, B., 2002, Satellite data reveals 26 January 2001 Kutch earthquake-induced ground changes and appearance of water bodies. *International Journal of Remote Sensing*, **23**, pp. 1749–1756.

SINVHAL, A., BOSE, P.R., PRAKASH, V., BOSE, A., SARAF, A.K. and SINVHAL, H., 2001, Damage, seismotectonics and isoseismals for the Kutch earthquake of 26th January 2001. *Proceedings of Workshop on Recent Earthquakes of Chamoli and Bhuj*, 22–23 May 2001, edited by H.R. Wason, A.K. Pachauri and V. Prakash, Department of Earthquake Engineering, University of Roorkee, pp. 61–70.

TRONIN, A.A., 1996, Satellite thermal survey—a new tool for the study of seismoactive regions. *International Journal of Remote Sensing*, **17**, pp. 1439–1455.

TRONIN, A.A., 2000, Thermal IR satellite sensor data application for earthquake research in China. *International Journal of Remote Sensing*, **21**, pp. 3169–3177.

QIANG, Z.-J., XU, X.-D. and DIAN, C.-G., 1991, Thermal infrared anomaly – precursor of impending earthquakes. *Chinese Science Bulletin*, **36**, pp. 319–323.

QIANG, Z.-J., DIAN, C.-G., LI, L., XU, M., GE, F., LIU, T., ZHAO, Y. and GUO, M., 1999, Satellite thermal infrared brightness temperature anomaly image – short-term and impending earthquake precursors. *Science in China*, **42**, pp. 313–324.

INT. J. REMOTE SENSING, 2004, prEview article

Taylor & Francis
Taylor & Francis Group

Cover

Satellite detects surface thermal anomalies associated with the Algerian earthquakes of May 2003

A. K. SARAF and S. CHOUDHURY

Department of Earth Sciences, Indian Institute of Technology Roorkee, Roorkee-247667, India; e-mail: saraffes@iitr.ernet.in

1. Introduction

On 21 May 2003, Algeria was hit by a powerful shallow focus earthquake of magnitude $M_w = 6.8$ (http://neic.usgs.gov/neis/bulletin/03_EVENTS/eq_030521/) at 18:44 (UTC) which led to the death of 2276 people, injured more than 11 000 people and left 200 000 people homeless (http://www.reliefweb.int/w/rwb.nsf/6686f45896f15dbc852567ae00530132/b49cf0730dc7884149256d480021ee90?OpenDocument). The geographical location of the epicentre was 36.90° N latitude and 3.71° E longitude (figure 1), just offshore from the province of Boumerdes, and about 60 km ENE of the capital city of Algiers. The province of Boumerdes, including the coastal city of Boumerdes, Thenia, Rouiba and the eastern district of Algiers are among the heavily damaged regions by this 'Boumerdes earthquake' (www.Reliefweb.int/w/rwb.Nsf/6686f45896f15dbc852567ae00530132/b342fd7d3ea5bb285256d4000671dce?OpenDocument). The earthquake has been named after the worst hit region, Boumerdes in Algeria. Notable large-scale concrete structure damage was witnessed in this earthquake. Since Algeria's independence from France in 1962, the country has seen a rapid rise in urbanization. There has been a growth in the building of concrete structures in the cities. The heavily damaged or collapsed buildings were mainly built within the last decade, some just completed or in the process of completion. Widespread liquefaction, rock falls, landslides and ground cracking were reported in the earthquake-affected region. However, no clear case of fault rupturing was reported (www-megacities.physik.uni-karlsruhe.de/wwwmega/downloads/QuakeReport1_2June03.pdf). A tsunami generated with an estimated wave height of 2 m caused damage to boats and underwater telephonic cables off the Balearic Islands, Spain (http://neic.usgs.gov/neis/bulletin/03_EVENTS/eq_030521/).

This major earthquake was followed by a number of low intensity earthquakes (table 1), which continued till 29 May 2003. Minutes after the 6.8 magnitude earthquake played havoc in northern Algeria, a 5.7 M_w earthquake occurred at 18:51 (UTC), with an epicentre at 36.97° N latitude and 3.85° E longitude (http://neic.usgs.gov/neis/bulletin/03_EVENTS/eq_030527/neic_uhbj_m.html). Other aftershocks of magnitude greater

International Journal of Remote Sensing
ISSN 0143-1161 print/ISSN 1366-5901 online © 2004 Taylor & Francis Ltd
http://www.tandf.co.uk/journals
DOI: 10.1080/01431160310001642359

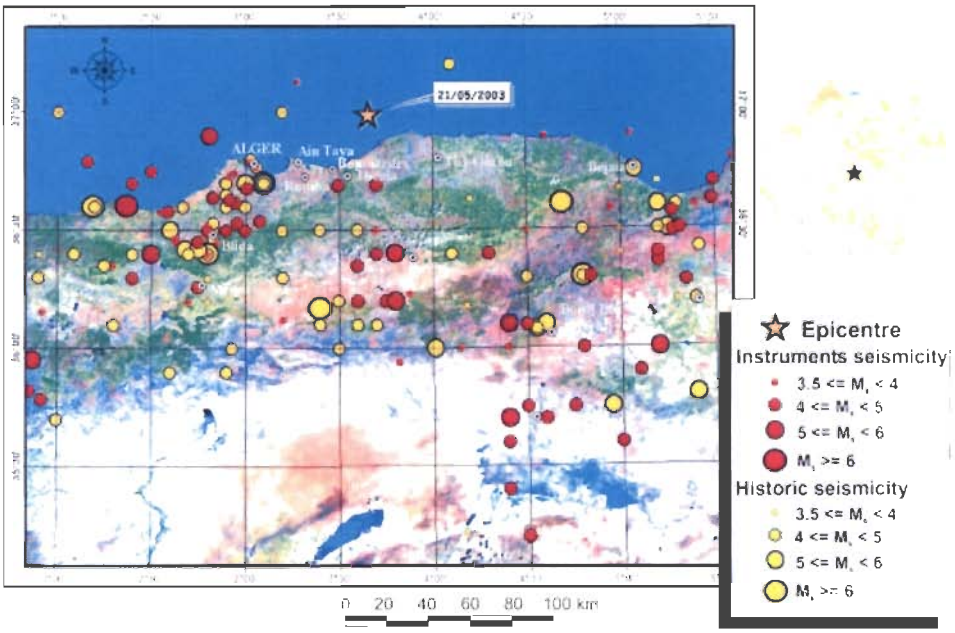

Figure 1. Map showing the study area, the location of the 21 May 2003 earthquake epicentre, affected places and locations of past earthquakes (both instruments and historic seismicity).

Table 1. List of recorded earthquakes in May 2003 in Algeria.

S. No.	Date	Magnitude (M_w)	Latitude (°N)	Longitude (°E)	Time (UTC)	Depth (km)
1	21 May 2003	6.8	36.89	3.78	18:44	10
2	21 May 2003	5.7	36.97	3.85	18:51	10
3	21 May 2003	5.2	36.80	3.76	19:02	10
4	21 May 2003	4.4	36.94	3.60	20:07	10
5	21 May 2003	4.0	36.97	3.53	21:53	10
6	21 May 2003	4.2	36.77	3.65	22:18	10
7	21 May 2003	4.4	36.87	3.90	23:18	10
8	21 May 2003	4.7	36.97	3.53	23:23	10
9	22 May 2003	4.4	36.78	3.65	1:39	10
10	22 May 2003	5.5	36.91	3.68	3:14	10
11	22 May 2003	4.2	36.71	3.76	4:29	10
12	22 May 2003	4.8	36.93	3.92	11:11	10
13	22 May 2003	4.3	36.81	3.68	12:51	10
14	23 May 2003	4.4	36.83	3.88	0:08	10
15	24 May 2003	4.4	36.93	3.96	19:21	10
16	25 May 2003	2.8	36.88	3.72	8:03	10
17	25 May 2003	2.6	36.78	3.98	10:19	10
18	25 May 2003	2.4	36.50	3.79	18:43	10
19	25 May 2003	2.5	36.82	3.66	18:59	10
20	27 May 2003	5.8	36.88	3.65	17:11	10
21	28 May 2003	5.0	36.74	3.45	6:58	10
22	29 May 2003	4.9	36.84	3.39	2:15	10

than 5 (M_w) occurred on 22, 27 and 28 May 2003. More than 21 aftershocks (table 1) were reported within nine days beginning from 21 May 2003, ranging in magnitude from 2.4 to 5.8 (M_w).

Land Surface Temperature (LST) maps generated from thermal images of NOAA-AVHRR datasets can be used to monitor the Earth's thermal regime for any change that might be induced by an earthquake. The thermal channels (4 and 5) of the sensor AVHRR onboard the NOAA series of satellites were used to study the LST for northern Algeria to look for any change in the thermal character of northern Algeria induced by the Boumerdes earthquake of 21 May 2003 and its aftershocks.

On analysis of the time series LST maps, a thermal anomaly was seen building up on the night of 13 May 2003. This anomaly showed a maximum rise on the night of 20 May 2003 just a few hours before the main shock. The earthquake occurred on 21 May 2003. A less intense anomaly was seen to persist towards the south of the Boumerdes epicentre (figure 2). This anomaly faded finally with the disappearance of the aftershocks.

Similar occurrence of thermal anomalies prior to earthquakes has also been studied and reported by Saraf and Choudhury (2003) for the Bhuj earthquake in Gujarat, India, which struck on 26 January 2001 at 23.39° N latitude and 70.31° E longitude. A thermal anomaly was seen to develop to a maximum on 23 January 2001 (three days before the main shock) south-east of the epicentre covering an area of around 300 km^2. On 23 January, the temperature was 28–31°C in the anomalous region (about 5–7°C higher than the normal temperature). The anomalous temperature disappeared after the 7.9 (M_s) magnitude earthquake (Saraf and Choudhury 2003). The idea that the thermal anomalies may be connected with seismic activity was also put to application in China, Russia and Japan (Qiang *et al.* 1991, 1999, Gorny and Shilin 1992, Tronin 1996, 2000) and interesting observations have been reported.

2. Geology, tectonics and seismicity of the region

The North African country of Algeria is surrounded by the Mediterranean Sea to the north (1200 km of shoreline), Morocco and Western Sahara to the west, Tunisia and Libya to the east and Mauritania, Mali and Niger to the south.

The development of the Mediterranean Alpine ranges in the northern fringe of the African plate along with their Algerian section is the result of the rotation of the African continent with respect to the Eurasian continental plate. This rotation is a slow drifting of the continents towards one another (www.mem-algeria.org/hydrocarbons.htm).

The African plate is moving north-west towards the Eurasian plate with a velocity of 6 mm per year. The relative plate motions create a compressional tectonic environment, which is manifested by a series of thrust-faulting and normal faulting (http://neic.usgs.gov/neis/bulletin/03_EVENTS/eq_030521/). The folded Paleozoic-Mesozoic sediments in the Atlas ranges extending from northern Tunisia through northern Algeria and Morocco are also an expression of this continent-continent convergence. This northern tectonic region of Africa therefore is seismically very active.

Examples of the manifestation of the compression due to the collision of the African-Eurasian plates are the east–west running South Atlas Fault (SAF) and the Middle Atlas Fault (MAF). The MAF runs parallel and lies to the north of the SAF. The upper plates of both these thrust fault zones lie to the north (figure 3 and

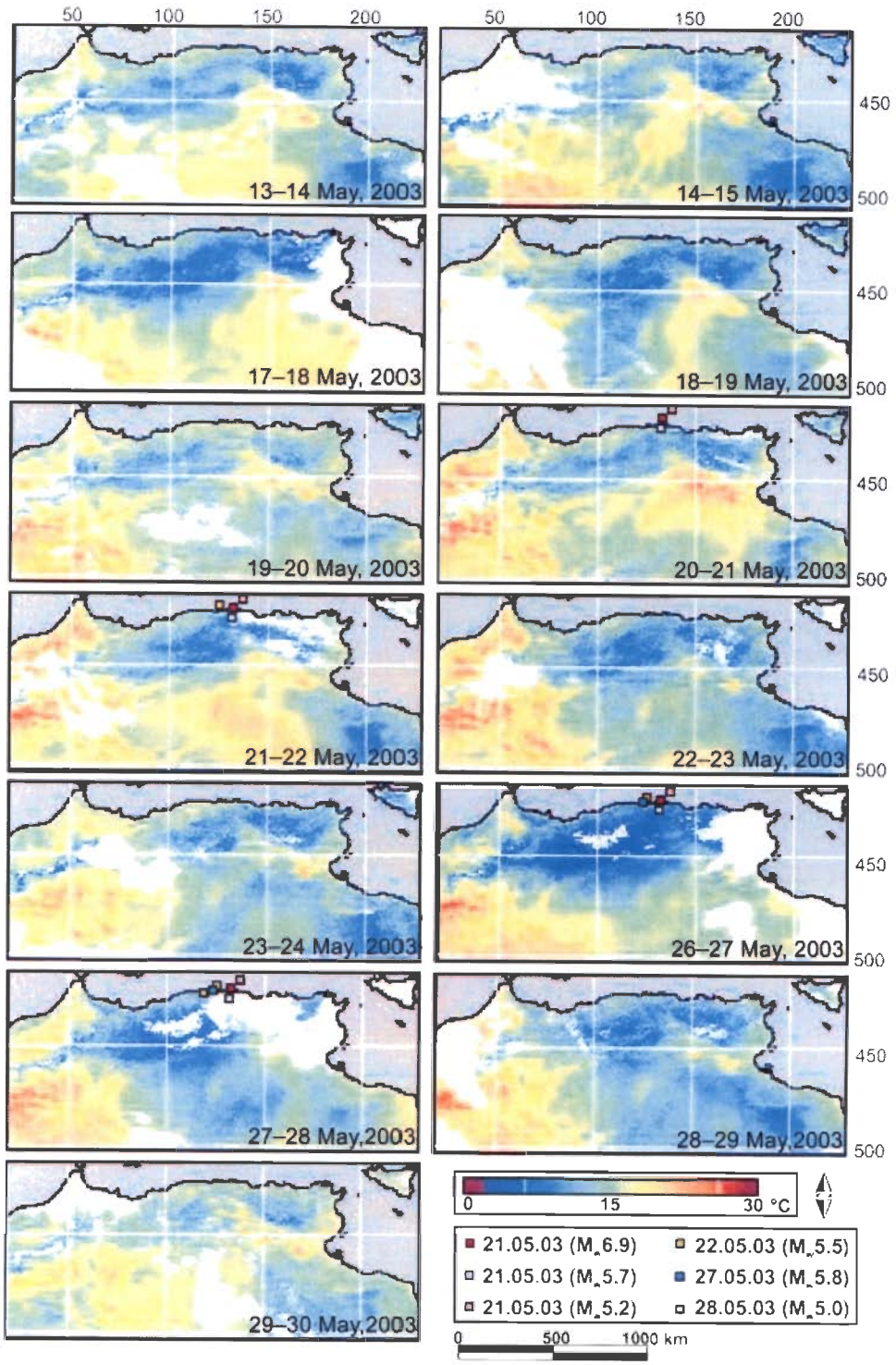

Figure 2. Time series night-time land surface temperature images. White areas show prevailing cloud conditions. The maximum thermal anomaly can be seen on the night-time image of 20–21 May 2003. The main shock occurred on 21 May 2003 at 18:44 (UTC). The figure also shows locations of all significant earthquake events occurring during May 2003. A detailed picture of 20–21 May 2003 night-time LST image along with structural features is also shown in figure 3.

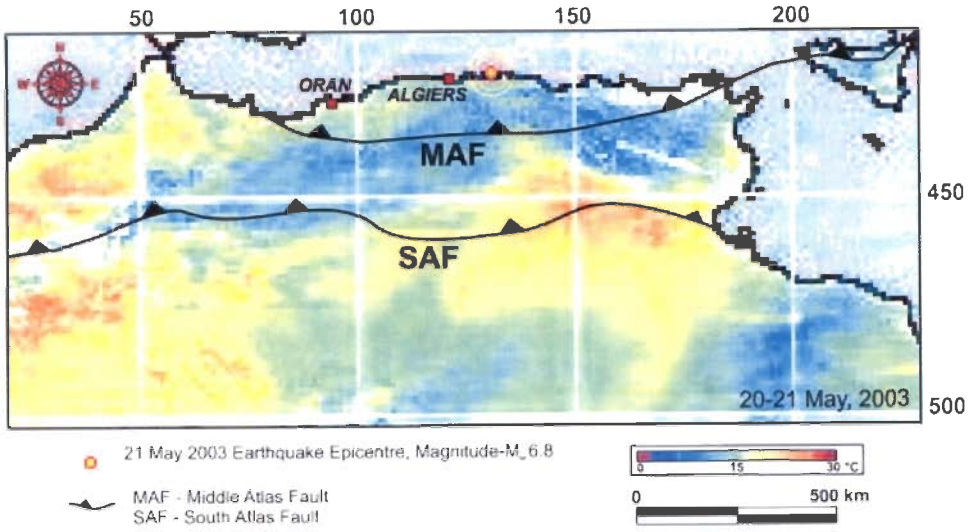

Figure 3. Location of the 21 May 2003 earthquake epicentre and South Atlas Fault (SAF) and Middle Atlas Fault (MAF). Also illustrates coincidence of surface thermal anomaly induced by the 21 May 2003 earthquake with the SAF.

on cover and figure 4) (http:monitoring.llnl.gov/regionalization/tect_map.html). Both the SAF and the MAF are low angle thrusts and are parallel to the African-Eurasian plate margins, which sketch along the coastline of North Algeria.

The linear orientation and location of the thermal anomaly, which was seen to surface as a prelude to the earthquakes, coincides with the SAF fault trace. Relatively low focal depth of 10 km infers the origin of the earthquake on the SAF plane (figure 4).

In the past, Algeria has experienced many destructive earthquakes. On 10 October 1980, the city of El Asnam (now Ech-Cheliff) situated approximately 220 km to the west of the 21 May 2003, 6.8 magnitude earthquake, had been hit by a 7.1 magnitude earthquake that killed at least 5000 people. The same city was

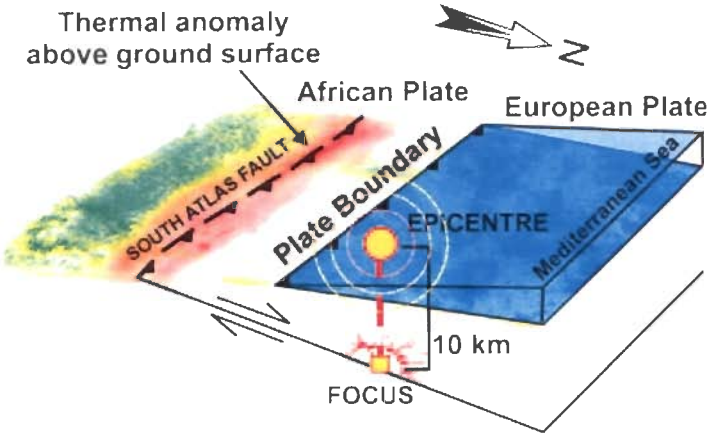

Figure 4. Schematic 3D model of the subsurface location of 21 May 2003 earthquake epicentre, focus and location of South Atlas Fault.

again heavily damaged on 9 September 1954, by a 6.7 magnitude earthquake that killed over 1000 people. On 29 October 1989, a 5.9 magnitude earthquake struck about 110 km to the west of the 21 May 2003 earthquake epicentre and killed 30 people (http://neic.usgs.gov/neis/bulletin/03_EVENTS/eq_030521/). All these events have been located in the Tellian Atlas of Algeria where approximately all seismic zones of Algeria have been observed to be located (http://www.ictp.trieste.it/~attia/algeriaseis.htm).

3. Data and methodology

Daily LST maps were obtained from the website http://eoweb.dlr.de.8080/servlets/template/welcome/entryPage.vm, wherein monthly, weekly and daily day-time and night-time LST composites are prepared from three daytime or nighttime NOAA-16-AVHRR images.

The generation of LST maps is based on the Becker and Li (1990) split window algorithm, which makes use of the differential absorption effects in channels 4 and 5 of NOAA-AVHRR for correcting atmospheric attenuation mainly caused by water vapour absorption. For estimating surface emissivity the relationship given by Van de Griend and Owe (1993) is applied. Thresholds of cloud detection scheme for night-time LST synthesis maps are based on AVHRR channels 3, 4 and 5. The climate zone in the lower latitude is also taken into account. Any pixels identified as cloud are excluded from LST calculation and shown as white areas in all LST maps (figure 2).

The data are remapped into a stereographic projection with a given geometrical resolution of 1.12 km at the centre of the satellite map at 51.00° N/15.00° E. The nearest neighbour technique is applied to resample the pixels into the map. The total size of the maps is 4100 samples × 4300 lines (http://eoweb.dlr.de.8080/servlets/template/welcome/entryPage.vm).

The required region of interest was extracted from the night-time LST maps (12 May–5 June 2003; figure 2). During the present study few night-time thermal images of NOAA-AVHRR obtained from Dundee Satellite Receiving Earth Station were also analysed (table 2).

Night-time LST maps from 12 May to 5 June 2003 were used for studying the daily thermal scenario over Algeria. Then detailed study was done for a period from 13 May to 30 May 2003 on the extracted LST images of the region of interest over northern Algeria for any pre- and post-earthquake thermal abnormality. Association with linear structures and fault systems located in northern Africa was observed. The selection of night-time images was made to avoid differential solar heating. Night-time data also deducts the chances of partial sun illumination due to topography and cloud shadow regions.

Table 2. Details of the NOAA-AVHRR digital datasets of Dundee Satellite Receiving Station used in the present study.

S. No.	Date	Time (IST)
Scene 1	14 May 2003	01:50
Scene 2	18 May 2003	02:46
Scene 3	19 May 2003	02:35
Scene 4	20 May 2003	02:24
Scene 5	21 May 2003	02:12
Scene 6	22 May 2003	02:01

The structural features and tectonics of northern Algeria were studied to ascertain the relation between the structures of the region with the series of earthquakes in May 2003 in Algeria. Fault and thrust locations and trends of the region were delineated and their relation to the location of the focus and epicentre was observed. The cause of the earthquake on 21 May 2003 along with the aftershocks appears to be due to the tectonic conditions in northern Africa, as was reported to be the force behind many past major seismic events in Algeria.

4. Results and discussion

Prior to an earthquake event, crustal deformation occurs due to stress fields. It is well-known that increases in pressure lead to increases in temperature. Due to the acting stress field, sub-surface pressure increases with a consequent increase in temperature. Such deviation from normal in the thermal regime can provide interesting observations in earthquake studies (figure 5; Saraf and Choudhury 2003). It is also known that an increase of stress may lead to release of greenhouse gases like CO_2, CH_4, N_2, etc., trapped in the pore spaces of the rocks, which escape to the lower atmosphere and create a localized greenhouse effect and thus augment the land surface temperature of the area (Qiang *et al.* 1999). An abnormality in the thermal properties of the Earth's surface, detected by thermal channels like AVHRR, can prove to be a valuable indicator of an impending earthquake.

Study of the LST scenario of Algeria before and after the series of earthquakes that rocked Algeria from 21 May to 29 May 2003 supports the above theory of an

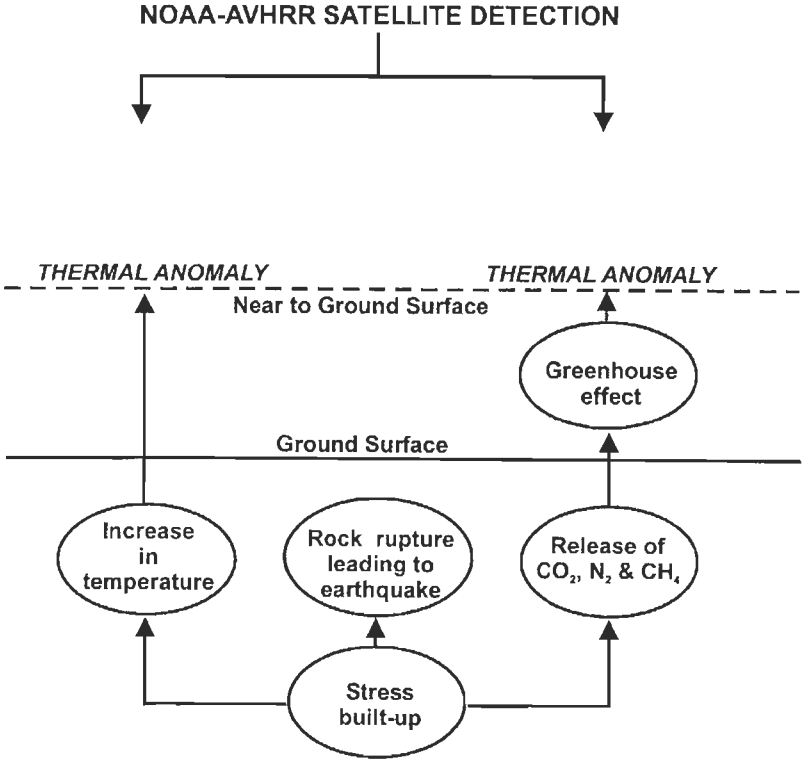

Figure 5. Conceptual model behind the generation of the pre-earthquake thermal anomaly (Saraf and Choudhury 2003).

earthquake precursor. On the night of 13 May 2003, a small area south of the epicentre of the Boumerdes earthquake had started to show a thermal anomaly as compared to the surrounding region (figure 2). This anomaly showed an intense rise on the night of 20 May 2003 covering an approximate area of 41 100 km^2. The temperature of the anomalous area was about 20–24°C, around 5–10°C higher than the surrounding area. The main shock struck Boumerdes province on 21 May 2003 at 18:44 (UTC). The anomaly decreased in intensity on the night of 21 May 2003. This anomaly was a precursor to a 5.5 magnitude earthquake, which occurred on 22 May 2003. The anomaly disappeared on the night of 22 May 2003. Again since the night of 23 May 2003, a weak thermal anomaly appeared on the LST images and faded out with the low intensity aftershocks. Clouds, which covered the study area, hampered the study of the development of any anomaly for the 5.8 magnitude earthquake on 27 May 2003. A weak anomaly was again noticed on the night of 28 May 2003. An earthquake of magnitude 4.9 rocked Algeria on 29 May 2003. The association of the thermal anomalies and the earthquakes is clear.

The location of the thermal anomaly concurs with the SAF (figures 3 and 4), which is a thrust running east to west in northern Algeria. The offshore location and shallow depth (10 km) of the epicentre indicates that the focus lies on the thrust plane of the SAF (figure 4). The coastline of northern Algeria along the Mediterranean Sea is the trace of a plate boundary, in which the African plate is subducted under the Eurasian plate. This compression leads to the creation of a series of thrusts and normal faults in northern Algeria. Therefore, the SAF, which is a part of such series of active structural features, may be regarded as the main cause of the 6.8 magnitude earthquake of 21 May 2003.

5. Conclusions

It may be inferred that the destructive earthquake of 21 May 2003 and the aftershocks were triggered by the tectonic setup of Algeria. The collision of the African-Eurasian plates and its associated thrust (SAF) in north Algeria was the cause of the shocks which is concluded from the location of the epicentre and the linear orientation and location of the thermal anomaly. The amplitude of the observed positive thermal anomaly studied using night-time LST maps generated from NOAA-AVHRR datasets was around 5–10°C. It spread over an area of around 41 100 km^2. The anomaly started building up and reached the peak just a few hours before the main shock. Lesser anomalies persisted till the aftershocks died out on 29 May 2003.

Analysis of meteorological and geological ground data of the study area may further help to understand the earthquake induced thermal anomalies.

Acknowledgment

We are greatly indebted to Department of Science and Technology (DST), New Delhi, India for financial assistance for carrying out this study, Dundee Satellite Receiving Station for providing the dataset and Prof. Robin A. Vaughan of University of Dundee, UK for his kind help.

Website URLs

1. http://www-megacities.physik.unikarlsruhe.de/wwwmega/downloads/QuakeReport1_2June03.pdf
2. http://neic.usgs.gov/neis/bulletin/03_EVENTS/eq_030521/

3. http://neic.usgs.gov/bulletin/03_EVENTS/index.html
4. http://neic.usgs.gov/neis/bulletin/neic_uhbj.html
5. http://neic.usgs.gov/neis/bulletin/03_EVENTS/eq_030527/neic_uhbj_m.html
6. http:monitoring.llnl.gov/regionalization/tect_map.html
7. http://www.mem-algeria.org/hydrocarbons.html
8. http://www.reliefweb.int/w/rwb.nsf/6686f45896f15dbc852567ae00530132/b49cf0730dc7884149256d480021ee90?OpenDocument
9. http://www.reliefweb.int/w/rwb.nsf/6686f45896f15dbc852567ae00530132/b342f1d7d3ea5bb285256d4000671dce?OpenDocument

References

BECKER, F., and LI, Z. L., 1990, Towards a local split window method over land surface. *International Journal of Remote Sensing*, **11**, 369–393.

GORNY, V. I., and SHILIN, B. V., 1992, Thermal method of remote sensing for study of natural resources. *Proceedings of the 18th Annual Conference of the Remote Sensing Society*, University of Dundee, 15–17 September 1992 (edited by A. P. Cracknell and R. A. Vaughan), pp. 245–263.

SARAF, A. K., and CHOUDHURY, S., 2003, NOAA-AVHRR detects thermal anomaly associated with the 26 January 2001 Bhuj earthquake, Gujarat, India. *International Journal of Remote Sensing* (in press).

TRONIN, A. A., 1996, Satellite thermal survey—a new tool for the study of seismoactive regions. *International Journal of Remote Sensing*, **17**, 1439–1455.

TRONIN, A. A., 2000, Thermal IR satellite sensor data application for earthquake research in China. *International Journal of Remote Sensing*, **21**, 3169–3177.

VAN DE GRIEND, A. A., and OWE, M., 1993, On the relationship between thermal emissivity and the normalized difference vegetation index for natural surfaces. *International Journal of Remote Sensing*, **14**, 1119–1137.

QIANG, Z.-J., XU, X.-D., and DIAN, C.-G., 1991, Thermal infrared anomaly—precursor of impending earthquakes. *Chinese Science Bulletin*, **36**, 319–323.

QIANG, Z.-J., DIAN, C.-G., LI, L., XU, M., GE, F., LIU, T., ZHAO, Y., and GUO, M., 1999, Satellite thermal infrared brightness temperature anomaly image—short-term and impending earthquake precursors. *Science in China*, **42**, 313–324.

J. Ind. Geophys. Union (July 2005)
Vol.9, No.3, pp.197-207

Thermal Remote Sensing Technique in the Study of Pre-Earthquake Thermal Anomalies

Arun K. Saraf and Swapnamita Choudhury
Department of Earth Sciences, Indian Institute of Technology Roorkee, Roorkee –247 667
Email: saraffes@iitr.ernet.in

ABSTRACT
Pressure built-up due to tectonic activities and also associated subsurface degassing might create changes in thermal regime prior to an earthquake event and if by any technique this change is detected, it can provide very important clues about future earthquake activities. Thermal satellite remote sensing which can sense the earth's surface emissivity at regular interval introduces a new way of analyzing this phenomenon. Using NOAA-AVHRR thermal datasets, few major past earthquakes (Bhuj (India), Boumerdes (Algeria), Bam (Iran) etc.) were analyzed for studying the thermal changes before and after the earthquakes. The study was successful in detecting pre-earthquake thermal anomalies prior to all these earthquakes. Significant thermal anomalies with a rise in temperature of about 5-10°C in the vicinity of the epicenters have been observed. The anomalies disappeared along with the earthquake events. Further, using passive microwave SSM/I sensor datasets from DMSP satellites the occurrence of the phenomenon of pre-earthquake thermal anomalies for few more earthquakes around the world were observed.

INTRODUCTION

Remote Sensing technology has been an unbiased monitor of the earth's surface. The use of thermal remote sensing has brought out new trends in earthquake research. Land surface temperature (LST) can be calculated with the aid of thermal sensors like Advanced Very High Resolution Radiometer (AVHRR) on board National Oceanic and Atmospheric Administration (NOAA), Multi-spectral Visible and Infrared Scan Radiometer (MVISR) on the Feng Yun (FY) Chinese series of satellites, Moderate Resolution Imaging Spectroradiometer (MODIS) on board satellites Terra and Aqua, Advanced Spaceborne Thermal Emission and Reflection Radiometer (ASTER) on board the satellite Terra, and other thermal Infrared sensors. The passive microwave radiometer, Special Sensor Microwave Imager (SSM/I) on board the Defense Meteorological Satellite Program (DMSP) has the advantage of being more transparent to clouds and has an all weather advantage to sense the thermal emission of the earth's surface.

Three earthquakes were analyzed using NOAA-AVHRR datasets in India, Algeria and Iran. The presence of thermal anomalies in regions around the earthquake epicenter prior to the earthquakes was observed in all these earthquakes. The anomalies disappeared along with the earthquakes [Saraf & Choudhury 2003, 2004 (a), (b) and (c)]. Further, SSM/I datasets were used to analyze a few earthquakes around the world, including the Bhuj Earthquake in India.

BHUJ EARTHQUAKE, GUJARAT, INDIA

The powerful Bhuj Earthquake struck Gujarat on 26 January 2001, at 03:16 (UTC) (local time 08:46 hrs) with a USGS magnitude of 7.9 (M_w). The location of the epicenter was at 23.40°N latitude and 70.31°E longitude, near Bhuj in the state of Gujarat. The earthquake is the result of an east-west thrusting attributed by stresses due to the Indian plate pushing northward into the Eurasian plate. However, no surface rupture was observed after this earthquake.

OBSERVATIONS

Thermal channel 4 of NOAA-AVHRR satellite data was used to calculate the LST of the study area. The LST calculation is based on the method provided in http://perigee.ncdc.noaa.gov/docs/podug/html/c1/sec1-410.htm. Cloud cover was delineated and avoided. The data of days which were cloudy could not be studied for thermal changes as AVHRR cannot penetrate clouds.

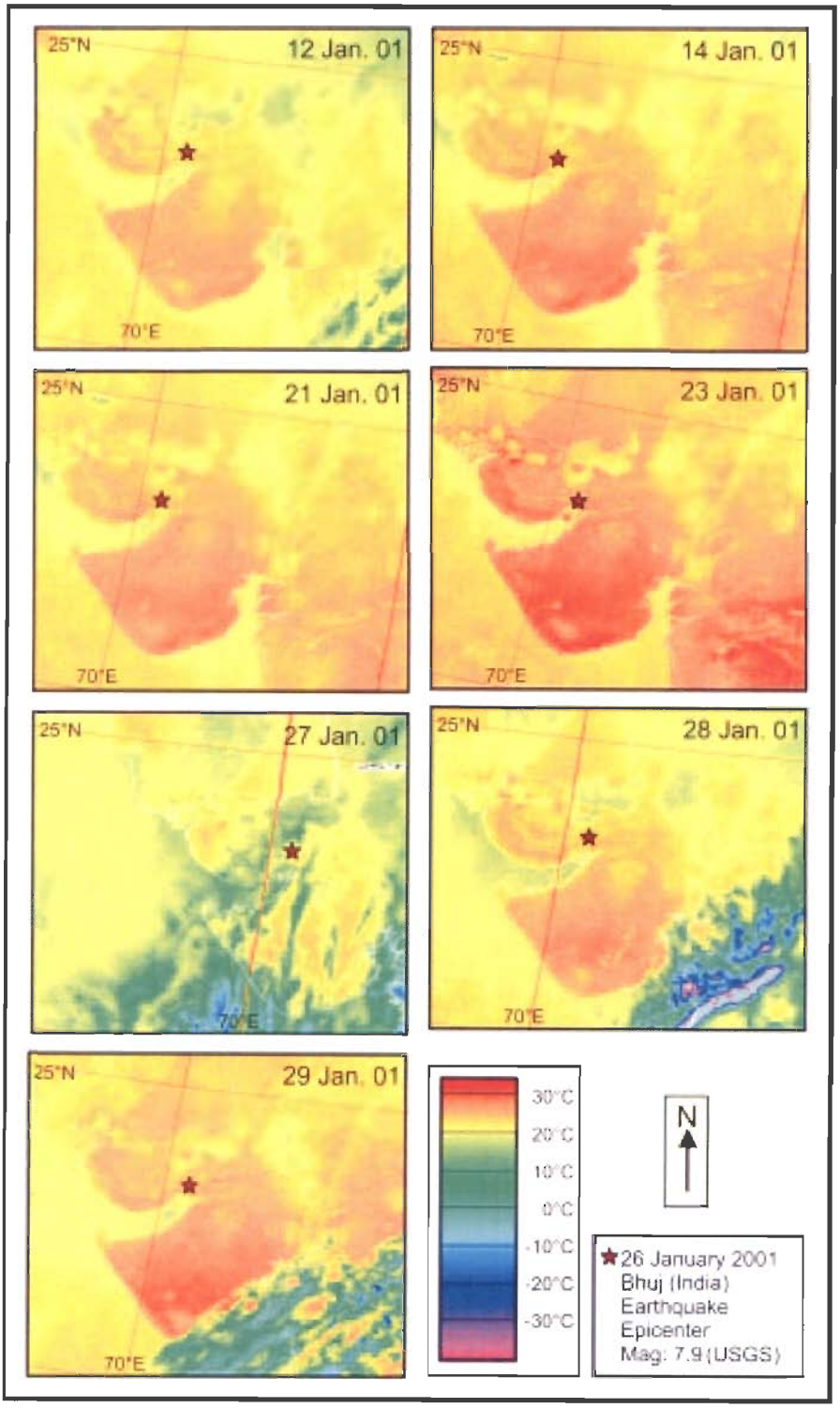

Figure 1 (a). Time series Land Surface Temperature (LST) maps prior to the earthquake of 26 January 2001 in Bhuj, India. Thermal anomaly over the region appeared on 14 January 2001 and was seen to be maximum on 23 January 2001.

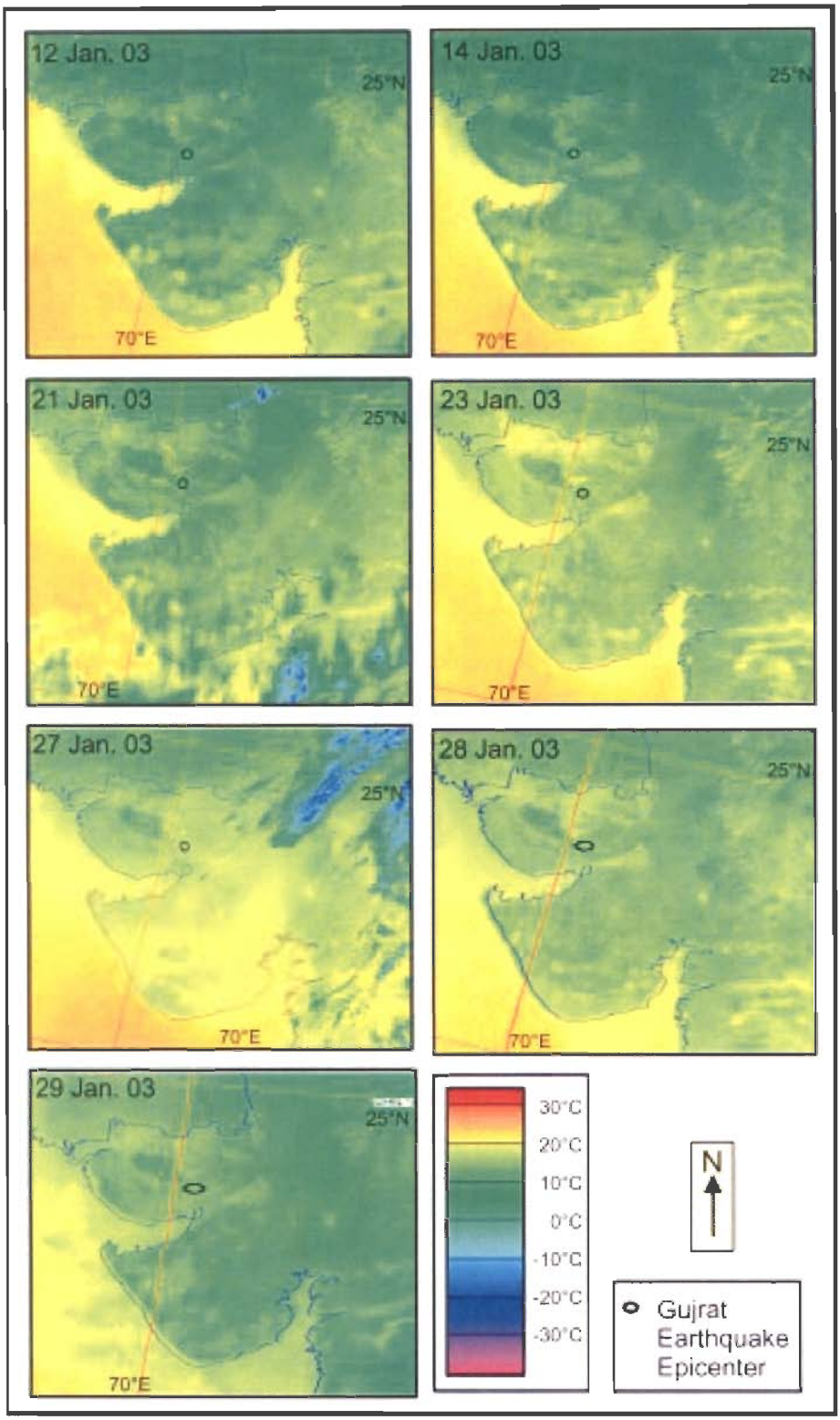

Figure 1 (b). Land Surface Temperature (LST) maps of the year 2003 over Gujarat shows normal thermal scenario.

Pre- and post- LST images revealed a positive thermal buildup on 14 January 2001 in southwest Gujarat with respect to the surrounding. The temperature increased to a maximum on 23 January 2001, just three days before the earthquake hit Gujarat (Fig.1a). On this day the LST was seen to be 28°C - 31°C. This rise in temperature was about 5-7°C higher than the usual temperature of the region. After this boost the temperature started to drop [Saraf & Choudhury 2003 and Saraf & Choudhury 2005]. NOAA-AVHRR data of the year 2003 of the same region and of the same dates were used to study the LST scenario. It was seen that in the year 2003, there was a completely normal thermal scenario in and around the epicenter (Fig. 1b).

To ascertain that this rise was due to the earthquake on 26 January 2001, the trend of the available weekly average temperature data (1951-1980) of a few India Meteorological Department (IMD) stations was analyzed. Using this weekly average temperature data as a base, the average weekly temperature for the period from December 1999 to February 2001 (3 months) of IMD stations around the epicenter was compared. The base period trend shows that in the third week of the year, the temperature for those years from 1951 to 1980 is lowest as compared to second and fourth weeks of those years (Fig. 2a). But in the year 2001 there was a peak of temperature increase in the third week (Fig. 2b) [Saraf & Choudhury 2003 and Saraf & Choudhury 2005]. This is in contrary to the observed trend for the past thirty years. This ground observation is in accord with the observed satellite thermal detection during January 2001.

BOUMERDES EARTHQUAKE, ALGERIA

A powerful shallow focus earthquake of magnitude 6.8 (M_w) hit Algeria on 21 May 2003 at 18:44 (UTC) with its epicenter located at 36.90°N latitude and 3.71°E longitude. This earthquake was accompanied by a series of aftershocks (ranging in magnitude from 5.7 to 2.4 (M_w)) in and around the epicenter in Boumerdes in Algeria, which continued till 28 May 2003. The African plate is moving towards the Eurasian plate along the Mediterranean coastline of Algeria at a rate of about 6 mm per year. This results in a compressional force, which manifests itself as a series of thrust and normal faulting. The movement of the South Atlas Fault (SAF) (which is considered to be responsible for the Boumerdes Earthquake) is a manifestation of such forces [Saraf & Choudhury 2004 (a)].

OBSERVATIONS

LST maps generated using three daily nighttime NOAA-AVHRR datasets obtained from German Aerospace Center (DLR), Koln, Germany were used to study the thermal conditions over Boumerdes before and after the Boumerdes earthquake. The calculation of LST is based on Becker & Li (1990) 'split window' algorithm, using the channels 4 and 5 of the AVHRR datasets. Use of nighttime images avoids solar heating during the day. Nighttime data also deducts the chances of partial sun illumination. Any cloud pixel was excluded from LST calculation.

The LST composite map of the night of 13 May 2003 showed the appearance of a positive thermal anomaly towards an area south of the Boumerdes earthquake epicenter. This anomaly intensified to a maximum buildup of thermal anomaly on the night of 20 May 2003, covering an approximate area of 91,100 km^2. The temperature rose to around 20-24°C, about 5-10°C higher than the surrounding area. After two main shocks occurred, of magnitudes 6.8 and 5.7(M_w), on 21 May 2003, the anomaly weakened. A less intense anomaly on the night of 21 May 2003 was probably a precursor to an earthquake of magnitude of 5.5 (M_w), which occurred on 22 May 2003 at 3:14 (UTC). The anomaly disappeared on the night of 22 May (Fig.3). A weak anomaly again appeared around the same area on the night of 23 May 2003. Clouds, which covered the study area, hampered the study of the development of any anomaly for the 5.8 magnitude earthquake on 27 May. A weak anomaly was again noticed on the night of 28 May (Fig.3). An earthquake of magnitude 4.9 rocked Algeria on 29 May. The location of the thermal anomaly concur with the South Atlas Fault (SAF), which is a thrust running east to west in northern Algeria. The offshore location and shallow depth (10 km) of the epicenter indicates that the focus lies on the thrust plane of the SAF [Saraf & Choudhury 2003 and Saraf & Choudhury 2004 (a)].

BAM EARTHQUAKE, IRAN

The devastating earthquake in Bam, Iran struck on 26 December 2003 at 01:55 (UTC) with a magnitude of 6.6 (M_w). The location of the focus was at a depth of 10 km and the epicenter was located at 29.00° N latitude and 58.33° E longitude near the 2000 years old ancient city of Bam, which was destroyed by the earthquake. The 26 December earthquake is generated by right-lateral strike-slip motion on the North-South trending Bam fault. The Bam fault passes from the vicinity of the city of Bam and between the cities of Bam and Baravat.

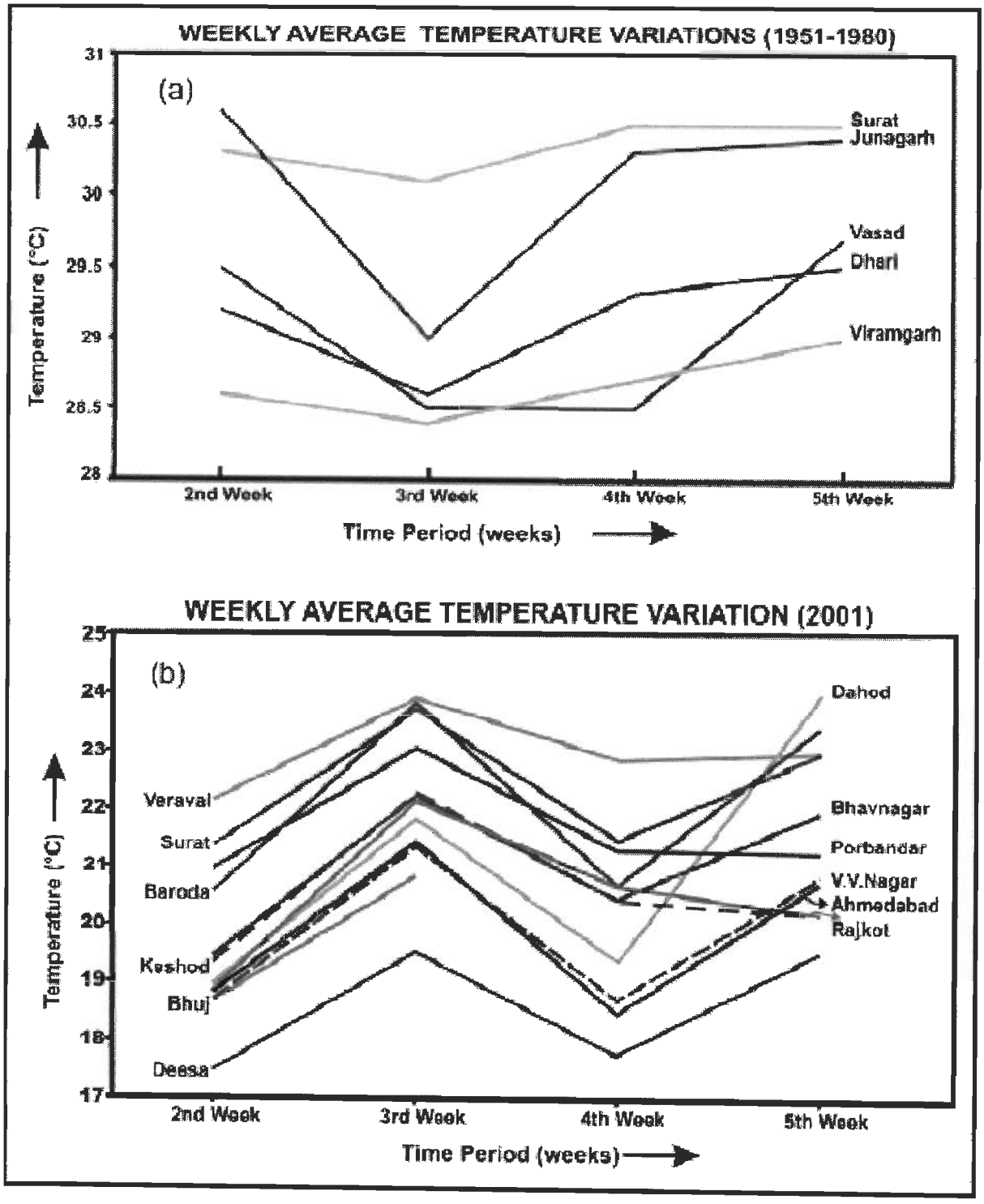

Figure 2. (a) Weekly average meteorological temperature trend in 30 years (1951-1980) shows a usual low in the third week of the year and (b) Weekly average meteorological temperature in the year 2001 shows a high in the third week (when the AVHRR-derived anomaly was observed).

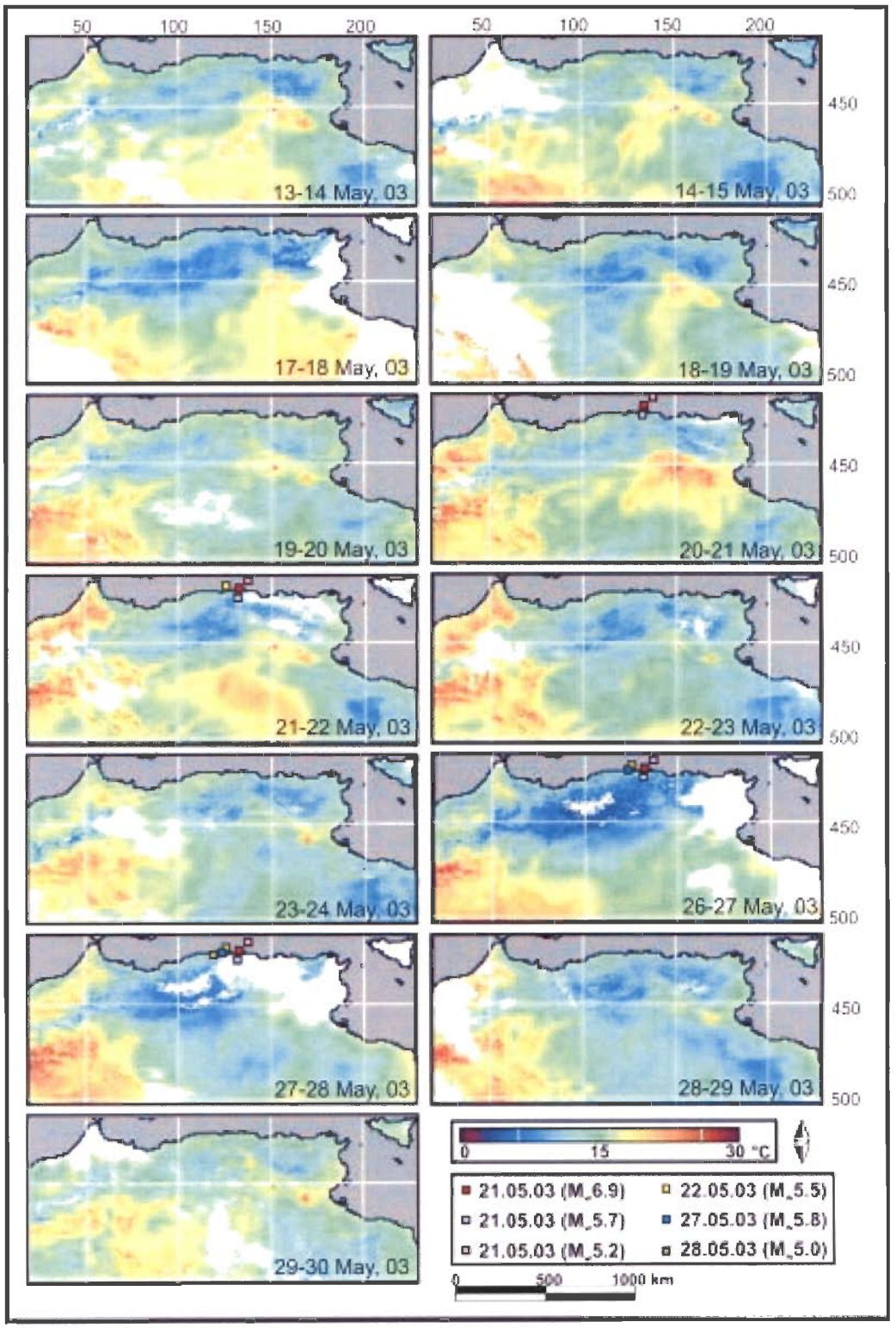

Figure 3. Time series composite maps of Algeria before and after the earthquake. The temperature was seen to be maximum on 20 May 2003.

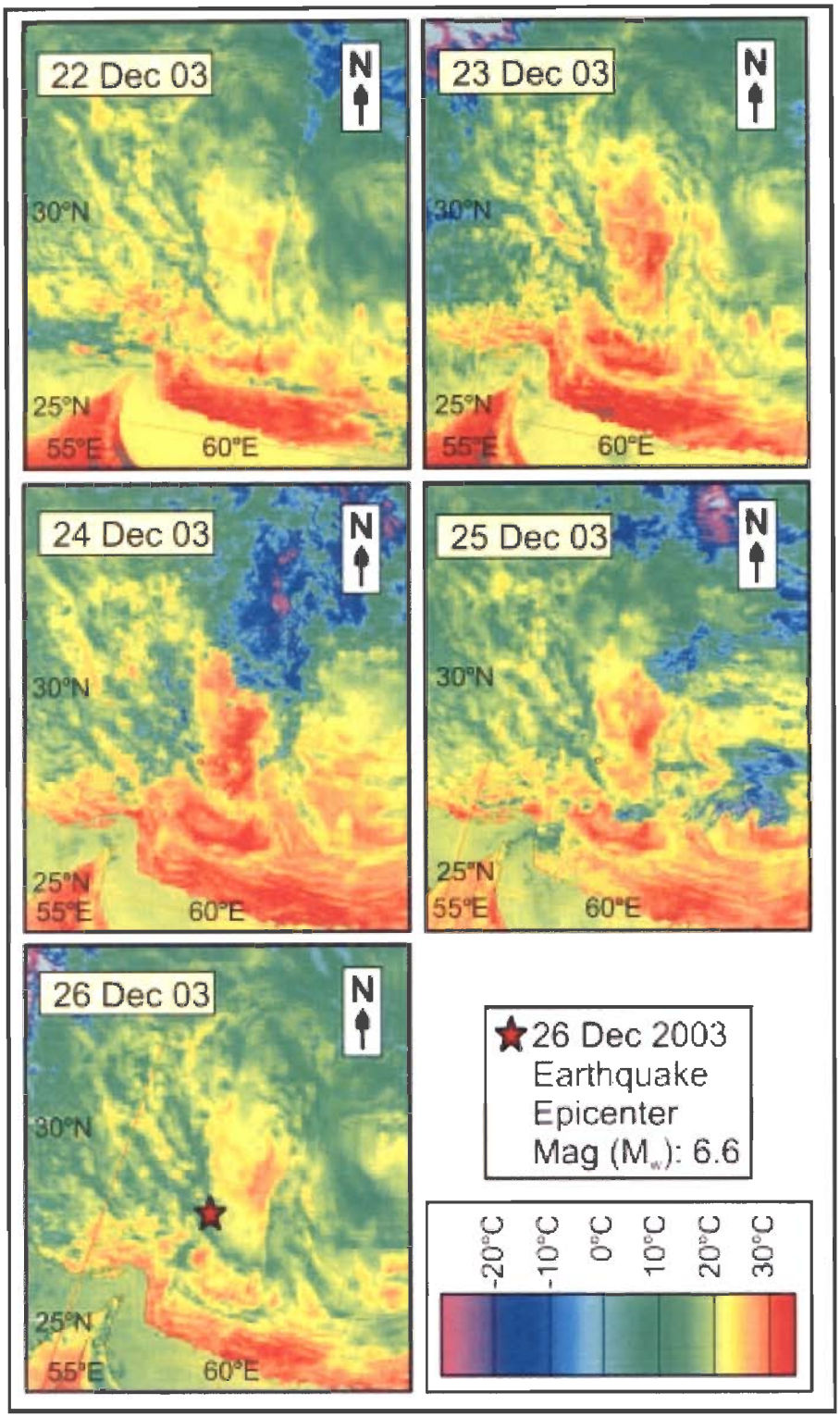

Figure 4. AVHRR-NOAA time series data show thermal anomaly before the 26 December 2003 BamEarthquake in Iran. The maximum anomaly was seen on 24 December 2003, two days before the earthquake.

LST maps for Iran were prepared using the channel 4 of the NOAA-AVHRR datasets using the method mentioned in http://perigee.ncdc.noaa.gov/docs/podug/html/c1/sec1-410.htm. Cloud covered pixels were delineated and masked.

OBSERVATIONS

A thermal anomaly was observed to appear before the devastating earthquake of 26 December 2003. The LST increase was about 5 - 7°C than the usual temperature of the region. At some places, the temperature was about 8 - 10°C higher than normal.

LST time series maps over Iran shows that the rise in temperature started from 22 December 2003 and stayed on till 24 December 2003 (figure 4). On 24 December, just two days prior to the earthquake, the temperature around the entire region and even surrounding the epicenter was around 8°C - 10°C higher than the normal temperature of the region. The rise in temperature dropped on 26 December, the day when the earthquake occurred.

KALAT EARTHQUAKE, PAKISTAN AND HINDUKUSH EARTHQUAKE, AFGHANISTAN

SSM/I on board the DMSP series of satellites is a passive microwave sensor having the advantage to penetrate clouds. The spatial resolution of this sensor is 30 km for all the products. Temperature anomalies derived from SSM/I data are with respect to the mean climatological values between the years from 1988 to 2002. Composite maps of seven days of satellite observation are prepared as a weekly derivative. The weekly anomaly is calculated with reference to 14 years mean temperature data. The temperature scale, therefore, actually represents thermal difference in degree Celsius with respect to the base period of 14 years. A value of +1 on the temperature scale will represent an increase of temperature of 1°C with respect to the base for that particular week on an average, i.e., the region was 1°C warmer than usual for that particular week of the year with respect to all the 14 years [Saraf & Choudhury 2004 (b)].

The Kalat Earthquake in Pakistan on 4 March 1990 (epicenter at 28.92° N and 66.33° E) and the Hindukush Earthquake in Afghanistan on 25 March 2002 (epicenter at 35.97° N and 69.18° E), both with magnitude 6.1 M_w (USGS), have shown interesting observation with SSM/I data. Both these earthquakes were preceded by thermal anomalies. The location of the epicenters of these earthquakes is in similar tectonic region, but these earthquakes have different focal depths. They are both shallow earthquakes, the Kalat Earthquake has a focal depth of 10 km, while the Hindukush has a focal depth of 33 km.

It was seen that the thermal anomaly of the earthquake with the deeper focus, i. e., the Hindukush Earthquake showed an anomaly with a greater spatial extent and the earthquake with the shallower focus, i.e., the Kalat Earthquake showed an anomaly with a lesser spatial extent (Fig.5).

Weekly temperature anomaly maps for the Kalat earthquake in Pakistan showed the development of a thermal anomaly close to the epicentral area two weeks before the earthquake hit the Kalat region in Pakistan. In the next week, the anomaly intensified to a maximum during 19-25 February 1990 with around 2-10°C difference of temperature than base temperature in the region. The anomaly remained for over a week and occupied a small area as a linear arch around the epicenter. This anomalous rise was seen to disappear in the week from 26 February -4 March 1990, i.e., just before the earthquake.

IZMIT EARTHQUAKE (KOCAELI), TURKEY

The active North Anatolian Fault, similar to the San Andreas Fault in California, generates numerous earthquakes in Turkey. SSM/I derived anomaly maps for the devastating 17 August 1999, magnitude 7.6 Izmit earthquake clearly show an increase in temperature of the region before the deadly earthquake. The anomaly, which started building in the week beginning from 6 August, 1999, was centered on the epicenter, but spread over a vast area over Western Turkey (Fig.6). The anomaly maps of this week show a difference in temperature of 2-6°C in the region. The next week probably with active degassing, witnessed a boost of temperature with an increase of 6-10°C with respect to the base period. This anomaly disappeared right after the 19 August 1999 earthquake and since 20 August 1999 showed similar temperature values as normal. The North Anatolian Fault is a strike slip fault, traversing the northern part of Turkey from east to west and forces the bulk of Turkey lying to the south of the fault to drift to the west for about 1200 km.

DISCUSSION AND CONCLUSIONS

The history of the application of thermal remote sensing in natural resources perhaps started in Russia in the nineteen sixties. Thermal data in seismic studies were first used in Russia. Such studies were carried out in Russia, Japan and China. Scientists in China, Russia and Japan observed the occurrence of thermal anomalies (Zu ji, Xiu-Deng & Chang-Gong.

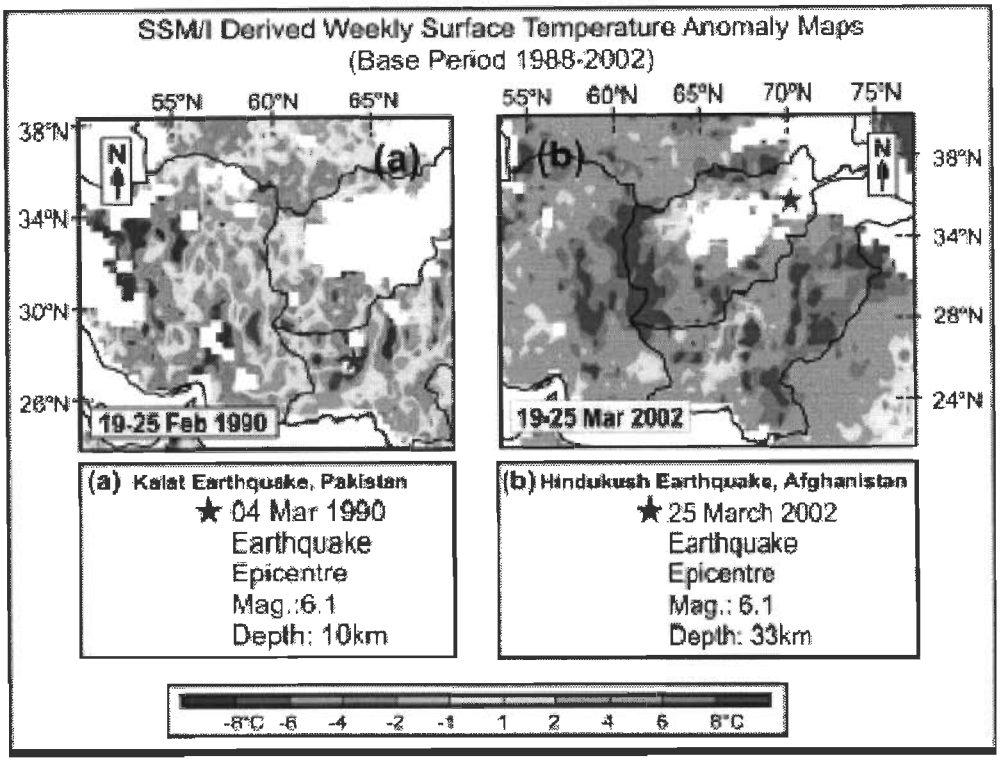

Figure 5. (a) Thermal anomaly prior to the 3 March 2002 earthquake and (b) Thermal anomaly prior to the 25 March 2002 earthquake. Both these earthquakes have the same magnitude, are located in similar tectonic locations but differ in their depth of focus.

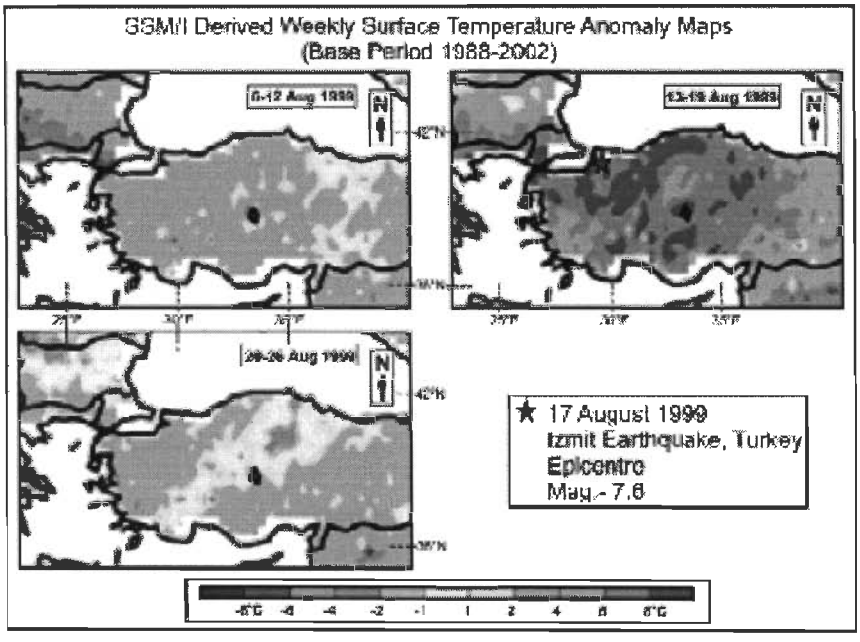

Figure 6. Thermal anomaly prior to the 17 August 1999, Izmit Earthquake in Turkey.

1991, Gorny & Shilin 1992, Tronin 1996, Zu ji et al. 1999, Tronin 2000). Zu ji et al. successfully studied and tried to predict a number of earthquakes based on thermal anomalies. Zu Ji, Xiu-Deng & Chang-Gong (1991) also state that rock breaking tests in laboratories have verified the escape of gases due to subsurface deformation. Infrared emission under action of enormous pressure has also been experimented upon and verified by Ouzounov and Freund (Ouzounov and Freund, 2003).

Prior to an earthquake, crustal deformation is due to a stress field. It is a known fact that increases in pressure leads to an increase in temperature. Due to the acting stress field, sub-surface pressure increases with the consequent increase in temperature. Such deviation from normal in the thermal regime can pose to be an interesting observation in earthquake studies. The strengthening of stresses in tectonic regions also results in the production and extension of micro-cracks. The gases trapped in these pores escape and create a localized green house effect and thus create a thermal anomaly near earth's surface. An abnormality in the thermal properties of the near earth's surface, detected by thermal channels like AVHRR, can prove to be a valuable indicator of an impending earthquake. As successfully demonstrated in the present study, the earthquakes in Bhuj (India), Boumerdes (Algeria), Bam (Iran), Izmit (Turkey), Hindukush (Afghanistan) and Kalat (Pakistan) were associated with the presence of pre-earthquake thermal anomalies. The anomalies appeared a few days to a few hours before the earthquakes. The increase in temperature ranges between 4-10°C. These anomalies are seen to disappear after the earthquakes.

ACKNOWLEDGEMENTS

We are indebted in gratitude to Department of Science and Technology (DST), New Delhi for financial assistance, National Institute of Oceanography (NIO), Goa, and India Meteorological Department (IMD), Ahmedabad, University of Dundee, UK, German Aerospace Center (DLR), Koln, Germany, Indian Institute of Technology Roorkee-Satellite Earth Station (IITR-SES), Department of Earth Sciences, IIT Roorkee and NOAA Satellite and Image Service, National Climatic Data Center (NCDC), USA for providing the valuable data.

REFERENCES

Becker, F. & LI, Z.L.,1990. Towards a local split window method over land surface, Int. J. Remote Sensing, 11 (3), pp. 369-393.

Gorny, V. I. &. Shilin, B.V., 1992. Thermal method of remote sensing for study of natural resources, Proceedings of the 18th Annual Conference of the Remote Sensing Society, 1992, University of Dundee, 15-17th September 1992 (edited by A. P. Cracknell and R.A.Vaughan), pp.245-263.

Ouzonov, D. & Freund, F., 2003. http://science.nasa.gov/headlines/ y2003/ 11 aug_ earthquakes.htm

Saraf, A. K. and Choudhury, S., 2003. Earthquakes and Thermal Anomalies, Geospatial Today, 2 (2), 18-20.

Saraf, A. K. & Choudhury, S., 2005. NOAA-AVHRR detects thermal anomaly associated with 26 January, 2001 Bhuj earthquake, Gujarat, India, Int. J. of Remote Sensing, 26 (6), 1065-1073.

Saraf, A. K. & Choudhury, S., 2004 (b). Satellite Detects Surface Thermal Anomalies Associated with the Algerian Earthquakes of May, 2003, Int. J. of Remote Sensing (in press).

Saraf, A. K. & Choudhury, S., 2004 (c). Satellite detects pre-earthquake thermal anomalies associated with past major earthquakes, Proceedings of Map Asia 2004 held at Beijing between 26-29 August 2004, organised by Chinese Academy of Surveying and Mapping, Bejing, China, pp. 40 (full paper in http://www.gisdevelopment.net/application/natural_hazards/earthquakes/ma04198abs.htm).

Tronin, A. A., 1996. Satellite thermal survey-a new tool for the study of seismoactive regions, Int. J. Remote Sensing, 17 (8), 1439-1455.

Tronin, A. A., 2000. Thermal IR satellite sensor data application for earthquake research in China, Int. J. Remote Sensing, 21(16), 3169-3177.

Zu-ji, Qiang, Xiu-Deng, XU & Chang-Gong, DIAN, 1991. Thermal infrared anomaly – precursor of impending earthquakes, Chinese Science Bulletin, 36 (4), 319-323.

Zu-ji, Qiang, Chang-gong, Dian, Lingzhi, LI, Min, XU, Fengsha GE, Tao, LIU, Yong, ZHAO & Manhong, GUO, 1999. Satellite thermal infrared brightness temperature anomaly image – short-term and impending earthquake precursors, Science in China, 42 (3), 313-324.

(Accepted 2005 May 12; Received 2005 March 14; in original form 2004 November 28)

Dr. Arun K. Saraf is M. Sc. (Applied Geology) from University of Roorkee (now Indian Institute of Technology, Roorkee) and Ph. D. (Remote Sensing) from University of Dundee, United Kingdom. Presently he is working in the Department of Earth Sciences, Indian Institute of Technology, Roorkee, India and teaches courses on Remote Sensing and GIS to post graduate students of Applied Geology. He was first in the country to introduce GIS course to post-graduate students in the year 1990. In 1986 he was awarded "National Fellowship to Study Abroad" by Govt. of India for his doctoral degree. Further, in 1994 he was awarded "Indo-US S&T Fellowship" and worked in Goddard Space Flight Centre, NASA, USA for Post Doctoral Research. This year he has been also awarded "National Remote Sensing Award-2001" by Indian Society of Remote Sensing, "GIS Professional of the Year Award-2001" by Map India 2002 and "Best Paper Award" in Map Asia 2004, Beijing, China. Earlier, he has also been given several Khosla Research Awards and Prizes by then University of Roorkee. In the year 2002, he has established NOAA & FY Satellite Earth Station (http://drarunsaraf.tripod.com/iitr-ses.htm) at IITR and has developed thermal remote sensing technique in earthquake studies. Email: saraffes@iitr.ernet.in.

Earthquakes and Thermal Anomalies

If earthquake forewarns us before it really strikes, can we pick up any clue?

ARUN K. SARAF and SWAPNAMITA CHOUDHURY
Department of Earth Sciences,
Indian Institute of Technology Roorkee

Earthquakes are probably the most unexpected and devastating natural phenomenon on earth. From time immemorial, scientists have tried to understand this devastating natural phenomenon, however, forecasting and prediction of an earthquake was a remote possibility and is still today. The role of tectonics as one of the causative factors behind an earthquake is now almost clear. Plate boundaries and fault zones are the most seismically active regions on the earth's crust and almost all past major earthquakes have been located along plate margins.

If earthquake forewarns us before it really strikes, can we pick up any clue? Can remote sensing technology provide us any approach to detect such clues?

Pressure induces a rise in temperature. This is well exemplified by the fact that when we place a coin on a slab of ice, the ice melts, because the weight of the coin exerts pressure on the ice. In a tectonically active region, stresses building up in rocks may lead to an increase in pressure and eventually to an increase in temperature. Sub-surface pressure can also reduce pore spaces in rocks and hence release gases trapped inside. Greenhouse gases like CO_2, NO_2, NH_3, etc., when released, escape to the lower atmosphere and create a green house effect on the earth's surface. The acting stresses may lead to rock rupture and eventually cause an earthquake. An increase in temperature induced by stresses in rocks, if possible to be detected and studied, may pose to be a possible indicator to an impending earthquake.

Thermal sensors like Advanced Very High Resolution Radiometer (AVHRR) on board National Oceanic and Atmospheric Administration (NOAA) series of satellites can be used to study earth's surface temperature. Any anomaly in the temperature regime of the earth can be detected by such sensor. The AVHRR is a multi-spectral (five channels) sensor working in the visible, near infra-red and thermal infra-red parts of the electromagnetic spectrum. Channels 4 and 5 of AVHRR are thermal channels, which detects earth's emissivity. Land surface temperature (LST) of any place can be calculated using these two channels. Channel 1 is used for daytime and channel 3 for nighttime cloud cover mapping.

The occurrence of thermal anomalies preceding major earthquakes was observed by scientists in China, Russia and Japan (Zuji et al., 1991, Gorny and Shilin 1992, Tronin, 1996, Zuji et al., 1999, Tronin, 2000). Positive results have also been obtained by observations and analyses of two interesting earthquakes; the Bhuj earthquake of 26 January 2001 and the Boumerdes earthquake of 21 May, 2003 and the associated aftershocks (Saraf and Choudhury, 2003a and Saraf and Choudhury, 2003b).

Bhuj Earthquake, Gujarat, India:

On 26 January 2001, Gujarat in India was hit by a devastating earthquake at 8:46 a.m. (IST) of USGS magnitude M_s=7.9 and epicenter located at 23° 23' 57" latitude and 70° 18' 51" longitude.

Major fault systems oriented around the epicenter of this earthquake are the Alla Bund Fault, the Katrol Hill Fault, the Kutch Mainland Fault, the Adhoi Fault, the Banni Fault, Khanpur Fault and the Island Belt Fault, embracing important places like Bhachau, Samakhiali, Rapar, Manfara, Chobari, Trambau, Vondh and Bhimasar which faced severe damage due to this earthquake (Saraf et al., 2002).

Evening time AVHRR satellite data, trying best to keep a consistency in time, consisting of pre- and post- earthquake scenes from NOAA-14 were analyzed for three months beginning from December 1999 to February 2001. For the year 2003, NOAA-17-AVHRR datasets of the same period

Earthquake and Economy

Three main categories of natural disasters account for 90% of the world's direct losses: floods, earthquakes, and tropical cyclones.These three events periodically revisit the same geographic zones. Often, the losses can be significant portions of GDP.

On our 51st Republic Day, January 26, 2001 an earthquake struck the Kutch district of Gujarat at 8.46 am. The Epicentre of the earthquake is 20 km North East of Bhuj, the headquarter of Kutch. The Indian Meteorological Department estimated the intensity of the earthquake at 6.9 Richter. According to the US Geological Survey, the intensity of the quake was 7.7 Richter. The quake was the worst in India in the last 180 years. Mr. Ashok K. Lahiri, Chief Economic Adviser, Government of India gave a presentation at the World Bank, Washington conference on Financing the Risks of Natural Disasters during June 2-3, 2003 on *The Impact of Catastrophes on National and Regional Economies: A Case Study of Gujarat.* Excerpts from the Presentation:

What Earthquakes can do?

- Casualties: loss of life and injury.
- Loss of housing.
- Damage to infrastructure.
- Disruption of transport and communications.
- Panic
- Looting.
- Breakdown of social order.
- Loss of industrial output.
- Loss of business.
- Disruption of marketing systems.

In Gujarath earthquake nearly 19,000 people died. Kutch alone reported more than 17,000 deaths.

1.66 lakh people were injured. Most were handicapped for the rest of their lives.

The dead included 7,065 children (0-14 years) and 9,110 women.

There were 348 orphans and 826 widows.

Output Loss

ADB and World Bank's Gujarat Earthquake Assessment Mission estimated the loss at Rs 99 billion and Reconstruction costs were estimated at Rs 106 billion. The annual loss of state domestic product was estimated at around Rs 20 billion (assuming an ICOR of 4) for the first 12 months.

Impact on GDP

- Applying ICOR
- Rs. 99 billion – deduct a third as loss of current value added.
- ICOR of 4
- Get GDP loss as Rs. 23 billion
- Adjust for heterogeneous capital, excess capacity, loss Rs. 20 billion.
- Reconstruction efforts.
- Likely to have been Rs. 15 billion.

Fiscal Accounts

- Differentiate among different taxes: sales tax, stamp duties and registration fees, motor vehicle tax, electricity duty, entertainment tax, profession tax, state excise and other taxes. Shortfall of Rs. 9 billion of which about Rs. 6 billion unconnected with earthquake.
- Earthquake related other flows.
- Expenditure:Rs. 8 billion on relief. Rs. 87 billion on rehabilitation.

Impact on Revenue

Sales tax losses for February and March 2001 were Rs 115 crore. For 2001-02, the losses were expected to be Rs 260 crore.

Motor vehicle tax collections were expected to fall short of budgeted figures by almost Rs 600 crore.

Monthly losses of Rs 4 crore each were projected for electricity duty and entertainment tax.

Professional taxes were expected to be lower by Rs 5 crore in the current year.

The impact on total tax revenues was estimated at Rs 286 crore, Rs 345 crore, and Rs 436 crore, in 2000-01, 2001-02, and 2002-03 respectively.

Total own taxes (as % of SDP) were expected to fall from budgeted estimate of 8.56% (2000-01) to 7.85% and further to 7.46% in 2001-02.

Total tax revenue (as% of SDP) was expected to decline from budgeted estimate of nearly 10% (2000-01) to 9.27% and further to 8.76% in 2001-02

Impact on Expenditure

- Total relief expenditure (food supplies, medical relief, debris removal, and cash compensation) was estimated at around Rs 840 crore.
- Total rehabilitation expenses were figured at Rs 8665 crore. Housing accounted for the highest expenditure (Rs 5148 crore), followed by education (Rs 837 crore) and drinking water (Rs 614 crore).
- Total (relief and rehabilitation) expenses amounted to Rs 9,345 crore.

Other Economic Impacts

Non-tax revenues : Interest receipts, irrigation receipts, and royalties were expected to remain largely unaffected.

Municipal finances: Almost 10% of municipal revenues were expected to be lost in a year.

Banking : 68 commercial bank branches were fully damaged and 80 branches were partially damaged.

Financial market: The wealth loss was expected to lead to reshuffling of peoples' portfolios and affect asset market behaviour.

Employment: Nearly 5 lakh people were expected to become unemployed. Employment in salt, ceramic, and small-scale industries (including refractories, powerlooms, colton ginning etc.) was worst affected ■

as of 2001 from the Indian Institute of Technology Roorkee-Satellite Earth Station (IITR-SES) was used to compare the analyses of the year 2001 and to create a background thermal regime of the area. Channel 4 of NOAA-AVHRR satellite data was used to calculate the LST of the study area. The LST calculation is based on the method provided at www.perigee.ncdc.noaa.gov/docs/podug/html/c1/sec1-410.htm. User specified temperature range of -40° C to 35° C was used and temperature outside this range was masked. Cloud cover was delineated and avoided during the LST estimations. Weekly average temperature data for a period from 1951 to 1980 (which was the only available past data) of the month of January were obtained from six IMD (India Meteorological Department) stations. Further weekly average temperature data of fourteen IMD stations of the same month for the year 2001 were also obtained. The above two weekly average temperature data sets were analyzed and the trend of weekly variation of temperature for the period in which the earthquake occurred was obtained.

Pre- and post- earthquake LST images when studied revealed a positive thermal buildup on 14 January 2001 (figure 1A). Probably with the increase and spread of degassing with further increase in stress, there was a spread and intensification of the thermal anomaly in the lower atmosphere. LST image on 23 January 2001 showed a maximum positive rise in intensity and area extent of the thermal anomaly, just three days before the earthquake rocked Gujarat (figure 1A). The maximum temperature was observed to be around 28° C - 31° C in the anomalous region, about 5° C - 7° C higher than the normal temperature in the surrounding region. This anomaly covered an approximate area of about 300 km^2 towards south of the epicentral location. This anomaly was seen to wane out after the earthquake on 26 January 2001 (figure 1A) (Saraf and Choudhury, 2003a).

A comparative study of LST images prepared with NOAA-AVHRR datasets of the year 2003 was done. These images show a completely normal thermal scenario over that period in the year 2003 (figure 1B).

Meteorological temperature data during the month of January also supports the presence of a thermal anomaly. It was observed that in the third week of January there was a peak in the weekly average temperature in Gujarat in the year 2001. The weekly average temperature from a period between 1951 and 1980 (almost thirty years) was also analyzed and it shows a prominent low in the third week (Saraf and Choudhury, 2003a).

Boumerdes Earthquake, Algeria

Towards the end of the month of May 2003, northern Algeria was rocked by a series of earthquakes. The most powerful shock was felt on 21 May 2003 having magnitude of 6.8 (M_w) (USGS) at 18:44 (UTC). Location of the epicenter is 36.90°N longitude and 3.71°E latitude, offshore near the locality of Zemmouri in the province of Boumerdes.

Following the main shock, a series of aftershocks were reported ranging in magnitude from 5.8 to 2.4 (M_w) (USGS), which continued till 28 May 2003.

Northern Africa is tectonically a very active region. The coastline of Algeria along the Mediterranean Sea is the plate boundary between the African plate and the Eurasian continental plate. The African plate is moving towards the Eurasian plate at a rate of 6 mm per year. This results in a compressional force, which manifests itself as a series of thrust and normal faulting. The east to west running low angle thrusts, namely, the South Atlas Fault (SAF) and the Middle Atlas Fault (MAF) are the best examples of manifestation of such forces. The MAF runs parallel to and lies to the north of the SAF. The upper plate of these thrusts lies to the north. Both these thrusts are parallel to the African-Eurasian plate boundary (www.monitoring.llnl.gov/regionalization/tect_map.html).

LST composite maps prepared from three daily nighttime scenes of NOAA-AVHRR data were analysed and used to study the thermal regime over northern Algeria for a period of two months from May to June. The algorithm used to prepare the LST maps is based on the Becker and Li (1990) 'split window' algorithm making use of the channels 4 and 5.

The study of LST composite map of the night of 13 May 2003 reveals a positive thermal anomaly buildup in an area south of the Boumerdes earthquake epicenter. This anomaly intensified to a maximum buildup of thermal anomaly on the night of 20 May 2003, covering an approximate area of 91,100 km² (figure 2). The temperature of the anomalous area was about 20° C -24° C, about 5° C -10° C higher than the surrounding area. After two main shocks occurred (of magnitudes 6.8 and 5.7(M_w)), on 21 May 2003, the anomaly weakened (Saraf and Choudhury, 2003b).

This less intense anomaly on the night of 21 May 2003 was probably a precursor to the earthquake of magnitude of 5.5 (M_w), which occurred on 22 May 2003 at 3:14 (UTC). The anomaly disappeared on the night of 22 May. A weak anomaly was again noticed on the night of 28 May. An earthquake of magnitude 4.9 rocked Algeria on 29 May (Saraf and Choudhury, 2003b).

An interesting observation is that the locations of the above anomalies coincide with the orientation and location of the thrust (SAF) running east to west parallel to the coast of North Africa. The origin of the earthquake may be inferred to be on a low angle fault plane obvious from the shallow location of the focus (10 km). The SAF may be regarded as the main cause of the 21 May 2003 Boumerdes earthquake.

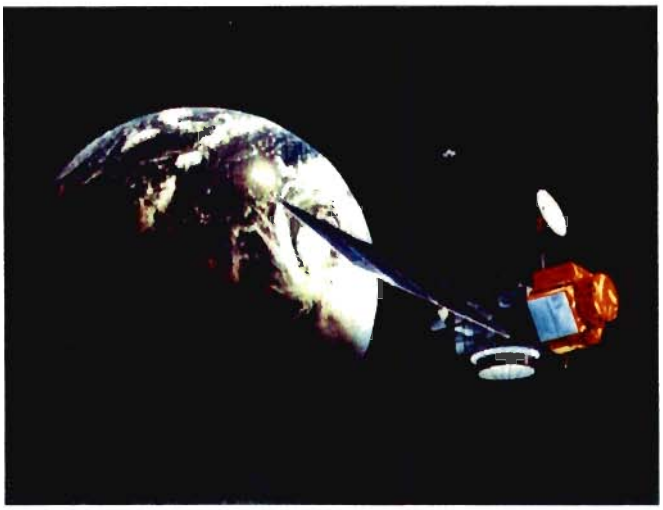

Conclusions

Remote sensing methods for detecting the earth's surface temperature with the help of thermal sensors like the AVHRR and its analysis have paved an avenue to recognize earthquake precursors in the form of a thermal anomaly in a tectonically active region.

The relation of the thermal anomaly with the tectonic setup of the region is significant. The generation of such an anomaly is induced by the activation of structures and fault systems.

Acknowledgement

We express our heartfelt thanks to Department of Science and Technology, New Delhi, National Institute of Oceanography, Goa and India Meteorological Department (IMD), Ahmedabad for their support in carrying out this research ■

References

Becker, F. and LI, Z.L., 1990, Towards a local split window method over land surface. Int. J. Remote Sensing, Vol. 11,No. 3, pp. 369-393.

Gorny, V. I. and B. V. Shilin, 1992, Thermal method of remote sensing for study of natural resources, Proceedings of the 18th Annual Conference of the Remote Sensing Society, 1992, University of Dundee, 15-17th September 1992 (edited by A. P. Cracknell and R. A. Vaughan), pp.245-263.

Saraf, A. K., Sinvhal, A., Sinvhal, H, Ghosh, P. and Sarma, B., 2002, Satellite data reveals 26 January 2001 Kutch earthquake-induced ground changes and appearance of water bodies, International Journal of Remote Sensing, Vol. 23, No. 9, pp.1749-1756.

Saraf, A. K., Choudhury, S., 2003a, NOAA-AVHRR detects thermal anomaly associated with 26 January, 2001 Bhuj earthquake, Gujarat, India, International Journal of Remote Sensing (submitted).

Saraf, A. K., Choudhury, S., 2003b, Satellite Detects Surface Thermal Anomalies Associated with the Algerian Earthquakes of May, 2003, International Journal of Remote Sensing (submitted).

Tronin, A. A., 1996, Satellite thermal survey-a new tool for the study of seismoactive regions, Int. J. Remote Sensing, Vol. 17, No. 8, pp. 1439-1455.

Tronin, A. A., 2000, Thermal IR satellite sensor data application for earthquake research in China, Int. J. Remote Sensing, Vol. 21, No. 16; pp. 3169-3177.

Zuji, Qiang, Xiu-Deng, XU and Chang-Gong, DIAN, 1991, Thermal infrared anomaly – precursor of impending earthquakes, Chinese Science Bulletin, Vol. 36, No. 4; pp. 319-323.

Zuji, Qiang, Chang-gong, Dian, Lingzhi, LI, Min, XU, Fengsha GE, Tao, LIU, Yong, ZHAO and Manhong, GUO, 1999, Satellite thermal infrared brightness temperature anomaly image – short-term and impending earthquake precursors, Science in China, Vol. 42, No. 3, pp. 313-324.

Dr. Arun K. Saraf** is Ph. D. (Remote Sensing) from University of Dundee, United Kingdom. Presently he is working in the Department of Earth Sciences, Indian Institute of Technology, Roorkee, India and teaches courses on Remote Sensing and GIS to post graduate students of Applied Geology. He was first in the country to introduce GIS course to post-graduate students in the year 1990.* **saraffes@iitr.ernet.in

***Swapnamita Choudhury** is M.Sc. in Geology from Gauhati University, Guwahati, India. At present she is pursuing her Ph.D. on Remote Sensing & GIS applications in earthquake studies under the supervision of Dr. Arun K. Saraf at Department of Earth Sciences, Indian Institute of Technology, Roorkee, India.*